A COMPREHENSIVE EVALUATION OF CAR SAFETY EVOLUTION USING MODEL CHANGE YEAR CLASSIFICATIONS AND TRAFFIC ACCIDENT DATA IN JAPAN

Kenji Kawaguchi

Institute for Traffic Accident Research and Data Analysis (ITARDA)

Japan

ABSTRACT

To reduce the number of traffic accidents and injuries caused by vehicles, crash safety performances for saving occupants and pedestrians have been improved, and also various advanced driver assistance systems have been introduced for a wide range of vehicles in recent years. The aim of this study was to elaborate on whether newer generations of car models have fewer casualty accidents due to such safety evolutions from a broader perspective. As for the classification of the cars, 411 models of standard passenger cars including SUVs were grouped into four categories by the year of full-model change (Mo.CY) which meant either fully remodeled or newly introduced to the Japanese market. Specifically, the classification were as follows; G1 (Generation 1): 2000-2002 Mo.CY, G2: 2003-2010, G3: 2011-2015, G4: 2016-2019.

Regarding accident data, fatal, serious, and minor injury accidents reported to the police in Japan between 2017 and 2020 were utilized. This applied in common to the four Mo.CY groups.

As the evaluation index, the numbers of accidents per 100,000 vehicles registered per year were used. Then it was assessed whether there was a difference among the groups of Mo.CY, i.e., whether the newer vehicle group has fewer accidents.

This evaluation was conducted from a comprehensive viewpoint including many safety systems and crash safety performance improvements, rather than strictly assessing the effectiveness of a specific safety system.

In conclusion, analyzing accident data for the same period of 2017 to 2020, the number of accidents for the newer Mo.CY groups in several types of accidents was lower than that for old ones.

Regarding fatal accidents, pedestrian and single-vehicle accidents accounted for a large percentage in the G1 group. Specifically, the analysis proved that the number of fatal accidents per 100,000 registered vehicles has dramatically decreased by 55% for pedestrians, and 69% for single-vehicle accidents from G1 to G4. In addition, the casualty accidents for rear-end collisions have greatly reduced by 64% from G1 to G4.

That was because the newer cars had more various safety features and better-improved passive safety performance. It was also clarified that the degrees of accident reduction depended on the severity of injury and the type of accident.

The method presented here, utilizing Japanese elaborate statistical accident data, demonstrated that it was possible to quantify the overall benefits of safety features and performances, or car safety evolution. Therefore it could lead to a better understanding of real-world performance and a way to go for a safer world.

INTRODUCTION

To decrease traffic accidents and injuries caused by vehicles, crash safety performances for occupants and pedestrians have been improved, and various advanced driver assistance systems have been introduced for a wide range of vehicles recently. New Car Assessment Program (NCAP) have been conducted in the U.S., Europe, Japan, etc., to evaluate such safety performance and systems. Several studies have been conducted to clarify how to contribute to the reduction of accidents and injuries [1] [2] [3].

In Japan, all police-reported accident data, not sampled, are recorded with model and type information, which is linked to the number of registered vehicles by model. Such an integrated accident database compiled by ITARDA would be extremely helpful for statistical analysis. The analysis enabled us to elaborate on whether a newer group of car models have fewer accidents and injuries from a broader perspective. The clarification of accident reduction by the severity of injury and type of accident could contribute to update of the traffic accident reduction strategies similar to those in the United States [4].

METHOD AND DATA SOURCES

The method used in this study contains five steps: vehicle model selection and grouping; counting accident data; counting numbers of registered vehicles; evaluation index calculation; results analysis.

Vehicle model selection and grouping

Firstly, the models fully remodeled or newly introduced on the Japanese market in 2000 or later were selected. As a result, 411 models of standard passenger cars including SUVs were chosen. The models were grouped into four categories by the year of full-model change (Mo.CY) as follows; G1 (Generation 1): 2000-2002 Mo.CY, G2: 2003-2010, G3: 2011-2015, G4: 2016-2019. The reasons why they were separated by those years are described below. The evaluation of ODB (Offset Deformable Barrier Frontal Test) was started in 2000 in JNCAP, and the initial group of vehicles with such basic performance was used for the comparison basis. Since this study initially started with pedestrian accident analysis, Mo.CY were segmented at the years of 2003 (when pedestrian head protection performance evaluation started in JNCAP), 2011 (pedestrian leg protection performance), and 2016 (pedestrian damage mitigation brakes.) However, these delimited years were kind of a guideline, not an absolute requirement. The fact that the year is not "model year" but "full-model change year" was significant. That is because the year means to be related to when a model was developed, not produced.

Counting accident data

In the second step, fatal, serious, and minor injury accident data related to each model between 2017 and 2020 in Japan were utilized. This applied in common to the four Mo. CY groups. The accident data reported to the police was obtained from National Police Agency and compiled by ITARDA. In this study, the targeted vehicle was focused on the primary-party in the accidents.

The injury severities in the accident database are defined as follows:

- Fatality: a death occurs within 24 hours of the accident and as a result of the accident
- Serious Injury: victim is treated for 30 or more days from the date of accident, including a death after more than 24 hours

- Minor Injury: victim is treated for less than 30 days from the date of accident

Counting numbers of registered vehicles

In the third step, the total number of registered vehicles from 2017 to 2020 for each group were counted. As data sources, the numbers of registered vehicles for each model as of the end of the year were got from Road Transport Bureau of Ministry of Land, Infrastructure, Transport and Tourism and compiled by ITARDA. To determine the effective number of registrations for the relevant year, the average of the number of registrations at the end of the previous year and that at the end of the current year was calculated. In the next step, the calculated number of registrations for each year was then added up for the four years: 2017-2020. In the final step, the numbers of registrations of each model for the four years were summed up among each Mo.CY group.

Evaluation index calculation

The fourth step calculated the evaluation index through dividing the number of accidents by the number of vehicles registered during the four years period. As the evaluation index, the numbers of accidents per 100,000 vehicles registered per year for each group were adopted.

Results analysis

In the final step, the evaluation index have been scrutinized by the severity of accidents and the type of accidents.

RESULTS

Table 1 showed the number of models for each group, varying from 63 to 164. Table 1 also included the total registered vehicle number for each group for four years. The number is from a minimum of about 8 million to a maximum of over 63 million. They were used as denominators when deriving the per-unit indicator. These sample sizes were quite large enough and nationally representative since the total registered number here accounted for about 80 percent of standard passenger car fleet in the Japanese market.

Table 1.

Classification of vehicle models, number of models and total registered number for each group

Group No.	G1	G2	G3	G4	Total G1-G4
Mo.CY	2000-2002	2003-2010	2011-2015	2016-2019	2000-2019
Number of models	86	164	98	63	411
Total of registered vehicle number for 4 years: 2017-2020	16,177,592	63,757,014	39,609,658	8,044,915	127,589,179

Table 2 displayed the number of fatal accidents by type of accident for each Mo.CY group. The similar tables for fatal and serious accident and for casualty one were shown in APPENDICES.

First of all, the total accident numbers in the bottom row of Table 2 were divided by the registered number in Table 1 for each group. Then the indicators "per 100,000 registered vehicles" were calculated.

Table 2.

Number of fatal accidents for each Mo.CY group and each type of accident

(Years of accident: 2017-2020, subject car: the primary-party)

	Number of fatal accidents for each Mo.CY group			
Type of accident	G1:2000-2002	G2:2003-2010	G3:2011-2015	G4:2016-2019
pedestrian	227	777	351	52
head-on	55	162	74	13
rear-end	19	69	27	9
crossing	43	160	89	18
turning right	36	95	53	8
turning left	0	8	6	1
single-car	141	272	108	23
others	13	68	27	4
Total	534	1,611	735	128

The results were shown in Figure 1, and there was a large difference between G1 and G2 in fatal case (left). On the other hand, in casualty cases (right), there was no difference between G1 and G2 but is a large difference between G3 and G4. Looking over these graphs it was found that the newer Mo.CY groups have lower accident possibilities than the older ones. In these figures, vertical lines indicated 95% confidence intervals and were used as a reference for determining whether there was a significant difference.
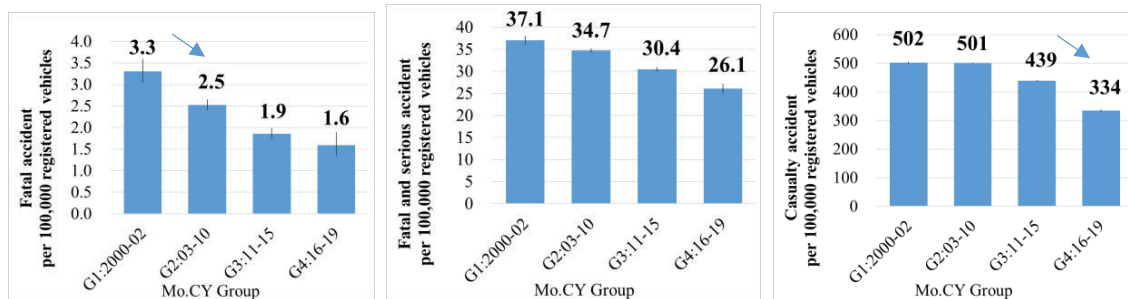

Figure 1. Number of accidents per 100,000 registered vehicles by Mo.CY group

(Years of accident: 2017-2020)

Fatal (left), fatal and serious (center), casualty (right) accident.

Next, Figure 2 (left) described a detailed look at type of accident in fatal accidents from Figure 1 (left).

In G1, pedestrian and single-car accidents were the most common types of accidents.

Comparing G1 to G4 for each type of accident, only those two types of accident had a significant difference. Therefore, the reduction tendency of both pedestrian and single-car accidents were shown in Figure2 (right), articulating a 55 percent decrease in pedestrian accidents and a 69 percent decrease in single-car accidents.
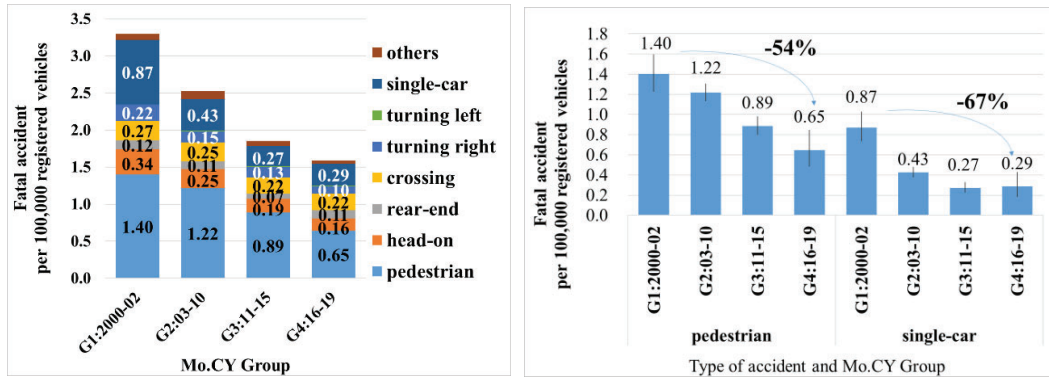

Figure 2. Number of <u>fatal</u> accidents per 100,000 registered vehicles by Mo.CY group

(Years of accident: 2017-2020)

Accumulated bar by type of accident (left), evolution for pedestrian and single-car collision (right).

Figure 3 illustrated the number of fatal and serious injury accidents per 100,000 registered vehicles by type of accident and Mo.CY group. It was illustrated that pedestrian and crossing collision were dominant types of accidents. There were some reductions for several types of accidents with comparison among Mo.CY Groups during the same period of the year of 2017-2020.
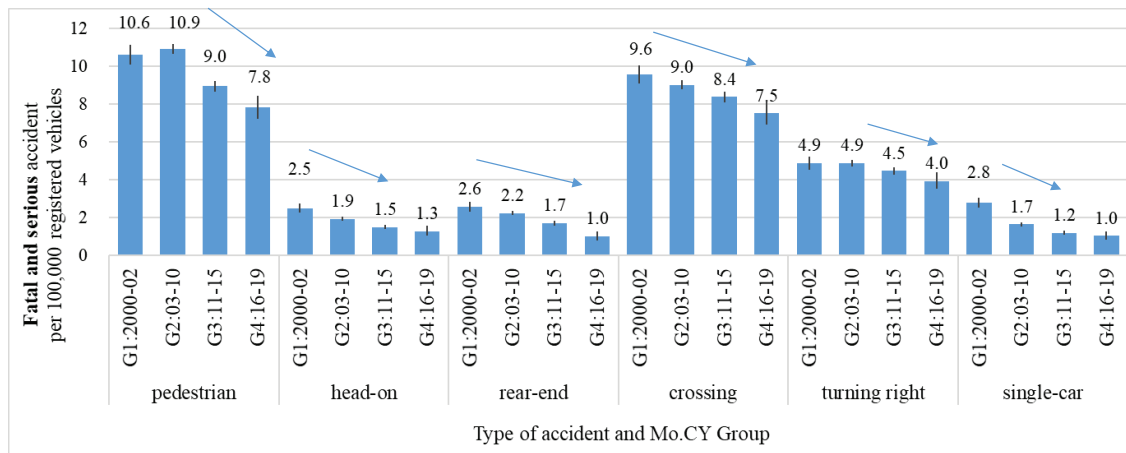

Figure 3. Number of <u>fatal and serious</u> accidents per 100,000 registered vehicles by Mo.CY group

(Years of accident: 2017-2020).

Figure 4 described the number of casualty accidents per 100,000 registered vehicles by type of accident and Mo.CY group. It was demonstrated that rear-end and crossing collisions were dominant types of accidents. A dramatically sharp drop for rear-end collision was clarified. Since rear-end collisions which were the most common type of accident have decreased, crossing collisions have become the most frequent type of accident in G4.
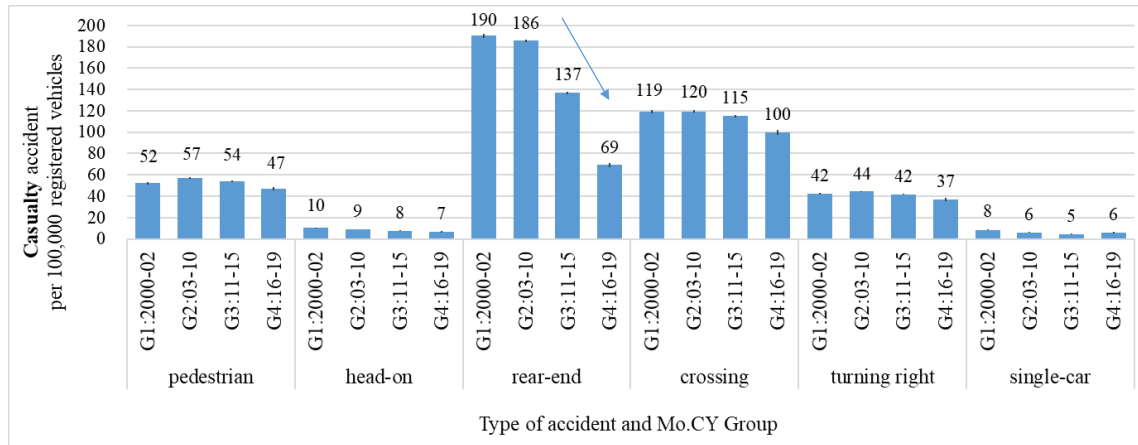

Figure 4. Number of <u>casualty</u> accidents per 100,000 registered vehicles by Mo.CY group
(Years of accident: 2017-2020).

Figure 5 summarized the reduction rates from G1 to G4 by type of accident for three severity levels of injury. The collision when turning left and the fatal type of accidents except for pedestrian and single-car had no significant difference between G1 and G4. Therefore, they were omitted from the graph.
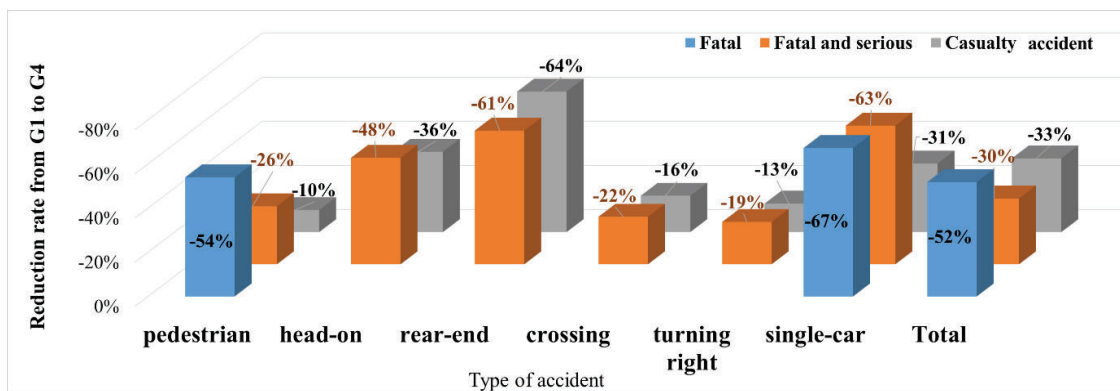

Figure 5. Reduction rates from G1 to G4 by type of accident for three severity levels of injury
(Years of accident: 2017-2020).

In addition, Figure 6 indicated absolute values of reduction per 100,000 registered vehicles. As shown in Figure 5 and Figure 6, it demonstrated that each reduction rate depended on the degree of injury and type of accident.
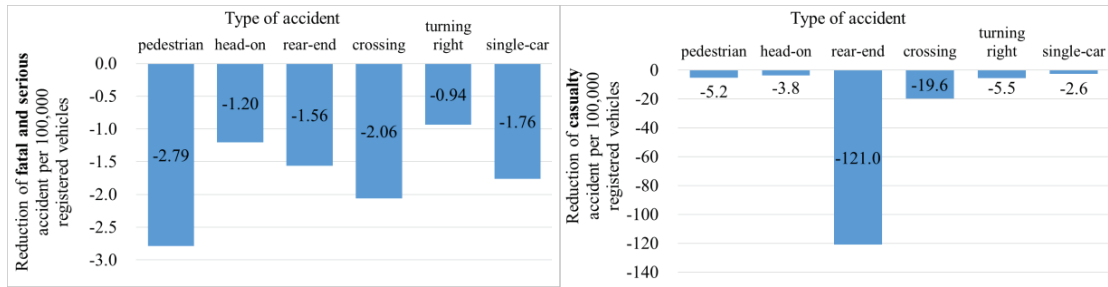

Figure 6. Reduction values per 100,000 registered vehicles from G1 to G4 by type of accident
Fatal and serious (left), casualty accident (right) (Years of accident: 2017-2020).

DISCUSSION AND LIMITATIONS

The status of accident reduction has been carefully and quantitatively scrutinized so far. Here, the presumed factors for these reductions would be discussed.

Regarding pedestrian fatality reduction, one of the factors could be the improvement of pedestrian head protection performance which JNCAP started to evaluate in 2003. That was because the primary part of injury in pedestrian fatalities was the head. In addition, the primary part of crash of vehicle against pedestrian in fatal case was the front as is well known.

As to head-on collision, in addition to the improvement of crash safety performance in Offset Deformable Barrier (ODB) frontal crash mode, the spread of Lane Departure Warning (LDW) system or Lane Departure Prevention System (LDPS) could play a leading role.

The largest decline in rear-end collisions including minor injury accidents, as shown in Figure 6 (right), could be attributed to the spread of Autonomous Emergency Braking (AEB) system. It can be said that AEB would be the most successful safety system.

For single-vehicle accidents, the spread of Electric Stability Control (ESC) system, LDW, and LDPS could contribute to the decrease in accidents.

However, all of these factors as mentioned above were presumptive ones. No causal relationship was quantified here. It would be difficult to extract the effectiveness of each system independently. For this purpose, further study should be needed, and at that time the differences in many accident conditions, such as collision velocity and drivers' age in different Mo.CY groups should be taken into account. Also, both the absolute number and the rate of reduction should be scrutinized to determine areas of future focus. The aim of this study was nonetheless successfully conducted to clarify that the newer generations of car models have fewer accidents and injuries from a broad perspective.

CONCLUSIONS

The 411 models of standard passenger cars including SUVs were grouped into four categories by the year of full-model change (Mo.CY). The number of accidents per 100,000 vehicles for a total of four years from 2017 to 2020 were compared to each other. The results showed the following improvements in vehicle safety for example.

Comparison between G1 (2000-2002) and G4 (2016-2019)

- Fatal accidents, 54% reduction for pedestrian accidents, 67% reduction for single-car ones
- Casualty accidents, as much as 64% reduction for rear-end collisions

The method presented in the study, utilizing Japanese elaborate statistical accident data, demonstrated that it was possible to quantify the overall benefits of safety features and performances based on the field data. Therefore, it could lead to a better understanding of real-world performance.

The results presented in this paper demonstrated the fruits of the great endeavors of many people including automotive engineers and others involved.

Moreover, the outcomes here could also mean a starting point for further research and measures toward vision zero.

REFERENCES

[1] Strandroth, J., Sternlund, S., Lie, A., Tingvall, C., Rizzi, M., Kullgre A., Ohlin, M. and Fredriksson, R. 2014. "Correlation Between Euro NCAP Pedestrian Test Results and Injury Severity in Injury Crashes with Pedestrians and Bicyclists in Sweden." 58th STAPP, No.2014-22-0009

[2] Samantha H. Hausa, S. H., Sheronyb, R., and Gablera, H. C. 2019. "Estimated benefit of automated emergency braking systems for vehicle–pedestrian crashes in the United States." Traffic Injury Prevention 2019, Vol.20

[3] Ogawa, S., Chen, Q., Kawaguchi. K., Narikawa, T., Yoshimura, M. and Lihua, S. 2013. "Effect of Visibility and Pedestrian Protection Performance on Pedestrian Accident." ESV2013, No.13-0365

[4] U.S. Department of Transportation. 2022. "National Roadway Safety Strategy."

APPENDICES

Table 3.

Number of <u>fatal and serious</u> accidents for each Mo.CY group and each type of accident

(Years of accident: 2017-2020, subject car: the primary-party)

Type of accident	Number of fatal and serious accidents for each Mo.CY group			
	G1:2000-2002	G2:2003-2010	G3:2011-2015	G4:2016-2019
pedestrian	1,718	6,961	3,548	630
head-on	404	1,241	599	104
rear-end	418	1,431	679	82
crossing	1,550	5,759	3,327	605
turning right	791	3,125	1,773	318
turning left	220	882	696	101
single-car	454	1,059	481	84
others	444	1,691	958	172
Total	5,999	22,149	12,061	2,096

Table 4.

Number of <u>casualty</u> accidents for each Mo.CY group and each type of accident

(Years of accident: 2017-2020, subject car: the primary-party)

Type of accident	Number of casualty accidents for each Mo.CY group			
	G1:2000-2002	G2:2003-2010	G3:2011-2015	G4:2016-2019
pedestrian	8,428	36,525	21,287	3,774
head-on	1,669	5,772	3,069	528
rear-end	30,770	118,442	54,264	5,571
crossing	19,317	76,192	45,618	8,026
turning right	6,872	28,244	16,622	2,977
turning left	3,592	14,274	9,800	1,690
single-car	1,350	3,962	1,851	463
others	9,203	36,042	21,369	3,870
Total	81,201	319,453	173,880	26,899

PEER REVIEW PAPER

This paper has been peer-reviewed and published in a special edition of Traffic Injury Prevention 24(S1), by Taylor & Francis Group. The complete paper will be available on the Traffic Injury Prevention website soon. To access ESV Peer-reviewed papers click the link below
https://www.tandfonline.com/toc/gcpi20/24/sup1?nav=tocList

Development of Simulation-Based Method for Benefit Estimation of Automatic Emergency Braking and Lane Departure Warning in Traffic Collisions

Mitsuaki Goto
Nana Takeuchi
Takao Matsuda
Yuichi Kitagawa
Toyota Motor Corporation
Japan

ABSTRACT

In this study, a simulation-based method was developed for benefit estimation of Automatic Emergency Braking (AEB) and Lane Departure Warning (LDW). The collision avoidance effect and the injury mitigation effect of AEB and LDW were probabilistically estimated through large-scale simulations of near-miss scenarios leading to traffic collisions. The top nine near-miss scenarios were selected from the fatal collision data in Japan. The simulation parameters such as vehicle speed and its position in the lane were varied based on the statistical data to realistically simulate various situations in the field. A total of 17,000 simulations were conducted for each with or without AEB or LDW in order to calculate the reduction of collisions cases. For the collision cases, crash simulations were conducted using a virtual human body model "THUMS" to predict the fatality risk. In this study, the head injury value, HIC_{15}, was used to determine whether the injury level was fatal. The benefit of AEB/LDW was estimated by multiplying their effect for each collision scenario by the percentage of the scenarios in the total number of fatal collisions in Japan. When neither AEB nor LDW were activated, collisions occurred in 117,031 out of 153,000 cases. When AEB or LDW was activated, collisions occurred in 48,030 cases. The collision avoidance effect by AEB or LDW was estimated to be 59.0 %. In the collision cases, there were 415 fatal cases where AEB was not activated while in 76 cases with AEB was activated. Based on the results, the injury mitigation effect was estimated to be 81.5 %. The simulation results for the top nine scenarios indicated 29.9 % for the benefit in collision avoidance and 52.4 % for the benefit in injury mitigation.

INTRODUCTION

Advanced driver-assistance systems (ADAS) are becoming widespread in many countries. The system alerts the driver when it detects a risk of collision. AEB activates the brakes when the driver does not apply the brakes despite the presence of a collision risk. The system tries to avoid the collision and mitigate the damage by lowering the vehicle speed. LDW alerts the driver when the vehicle is about to depart from the lane for some reason such as distraction. It tries to avoid the collisions with an oncoming vehicle or obstacles such as guard rails. The performance of ADAS functions is evaluated in vehicle tests under prescribed conditions assuming common collision scenarios [1-3]. The performance tests of AEB in Euro NCAP are conducted on the target assuming near-miss situations with pedestrians, bicycles, and vehicles ahead. The AEB rating for pedestrians assumes that pedestrians are crossing. The test scores are calculated from the result of 110 test cases with different vehicle speed, direction of pedestrian, presence of blind spots, and day/night conditions. However, there could be many types of actual collision scenarios. This makes it difficult to quantitatively estimate the effectiveness of ADAS in the field. Previous study reported the performance of ADAS in actual traffic conditions based on the past accident database [4]. It takes several years to accumulate the necessary number of accident data for such a study. It is difficult to predict the effectiveness of new safety features under development. Few studies have quantitatively investigated the effectiveness of ADAS on human injury mitigation. The objective of this study is to develop a simulation-based method to estimate the effectiveness of AEB and LDW in terms of collision avoidance and injury mitigation, considering the variation traffic collisions. The benefit of AEB and LDW in fatal collisions is also estimated at the national level using this method.

METHOD

The effectiveness of AEB and LDW was estimated by combining two simulations: vehicle dynamics simulation and crash simulation. The purpose of vehicle dynamics simulation was to estimate the reduction in the number of collision cases by activating AEB. The purpose of crash simulation was to estimate the reduction in the number of fatalities (Figure 1) in collision cases. For AEB, the effectiveness in both collision avoidance and injury mitigation was estimated. For LDW, the collision avoidance effect was estimated. Note that LDW works to prevent lane departure.
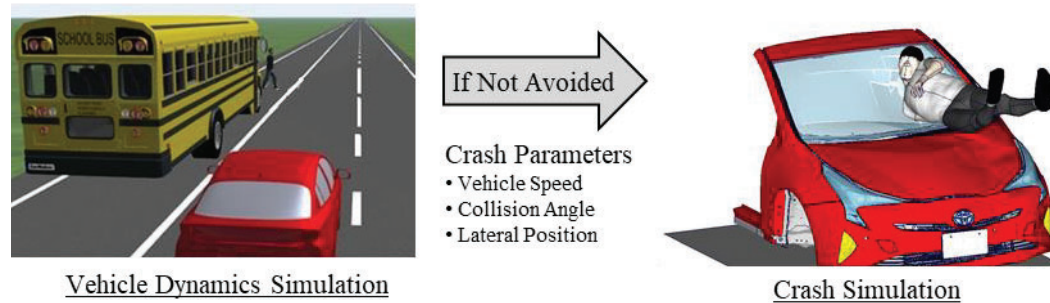

Figure 1. Simulations for estimating effectiveness of AEB and LDW.

Vehicle Dynamics Simulation
The vehicle dynamics simulations assumed various near-miss scenarios that could lead to collisions. The simulations were conducted assuming top nine fatal collision scenarios in the traffic collision database in Japan (Table 1). The top nine scenarios are pedestrian crossing, collision with a bicycle or a motorcycle at an intersection, collision when the vehicle was turning right or left, single-vehicle collision, and head-on collision. It accounted for approximately 80% of fatal traffic collisions reported in Japan [5]. The pedestrian crossing assumed the scenario (i) where a pedestrian appeared from the blind spot of a parked vehicle. Intersection scenarios assumed situations where bicycle (scenario (ii)) or motorcycle (scenario (iii)) entered the intersection from the crossing road. The right/left turn scenarios assumed the situations where the turning vehicle came close to a pedestrian (scenario (iv), (vi)) or a bicycle (scenario (v), (vii)) moving in the same direction or the opposite direction. The single-vehicle collision assumed the scenarios where the vehicle departed from the lane and came close to obstacles such as guard rails and a pole. The other case assumed a head-on collision with an oncoming vehicle. In each scenario, parameters such as vehicle speed/position, pedestrian walking speed/direction, those of bicycle/motorcycle, other road environment features were stochastically varied based on actual statistical data [6-11] and human behavioral characteristics to represent the variety in actual traffic collisions. A total of 17,000 simulation cases were generated for each scenario (Figure 2, Table 2). A pair of the simulation sets were performed with and without AEB/LDW. A total of 153,000 (17,000 cases for each of the nine scenarios) simulations were conducted in this study. The reduction of collision cases by AEB/LDW was calculated for each scenario. The benefit of AEB/LDW was estimated by multiplying the effectiveness of AEB/LDW in each scenario by the percentage of the scenario in the total number of fatal collisions in Japan. The effectiveness of AEB was estimated for the scenarios of pedestrian crossing and right/left turning at intersections. The effectiveness of LDW was estimated for the scenarios of single vehicle collision and head-on collision. The simulation model assumed a medium-sized sedan as the subject vehicle. The vehicle model replicated a real vehicle with a sensor and brake performance. The AEB model was added to the vehicle model to activate the brakes when the time to collision (TTC) with an object fell below a threshold value. The field of view was set to the range where the view angle of the millimeter wave radar and the monocular camera overlapped (46deg). The driving environment was assumed to be daytime on a sunny day. It was assumed that the object was detected as soon as it entered the field of view. There was no additional time (latency) between the detection and the initiation of braking. Assuming the dry condition for the road surface, a constant braking deceleration was defined for AEB model with the maximum jerk of 16.7 m/s^3 and the maximum deceleration of 9.8 m/s^2 as shown in Figure 3(a). A human driver model was used for the cases where AEB was not activated. The braking operation was simulated considering individual differences (Figure 3(b)). Based on the volunteer test data [12], the variation in idle time (0.2 ~ 5.1s), jerk (0.5~16.7m/s^3) and maximum deceleration (0.5~9.8m/s^2) were reproduced in the human driver model. The field of view was assumed to be 100 degrees. The driver detected the object as soon as it entered the field of view. In the right/left turning scenarios without AEB, it was assumed that the driver missed detecting the obstacle despite it entered in the field of view. As for LDW, the system alerted the driver when the vehicle deviated from the center of the lane and approached an obstacle. The driver model

was designed to return to the center of the lane after hearing the alert. Based on the volunteer test data [13], the variations in reaction time (0.3~2.1s), steering angular velocity (0~320deg/s) and maximum steering angle (0~160deg) were reproduced (Figure 4) in the driver model. In the cases without LDW, the vehicle continued the motion without appropriate steering operation to stay in the lane. CarMaker of IPG Automotive was used for vehicle driving simulation. The simulation models of AEB, LDW, and the human driver were developed in MATLAB/Simulink from MathWorks and incorporated into CarMaker's vehicle model.

Table 1.
Simulation scenarios.

No.	Collision Scenario	Description	ADAS	Number of Simulations
(i)	Pedestrian Crossing	Crossing - Pedestrian from left/right side	AEB	17,000
			-	17,000
(ii)	Bicyclist Crossing	Crossing - Bicyclist from oncoming bicycle lane left/right and straight	AEB	17,000
			-	17,000
(iii)	Motorcyclist Crossing	Crossing - Motorcyclist from left/right and driving straight	AEB	17,000
			-	17,000
(iv)	Pedestrian in right-turn	Right turning vehicle and pedestrian in same/opposite direction	AEB	17,000
			-	17,000
(v)	Bicyclist in right-turn	Right turning vehicle and bicyclist from bicycle lane in same/opposite direction	AEB	17,000
			-	17,000
(vi)	Pedestrian in left-turn	Left turning vehicle and pedestrian in same/opposite direction	AEB	17,000
			-	17,000
(vii)	Bicyclist in left-turn	Left turning vehicle and bicyclist from bicycle lane in same/opposite direction	AEB	17,000
			-	17,000
(viii)	Single-Vehicle Collision	Other accident - Fix obstacle	LDW	17,000
			-	17,000
(ix)	Head-on Collision with Vehicle	Head on - Encountering vehicles in curve	LDW	17,000
			-	17,000
Total				153,000×2
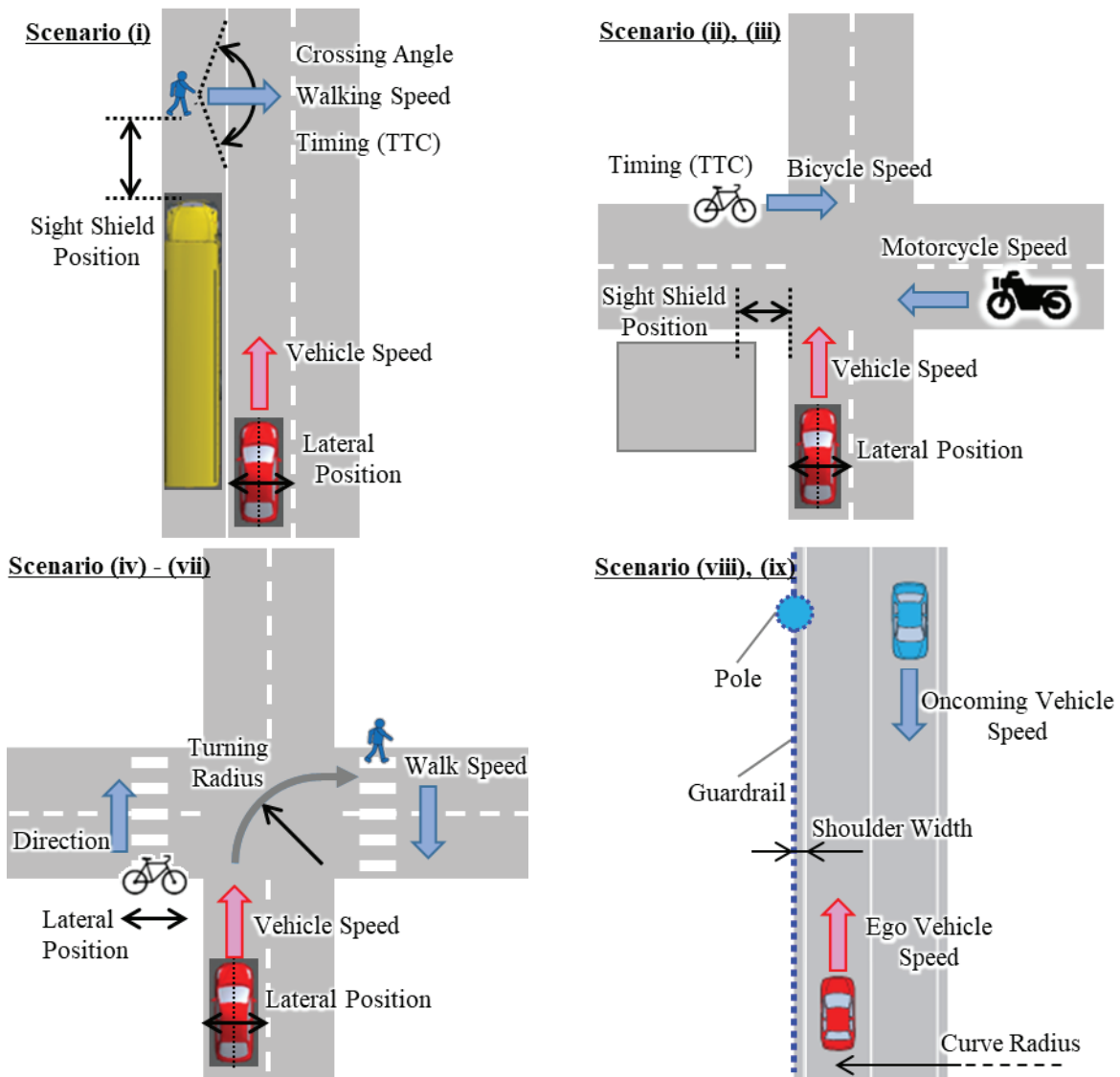
Figure 2. Simulation scenarios.

Table 2.
Simulation parameters and ranges.

No.	Collision Scenario		Parameter	Unit	Range	Distribution
(i)	Pedestrian Crossing	Pedestrian	Speed	m/s	0.8 - 2.0	Gaussian
			Crossing Angle	deg.	-70 - +70	Gaussian
			Timing	s	0.7 - 10	Log-normal
		Vehicle	Speed	km/h	10 - 60	Gaussian
			Lateral Position	m	-0.8 - +0.8	Gaussian
		Others	Sight Shield Position	m	4 - 24	Logarithmic
(ii)	Bicyclist Crossing	Bicyclist	Speed	km/h	3 - 21	Uniform
			Lateral Position	-	Sidewalk/Bicycle Lane	Uniform
			Direction	-	Left/Right	Uniform
			Timing	s	-0.2 - +0.2	Uniform
		Vehicle	Speed	km/h	10 - 60	Uniform
			Lateral Position	m	-0.8 - +0.8	Uniform
		Others	Sight Shield Position	m	0 - 35	Uniform
(iii)	Motorcyclist Crossing	Motorcyclist	Speed	km/h	10 - 60	Uniform
			Lateral Position	-	Roadway	Uniform
			Direction	-	Left/Right	Uniform
			Timing	s	-0.2 - +0.2	Uniform
		Vehicle		same as (ii)		
		Others		same as (ii)		
(iv)	Pedestrian in Right-Turn	Pedestrian	Speed	km/h	3 - 8	Gaussian
			Lateral Position	m	-0.5 - +0.5	Uniform
			Direction	-	Same/Opposite	Uniform
		Vehicle	Speed	km/h	12 - 36	Gaussian
			Turning Radius	m	5 - 10/5 - 16	Gaussian
			Lateral Position	m	-0.8 - +0.8	Uniform
(v)	Bicyclist in Right-Turn	Bicyclist				
			Lateral Position	m	-0.5 - +0.5	Uniform
			Direction	deg	Same/Opposite	Uniform
		Vehicle	Speed	km/h	12 - 36	Gaussian
			Turning Radius	m	5 - 10/5 - 16	Gaussian
			Lateral Position	m	-0.8 - +0.8	Uniform
(vi)	Pedestrian in Left-Turn	Pedestrian		same as (iv)		
		Vehicle		same as (iv)		
(vii)	Bicyclist in Left-Turn	Bicyclist		same as (v)		
		Vehicle		same as (v)		
(viii)	Single-Vehicle Collision	Vehicle	Speed	km/h	50 - 80	Gaussian
			Departure Angle	deg	0 - 25/0 - 30	Gaussian
		Road	Curve Radius	m	150 - 1050/Straight	Log-normal
			Shoulder Width	m	0.5/0.75	-
		Other	Fix Obstacle	-	Pole/Guardrail	Uniform
(ix)	Head-on Collision with Vehicle	Ego Vehicle	Speed	km/h	50 - 80	Gaussian
			Departure Angle	deg	0 - 25/0 - 30	Gaussian
		Oncoming Vehicle	Speed	km/h	0 - 80	Gaussian
		Road	Curve Radius	m	150 - 1050/Straight	Log-normal

Max. Deceleration
(9.8[m/s²])

Jerk
(Max. 16.7[m/s³])

Detect

Detect & React
(46 deg.)

Detect

Deceleration [m/s²]

TTC [s]

Sensing Range

Deceleration Property

(a) AEB model

Max. Deceleration
(0.5~9.8[m/s²])

Brake Reaction Time
(0.2~5.1[s])

A-Pedal Off   Change Pedal

Jerk
(0.5~16.7[m/s³])

Detect & React
(100 deg.)

Deceleration [m/s²]

Detect

TTC [s]

Sensing Range

Deceleration Property
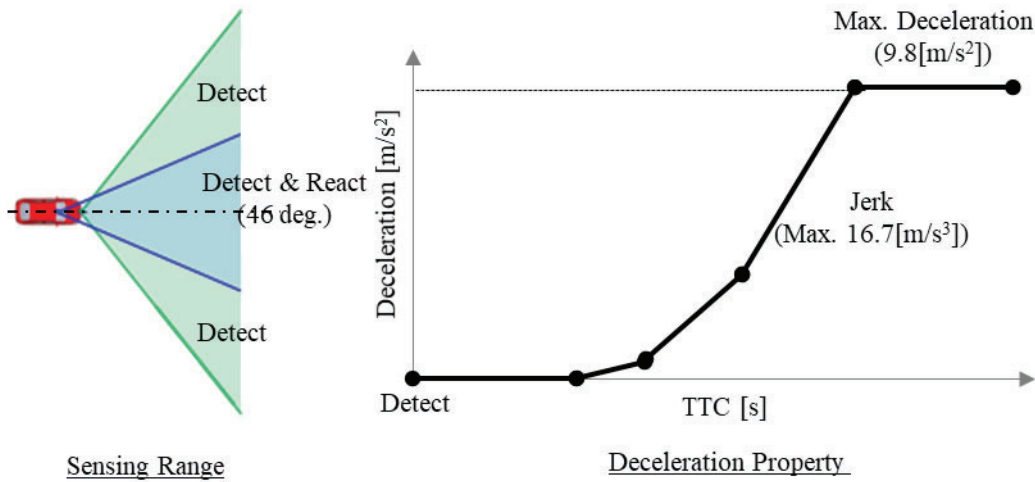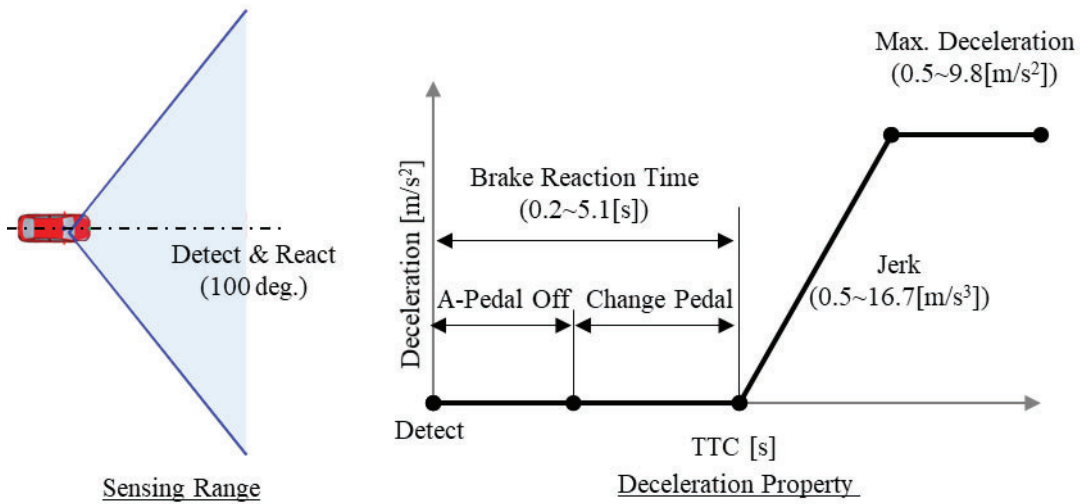
(b)Driver's braking model

Figure 3. Properties for AEB and driver's braking
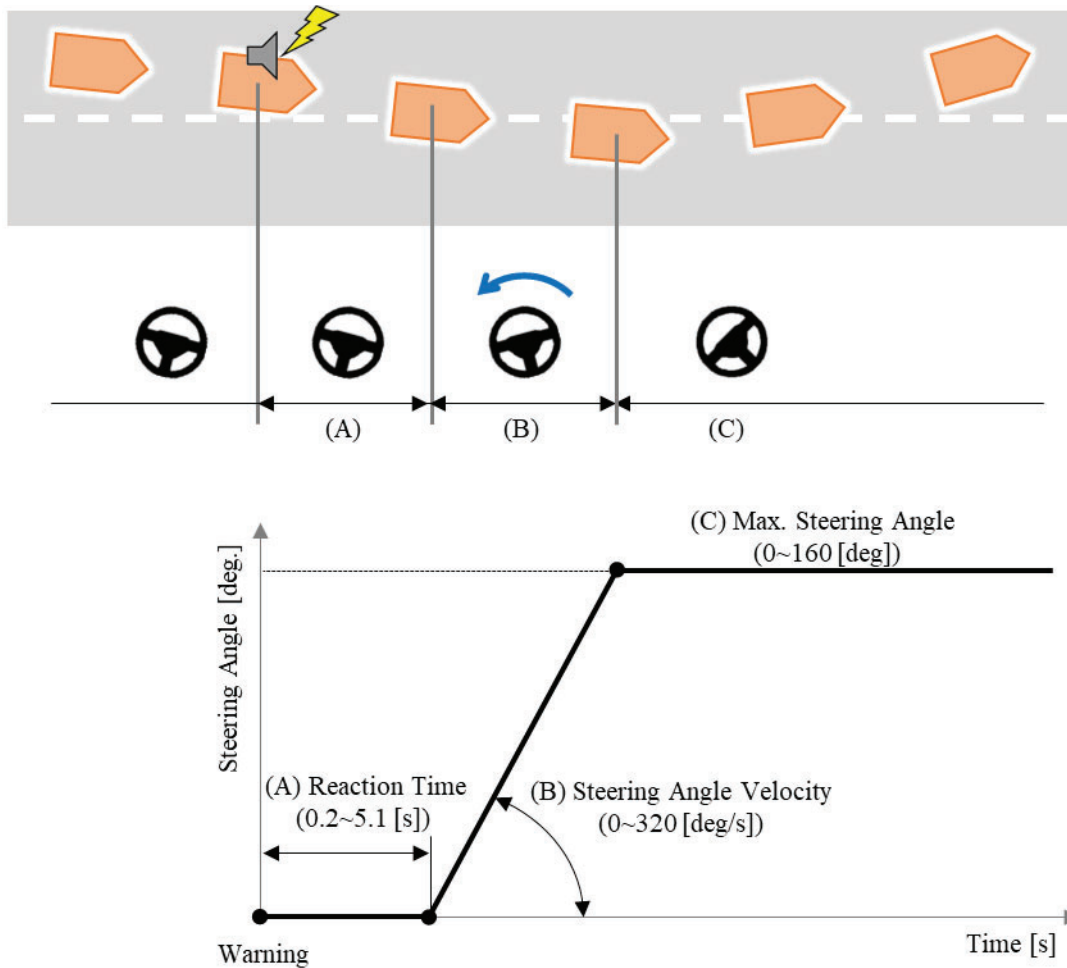
Figure 4. Property of driver steering to the center of the lane.

Crash Simulation

In the crash simulation, the fatal injury risk was estimated for the collision cases in the vehicle dynamics simulations. The virtual human body model THUMS (Total HUman Model for Safety) [14] was used to predict the fatal injury risk. The study focused on head injury as a representative form of fatal injury. The head injury criterion HIC_{15} was used to determine whether the injury level was fatal. First, crash simulations were conducted without AEB then the fatal injury risk was calculated. Next, crash simulations were conducted with AEB then the fatal injury risk was calculated again. The effectiveness of AEB was defined as the percentage of the reduction in the number of fatal injury cases by AEB. The benefit of AEB in injury mitigation was estimated by multiplying the fatality reduction rate by the percentage of the collision scenario in the total fatal collisions in Japan. The injury prediction method for pedestrians and occupants in the collision cases is described below. Figure 5 illustrates the flow of prediction process. First, crash simulations were conducted using THUMS and the vehicle model to construct a database indicating the relationship between the crash conditions and the HIC_{15} values. Using the database, a Reduced Order Model (ROM) was generated to calculate the injury value from the given crash conditions in a short time. A neural network was used to generate the ROM. The ROM calculated the injury values in tens of thousands of collision cases in a very short time. The conditions of a collision case were the input data to the ROM and the HIC_{15} value was the output. If the HIC_{15} value exceeded 700, it was regarded as a fatal collision case. LS-DYNA from ANSYS was used for the crash simulations. LS-OPT from ANSYS was used to generate the ROM and to calculate injury values.
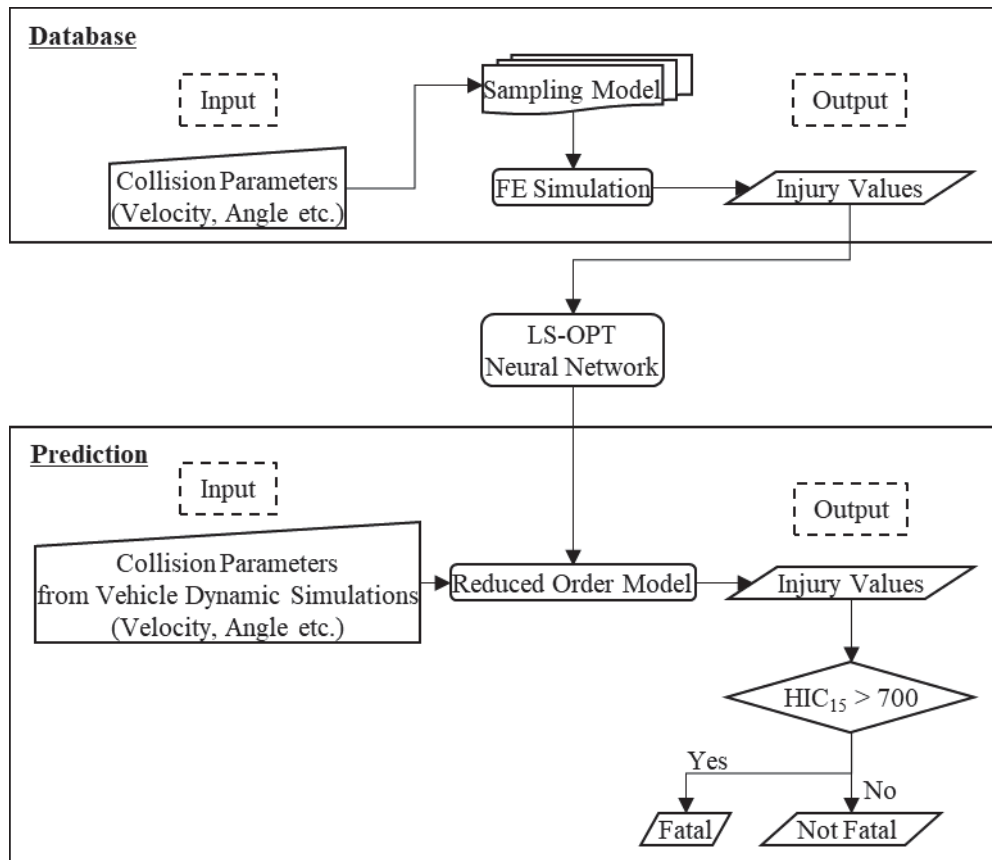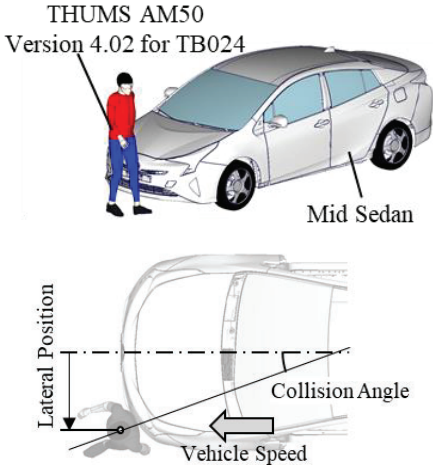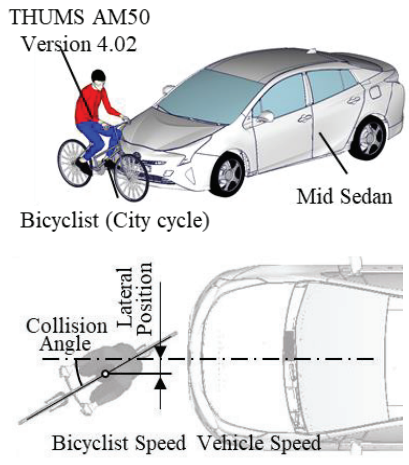
Figure 5. Flow of injury prediction process.

Crash Simulation Model THUMS AM50 Version 4.02 was used to represent the pedestrian or occupant in crash simulations. A midsize sedan was assumed as the subject vehicle (Figure 6). The collision conditions were changed parametrically by varying the numerical values. The parameter range of crash simulation covered all the collision cases in the vehicle dynamics simulation (Table 3). For pedestrian crossing, it was assumed that a pedestrian crossed the road in front of the vehicle then collided. The pedestrian collisions at the intersection occurred when the vehicle was turning right or left. The pedestrian posture was adjusted to comply with EuroNCAP TB024 [15]. The vehicle speed was varied from 10 to 60 kph, the collision angle was varied from 20 to 160 deg, and the collision position was varied from -700 to 700 mm in the vehicle width direction. A total of 225 crash simulations were performed. The bicycle collisions at the intersection occurred when the bicycle entered the intersection from the crossing road and collided with the vehicle's front. The other scenario was that the vehicle turned right or left at the intersection, and then collided with the bicycle. A city cycle was assumed. THUMS was placed on to the bicycle model. The vehicle speed varied from 10 to 60 kph, the bicycle speed varied from 3 to 23 kph, the collision angle varied from 0 to 180 deg, and the position varied from -650 to 1850 mm in the vehicle width direction. A total of 700 crash simulations were performed. The motorcycle collisions occurred when the motorcycle entered the intersection, and then collided with the vehicle front. A standard motorcycle was assumed. THUMS was placed on to the motorcycle model. The vehicle speed varied from 10 to 60 kph, the motorcycle speed varied from 10 to 60 kph, and the position varied from -440 to 1660 mm in the vehicle width direction. A total of 350 crash simulations were performed. The crash simulations were performed until the head contacted the vehicle and the head acceleration reached the maximum peak. It was assumed that pedestrians, bicyclists, and motorcyclists did not perform any avoidance or defensive actions before the collision.
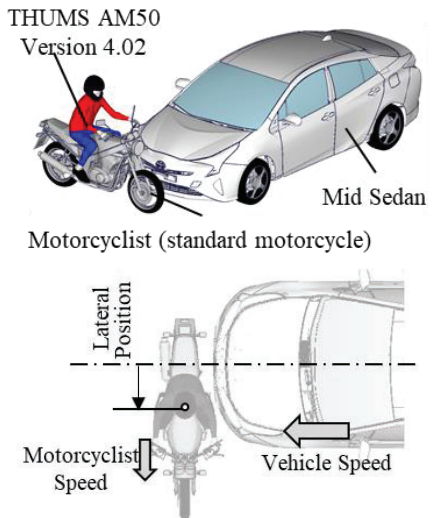
(a) Pedestrian (Scenario (i), (iv), (vi))

(b) Bicyclist (Scenario (ii), (v), (vii))

(c) Motorcyclist (Scenario (iii))

Figure 6. Crash simulation models.

Table 3.
Crash simulation parameters and ranges.

		Parameters				Number of Simulations
		Vehicle Speed	Bicyclist/Motorcyclist Speed	Collision Angle	Lateral Position	
	Unit	kph	kph	deg	mm	
Range	Pedestrian	10 ~ 60	0	20 ~ 160	-700 ~ 700	225
	Bicyclist	10 ~ 60	3 ~ 23	0 ~ 180	-650 ~ 1850	700
	Motorcyclist	10 ~ 60	10 ~ 60	90	-440 ~ 1660	350

RESULT

Vehicle Dynamics Simulation

    <u>**Collision Avoidance Effect of AEB and LDW**</u> A total of 153,000 cases were performed in the vehicle dynamics simulation, replicating the top nine collision scenarios in Japan. Without AEB or LDW, collision occurred in 117,031 out of 153,000 cases. With AEB or LDW, collision occurred in 48,030 cases. The reduction by AEB/LDW was calculated as 59.0 %. The benefit of AEB/LDW in collision avoidance was estimated as 29.9 % (Table 4). The contribution of AEB and LDW was 28.8 % and 1.1 %, respectively.

Table 4.
Benefit of AEB/LDW in collision avoidance.

No.	ADAS	Collision Scenario	Percentage of Collision in the Field	Number of Collision (ADAS inactivated)	Number of Collision (ADAS activated)	Collision Avoidance Effect	Benefit of AEB/LDW in Collision Avoidance
(i)	AEB	Pedestrian Crossing	6.2%	3,054	491	83.9 %	28.8%
(ii)		Bicyclist Crossing	24.5%	4,108	605	85.3 %	
(iii)		Motorcyclist Crossing		7,869	6,011	23.6 %	
(iv)		Pedestrian in Right-Turn	12.7%	17,000	4,265	74.9 %	
(v)		Bicyclist in Right-Turn		17,000	1,353	92.0 %	
(vi)		Pedestrian in Left-Turn		17,000	7,273	57.2 %	
(vii)		Bicyclist in Left-Turn		17,000	32	99.8 %	
(viii)	LDW	Single-Vehicle Collision	2.7%	17,000	13,390	21.2 %	1.1 %
(ix)		Head-on Collision with Vehicle	3.5%	17,000	14,610	14.1 %	
Total			-	117,031	48,030	59.0 %	29.9 %

Pedestrian Crossing In scenario (i), pedestrians crossing, collisions occurred in 3,054 out of 17,000 cases without AEB, while 491 cases were with AEB. The reduction of collision cases by AEB was 83.9 %. Figure 7 shows the time history curve of the vehicle speed for one of the non-collision cases with AEB (vehicle speed 54.2 kph, crossing angle 0 deg, pedestrian speed 1.3 kph). Figure 8 shows the vehicle behavior in the same case. Without AEB, the driver applied the brake at 0.6 seconds after recognizing the pedestrian who suddenly appeared. The 0.6 seconds corresponds to the time needed for the driver to make a decision and step on the brake pedal. In this case, the vehicle did not stop in front of the pedestrian. The vehicle speed was 41.9 kph at the time of collision. With AEB, the brake was activated immediately after the sensor detected the pedestrian. In that case, the vehicle stopped in front of the pedestrian. Figure 9 shows the frequency distribution of vehicle speed reduction in the 3,054 cases with and without AEB. The average speed reduction with AEB was 48.4 kph, which was 6.2 kph greater than that without AEB.
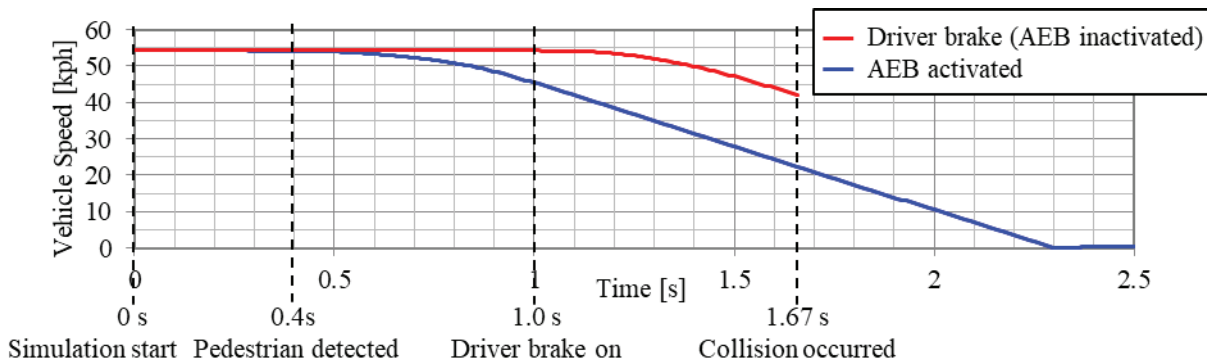

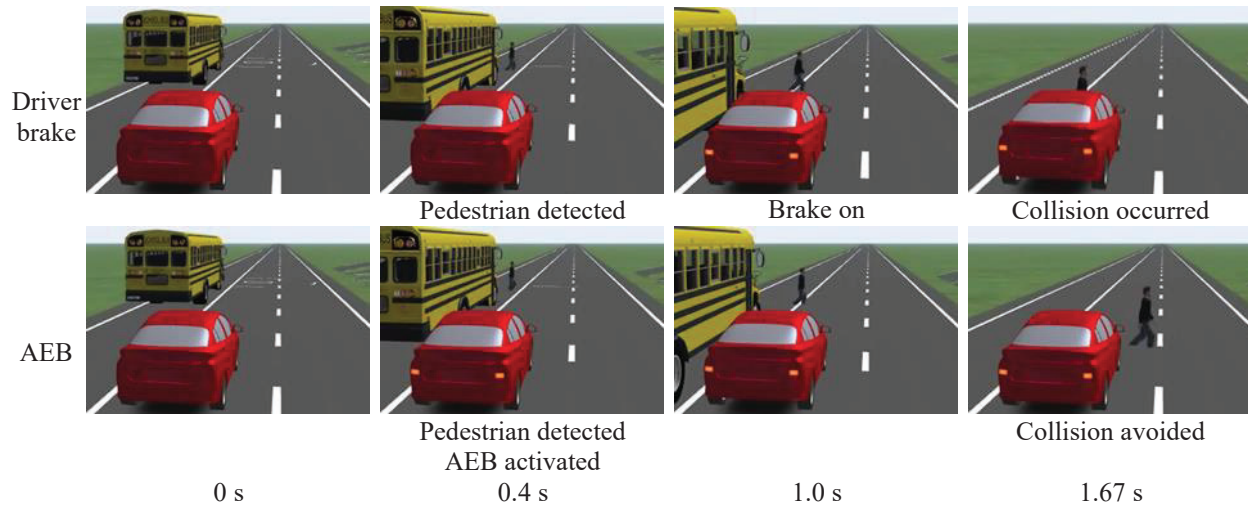*Figure 7. Time history curves of vehicle speed.*

	0 s	0.4 s	1.0 s	1.67 s
Driver brake		Pedestrian detected	Brake on	Collision occurred
AEB		Pedestrian detected AEB activated		Collision avoided

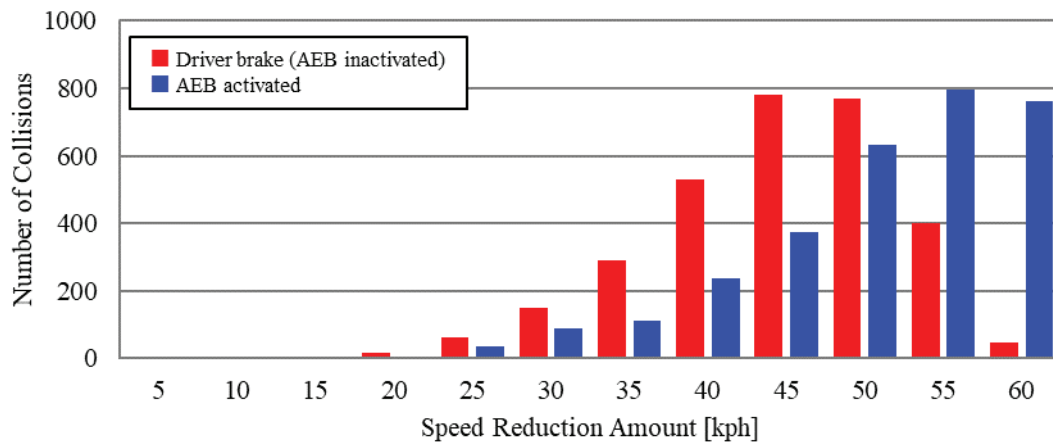*Figure 8. Vehicle behaviors.*

Figure 9. Frequency distribution of vehicle speed reduction.

Bicyclist/Motorcyclist Crossing In scenario (ii), bicyclist collision at the intersection, collisions occurred in 4,108 out of 17,000 cases without AEB, while 605 cases with AEB. The collision reduction rate by AEB was calculated as 85.3 %. In scenario (iii), motorcyclist collision at the intersection, collisions occurred in 7,869 out of 17,000 cases without AEB, while 6,011 cases with AEB. The collision reduction rate by AEB was calculated as 23.6 %. Figure 10 shows the time history curve of the vehicle speed in one of the non-collision cases with AEB (vehicle speed 59.9 kph, bicycle speed 15.3 kph). Figure 11 shows the vehicle behavior in the same case. Without AEB, the driver applied the brakes at 0.8 seconds after recognizing the bicycle suddenly appeared in the intersection. In this case, the vehicle did not stop in front of the bicycle. The vehicle speed was 39.8 kph at the time of collision. With AEB, the system activated the brake immediately after the sensor detected the bicycle. In that case, the vehicle stopped in front of the bicycle. Without AEB, collision occurred in 4,108 cases in scenario (ii), and 7,869 cases in scenario (iii). Figure 12 shows the frequency distribution of vehicle speed reduction in the collision cases with bicycle or motorcycle. In scenario (ii), the average speed reduction with AEB was 44.5 kph. It was greater than that without AEB by 6.8 km/h. In scenario (iii), the average speed reduction with AEB was 35.2 kph, which was 2.4 km/h greater than that without AEB.
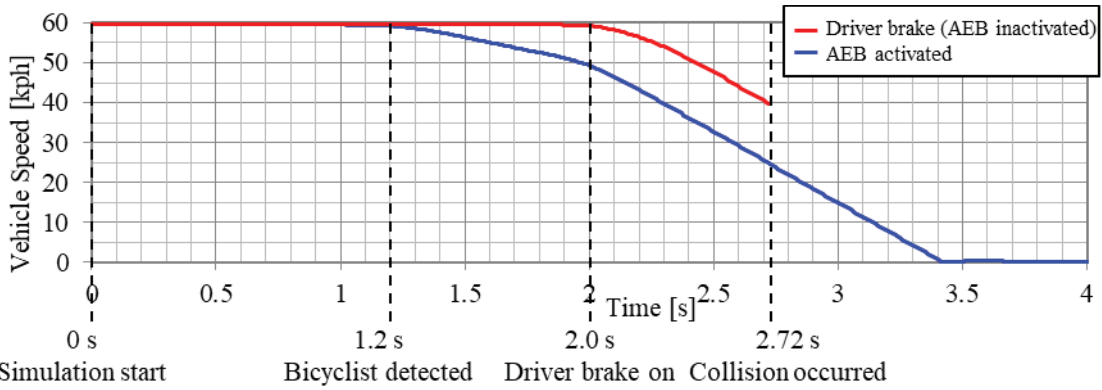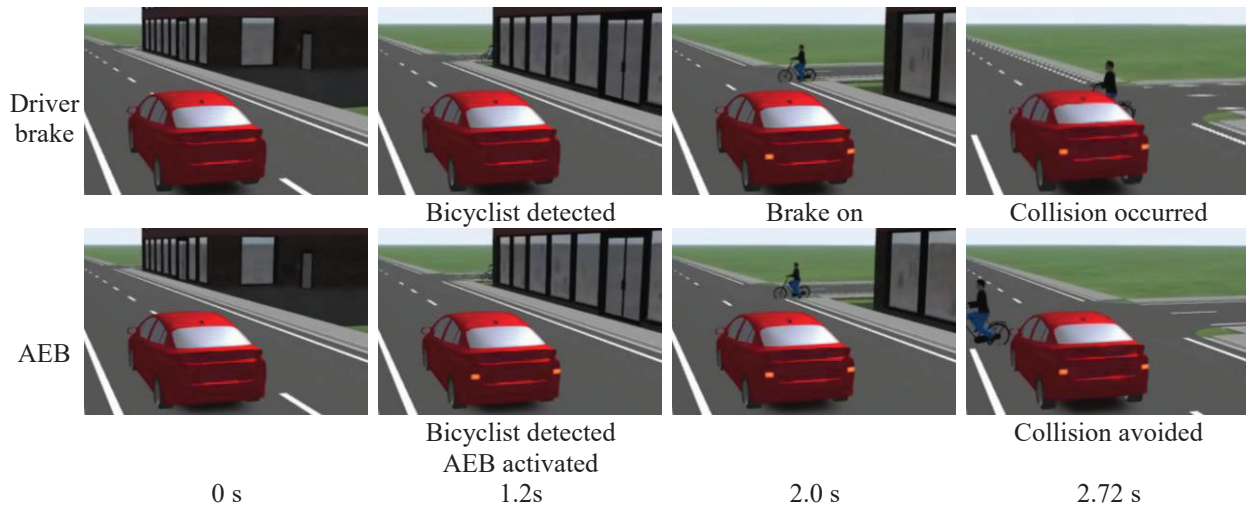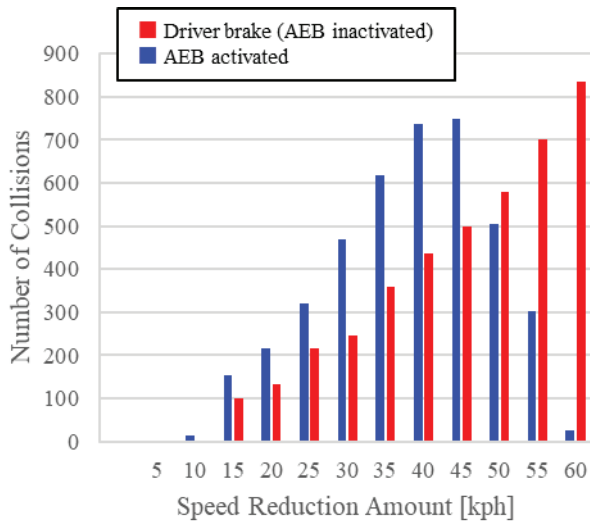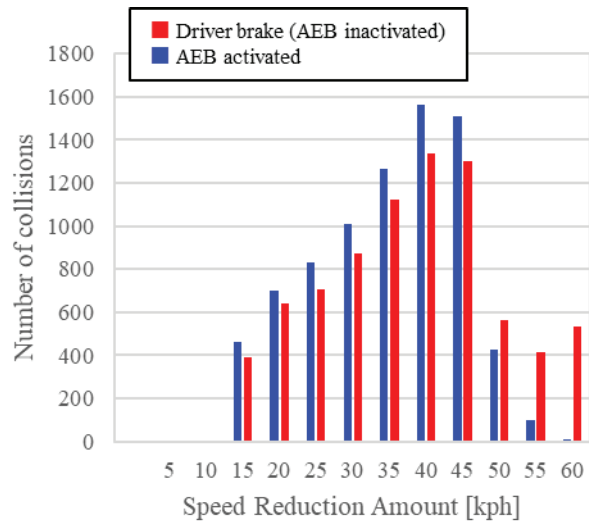
Figure 10. Time history curves of vehicle speed.

Figure 11. Vehicle behaviors.

(a) Scenario(ii) Bicycle crossing *(b) Scenario(iii) Motorcycle crossing*

Figure 12. *Frequency distribution of vehicle speed reduction.*

Pedestrian/Bicyclist in Turning In scenario (iv)-(vii), collisions with pedestrians and bicyclists when the vehicle is turning right or left at an intersection, it was assumed that the driver missed the pedestrian or the bicyclist and did not apply the brake. Without AEB, collisions occurred in all 17,000 cases. With AEB, collisions occurred in 4,265 out of 17,000 cases in scenario (iv), 1,353 cases in scenario (v), 7,273 cases in scenario (vi), and 32 cases in scenario (vii). The collision avoidance effect by AEB was 74.9 % in scenario (iv), 92.0 % in scenario (v), 57.2 % in scenario (vi), and 99.8 % in scenario (vii). Figure 13 shows the time history curve of the vehicle speed in one of the non-collision cases with AEB (scenario (iv), vehicle speed 19.6 kph, pedestrian speed 1.3 kph). Figure 14 shows the vehicle behavior in the same case. Without AEB, the vehicle continued turning right despite the presence of pedestrian. A collision occurred in this case. With AEB, the sensor detected the pedestrian during the right turn and the system stopped the vehicle in front of the pedestrian. Figure 15 shows the frequency distribution of the vehicle speed reduction in the collision cases with AEB. The average reduction in speed was 12.9 kph in scenario (iv), 16.2 kph in scenario (v), 15.9 kph in scenario (vi), and 15.3 kph in scenario (vii) with AEB activated. Table 5 compares the collision avoidance effects between the moving directions. When pedestrians or bicyclists moved in the same direction of the vehicle, the collision avoidance effects were 49.8 % in scenario (iv), 84.1 % in scenario (v), 19.2 % in scenario (vi), and 99.6 % in scenario (vii). When moving in the opposite direction of the vehicle, the collision avoidance effects were 100 % in scenario (iv), (v), and (vii) and 97.3 % in scenario (vi).
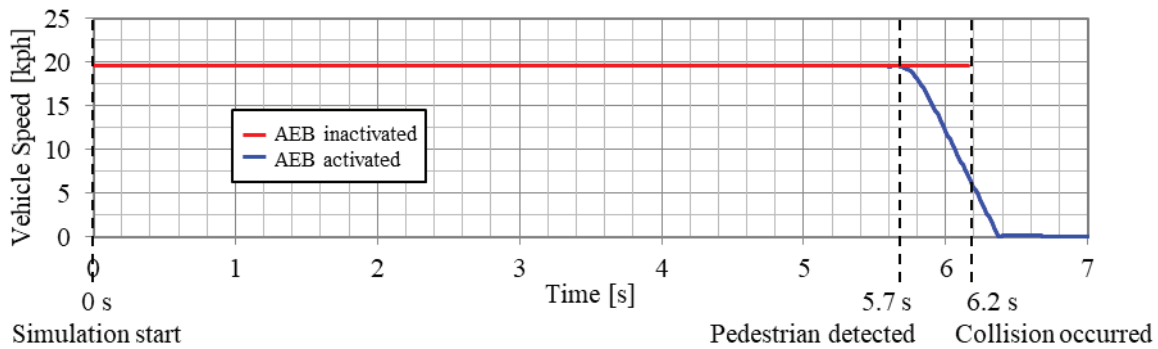

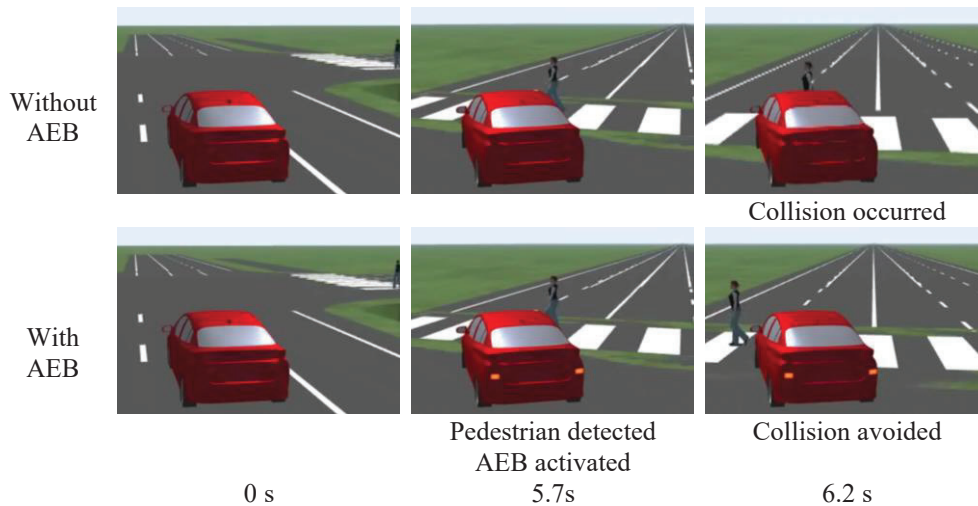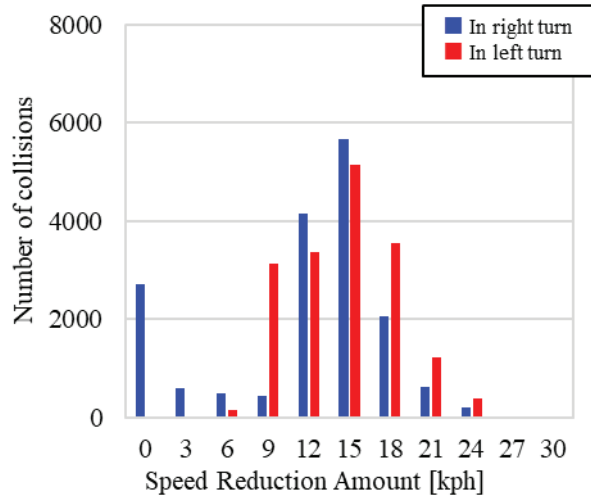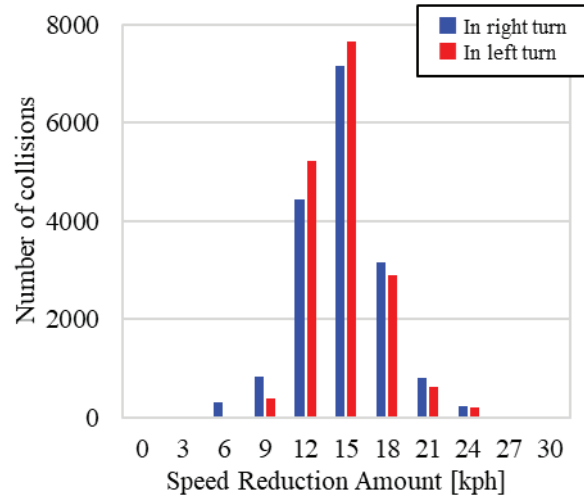*Figure 13. Time history curves of vehicle speed.*

Figure 14. Vehicle behaviors.

(a) Scenario(iv), (vi) Pedestrian in right/left turn   (b) Scenario(v), (vii): Biyclist in right/left turn

Figure 15. Frequency distribution of vehicle speed reduction.

Table 5.
Reduction rates in collisions where the pedestrian/bicyclist coming from same/opposite direction while the vehicle is turning.

Scenario	ADAS	Collision Scenario	Direction	Number of Collision (ADAS inactivated)	Number of Collision (ADAS activated)	Collision Avoidance Effect
(iv)	AEB	Pedestrian in Right-Turn	Same	8,500	4,265	49.8 %
			Opposite	8,500	0	100 %
(v)		Bicyclist in Right-Turn	Same	8,500	1,353	84.1 %
			Opposite	8,500	0	100 %
(vi)		Pedestrian in Left-Turn	Same	8,500	7,051	19.2 %
			Opposite	8,500	222	97.3 %
(vii)		Bicyclist in Left-Turn	Same	8,500	32	99.6 %
			Opposite	8,500	0	100 %

Lane Departure In scenario (viii), (ix), lane departure and collision with a fixed obstacle (single vehicle collision) or an oncoming vehicle (head-on collision), it was assumed that the driver did not control the steering without recognizing the risk. Without LDW, collisions occurred in all 17,000 cases. With LDW, collisions occurred in 13,390 out of the 17,000 cases in scenario (viii) and 14,610 cases in scenario (ix). The collision avoidance effect by LDW was 21.2 % for single vehicle collisions and 14.1 % for head-on collisions. Figure 16 shows the time history curve of the steering angle in one of the non-collision cases with LDW (scenario (viii), vehicle speed 56.6 kph, curve radius 450 m). Figure 17 shows the vehicle behavior in the same case. Without LDW, the vehicle deviates from the lane and collided with the guardrail. With LDW, the driver controlled the steering at 0.7 s after the warning. The delay time represented the driver's reaction time. The vehicle returned to the lane before colliding with the guardrail. Figure 19 shows the relationship between collision avoidance effect and vehicle departure speed/angle. The collision avoidance effect ranged from 10 to 30 % for all speed ranges. As for the departure angle, the collision avoidance effect

ranged from 26 to 50 % when the angle was less than 5 degrees. The collision avoidance effect was lower than 14 % when the angle was 5 degrees or greater.
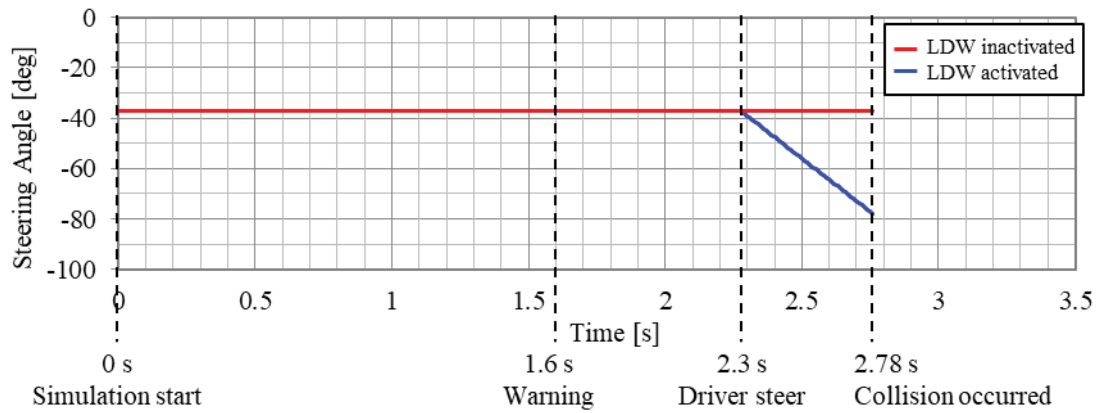

Figure 16. Time history curves of steering angle.
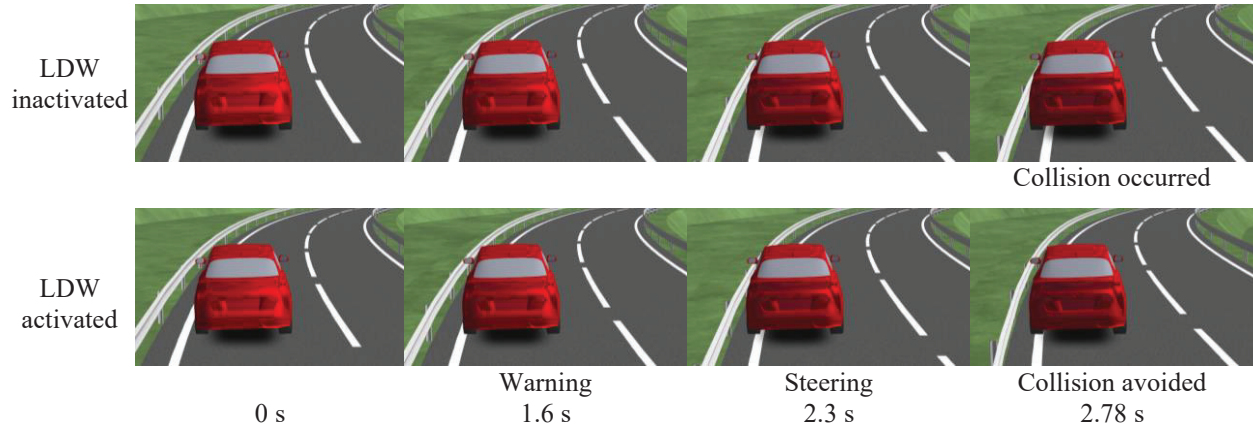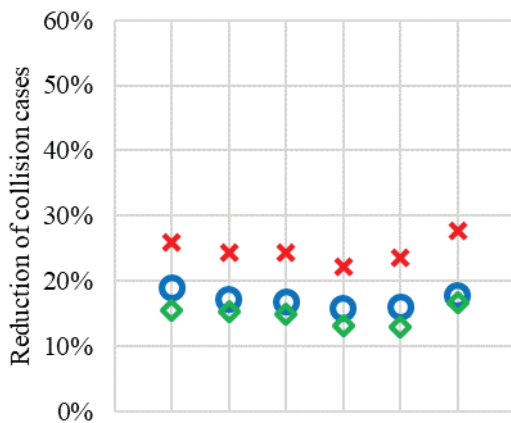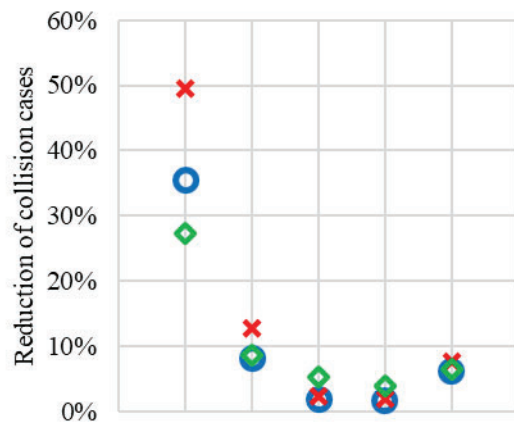

Figure 17. Vehicle behaviors.

Relationship between collision avoidance effect and vehicle departure speed

Relationship between collision avoidance effect and vehicle departure angle

Figure 18. Reduction of collision cases.

Crash Simulations

Kinematics and Head Impact Response Crash simulations were conducted using THUMS and the vehicle model in order to generate a ROM for rapid injury prediction. The paper focuses on the case where the vehicle speed was 60 kph, the collision angle was 90deg, and the head contact position was 600 mm from the vehicle center in the width direction. Figure 19 shows the whole-body behavior of the pedestrian during the collision. Figure 20 shows the time history curve of the head acceleration. The upper body rotated after the lower limbs contacted the bumper and the pelvis contacted the hood. The shoulder contacted the rear end of the hood. Approximately 110 ms after the start of the collision, the head contacted the A-pillar. The head displacement was 40 mm in the vehicle width direction. The head acceleration reached the maximum peak (241 G) when contacting with the A-pillar. The HIC_{15} value was calculated as 1,522. Figure 21 shows the whole-body behavior of the bicyclist traveling at 23 kph. Figure 22 shows the time history curve of the head acceleration. Initially, the lower limbs contacted the bumper. The upper body rotated after the pelvis contacted the hood. Then, the shoulder contacted the windshield glass (W/S). Approximately 130 ms after the start of the collision, the head contacted the roof. The head displacement was 730 mm in the vehicle width direction. The head acceleration reached the maximum peak (94G) at the timing when contacting the roof. The HIC_{15} value was calculated as 640. Figure 23 shows the whole-body behavior of the motorcyclist when colliding with the vehicle traveling at a speed of 40 kph. Figure 24 shows the time history curve of the head acceleration. Initially, the lower limbs and the motorcycle body contacted the vehicle front, and the hood was deformed. The upper body rotated after the pelvis contacted the hood. After that, the shoulder contacted the W/S. The head contacted the A-pillar at about 140 ms from the start of the collision. The head displacement was 1,285 mm in the vehicle width direction. The head acceleration reached the maximum peak (188 G) at the timing when contacting the A-pillar. The HIC_{15} value was calculated as 1,573.
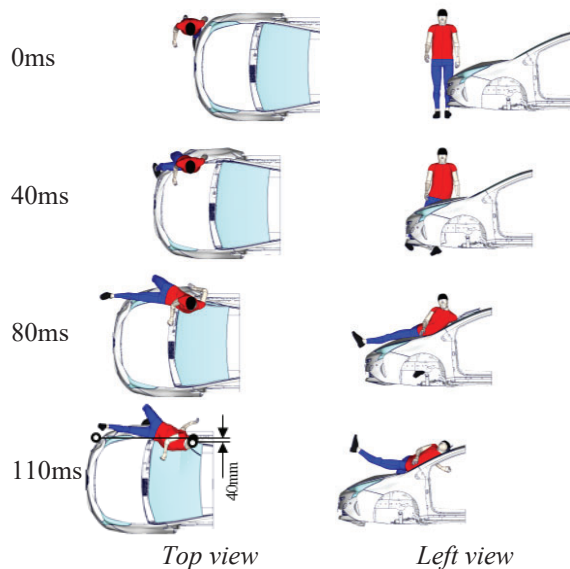
Top view   Left view
Figure 19. Whole-body behavior.
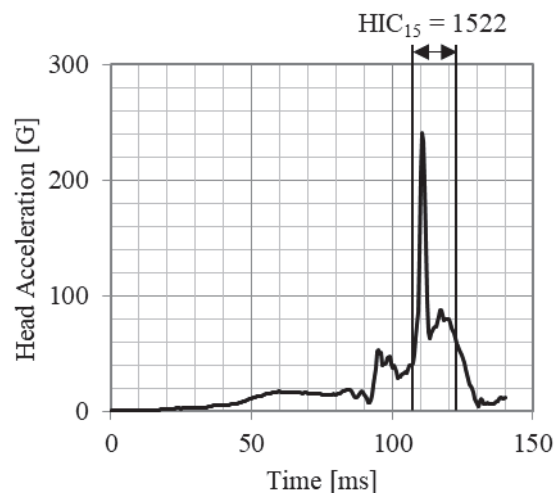
Figure 20. Time history curve of acceleration of pedestrian's head.

0ms
40ms
80ms
110ms
730mm

Top View   *Left View*
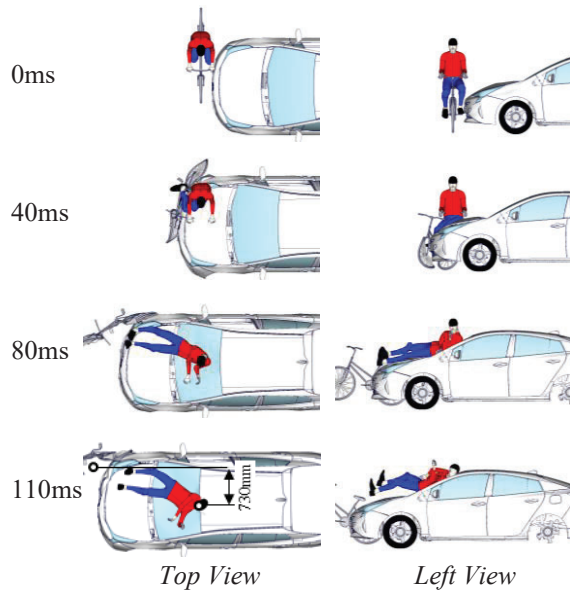
Figure 21. Whole-body behavior.
(Bicycle speed = 23 kph)

$HIC_{15} = 640$

Head Acceleration [G]

Time [ms]
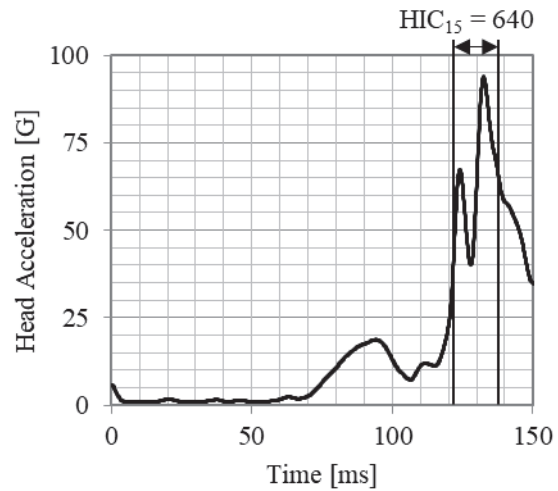
Figure 22. Time history curve of acceleration of bicyclist's head.

0ms
40ms
80ms
110ms
1285mm

Top View   *Left View*
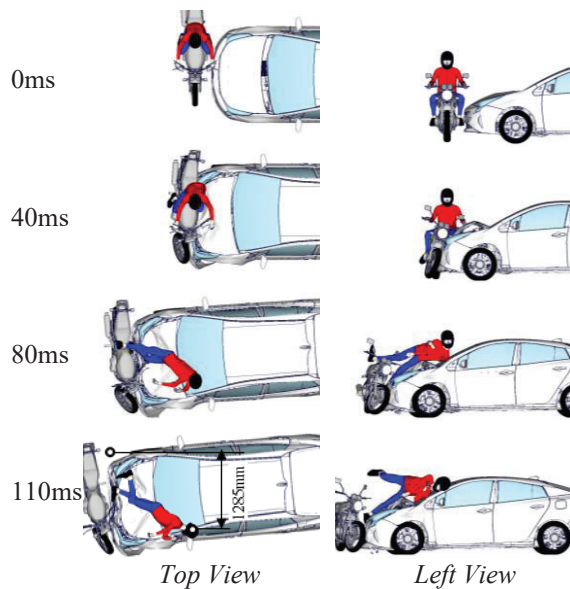
Figure 23. Whole-body behavior.
(Motorcycle speed = 40 kph)

$HIC_{15} = 1573$

Head Acceleration [G]

Time [ms]
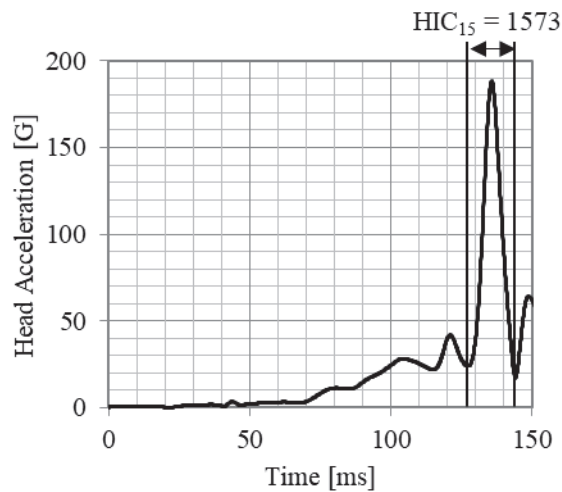
Figure 24. Time history curve of acceleration of motorcyclist's head.

Head Impact Conditions Figure 25 shows the distribution of HIC_{15} (over 700/not over 700) for the pedestrians, bicyclists, and motorcyclists in relation to the head contact points on the vehicle. In the pedestrian cases, the head contact points distributed above the W/S. The points with the HIC_{15} values over 700 were found near the A pillar. In the bicyclist cases, the head contact points distributed on the hood, W/S, and roof. The points with the HIC_{15} values over 700 appeared near the A-pillar and the roof header. In the motorcyclist cases, the head contact points distributed from the hood to the W/S. The points with the HIC_{15} values over 700 were mostly observed near the A pillar.

(a) Pedestrian   *(b) Bicyclist*   *(c) Motorcyclist*
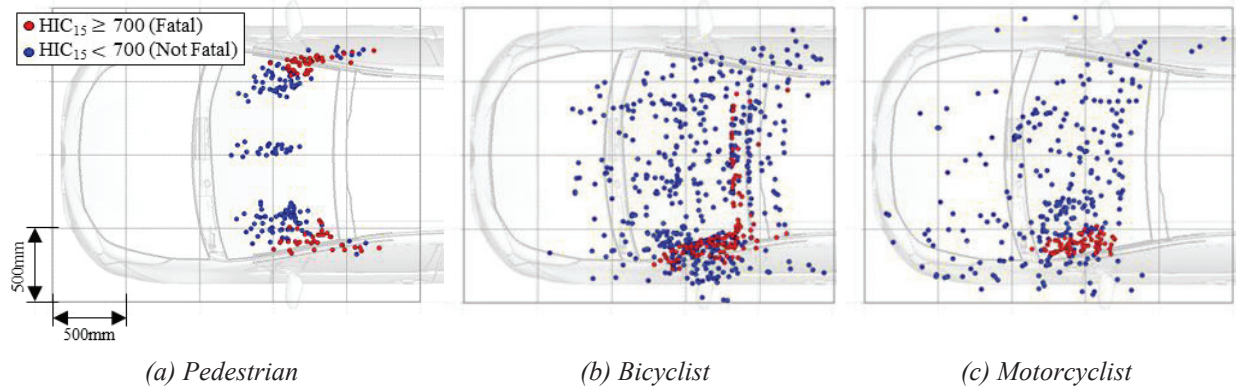
Figure 25. Distributions of HIC₁₅ value.

 Reduced Order Model The collision parameters and the resultant HIC_{15} values were stored in the database. A ROM was generated to predict HIC_{15} values from the given collision conditions. A neural network was used to generate the ROM. The prediction accuracy of the generated ROM was verified by the leave-one-out cross-validation test. Figure 26 shows the validation results. The vertical axis is the predicted value by the ROM, and the horizontal axis is the HIC_{15} (true value) calculated by THUMS. The area under the curve (AUC) of the receiver operating characteristic (ROC) curve, a binary classification, was used as the evaluation index [16]. The ROMs generated for pedestrians, bicyclists, and motorcyclists were validated through the validation process described above. The AUC values were about 0.9 for all cases. Based on the results, it was confirmed that the generated ROMs had sufficient prediction accuracy.

| AUC | 0.89 | 0.93 | 0.99 |

(a) Pedestrian   *(b) Bicyclist*   *(c) Motorcyclist*
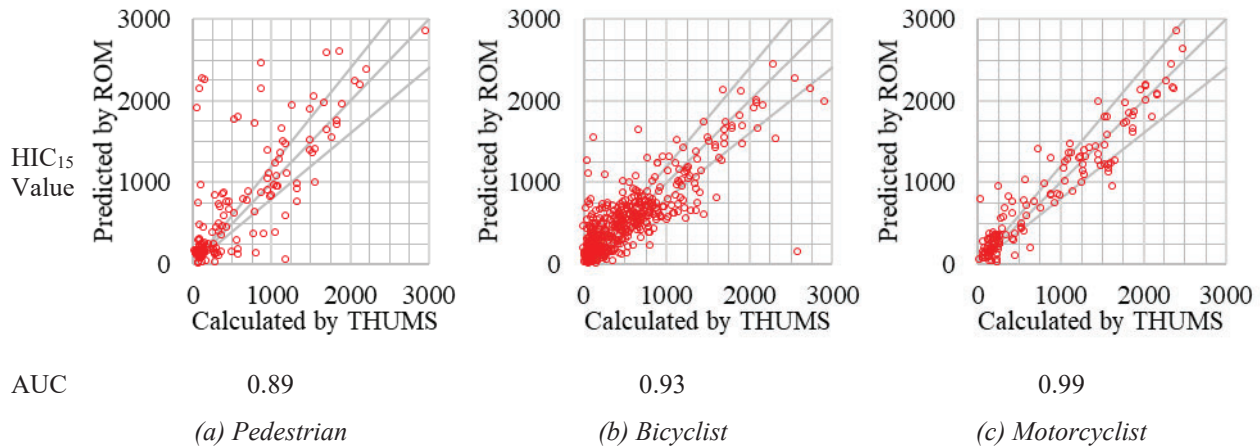
Figure 26. Validations HIC₁₅ value.

 Injury Mitigation Effect of AEB The HIC_{15} values were predicted by ROM for the collision cases in vehicle dynamics simulations. Without AEB, fatal injuries were predicted in 415 out of 117,031 cases. With AEB, fatal injuries were predicted in 76 out of 48,030 cases. Based on these numbers, the injury mitigation effect of AEB was estimated to be 81.7 %. The benefit of AEB in injury mitigation in Japan, was estimated as 52.5 % (Table 6)

Table 6.
Benefit of AEB in injury mitigation.

No.	ADAS	Collision Scenario	Percentage of Fatalities in the Field	Number of Fatalities (ADAS inactivated)	Number of Fatalities (ADAS activated)	Injury Mitigation Effect	Benefit of AEB in Injury Mitigation
(i)	AEB	Pedestrian Crossing	40.2 %	123	5	95.9 %	52.5 %
(ii)		Bicyclist Crossing	6.7 %	142	0	100 %	
(iii)		Motorcyclist Crossing	3.9 %	122	71	42.0 %	
(iv)		Pedestrian in Right-Turn	1.9 %	10	0	100 %	
(v)		Bicyclist in Right-Turn		0	0	100 %	
(vi)		Pedestrian in Left-Turn	1.0 %	18	0	100 %	
(vii)		Bicyclist in Left-Turn		0	0	100 %	
(viii)	LDW	Single-Vehicle Collision	-	-	-	-	-
(ix)		Head-on Collision with Vehicle	-	-	-	-	
Total			-	415	76	81.7 %	52.5 %

Pedestrian Crossing Without AEB in scenario (i) of pedestrian crossing, fatal injuries were predicted in 123 out of 3,054 cases. With AEB, fatal injuries were predicted in 5 out of 491 cases. Based on these numbers, the injury mitigation effect by AEB was estimated as 95.9 %. Figure 27 shows the distribution of HIC_{15} (over 700/under 700) predicted by ROM in relation to the head contact point on the vehicle. The contact points were distributed from the A-pillar to the W/S. The points with the HIC_{15} values over 700 appeared near the A pillar.

(a) Driver brake (without AEB)   *(b) With AEB*
Figure 27. Distribution of HIC_{15} value.

Bicyclist/Motorcyclist Crossing Without AEB in scenario (ii) of bicycle collision at the intersection, fatal injuries were predicted in 142 out of 4,108 case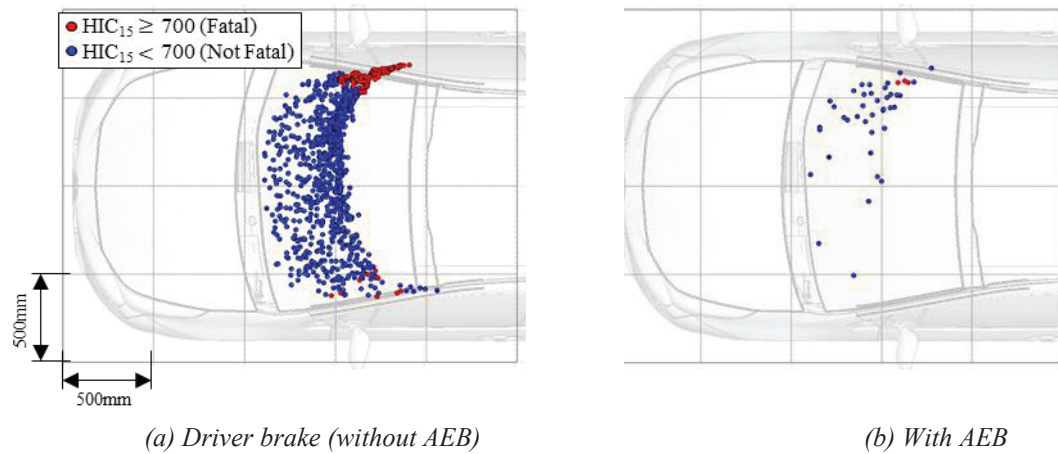s. With AEB, fatal injuries were not predicted. Based on these numbers, the injury mitigation effect by AEB was estimated as 100 %. Figure 28 shows the distribution of HIC_{15} values (over 700/under 700) predicted by ROM in relation to the head contact points on the vehicle. The contact points distributed from the hood, W/S, and roof header. The contact points with the HIC_{15} values over 700 mostly appeared near the A pillar and roof header. With AEB, the head did not contact the A-pillar or roof header. Without AEB in scenario (iii) of motorcycle collision at the intersection, fatal injuries were predicted in 122 out of 7,869 cases. With AEB, fatal injuries were predicted in 71 out of 6,011 cases. Based on these numbers, the injury mitigation effect by the AEB was estimated to be 42.0 %. Figure 29 shows the distribution of the HIC_{15} values (over 700/under 700) predicted by ROM in relation to the head contact points on the vehicle. The head contact points distributed from the hood to the W/S. The points with the HIC_{15} values over 700 appeared near the A pillar.

| (a) Driver brake (without AEB) | (b) With AEB |
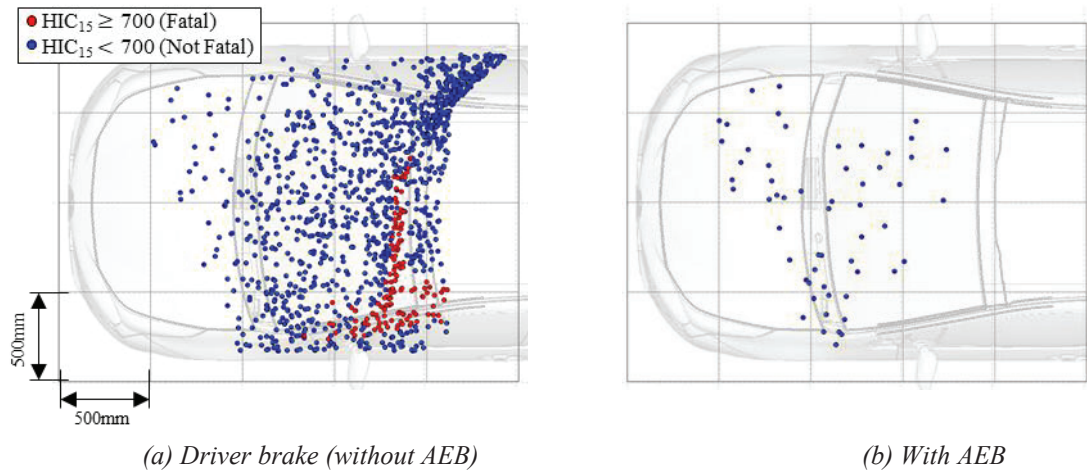
Figure 28. Distribution of HIC₁₅ value. (Scenario (ii): Bicyclist)

| (a) Driver brake (without AEB) | (b) With AEB |
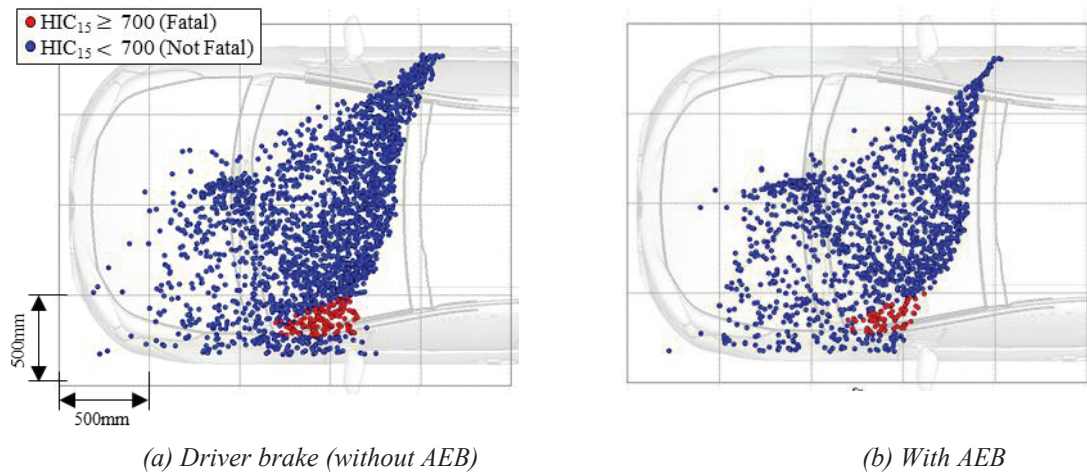
Figure 29. Distribution of HIC₁₅ value. (Scenario (iii): Motorcyclist)

Pedestrian/Bicyclist in Turning In scenario (iv) and (vi), pedestrian collision in turning right/left at the intersection without AEB, fatal injuries were predicted in 10 out of 17,000 cases in the right-turn scenarios (iv) and 18 out of 17,000 cases in the left-turn scenarios (vi). With AEB, fatal injuries were not predicted. Figures 30 and 31 show the distribution of the HIC_{15} values (over 700/under 700) predicted by ROM in relation to the head contact points on the vehicle. The head contact points distributed from the A pillar to W/S. The points with the HIC_{15} values over 700 mostly appeared near the A pillar. In scenario (v) and (vii), bicyclist collision in turning right/left at the intersection

without AEB, fatal injuries were not predicted. Figures 32 and 33 show the distribution of the HIC_{15} values (over 700/under 700) predicted by ROM in relation to the head contact points on the vehicle. Without AEB, the head contact points distributed from the hood and W/S. With AEB the bicyclist head did not contact the vehicle.
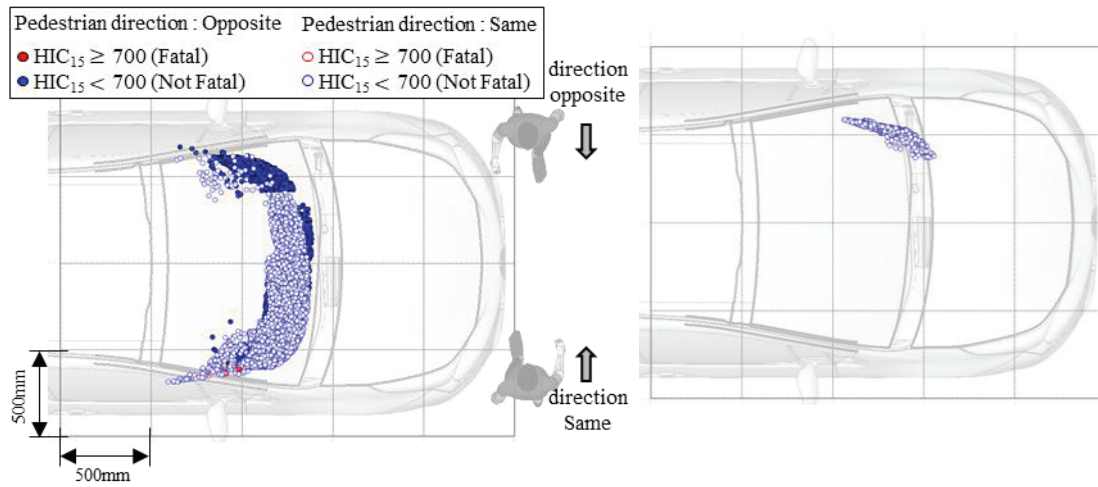
(a) Without AEB   (b) With AEB

Figure 30. Distribution of HIC_{15} value. (Scenario (iv): Pedestrian in right turn)
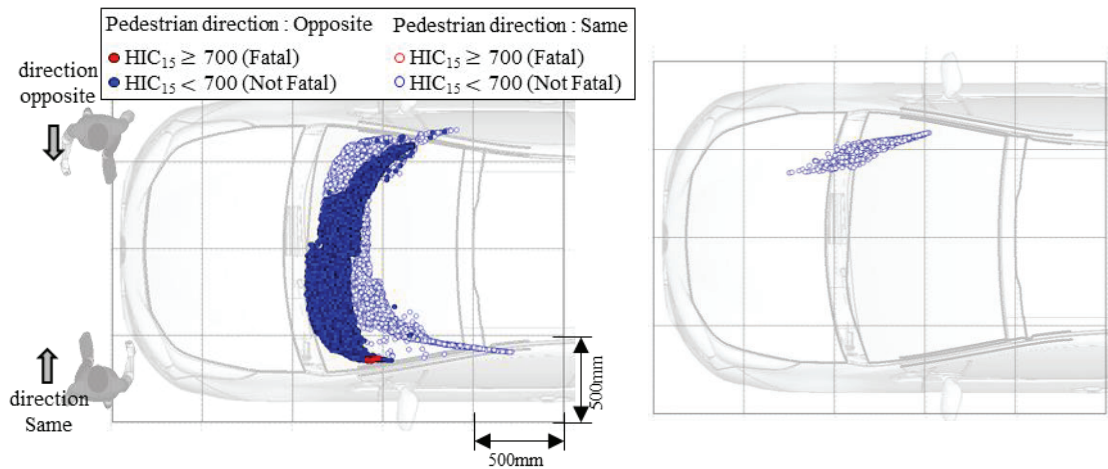
(a) Without AEB   (b) With AEB

Figure 31. Distribution of HIC_{15} value. (Scenario (vi): Pedestrian in left turn)

(a) Without AEB   *(b) With AEB*
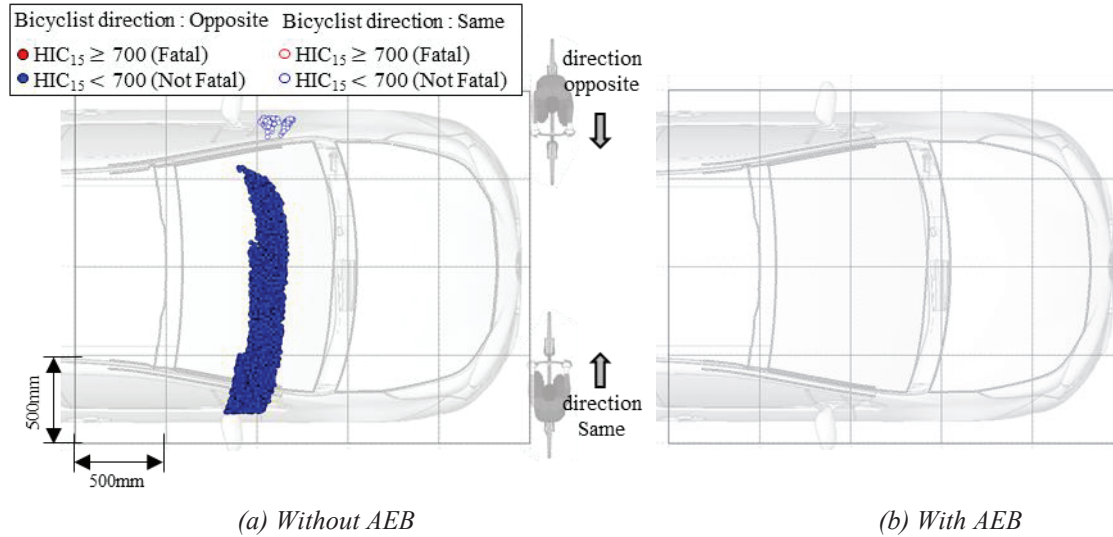
Figure 32. Distribution of HIC$_{15}$ value. (Scenario (v): Bicyclist in right turn)

(a) Without AEB   *(b) With AEB*
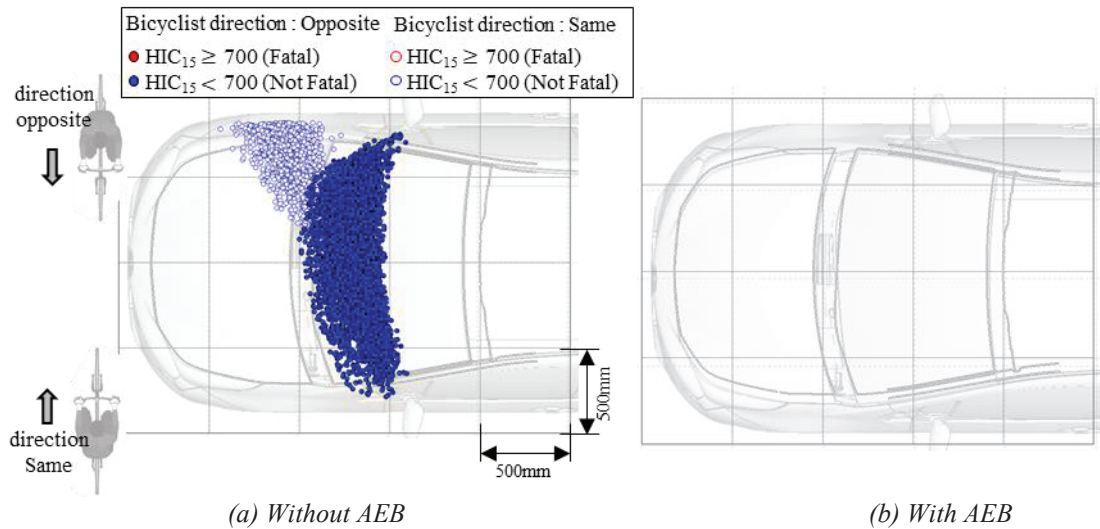
Figure 33. Distribution of HIC15 value. (Scenario (vii): Bicyclist in left turn)

DISCUSSION

The effectiveness of AEB/LDW was analyzed for the nine scenarios assumed in this study. In scenario (i) of pedestrian crossing, the collisions were avoided by the AEB in many cases and the number of fatal injuries was lower than the cases without AEB where the driver applied brake. Comparing the results of scenario (ii) and (iii), collisions with bicyclist and motorcyclist at the intersection, the collision avoidance effect by AEB was higher in the bicyclist cases than in the motorcyclist cases. In scenario (iv)-(vii), collisions with pedestrians and bicyclist while the vehicle was turning right or left at the intersection, the collision avoidance effect was higher when the pedestrian or bicyclist moved in the opposite direction of the vehicle than when they moved in the same direction. In scenario (viii) and (ix) of lane departure, the collision avoidance effect by LDW was higher in the cases against a fixed obstacle than those colliding with an oncoming car.

Pedestrian Crossing
In scenario (i) of pedestrian crossing, the collision avoidance effect by AEB was estimated to be 83.9 % and the injury mitigation effect was estimated to be 95.9 %. The study assumed the situation that a pedestrian appeared from the

blind spots of a parked vehicle. There was no significant difference in TTC at detection between AEB and the human driver (Figure 34). With AEB, the average stopping distance was shorter than that without AEB (human driver) by 4.9 m. The reduction in stopping distance contributed to the collision avoidance (Figure 35). In collision cases with AEB, the average collision speed was lower than that without AEB by 6.7 kph. The reduction in collision speed contributed to injury mitigation (Figure 36).
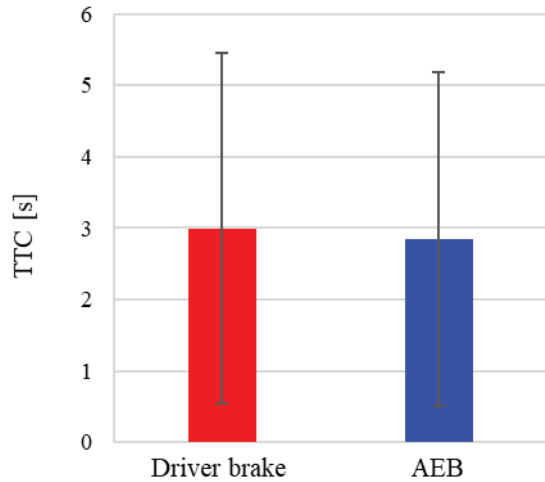
Figure 34. TTC by driver's braking and AEB.
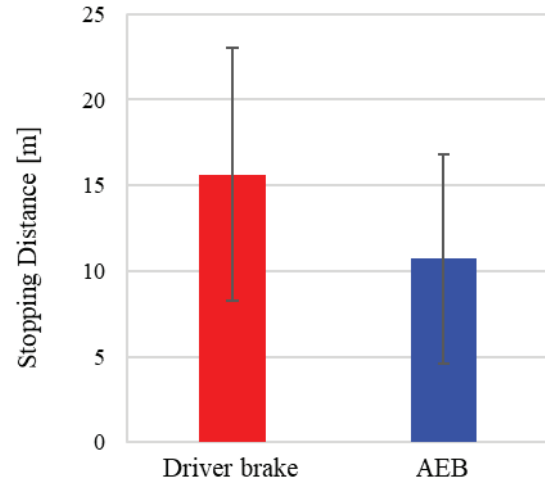
Figure 35. Stopping distance by driver's braking and AEB.
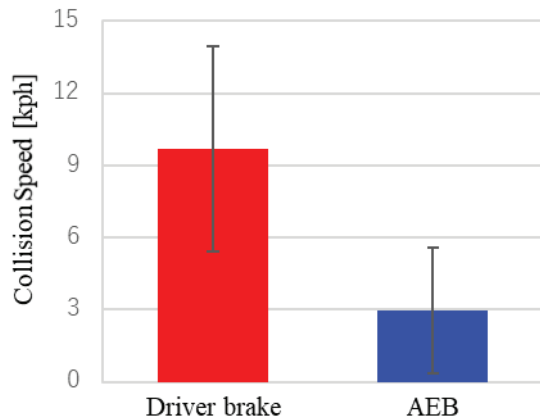
Figure 36. Collision speed.

Bicyclist/Motorcyclist Crossing

In scenarios (ii) and (iii), collisions with bicyclist and motorcyclist at the intersection, the collision avoidance effect by AEB was higher for bicyclist than for motorcyclist. Without AEB, the reduction in vehicle speed was 9.3 km/h greater (on an average) in collisions with bicyclist than those with motorcyclist. The speed of bicyclist was lower than the motorcyclist. The TTC values at detection were generally longer for bicyclists than those of motorcyclist. The longer TTC contributed to the collision avoidance (Figure 37).
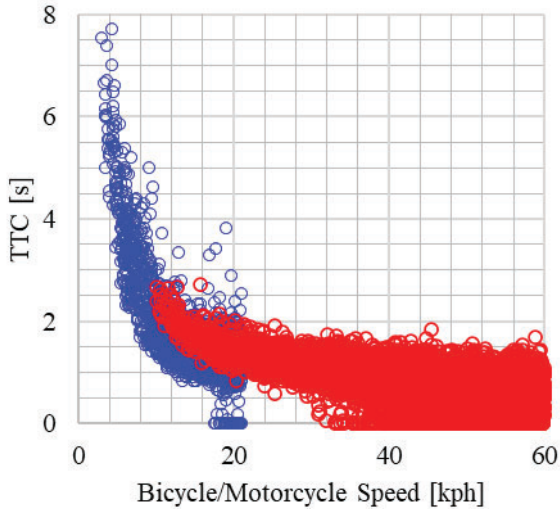
Figure 37. Distribution of TTC.

Pedestrian/Bicyclist in Turning

In scenario (iv)-(vii), collisions with pedestrians or bicyclists during right or left turn at the intersection, the collision avoidance effect when the pedestrian or bicyclist moved in the opposite direction of the vehicle was higher than that in the same direction. The pedestrians approaching from the opposite direction were detected early as they entered the field of view. Pedestrians moving in the same direction were not detected early as they stayed diagonally behind the vehicle in the sensor's blind spot for a long time (Figure 38).
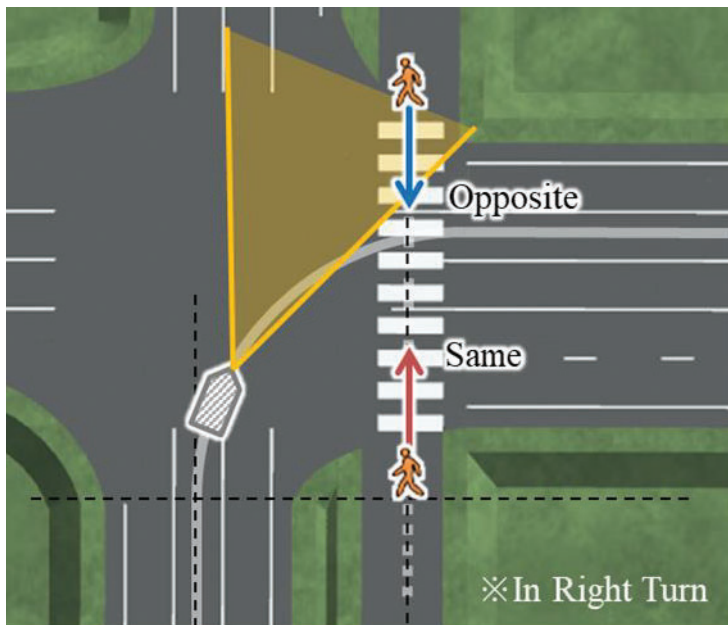
Figure 38. Field of view of a turning vehicle.

Lane Departure

In scenario (viii) and (ix) of lane departure, the collision avoidance effect by LDW was higher in the cases colliding with a fixed obstacle than those with an oncoming car. The collision avoidance effect decreased with the increase of deviation angle (Figure 18). For deviation angles of less than 5 degrees, the collision avoidance effect in the cases colliding with poles was higher than that with the guardrail or oncoming vehicles. The guardrail was a continuous structure along the road and could be a large obstacle for the vehicle. On the other hand, the pole was located at a specific position of the roadside. At the same deviation angle, collision with the guardrail could occur earlier than that

with the pole. This tendency appeared remarkably at small departure angles. The oncoming vehicle approached with speed and the time to avoid the collision was shortened. The time to the collision from the alert was longer in the cases with the pole and contributed to the higher collision avoidance effect (Figure 39).
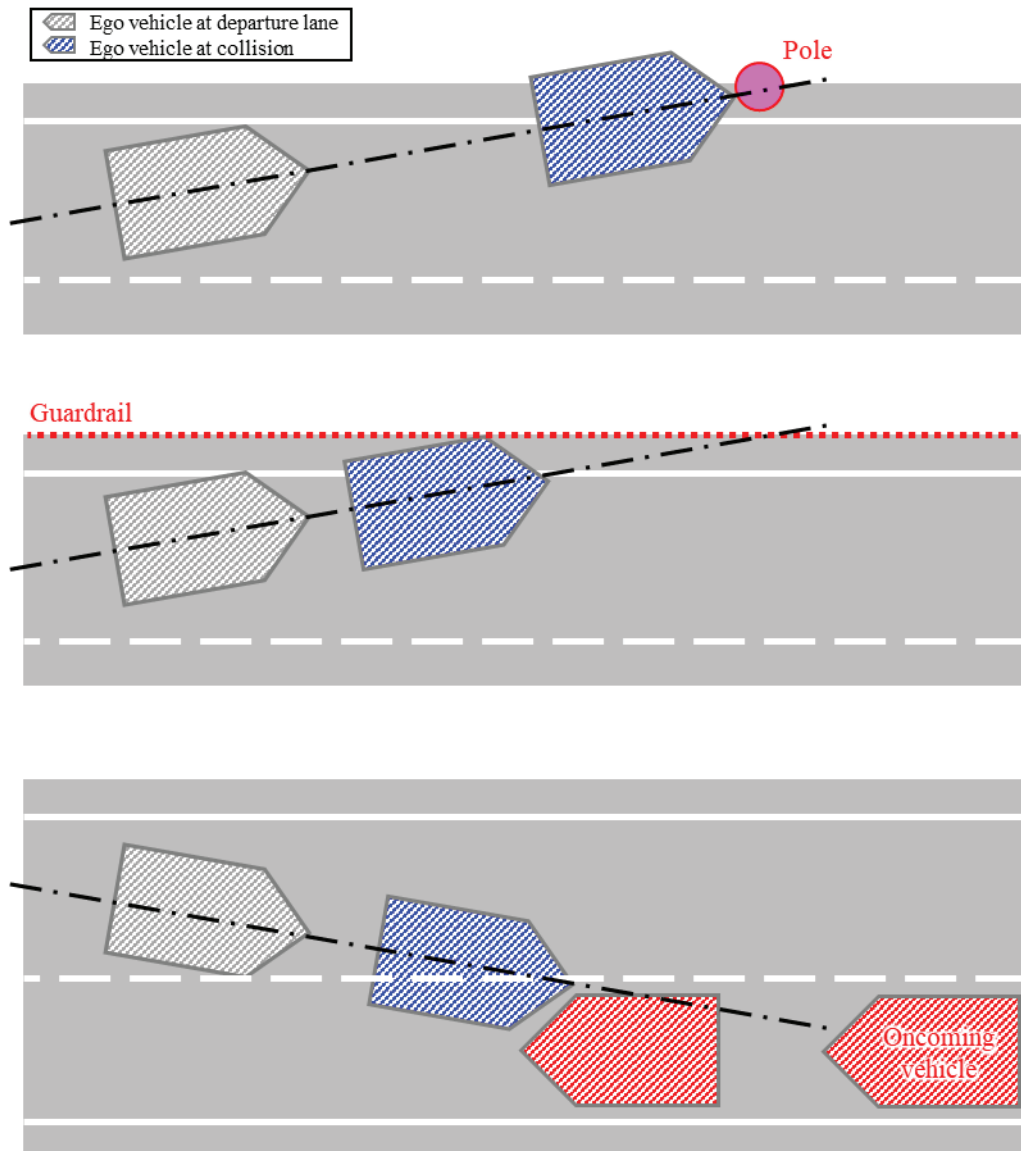
Figure 39. Behaviors of a vehicle deviates from its lane.

LIMITATION

In this study, the effectiveness of AEB/LDW were estimated through the vehicle dynamic simulations and crash simulations. The parameters of simulations varied to widely cover possible situations in the field. However, it did not perfectly cover all actual collision cases. In the simulation model, the sensor properly detected the obstacles and the system immediately activated AEB or LDW at the maximum performance. The real traffic environment has a wide range of variety in brightness, visibility and road surface conditions etc. There were other assumptions such as a midsize sedan for the vehicle type and a midsize adult male person for the occupant. The study used the head injury criterion for the judgement of fatal injury. In collisions with VRU, only collisions with vehicles were counted in the study while there were also road surface collisions in the field. Thus, actual collisions may have much more variety than the range assumed in this study. It is important to consider actual accident data to verify the accuracy of this

method for benefit estimation, and to consider the variation and diversity of factors that have a large impact on prediction accuracy.

CONCLUSION

In this study, a simulation-based method was developed to probabilistically estimate the collision avoidance effect and injury mitigation effect of AEB and LDW assuming various near-miss situations leading to collisions. For the top 9 fatal traffic collision scenarios in Japan, the benefit of AEB and LDW in collision avoidance and injury mitigation was estimated quantitatively using this method.

REFERENCES

[1] Euro NCAP. Apr. 2021. "Euro NCAP AEB VRU Test Protocol v3.0.4." Internet: https://cdn.euroncap.com/media/62795/euro-ncap-aeb-vru-test-protocol-v304.pdf, Date Updated Nov. 2022

[2] Euro NCAP. July. 2019. "Euro NCAP LSS Test Protocol v3.0.2." Internet: https://cdn.euroncap.com/media/64973/euro-ncap-lss-test-protocol-v302.pdf. Date Updated Nov. 2022

[3] Euro NCAP. Apr. 2021. "Euro NCAP AEB Car-to-Car Test Protocol v3.0.3." Internet: https://cdn.euroncap.com/media/62794/euro-ncap-aeb-c2c-test-protocol-v303.pdf. Date Updated Nov. 2022

[4] Reßle, A., Lienkamp, M., & Fürst, F. 2011. "Method to Estimate the Field Effectiveness of an Automatic Braking System in Combination with an Adaptive Restraint System in Frontal Crashes." Proceedings of the 22nd ESV Conference

[5] Cabinet Office. Mar. 2018. "Research on analysis methods for estimating the effect of reducing traffic accident fatalities and injuries." Cross-ministerial Strategic Innovation Promotion Program

[6] Ministry of Economy, Trade and Industry. Mar. 2019. "Development and demonstration of simulation technology for estimating detailed effects of traffic accident reduction." Cross-ministerial Strategic Innovation Promotion Program

[7] Saito, Y., Inoue, H., & Raksincharoensak, P. 2018. "Safety Cushion: Potential Risk Estimation Based on Driving Context and Driving Behavior State (First Report)." Society of Automotive Engineers of Japan

[8] Yamamoto, A., Owaki, T., & Uesaka, K. 2011. "Analysis of differences in travel speed due to differences in bicycle riding space, etc." Japan Society of Civil Engineers

[9] Institute for Traffic Accident Research and Data Analysis. 2014. "Serious accidents involving four-wheeled vehicles traveling at low speeds when encountering two-wheeled vehicles." ITARDA INFORMATION No. 105

[10] Institute for Traffic Accident Research and Data Analysis. 2017. "Accidents between bicycles and four-wheeled vehicles." ITARDA INFORMATION No. 122

[11] Shikura, K. 2008. "Traffic Accident Case Study Analysis Study Group Analysis Study." Car Seminar, Vol.47, No. 11, 69-85

[12] Iwaki, R., Wakasugi, T., Teraoka, E. Y., Tanaka, S., & Uchida, N. 2013. "Analysis of driver response to road crossing pedestrian." Society of Automotive Engineers of Japan

[13] Iwaki, R., Wakasugi, T., Mochida, T., & Yoshida, S. 2013. "Modelling Lane Return Steering Behaviour When a Lane Departure Warning is Issued." Society of Automotive Engineers of Japan

[14] Yasuki, T., Kitagawa, Y., & Shigeta, K. 2009. "Development of next generation human body FE model capable of organ injury prediction." Proceedings of the 21st ESV Conference

[15] Euro NCAP. Oct. 2018. "Pedestrian Human Model Certification Version 1.1." Internet: https://cdn.euroncap.com/media/41783/tb-024-pedestrian-human-model-certification-v11.201811141155007002.pdf. Date Updated Nov. 2022

[16] Fischer, J. E., Bachmann, L. M., & Jaeschke, R. (2003). "A readers' guide to the interpretation of diagnostic test properties: clinical example of sepsis." Intensive Care Medicine.

EDR REPORTED DRIVER USAGE OF CRASH AVOIDANCE SYSTEMS FOR HONDA VEHICLES

Christopher Wiacek
Lauren Firey
Mark Mynatt
National Highway Traffic Safety Administration
USA

Paper Number 23-0040

ABSTRACT

Starting with the 2016 Model Year, Honda Motor Co. (Honda) began to phase-in vehicles equipped with an Event Data Recorder (EDR) that captures the status and activation of crash avoidance technologies such as forward collision warning/automatic emergency braking and lane departure warning/lane keeping assist. While not defined under the National Highway Traffic Safety Administration's (NHTSA) EDR regulation 49 CFR Part 563, Honda has elected to add these data elements. For this study, Honda EDR data were collected from the NHTSA's 2017 – 2021 Crash Investigation Sampling System (CISS) for vehicles equipped with this recording capability. The data were then assessed to identify the use and activation statuses of these crash avoidance technologies at the time of their respective crash events. If drivers choose to disable these technologies, they will not be afforded the potential collision avoidance and/or severity mitigation benefits of these systems in relevant crashes.

The 150 crash-involved Honda vehicles in this study are equipped with EDRs that captured data elements related to the function and alert status of several crash avoidance systems in the time leading up to the crash event. The results indicate that drivers of Honda vehicles equipped with crash avoidance systems are much more likely to have forward collision warning/automatic emergency braking systems "On" and the lane departure warning/lane keeping assistance systems "Off." Specifically, 99% of drivers for this study had the forward collision warning/automatic emergency braking systems "On" in the time leading up to the crash and thus could be afforded the potential benefits of these systems if they were involved in a system relevant crash situation. With respect to lane departure warning/lane keeping assistance, 49% of the drivers had these systems "Off" at the time of the crash, and therefore were not afforded the potential benefits of these systems during an appropriate situation. Differences were not identified for drivers that had the lane departure warning/lane keeping assistance "On" compared to those that had it "Off" with respect to the driver's sex, age, and race/ethnicity.

Since data on these crash avoidance technologies are collected on the vehicle's Bosch compatible EDR, information regarding the status for these systems at the time of the crash event is readily accessible. This will permit a future assessment for whether a system relevant crash event may have occurred because the system was turned "Off." Alternatively, if the system was turned "On," follow up assessment could be conducted for whether the system "Engaged" and mitigated the severity of the crash. If the system was "On" but is reported as "Not Engaged," further investigation may be warranted to understand factors that may have prevented system activation.

Vehicle level crash avoidance system data captured in the EDR is invaluable and relevant for assessing new field data collection, which will in turn contribute to assessing the real-world benefits of these crash avoidance technologies.

INTRODUCTION

Vehicles equipped with crash avoidance systems have the potential to prevent crashes or mitigate crash severity. As these technologies become more broadly available, it is important to quantify the effectiveness of these systems when evaluating real-world crashes. Existing studies conducted by the University of Michigan Transportation Research Institute (UMTRI), Impact Research, and the Insurance Institute for Highway Safety (IIHS) applied statistical methodologies to police reported crash data to estimate the effectiveness of crash avoidance systems such as forward collision warning (FCW), automatic emergency braking (AEB), lane departure warning (LDW) and lane keeping assistance (LKA). High level results from these studies are represented in Tables 1 and 2 below.

Table 1 estimates the effectiveness in reducing rear-end crashes for vehicles equipped only with FCW at 20-27% compared to vehicles equipped with both FCW and AEB at 41-50%. These results suggest that FCW in conjunction with the active AEB improves overall system effectiveness.

Table 1.
FCW and AEB rear-end crash avoidance effectiveness estimates

Study	FCW	FCW + AEB
UMTRI 2022 [1]	20%	41%
Impact Research 2021 [2]	–	43%
IIHS 2017 [3]	27%	50%

Table 2 estimates the effectiveness of LDW and LKA in reducing lane departure related crashes. The UMTRI and Impact Research studies were limited to single vehicle crashes involving road departure while the IIHS study also included head-on and side swipe crashes. Crash reduction for vehicles equipped only with LDW ranged from 8-11% while vehicles equipped with both LDW and LKA ranged from 9-17%. These findings suggest that LDW in conjunction with the active LKA improves overall system effectiveness.
.

Table 2.
Lane departure (LDW/LKA) crash avoidance effectiveness

Study	LDW	LDW + LKA
UMTRI 2022 [1]	8%	17%
Impact Research 2021 [4]	–	9%
IIHS 2018 [5]	11%	–

One limitation of the three studies cited above is that they are constrained to identifying vehicles in the crash data that are *"equipped"* with the crash avoidance technologies. This means identified vehicles were confirmed to be manufactured with a specified crash avoidance technology, but there is no information available to indicate system performance or variation at the vehicle or driver levels. For example, a vehicle may be equipped with AEB, however, if the driver turns the AEB system off, they would not be afforded the benefits of AEB slowing their vehicle if the vehicle in front of theirs stopped suddenly. Furthermore, if the AEB system was engaged at the time of a crash, there is no way to determine whether the system may have performed as designed, mitigating crash severity even if the rear end collision itself was not avoided. Therefore, information about the operation and engagement of collision avoidance systems at the vehicle level is imperative to fully assess the performance of these systems and understand how/whether the systems are being used.

Honda was identified as a manufacturer who, beginning with Model Year 2016 vehicles, captured and recorded the status and activation of crash avoidance technologies such as FCW/AEB and LDW/LKA directly through the vehicle's EDR. Honda EDR data is readily accessible as it can be imaged using the Bosch Crash Data Retrieval (CDR) tool. Using NHTSA's 2017 – 2021 CISS database, data collected on vehicles equipped with this EDR recording capability can be used to identify driver usage of crash avoidance technologies at the time of the recorded crash events. This will enhance future analyses of crash data to determine whether a crash event may have occurred from an avoidance system being turned "Off" or if a system was turned "On" and was "Engaged" to mitigate the severity of the crash. If the system was "On" but is reported as "Not Engaged," further investigation may be warranted to understand factors that may have prevented system activation, such as the crash event was not a crash type that could potentially be addressed by FCW/AEB or LDW/LKA systems.

This paper provides a detailed overview of the recording capabilities of model year 2016 and newer Honda EDRs. It contains a compilation of the status of the CISS reported subject vehicle's crash avoidance technologies and driver demographic data Examples detailing how EDR vehicle data can provide insight for the performance of these systems during a crash event are also included.

Any conclusions about consumer usage of Honda's driver assistance technologies may be biased towards Honda's implementation of these technologies and may not be comparable to other vehicle manufacturers with similar systems. This study does not assess behavioral reasons why consumers have Honda's crash avoidance systems "On" or "Off." CISS and EDR data are limited to reporting vehicle and driver status at the time of the recorded crash event. They do not distinguish whether the driver of the subject Honda vehicle may have turned a crash avoidance system, such as LDW and LKA, "On" or "Off." This study also does not address how effective Honda's crash avoidance technologies are at preventing or mitigating applicable crash events.

METHODOLOGY

Honda Crash Avoidance and Driver Assistance System Terminology

Honda has described crash avoidance and driver assistance systems within their EDR using their specific marketing terms. Table 3 maps the Honda terminology listed within their owner's manual [6] to what industry accepts as more traditional nomenclature for these systems. The common terminology for these systems will be used for this paper.

Table 3.
Terminology mapping

Honda EDR Terms	Common Terms	Abbreviation	System Design/Operation
Forward Collision Warning/Collision Mitigation Braking System	Forward Collision Warning/Automatic Emergency Braking	FCW/AEB	Detects a potential collision with a vehicle ahead and provides a warning to the driver. Automatically applies the vehicle's brakes in time to avoid or mitigate an impending forward crash with another vehicle.
Lane Departure Warning/Road Departure Mitigation	Lane Departure Warning/Lane Keeping Assistance	LDW/LKA	Monitors lane markings and alerts the driver when it detects that the vehicle is drifting out of its lane. Helps prevent the vehicle from unintentionally drifting out of its lane
Lane Keeping Assist	Lane Centering Assistance	LCA	Monitors the vehicle's lane position and automatically and continuously applies steering input needed to keep the vehicle centered within its lane.
Adaptive Cruise Control	Adaptive Cruise Control	ACC	Automatically adjusts the vehicle's speed to keep a pre-set distance between it and the vehicle in front of it.

Honda Event Data Recorder

The Honda EDRs used for this study capture and report five seconds of pre-crash data at 0.5 second recording increments from the Algorithm Enable (AE) crash event. Honda generates 3 standard pre-crash output tables per event, represented by Figures 1, 2 and 3 below.

Figure 1 shows EDR output Table 1 of 3, which contains records for Vehicle Speed, Accelerator Pedal Position, Service Brake, Anti-Lock Brake System (ABS) Activity, Stability Control, Steering Input and Engine Revolutions per Minute (RPM). These elements are required and/or optional pre-crash data elements established by NHTSA regulation 49 CFR Part 563. Note that an output of "On" for Service Brake indicates the driver is physically applying the brake pedal and "On" for ABS Activity means ABS is activated during the specified pre-crash time interval. For Stability Control, "On" (time increment output value "On Non-Engaged") means the system is available for use but was not activated during pre-crash recording, "Off" (output value "Not Engaged") specifies that the system is deactivated by the driver and therefore is not available for the duration of the event, and "Engaged" (output value "On Engaged") indicates the system is available and in use during the event.

Pre-Crash Data -5 to 0 sec [2 samples/sec] (Event Record 1) - Table 1 of 3

Time Stamp (sec)	Speed, Vehicle Indicated (MPH [km/h])	Accelerator Pedal Position, % full	Service Brake (On, Off)	ABS Activity (On, Off)	Stability Control (On, Off, Engaged)	Steering Input (deg)	Engine RPM
-5.0	80 [128]	16	Off	Off	On Non-Engaged	-5	2,100
-4.5	80 [128]	8	Off	Off	On Non-Engaged	-5	2,100
-4.0	80 [128]	11	Off	Off	On Non-Engaged	-5	2,100
-3.5	80 [128]	13	Off	Off	On Non-Engaged	-5	2,100
-3.0	80 [128]	18	Off	Off	On Non-Engaged	-5	2,100
-2.5	80 [128]	18	Off	Off	On Non-Engaged	-5	2,100
-2.0	80 [128]	17	Off	Off	On Non-Engaged	-5	2,100
-1.5	80 [128]	0	Off	Off	On Non-Engaged	0	2,000
-1.0	79 [127]	0	On	Off	On Non-Engaged	0	1,800
-0.5	65 [105]	0	On	On	On Non-Engaged	0	1,600
0.0	65 [105]	0	On	On	On Non-Engaged	10	1,400

Figure 1. Exemplar Honda EDR Table 1 of 3 pre-crash output.

The output data elements for EDR Table 2 of 3, represented by Figure 2, show the status of the active and passive crash avoidance safety systems during the recorded crash event. A value of "On" for the column titled Collision Mitigation Braking System, Forward Collision Warning (On/Off) and the Road Departure Mitigation, Lane Departure Warning (On/Off) states the system is available and ready to engage if a system relevant crash event is qualified. However, a value of "Off" indicates the driver turned off the safety features, so they were not available during the recorded crash event. The columns Forward Collision Warning, Collision Mitigation Braking System, Lane Departure Warning and Road Departure Mitigation note the time when the passive systems are "Warning" or "Not warning" and active safety systems are "Engaged" or "Not engaged." By default, a value of "Off" for Collision Mitigation Braking System, Forward Collision Warning (On/Off) and Road Departure Mitigation, Lane Departure Warning (On/Off) will output values "Not warning" and "Not engaged" for their respective warning status and system engagement columns.

Pre-Crash Data -5 to 0 sec [2 samples/sec] (Event Record 1) - Table 2 of 3

Time Stamp (sec)	PCM Derived Accelerator Pedal Position, % full	Forward Collision Warning (Not Warning/ Warning)	Collision Mitigation Braking System (Not Engaged/ Engaged)	Collision Mitigation Braking System, Forward Collision Warning (On/Off)	Lane Departure Warning (Not Warning/ Warning)	Road Departure Mitigation (Not Engaged/ Engaged)	Road Departure Mitigation, Lane Departure Warning (On/Off)
-5.0	16	Not warning	Not engaged	On	Not warning	Not engaged	Off
-4.5	8	Not warning	Not engaged	On	Not warning	Not engaged	Off
-4.0	11	Not warning	Not engaged	On	Not warning	Not engaged	Off
-3.5	13	Not warning	Not engaged	On	Not warning	Not engaged	Off
-3.0	18	Not warning	Not engaged	On	Not warning	Not engaged	Off
-2.5	18	Not warning	Not engaged	On	Not warning	Not engaged	Off
-2.0	17	Not warning	Not engaged	On	Not warning	Not engaged	Off
-1.5	0	Warning	Engaged	On	Not warning	Not engaged	Off
-1.0	0	Warning	Engaged	On	Not warning	Not engaged	Off
-0.5	0	Warning	Engaged	On	Not warning	Not engaged	Off
0.0	0	Warning	Engaged	On	Not warning	Not engaged	Off

Figure 2. Exemplar Honda EDR Table 2 of 3 pre-crash output.

Honda also provides data elements for the driver assistance systems in the EDR's Table 3 of 3 outputs as shown in Figure 3. The "On/Off" columns for Adaptive Cruise Control, Lane Keeping Assist and Cruise Control indicate whether the driver had these systems "On" and available during the current drive cycle or "Off" leading up to the crash. The remaining data elements specify whether these systems were "Engaged" or "Not engaged" at any time during the pre-crash time interval, leading up to the crash event.

Pre-Crash Data -5 to 0 sec [2 samples/sec] (Event Record 1) - Table 3 of 3

Time Stamp (sec)	Adaptive Cruise Control (Not Engaged/ Engaged)	Adaptive Cruise Control (On/Off)	Lane Keeping Assist (Not Engaged/ Engaged)	Lane Keeping Assist (On/Off)	Cruise Control (Not Engaged/ Engaged)	Cruise Control (On/Off)
-5.0	Not engaged	On	Not engaged	On	Not Engaged	On
-4.5	Not engaged	On	Not engaged	On	Not Engaged	On
-4.0	Not engaged	On	Not engaged	On	Not Engaged	On
-3.5	Not engaged	On	Not engaged	On	Not Engaged	On
-3.0	Not engaged	On	Not engaged	On	Not Engaged	On
-2.5	Not engaged	On	Not engaged	On	Not Engaged	On
-2.0	Not engaged	On	Not engaged	On	Not Engaged	On
-1.5	Not engaged	On	Not engaged	On	Not Engaged	On
-1.0	Not engaged	On	Not engaged	On	Not Engaged	On
-0.5	Not engaged	On	Not engaged	On	Not Engaged	On
0.0	Not engaged	On	Not engaged	On	Not Engaged	On

Figure 3. Exemplar Honda EDR Table 3 of 3 pre-crash output.

Crash Investigation Sampling System

NHTSA has collected crash data since the early 1970s to support its mission to reduce motor vehicle crashes, injuries, and deaths on our Nation's highways. CISS [7] collects detailed crash data to help scientists and engineers analyze motor vehicle crashes and injuries. CISS collects data on a representative sample of minor, serious, and fatal crashes involving at least one passenger vehicle – cars, light trucks, sport utility vehicles, and vans – towed from the scene.

After a crash has been randomly sampled, trained Crash Technicians collect data from crash sites by documenting scene evidence such as skid marks and struck objects. They locate the vehicles involved, document the crash damage, inspect the vehicle's safety equipment such as air bags and seatbelts, identify interior components that were contacted by the occupants and image the EDR when supported. On-site inspections are followed-up with confidential interviews of the crash victims and a review of medical records for injuries sustained in the crash. CISS uses emerging technologies and methods to acquire quality data.

The data collected by the CISS field teams is used by NHTSA and others for a variety of purposes, such as:

- Identifying existing and emerging highway safety problems;
- Obtaining detailed crash performance data for passenger vehicles, including the vehicle safety systems and designs;
- Learning more about the nature of crash-related injuries and the relationship between the type and severity of a crash and the resulting injuries; and
- Assessing the effectiveness of motor vehicle standards and highway safety programs.

CISS data from case years 2017 – 2021 were examined during this study. This data set was filtered for 2016 model year or newer Honda vehicles. Since these vehicles were towed from the scene, the EDR algorithm enabled threshold should have been sufficient to capture crash and pre-crash vehicle information, including the status and activation of crash avoidance systems.

The assessed crashes were not filtered by CISS' crash type variable, meaning the scope for this study is limited to identifying whether the Honda vehicle was equipped with an EDR capable of capturing pre-crash data for crash avoidance system and, if so, reviewing the status of these systems (on/off, engaged/not engaged) at the time of the recorded event. At a high level, this Honda CISS data was then examined for whether the subject vehicle experienced a relevant crash where a crash avoidance system may have mitigated the severity of the reported crash.

There were 150 crashes involving Honda vehicles equipped with the relevant crash avoidance EDR data in CISS.

RESULTS

All Honda EDR data are compiled to assess the status of FCW/AEB and LDW/LKA at the time of each crash and determine which systems were "On" and would be available during a system relevant pre-crash event. Driver demographic information including sex, race/ethnicity, and age are also reported to provide insight into driver usage of these systems. The results for this study are limited to reporting vehicle status of the crash avoidance systems and demographics for the respective driver of the Honda for the relevant crash event. Examples for three specific CISS crashes where the crash avoidance or driver assistance systems were engaged any time during the 5 second pre-crash interval are also listed.

Crash Avoidance System Status
Table 4 presents the status of the FCW/AEB and LDW/LKA crash avoidance systems at the time of the crash for the reported CISS case. Of the 150 CISS cases reviewed, 149 drivers (99%) had FCW/AEB "On" at the time of the crash. With respect to LDW/LKA, 73 drivers (49%) had the system "On" at the time of the crash.

Table 4.
EDR status of crash avoidance systems

Crash Avoidance Systems	On	Off	Total
Forward Collision Warning/Automatic Emergency Braking (FCW/AEB)	149	1	150
Lane Departure Warning/Lane Keeping Assistance (LDW/LKA)	73	77	150

Driver Demographics

Driver demographic data for the 150 CISS cases reviewed are listed in Tables 5 and 6. The driver is reported as female in 92 cases (61%), male in 54 cases (36%), and unknown or not reported in 4 cases (3%). Regarding race/ethnicity, 70 drivers (47%) are reported as White (Not Hispanic or Latino), 20 drivers (13%) as Hispanic or Latino, 9 drivers (6%) as Black or African American, 7 drivers (5%) as Asian, 4 drivers (3%) as American Indian or Alaska Native, 2 drivers (1%) as Native Hawaiian or Other Pacific Islander, and 2 drivers (1%) as Other. The race/ethnicity was unknown for 36 drivers (24%). The average driver age is 44-years-old, with the youngest and oldest drivers reported to be 16-years-old and 91-years-old, respectively.

Table 5.
Driver demographics by sex and race/ethnicity

Race/ethnicity	Sex				Total
	Female	Male	Unknown	Not Reported	
White	43	27	0	0	**70**
Hispanic or Latino	10	10	0	0	**20**
Black/African American	6	3	0	0	**9**
Asian	5	2	0	0	**7**
American Indian/ Alaska Native	3	1	0	0	**4**
Native Hawaiian/Other Pacific Islander	2	0	0	0	**2**
Other	2	0	0	0	**2**
Unknown	21	11	2	2	**36**

To evaluate driver usage of the FCW/AEB and LDW/LKA systems at the time of the crash, demographic information was compiled and is reported below. As shown in Figures 4 and 5, FCW/AEB was reported as "On" in 149 of 150 cases. Only one driver, a 37-year-old white male, had the system "Off" during the crash event (CISS Case No. 1-26-2019-061-02). This data indicates widespread usage for Honda's FCW/AEB system, regardless of driver sex, race/ethnicity, and age.
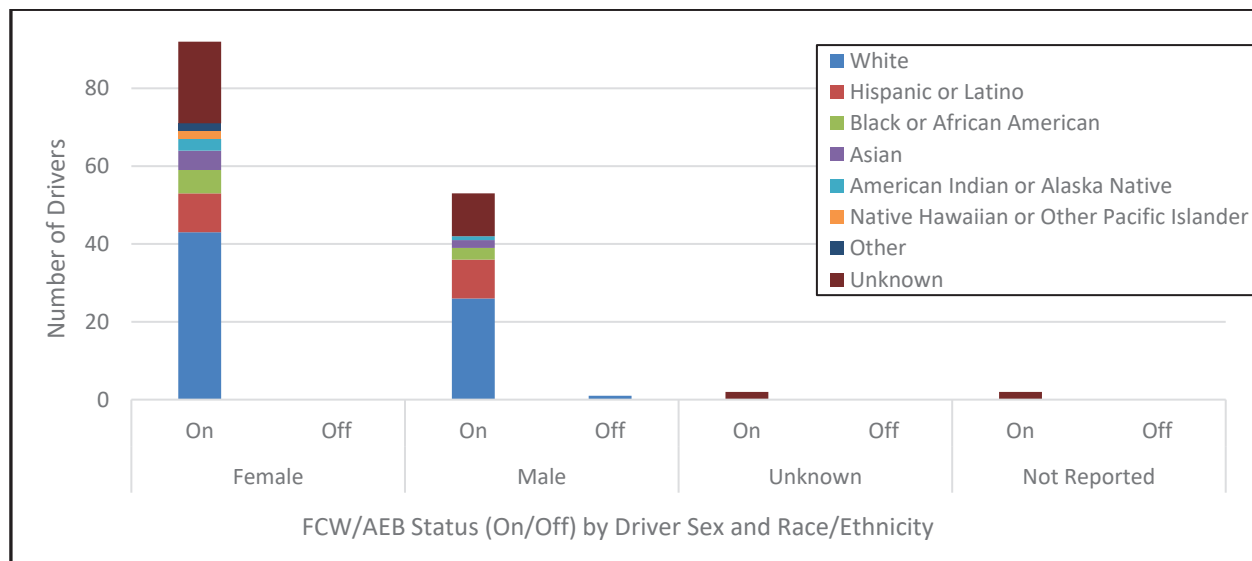
Figure 4. FCW/AEB system status by driver sex and race/ethnicity.
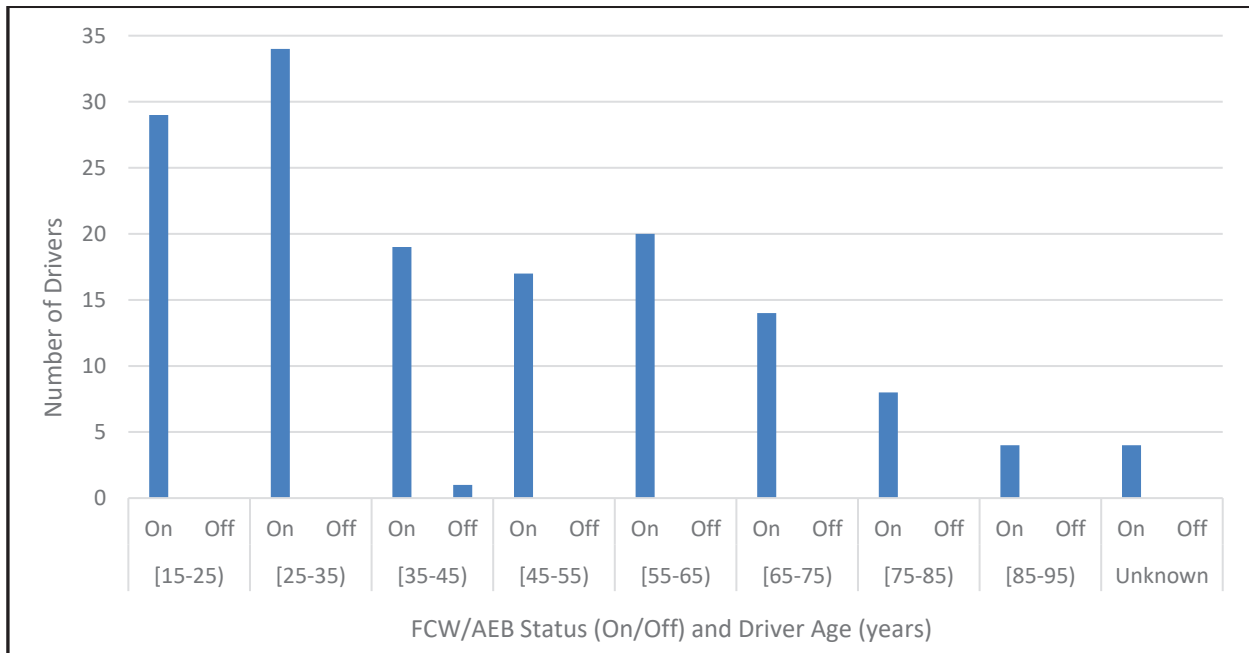
Figure 5. FCW/AEB status by driver age.

The distribution for the status of the LDW/LKA system by driver sex and race/ethnicity are shown in Figure 6 while the status by driver age is represented by Figure 7. The percent difference between drivers who had the LDW/LKA system "On" compared to those who turned it "Off" is 9% for females and 7% for males. Given the disproportionate number of drivers categorized by reported race/ethnicity, results evaluating usage of LDW/LKA by this demographic are inconclusive. The average age of drivers with LDW/LKA "On" is 42 years old and "Off" is 45 years old, which implies usage is independent of driver age. Since the percent difference between overall drivers who had LDW/LKA "On" vs. "Off" is 5%, the CISS data indicate that roughly half of Honda drivers leave the LDW/LKA system "On," regardless of sex, race/ethnicity, and age.
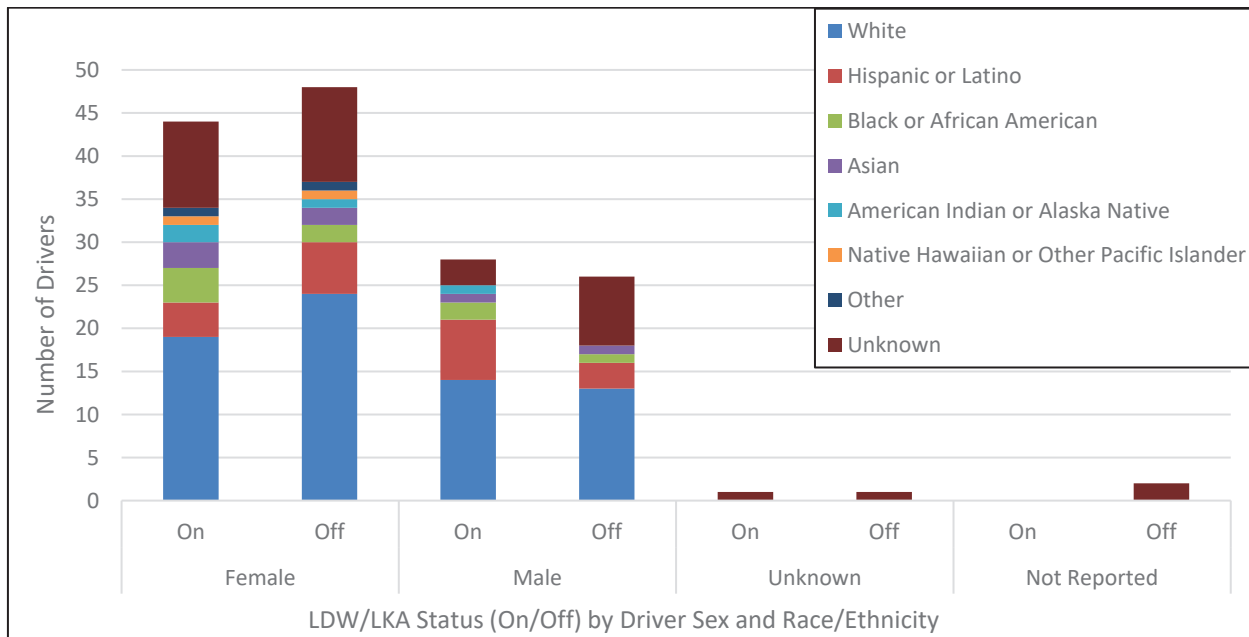
Figure 6. LDW/LKA status by driver sex and race/ethnicity.
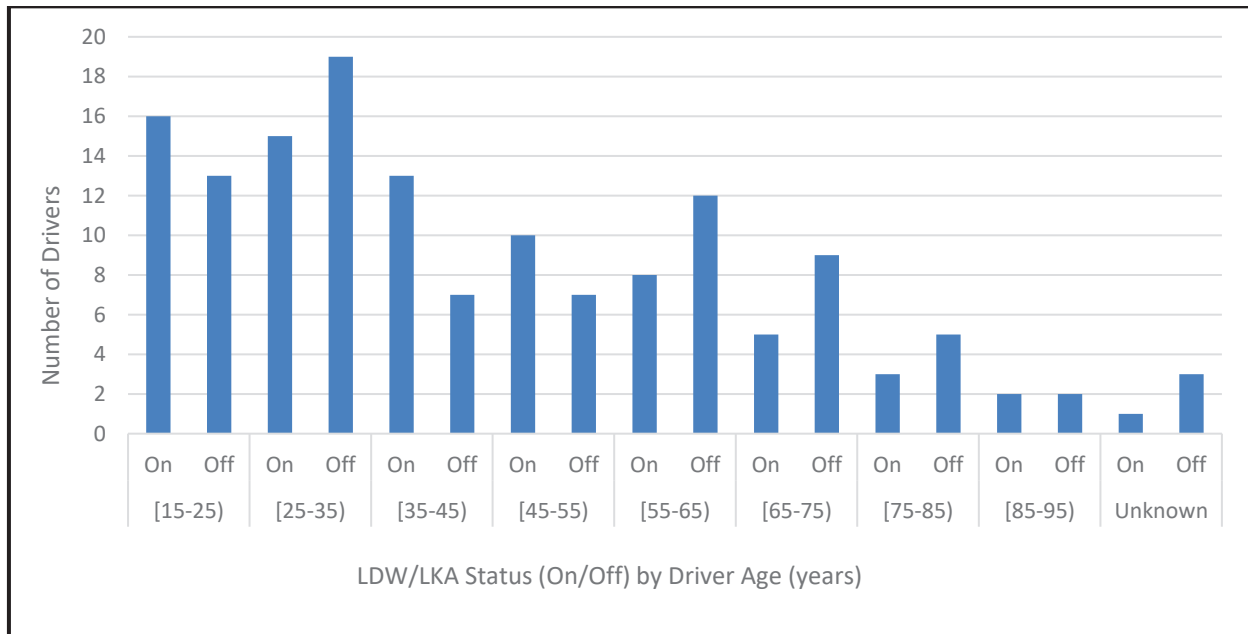
Figure 7. LDW/LKA status by driver age.

Crash Avoidance and Driver Assistance System Activated

There are 21 cases identified in the CISS data where the subject Honda's crash avoidance or driver assistance systems were reported as active during the EDR's 5 seconds of pre-crash data. Note that Honda uses the term "Engaged" to specify that the system was active (i.e., not just switched on, but actually in operation) during the pre-crash recording interval.

Table 6 lists the six cases where FCW provided a warning to the driver prior to the recorded crash event. Half of these cases simultaneously engaged AEB while the FCW system was active. Table 7 specifies the fifteen cases where a driver assistance system engaged. Of these cases, 7 engaged ACC, 5 engaged LCA, and 3 engaged both ACC and LCA prior to impact. None of the CISS cases identified activation of the LDW or LKA systems. There were no cases where an active crash avoidance system (Table 6) also had an active driver assistance system (Table 7).

Table 6.

EDR reported crash avoidance system engaged

Case No.	FCW Warning	AEB Engaged
1-26-2018-135-03	X	X
1-29-2019-079-08	X	
1-16-2020-002-02	X	X
1-21-2020-013-04	X	X
1-27-2020-063-04	X	
1-24-2021-070-03	X	

Table 7.

EDR reported driver assistance system engaged

Case No.	ACC Engaged	LCA Engaged
1-12-2021-012-01	X	X
1-17-2021-009-04	X	X
1-18-2020-088-03	X	
1-19-2020-106-03	X	
1-19-2021-106-03	X	
1-20-2021-022-03		X
1-20-2021-072-03		X
1-20-2021-142-04	X	
1-20-2021-168-04	X	
1-23-2021-142-04		X
1-24-2019-007-03	X	
1-24-2019-122-02		X
1-24-2020-181-02	X	X
1-31-2021-060-03		X
1-66-2018-064-04	X	

DISCUSSION

The EDR data suggests high usage of Honda's FCW/AEB. In all but one crash, the system was "On" and available if the vehicle encountered a system relevant crash. However, usage of LDW/LKA was not as high, given the system was turned "Off" in over 50% of the crashes. The results of this EDR study are consistent with an earlier IIHS investigation into consumer usage of passive crash avoidance systems [8]. In a survey of Honda vehicles brought into Honda dealerships for service equipped with both FCW and LDW, IIHS researchers found that for 184 vehicles, only a third of the vehicles had LDW "On," whereas all but one vehicle had FCW turned "On."

Demographic data supports driver usage of FCW/AEB, regardless of sex, race/ethnicity, or age. Driver usage of LDW/LKA is split almost equally in half between those that have the system "On" compared to those that have the system "Off." LDW/LKA system usage does not appear to have a distinct sex or age bias. There are no conclusive determinations for system usage based on race/ethnicity. Biases may exist in this dataset, given that this study is limited to the Honda vehicles themselves, the demographics for individuals that purchase and drive these vehicles, and the usage for these systems is specific to Honda's implementation.

Data from this EDR study provides additional insight to actual FCW, AEB, LDW and LKA system status availability and engagement during a collision, which was not available in prior studies that have estimated the operation of these systems thus far. Instead, prior studies relied on police reported crash data, and therefore did not benefit from detailed vehicle level reported data. This study shows over a 99% driver usage rate for FCW/AEB, meaning Honda vehicles equipped with this system should be affording maximum crash severity reduction benefits to these vehicle drivers. However, the potential benefits for LDW/LKA could be improved to optimize driver usage, as this data indicates that approximately 50% of drivers turn the system off. Additional research is warranted to further understand the disparity between drivers who have the system on and those have the system off. Moreover, additional vehicle data analyses can be conducted to provide further insight into the specific crash event which, combined with an on-site crash investigation, may begin to explain system effectiveness.

There were 21 cases (14%) identified in this study where the crash avoidance or driver assistance system was engaged within the five seconds pre-crash time interval captured in the EDR. Three example CISS cases, provided below, show how EDR vehicle data can be used to assess the performance of these technologies in system relevant crashes.

FCW/AEB - Example 1

In CISS Case No. 1-21-2020-013-04, a 2018 Honda Accord was traveling south on a median divided trafficway with positive barrier. The roadway width was reduced by cone barriers for a construction zone. The Honda was approaching a 2006 Chevrolet Medium/Heavy truck, which was also traveling south, in the same lane at a lower, steady speed. The front of the Honda contacted the back of the Chevrolet. The Honda came to rest facing a southerly direction in lane two, and the Chevrolet was driven to the shoulder. Figure 8 is a post-crash photo of the Honda showing the vehicle underrode the Chevrolet truck.
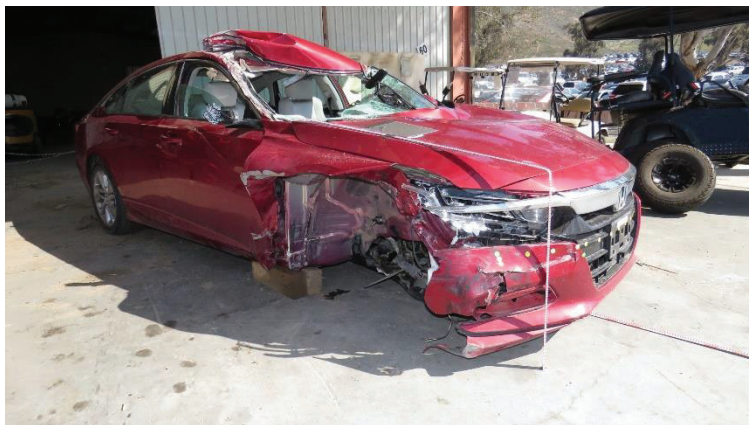
Figure 8. CISS Case No. 1-21-2020-013-04 damage.

A review of the Table 1 EDR data in Figure 9, shows the Honda was traveling at 96 mph at 5 seconds prior to the impact with the Chevrolet. Figure 10, Table 2 of 3 EDR data, reported the driver received a FCW alert at 3 seconds prior to the crash, with AEB (Honda's Crash Mitigation Braking System) engaging at 1.5 seconds prior to the crash. According to the EDR, the driver depressed the brake at 0.5 seconds, which also engaged ABS. The data indicate that the manual brake activation and the steering wheel input that occurred at 0.5 seconds prior to the crash also coincided with the suppression of both the FCW warning and AEB activation. The EDR reported vehicle speed information does not appear to coincide with the AEB and driver brake activation, although the EDR reported crash severity indicates a speed reduction. The EDR reported that the maximum longitudinal change in velocity (Delta-V) from the crash was 15 mph. Considering the 96 mph travel speed, prior to any brake activation by the AEB or driver, there was a significant speed reduction, likely resulting from AEB activation, prior to impact.

Pre-Crash Data -5 to 0 sec [2 samples/sec] (Event Record 1) - Table 1 of 3

Time Stamp (sec)	Speed, Vehicle Indicated (MPH [km/h])	Accelerator Pedal Position, % full	Service Brake (On, Off)	ABS Activity (On, Off)	Stability Control (On, Off, Engaged)	Steering Input (deg)	Engine RPM
-5.0	95 [153]	45	Off	Off	On Non-Engaged	0	3,200
-4.5	95 [153]	46	Off	Off	On Non-Engaged	-5	3,200
-4.0	96 [154]	42	Off	Off	On Non-Engaged	-5	3,200
-3.5	96 [155]	48	Off	Off	On Non-Engaged	-5	3,200
-3.0	96 [155]	48	Off	Off	On Non-Engaged	-5	3,300
-2.5	97 [156]	48	Off	Off	On Non-Engaged	-5	3,300
-2.0	98 [157]	48	Off	Off	On Non-Engaged	-5	3,300
-1.5	98 [157]	64	Off	Off	On Non-Engaged	-5	3,300
-1.0	97 [156]	0	Off	Off	On Non-Engaged	0	3,400
-0.5	84 [135]	0	On	On	On Non-Engaged	100	2,800
0.0	84 [135]	0	On	On	On Non-Engaged	85	2,600

Figure 9. CISS Case No. 1-21-2020-013-04 Table 1 EDR data.

Pre-Crash Data -5 to 0 sec [2 samples/sec] (Event Record 1) - Table 2 of 3

Time Stamp (sec)	PCM Derived Accelerator Pedal Position, % full	Forward Collision Warning (Not Warning/ Warning)	Collision Mitigation Braking System (Not Engaged/ Engaged)	Collision Mitigation Braking System, Forward Collision Warning (On/Off)	Lane Departure Warning (Not Warning/ Warning)	Road Departure Mitigation (Not Engaged/ Engaged)	Road Departure Mitigation, Lane Departure Warning (On/Off)
-5.0	45	Not warning	Not engaged	On	Not warning	Not engaged	Off
-4.5	46	Not warning	Not engaged	On	Not warning	Not engaged	Off
-4.0	42	Not warning	Not engaged	On	Not warning	Not engaged	Off
-3.5	48	Not warning	Not engaged	On	Not warning	Not engaged	Off
-3.0	48	Warning	Not engaged	On	Not warning	Not engaged	Off
-2.5	48	Warning	Not engaged	On	Not warning	Not engaged	Off
-2.0	48	Warning	Not engaged	On	Not warning	Not engaged	Off
-1.5	64	Warning	Engaged	On	Not warning	Not engaged	Off
-1.0	0	Warning	Engaged	On	Not warning	Not engaged	Off
-0.5	0	Not warning	Not engaged	On	Not warning	Not engaged	Off
0.0	0	Not warning	Not engaged	On	Not warning	Not engaged	Off

Figure 10. CISS Case No. 1-21-2020-013-04 Table 2 EDR data.

LDW/LKA - Example 2
CISS Case No. 1-19-2020-162-04 documents a single vehicle roadway departure crash of a 2019 Honda Accord equipped with LKA (Honda's Road Departure Mitigation), which the EDR reported as "On" leading up to the incident. In this case the Honda was traveling southwest on a two-lane undivided roadway, negotiating a left curve. The Honda departed the roadway (Figure 11) to the right and traveled a short distance before the front plane contacted a tree, coming to a final rest to the right of the road.

Figure 11. CISS Case No. 1-19-2020-162-04 roadway departure.

The Table 1 EDR data reported (Figure 12), shows the Honda was traveling at 34 mph, 5 seconds prior to the impact with a tree at 24 mph, resulting in a 19-mph longitudinal Delta-V crash severity. The driver applied the service brake at 4.5 second and there was a steering angle input to the left starting at 4 seconds prior to the crash. Table 2 EDR data shown in Figure 13 confirms LDW/LKA was "On," however, the LDW did not provide a warning and LKA did not engage prior to the crash. Cruise control and all other driver assistance systems were "Off" and therefore were not available leading up to the crash. The driver of the Honda was coded in CISS as attentive or not distracted.

Pre-Crash Data -5 to 0 sec [2 samples/sec] (Event Record 1) - Table 1 of 3

Time Stamp (sec)	Speed, Vehicle Indicated (MPH [km/h])	Accelerator Pedal Position, % full	Service Brake (On, Off)	ABS Activity (On, Off)	Stability Control (On, Off, Engaged)	Steering Input (deg)	Engine RPM
-5.0	34 [55]	0	Off	Off	On Non-Engaged	0	1,200
-4.5	34 [55]	0	On	Off	On Non-Engaged	0	1,200
-4.0	34 [54]	0	On	Off	On Non-Engaged	15	1,200
-3.5	32 [51]	0	On	Off	On Non-Engaged	30	1,200
-3.0	29 [47]	0	On	Off	On Non-Engaged	35	1,200
-2.5	29 [47]	0	Off	Off	On Non-Engaged	50	1,200
-2.0	27 [43]	0	Off	Off	On Non-Engaged	45	1,200
-1.5	26 [42]	0	Off	Off	On Non-Engaged	35	1,100
-1.0	25 [41]	0	Off	Off	On Non-Engaged	45	1,100
-0.5	24 [39]	0	Off	Off	On Non-Engaged	70	1,100
0.0	24 [39]	0	Off	Off	On Non-Engaged	65	1,100

Figure 12. CISS Case No. 1-19-2020-162-04 Table 1 EDR Data.

According to the Honda owner's manual [9], the LDW/LKA system becomes ready to start searching for lane markings when all the following conditions are met:
• The vehicle is traveling between about 45 and 90 mph (72 and 145 km/h).
• The vehicle is on a straight or slightly curved road.
• The turn signals are off.
• The brake pedal is not depressed.
• The wipers are not in high-speed operation.
• The vehicle is not accelerating or braking, and the steering wheel is not being turned.
• The system makes a determination that the driver is not actively accelerating, braking or steering.

There were several factors in the crash scenario that likely prevented the LDW/LKA system from engaging. Figure 11 shows there were no lane markings on the roadway, which are required for system operation. The EDR reported vehicle travel speed (24mph) was lower than the system activation travel speed (45mph) per the owner's manual. EDR data also show that the brake pedal was depressed, and steering wheel was turned before the vehicle departed the roadway. Comparing the system limitations listed in the owner's manual and the subject Honda's status for the systems listed above, the LDW/LKA system would not be expected to activate during this crash event. The LDW/LKA system appears to have operated as designed.

Time Stamp (sec)	PCM Derived Accelerator Pedal Position, % full	Forward Collision Warning (Not Warning/ Warning)	Collision Mitigation Braking System (Not Engaged/ Engaged)	Collision Mitigation Braking System, Forward Collision Warning (On/Off)	Lane Departure Warning (Not Warning/ Warning)	Road Departure Mitigation (Not Engaged/ Engaged)	Road Departure Mitigation, Lane Departure Warning (On/Off)
-5.0	0	Not warning	Not engaged	On	Not warning	Not engaged	On
-4.5	0	Not warning	Not engaged	On	Not warning	Not engaged	On
-4.0	0	Not warning	Not engaged	On	Not warning	Not engaged	On
-3.5	0	Not warning	Not engaged	On	Not warning	Not engaged	On
-3.0	0	Not warning	Not engaged	On	Not warning	Not engaged	On
-2.5	0	Not warning	Not engaged	On	Not warning	Not engaged	On
-2.0	0	Not warning	Not engaged	On	Not warning	Not engaged	On
-1.5	0	Not warning	Not engaged	On	Not warning	Not engaged	On
-1.0	0	Not warning	Not engaged	On	Not warning	Not engaged	On
-0.5	0	Not warning	Not engaged	On	Not warning	Not engaged	On
0.0	0	Not warning	Not engaged	On	Not warning	Not engaged	On

Figure 13. CISS Case No. 1-19-2020-162-04 Table 2 EDR data.

Driver Assistance System - Example 3
CISS Case No. 1-24-2020-181-02 is an example where the EDR reported the driver assistance systems were engaged leading up to the crash. In this case, a 2014 Chevrolet Equinox was traveling eastbound on a four lane, two-way, painted median roadway. The Chevrolet was stopped on the roadway, waiting to make a left turn into a driveway. A 2020 Honda Civic was traveling eastbound on the same roadway directly behind the Chevrolet. The back plane of the Chevrolet was contacted by the front plane of Honda. Both vehicles came to final rest on the roadway near the point of impact.

In Figure 14, the Table 1 EDR data shows the vehicle was traveling at a steady speed of 67 mph pre-crash. There was no reported accelerator pedal position travel, the engine RPMs were generally steady and there was negligible steering input from the 5 seconds to 1 second pre-impact intervals. FCW/AEB was reported "ON," but did not provide a warning or activate the automatic braking prior to the rear end crash as shown in Figure 15. Figure 16 reports that the ACC and LCA (Honda's Lane Keeping Assist System) were engaged until 1 second prior to impact. EDR data shows the driver begins to steer at 1 second, depresses the service brake at 0.5 seconds which corresponds with the override of both ACC and LCA. The oblique rear-end impact resulted in a 25-mph longitudinal and 8-mph lateral Delta-V crash severity in response to the steering input beginning at 1 second prior to impact.

The driver of the Honda was coded in CISS as being distracted or inattentive.

Pre-Crash Data -5 to 0 sec [2 samples/sec] (Event Record 1) - Table 1 of 3

Time Stamp (sec)	Speed, Vehicle Indicated (MPH [km/h])	Accelerator Pedal Position, % full	Service Brake (On, Off)	ABS Activity (On, Off)	Stability Control (On, Off, Engaged)	Steering Input (deg)	Engine RPM
-5.0	67 [108]	0	Off	Off	On Non-Engaged	0	1,800
-4.5	67 [108]	0	Off	Off	On Non-Engaged	0	1,800
-4.0	67 [108]	0	Off	Off	On Non-Engaged	0	1,800
-3.5	67 [108]	0	Off	Off	On Non-Engaged	-5	1,800
-3.0	67 [108]	0	Off	Off	On Non-Engaged	-5	1,800
-2.5	67 [108]	0	Off	Off	On Non-Engaged	-5	1,700
-2.0	67 [108]	0	Off	Off	On Non-Engaged	0	1,700
-1.5	67 [108]	0	Off	Off	On Non-Engaged	0	1,800
-1.0	67 [108]	0	Off	Off	On Non-Engaged	-10	1,700
-0.5	67 [108]	0	On	On	On Engaged	-110	1,700
0.0	67 [108]	0	On	On	On Engaged	-115	1,700

Figure 14. CISS Case No. 1-24-2020-181-02 Table 1 EDR data.

Pre-Crash Data -5 to 0 sec [2 samples/sec] (Event Record 1) - Table 2 of 3

Time Stamp (sec)	PCM Derived Accelerator Pedal Position, % full	Forward Collision Warning (Not Warning/ Warning)	Collision Mitigation Braking System (Not Engaged/ Engaged)	Collision Mitigation Braking System, Forward Collision Warning (On/Off)	Lane Departure Warning (Not Warning/ Warning)	Road Departure Mitigation (Not Engaged/ Engaged)	Road Departure Mitigation, Lane Departure Warning (On/Off)
-5.0	10	Not warning	Not engaged	On	Not warning	Not engaged	Off
-4.5	10	Not warning	Not engaged	On	Not warning	Not engaged	Off
-4.0	10	Not warning	Not engaged	On	Not warning	Not engaged	Off
-3.5	10	Not warning	Not engaged	On	Not warning	Not engaged	Off
-3.0	10	Not warning	Not engaged	On	Not warning	Not engaged	Off
-2.5	10	Not warning	Not engaged	On	Not warning	Not engaged	Off
-2.0	10	Not warning	Not engaged	On	Not warning	Not engaged	Off
-1.5	10	Not warning	Not engaged	On	Not warning	Not engaged	Off
-1.0	10	Not warning	Not engaged	On	Not warning	Not engaged	Off
-0.5	0	Not warning	Not engaged	On	Not warning	Not engaged	Off
0.0	0	Not warning	Not engaged	On	Not warning	Not engaged	Off

Figure 15. CISS Case No. 1-24-2020-181-02 Table 2 EDR data.

Honda's owner's manual states [10] that the FCW/AEB system may activate when:
- The speed difference between the Honda vehicle and a vehicle or pedestrian detected in front of the Honda becomes about 3 mph (5 km/h) and over with a chance of a collision.
- The Honda's vehicle speed is about 62 mph (100 km/h) or less and the system determines there is a chance of a collision with:
  - Vehicles detected in front of the Honda that are stationary, oncoming, or traveling in the same direction.

- A pedestrian who is detected in front of the Honda.
- The Honda's vehicle speed is above 62 mph (100 km/h), and the system determines there is a chance of a collision with a vehicle detected in front of the Honda traveling in the same direction.

Therefore, it is possible that the Honda's 67 mph travel speed exceeded the system limitation of 62mph, which prevented the system from recognizing and providing an FCW/AEB response to the stationary Chevrolet vehicle during this crash event.

Pre-Crash Data -5 to 0 sec [2 samples/sec] (Event Record 1) - Table 3 of 3

Time Stamp (sec)	Adaptive Cruise Control (Not Engaged/ Engaged)	Adaptive Cruise Control (On/Off)	Lane Keeping Assist (Not Engaged/ Engaged)	Lane Keeping Assist (On/Off)	Cruise Control (Not Engaged/ Engaged)	Cruise Control (On/Off)
-5.0	Engaged	On	Engaged	On	Engaged	On
-4.5	Engaged	On	Engaged	On	Engaged	On
-4.0	Engaged	On	Engaged	On	Engaged	On
-3.5	Engaged	On	Engaged	On	Engaged	On
-3.0	Engaged	On	Engaged	On	Engaged	On
-2.5	Engaged	On	Engaged	On	Engaged	On
-2.0	Engaged	On	Engaged	On	Engaged	On
-1.5	Engaged	On	Engaged	On	Engaged	On
-1.0	Engaged	On	Engaged	On	Engaged	On
-0.5	Not engaged	On	Not engaged	On	Not Engaged	On
0.0	Not engaged	On	Not engaged	On	Not Engaged	On

Figure 16. CISS Case No. 1-24-2020-181-02 Table 3 EDR data.

These three examples show real world crashes where Honda EDRs recorded the status of crash avoidance and driver assistance systems during crash events. This information provides insight into the performance of these technology systems during relevant crash events that could not otherwise be assessed. This vehicle level data could provide some understanding for consumer usage and acceptance of these systems. As stated earlier, using police crash reports alone to determine system effectiveness is limited. Evaluating vehicle level EDR data, in combination with a comprehensive crash investigation, will identify opportunities for the improvement and advancement of crash avoidance and driver assistance technologies.

CONCLUSION

Starting with the 2016 Model Year, Honda began to phase-in vehicles equipped with an EDR that captures the status and activation of crash avoidance technologies. To understand driver usage of these technologies, Honda EDR data were collected from the 2017 – 2021 CISS for vehicles equipped with this recording capability. Vehicle level crash avoidance system data captured in the EDR is invaluable and relevant for assessing new field data collection. This will in turn contribute to assessing the real-world benefits of these crash avoidance technologies. The 150 Honda vehicles in this study are equipped with EDRs that captured data elements related to the function and alert status of several crash avoidance systems in the time leading up to a crash event. The results indicate that Honda drivers of vehicles equipped with crash avoidance systems seem to be more likely to have FCW/AEB systems "On" and LDW/LKA systems "Off." Specifically, almost all drivers (99%) had the FCW/AEB systems "On" and thus will be afforded the potential benefits of these systems if they are involved in a relevant crash situation. With respect to LDW/LKA, about half (51%) of drivers had these systems "Off" and therefore would not be afforded the potential benefits of these systems during an appropriate situation. Driver demographic information did not identify any clear differences in usage of LDW/LKA with respect to the driver's sex, age, or race/ethnicity.

REFERENCES

[1] A. J. Leslie, R. J. Kiefer, C. A. Flannagan, B. A. Schoettle and S. H. Owen, "Analysis of the Field Effectiveness of General Motors Model Year 2013-2020 Advanced Driver Assistance System Features," University of Michigan Transportation Research Institute, Ann Arbor, 2022.

[2] R. Spicer, A. Vahabaghale, D. Murakhovsky, S. St. Lawrence, B. Drayer and G. Bahouth, "Do driver characteristics and crash conditions modify the effectiveness of automatic emergency braking?," SAE International, 2021.

[3] J. Cicchino, "Effectiveness of Forward Collision Warning and Autonomous Emergency Braking Systems in Reducing Front-to-rear Crash Rates," Accident Analysis and Prevention, vol. 99, pp. 142-152, 2017.

[4] R. Spicer, A. Vahabaghale, D. Murakhovsky, G. Bahouth and B. Drayer, "Effectiveness of Advanced Driver Assistance Systems in Preventing System-Relevant Crashes," SAE International, 2021.

[5] J. B. Cicchino, "Effects of lane departure warning on police-reported crash rates," Journal of Safety Research, vol. 66, pp. 61-70, 2018.

[6] https://owners.honda.com/vehicle-information/manuals

[7] https://www.nhtsa.gov/crash-data-systems/crash-investigation-sampling-system.

[8] Insurance Institute for Highway Safety (2016, January 28), Most Honda owners turn off lane departure warning, Status Report, Vol. 51, No. 1, page 6.

[9] https://owners.honda.com/vehicle-information/information/2019/Accord%20Sedan/manuals

[10] https://owners.honda.com/vehicle-information/information/2020/Civic-Sedan/manuals

PEER REVIEW PAPER

This paper has been peer-reviewed and published in a special edition of Traffic Injury Prevention 24(S1), by Taylor & Francis Group. The complete paper will be available on the Traffic Injury Prevention website soon. To access ESV Peer-reviewed papers click the link below
https://www.tandfonline.com/toc/gcpi20/24/sup1?nav=tocList

REPRESENTATIVE PEDESTRIAN COLLISION INJURY RISK DISTRIBUTIONS FOR A DENSE-URBAN US ODD USING NATURALISTIC DASH CAMERA DATA

Eamon T. Campolettano
John M. Scanlon
Trent Victor
Waymo, LLC
United States

ABSTRACT

Automated Driving Systems (ADS; SAE levels 3 through 5 technologies) are currently being deployed in several dense-urban operational design domains (ODDs) within the United States (US). Within these dense-urban areas, vulnerable road users (VRU) generally comprise the vast majority of injury and fatal collisions. One challenge with the study of VRU collisions is a lack of crash data sources with pre-impact kinematics. Understanding the pre-impact kinematics is a key factor in assessing the potential injury risk for pedestrian-vehicle impacts. The purpose of this study was to determine injury distributions for pedestrians within a dense-urban ODD (Los Angeles, California) using data from vehicles instrumented with forward-facing cameras and vehicle sensors. This study leveraged data from a fleet of vehicles equipped with aftermarket, in-cabin dash cameras operating in Los Angeles, California. From approximately 66 million miles of driving data, 42 collisions were identified. Each vehicle was equipped with a forward-facing camera, an accelerometer sampling at 20 Hz, and GPS. A global optimization routine was used on the accelerometer, GPS, and video data to correct for sensor orientation and asynchronicity in data sampling. For each event, two key video frames were identified: the frame associated with impact and a frame associated with key vehicle kinematics (e.g., vehicle start/stop, hard braking [> 0.2 g]). These key frames were then mapped to the processed vehicle speed kinematics to determine vehicle speed at impact.

For the events included in this dataset, impact speeds ranged from approximately 1.6 kph (1 mph) to 65 kph (40 mph). In most events, the front of the vehicle struck the pedestrian. Existing pedestrian injury risk curves were then used to calculate the level of risk associated with the reconstructed impacts, and the probability of AIS3+ injury risk was observed to vary from minimal risk (<2%) to approximately 55%. These data highlight the wide range of impact speeds and injury risk that may occur during vehicle-pedestrian collisions.

Assessing injury severity for collisions involving VRUs is highly impactful for the continued development of traffic safety, including ADAS, ADS, and roadway design. Using naturalistic VRU collision data collected from dashboard cameras, a methodology for assessing event severity by pairing accelerometer and GPS data with video to compute impact speed was presented. This is the first known analysis of pedestrian severity distributions using a naturalistic US database. The methods presented in this study may be applied to larger datasets or other sensing systems to enable further ODD-specific modeling.

INTRODUCTION

Pedestrians represent a vulnerable group of road users who do not have the same crash protections as vehicle occupants during a collision event. According to the most recent data available from NHTSA, over 6,000 pedestrians were fatally injured in 2019, compared to over 75,000 who sustained injuries in traffic-related crashes [1]. Furthermore, pedestrians represent 17% of all police-reported traffic collision-related fatalities, but only 3% of all such injuries [1]. In general, fatal pedestrian collisions were most likely to occur in urban areas (82%), at non-intersections (73%), and 90% of all fatal collisions occurred due to contact with the front of the vehicle [1].

The majority of pedestrian impact events in human collision data occur with the front structures of some forward moving vehicle [1-4]. Accordingly, injury risk models are often built using this frontal striking data. During these events, some pedestrian actor is within the trajectory of some vehicle actor when the engagement occurs. Injuries generally occur following some engagement of the front bumper structure. This is followed by potential movement of the pedestrian onto the hood, windshield, A-pillar, and other structures. Lastly, there can be potential ground contact. Injuries can occur during any phase of this engagement. Because of these injury-causing mechanisms, the

previously developed models overwhelmingly utilize vehicle impact speed as a key independent variable dictating injury risk [5-10].

Analysis from an in-depth, German collision database called German In-Depth Accident Study (GIDAS) has shown that approximately 88% of collisions involving pedestrians resulted in a maximum injury severity of MAIS2 or lower [11]. Regardless of severity, the lower extremity is the most often-injured body region (injured in 67% of cases), followed by the head (~50% of the time), and upper extremity (38% of the time). The lower extremity is most often injured by contact with the front end of the striking vehicle, while the most common injury source for the head is engagement with the windshield, followed by the ground [12-14].

From 1994 to 1998, the National Traffic Highway Safety Administration (NHTSA) oversaw the Pedestrian Crash Data Study (PCDS). PCDS compiled data from crashes involving pedestrians in 6 geographic areas and resulted in in-depth analysis on 549 total collision events [15]. To date, PCDS represents the most comprehensive large-scale pedestrian crash database in the United States with objective injury outcome data; however, the data is not recent, not of a representative sample, and only considers frontal impacts and not all pedestrian-vehicle events. When relating injury risk to vehicle impact speed, Tefft noted that the age of PCDS may affect the relationship due to "changes in medical care, vehicle design, or the composition of the vehicle fleet [10]."

Previously, researchers have utilized taxicabs instrumented with forward-facing cameras and vehicle sensors in South Korea to investigate injury severity for collisions involving pedestrians. Notably, injury severity was only presented on an ordinal scale based on data from police reports rather than utilizing an existing probabilistic injury risk model. As in previous research, crash speed was highly related to injury severity [16].

ADS fleets are currently being deployed in several dense-urban US operational design domains (ODDs). For example, Waymo has commercial ride-hailing operations in downtown Phoenix and the Phoenix East Valley [17], and has been testing without an autonomous specialist behind the wheel in San Francisco since early 2022 [18]. Within these dense-urban areas, vulnerable road users (VRU), such as pedestrians, generally comprise the vast majority of injury and fatal collisions [1, 3-4]. One challenge with the study of VRU collisions is a lack of crash data sources with objective pre-impact kinematics. Understanding the pre-impact kinematics is a key factor in assessing the potential injury risk for pedestrian-vehicle impacts. The purpose of the present study was to determine injury risk distributions for pedestrians within a dense-urban ODD (Los Angeles, California) using data from vehicles instrumented with forward-facing cameras and vehicle sensors in conjunction with established pedestrian injury risk models.

METHODOLOGY

Data Source
This study leveraged data from a fleet of vehicles equipped with aftermarket in-cabin dash cameras operating in Los Angeles, California. For this study, only collision events and driving miles on S1400 roads were included. S1400 roads are defined as "local neighborhood road, rural road, city street [19]." From approximately 66 million miles of driving data, 42 collisions involving pedestrians were identified and considered in this study.

Each vehicle was equipped with a forward-facing camera, an accelerometer sampling at 20 Hz, and GPS.

Video Review
Video of each collision was reviewed and agreed upon by two of the authors to determine several, mostly qualitative factors associated with the collision event. Specifically, the nature of the vehicle engagement with the pedestrian (frontal strike, sideswipe, side collision, rear strike), the location on the vehicle of the initial contact (e.g., front left, right front, rear), the relative direction of engagement between the pedestrian and vehicle (i.e., perpendicular vs. parallel), whether the pedestrian engaged with side structures of the vehicle, how many pedestrians were involved in the collision event, and whether the pedestrian was knocked down were all evaluated. These data were utilized as part of the ensuing analysis leveraging the on-board sensor data.

Vehicle Impact Speed Determination
To make an injury risk assessment, vehicle impact speed measurements were required (a key input to the injury risk function evaluation). A vehicle speed measurement was provided via the GPS sensor. However, the GPS speed had

inconsistent sampling and limited resolution. Accordingly, the GPS speed was coupled with accelerometer data. Accelerometer data was available for all cases with either a low pass filter at 0.5 Hz or 5 Hz applied to the data. The traces filtered at 5 Hz were used for this analysis considering collision events because the jerk associated with vehicle hard braking was captured with this signal and not smoothed as part of the filtering process like it was for the 0.5 Hz data. A series of steps were required to (a) correct for inconsistent sensor orientation within the vehicle and (b) align the speed and accelerometer data due to asynchronous data collection. These steps to generate a single, corrected vehicle speed are covered in the subsequent subsections.

Sensor Orientation Correction The installed dash cams used in this study were found to have considerable variability in their orientation within the vehicle. Specifically, although the dash camera unit was oriented largely in the forward direction, there was some notable pitch as evidenced by non-zero acceleration z-direction (upwards and downwards; after correcting for acceleration due to gravity) while the equipped vehicle was stopped. To correct for this pitch, a correction routine was applied. This routine assumed that the true signal for longitudinal vehicle acceleration ($acc_{x, corrected}$) was measured in part by the longitudinal and vertical accelerometer data as shown in Equation 1, where θ corresponds to the angular pitch offset of the sensor with respect to the z-direction being up and down.

$$acc_{x, corrected} = acc_x cos(\theta) + acc_z sin(\theta) \qquad \text{Equation (1)}$$

Further, any periods of time during which the vehicle was not accelerating (i.e., constant travel speed or a stopped vehicle) the x-component as measured by the accelerometer should be approximately equal to 0 as well. By integrating over these time periods (where both the change in velocity in the x and z directions should be zero; equation 2), an estimate of the sensor pitch (θ) can be determined (Equation 3).

$$0 = \int acc_x cos(\theta)dt + \int acc_z sin(\theta)dt \qquad \text{Equation (2)}$$

$$tan(\theta) = -\frac{dv_x}{dv_z} \qquad \text{Equation (3)}$$

With the sensor pitch defined, the longitudinal vehicle acceleration could be calculated using the x and z accelerometer signals.

Speed and Acceleration Optimization Given the lower sampling rate for the speed data from the GPS, the accelerometer data were leveraged, through integration, to generate a higher sampling rate speed vector. The accelerometer and GPS data were collected asynchronously from one another, which prevented straightforward integration. A global optimization routine was used to perform a temporal correction on these data to align the GPS speed and accelerometer data for each case. An iterative routine was carried out that applied a temporal shift to the accelerometer data prior to integrating to generate velocity values. These velocity values were then compared to those provided by the GPS data, and the difference between the integrated accelerometer speed and the GPS speed represented integration drift, or the error in the velocity signal. The time shift that minimized the velocity error was selected as the optimal outcome and was saved for continued data analysis.

The accelerometer data were used to calculate what the expected velocity would be based on the mean acceleration between two time points and the preceding known velocity. At the unique velocities extracted from the GPS data, the error between the measured and expected velocities was calculated. Lastly, as shown in Equation 4, the corrected vehicle speed ($v_{corrected, i}$) was calculated at successive time points using the expected speed for that time point ($v_{expected, i}$) in conjunction with a time-scaled version of the calculated velocity error ($Error_j$). To account for noise associated with small velocity values, all velocity values below 0.5 mph were set to 0 mph.

$$v_{corrected, i} = v_{expected, i} + Error_j * \frac{t_i - t_{j-1}}{t_j - t_{j-1}} \qquad \text{Equation (4)}$$

where i is as defined above and represents indexing over the entire length of the velocity trace and j represents indexing over the vector of unique velocity values. Thus, at all times when $t_i = t_j$, no time-scaling was necessary and the corrected velocity reduces to the sum of the expected velocity and the error term. This method also ensures that the corrected speed was equal to the GPS speed at each of the unique velocity value timepoints previously identified. This optimization process was repeated for each time shift evaluated (increments of 0.05 s), and the temporal shift which resulted in the minimum mean absolute velocity error was selected as the optimized version to carry forward in analysis. An example of the results of the optimization process is shown in Figure 1.
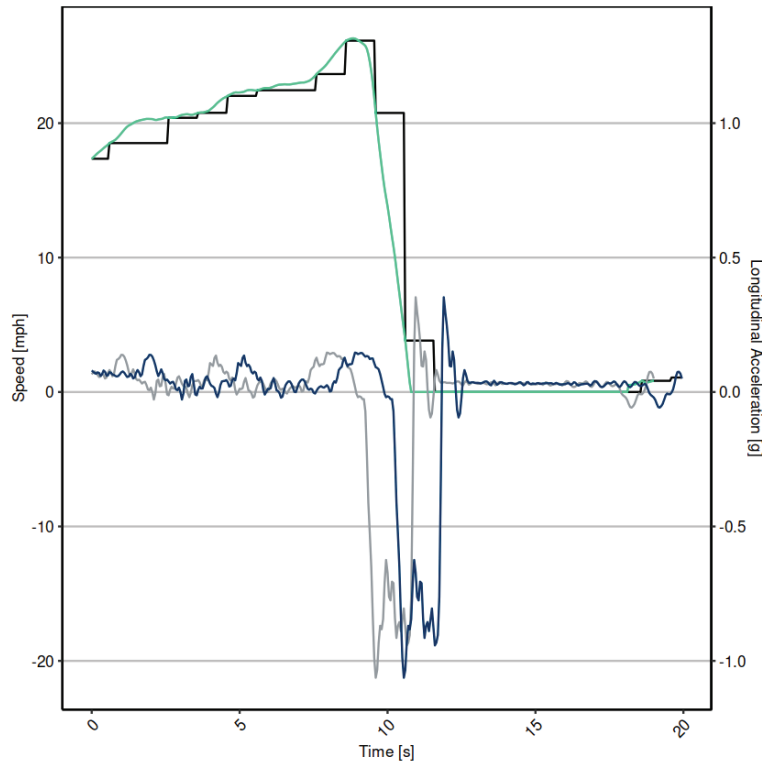

Figure 1. Exemplar sensor optimization trace. Gray line represents original longitudinal vehicle acceleration, dark blue line represents time-shifted longitudinal vehicle acceleration, black line represents GPS speed, and green line represents the corrected vehicle velocity trace.

Impact Speed Determination The final step in determining vehicle impact speed was to align the video with the imputed vehicle speed. Key, easily identifiable kinematic time points from the video were associated to kinematic signatures from the vehicle speed time series. Depending on the specific collision, different alignment routines were applied. In all collisions, two video frames were identified: the frame associated with vehicle impact and a frame associated with key vehicle kinematics (e.g., vehicle start/stop, hard braking [> 0.2 g]; see Table 1). These key frames were then mapped to the processed vehicle speed kinematics outlined above to determine vehicle speed at impact. Given the video frame rate (4 Hz), the exact time of impact was generally not captured. Accordingly, the nearest frame preceding collision was used. The speed at the time point closest to this time was taken to be the vehicle impact speed. All collision videos were sampled at 4 frames per second and were 20 or 30 seconds in length. Individual frames were extracted from downloaded collision videos using ffmpeg (ffmpeg.org).

Table 1.

Vehicle kinematics used for key frame for determination of vehicle speed at impact and description of how specific frame was defined

Vehicle Kinematics	Description
Vehicle stop	Vehicle stop was determined based on video-observed braking to a stop. With the available vehicle speed data collected by the accelerometers, the time point at which the vehicle's speed first achieved a value of 0 mph was found. The nth stop was used, with the time associated with the beginning of each stop found using the accelerometer data.
Minimum/maximum speed	When a kinematic visual cue was not available, the vehicle's minimum or maximum speed was used as a reference point. This method required an iterative process involving simultaneous review of the accelerometer data and collision video. The time point in the accelerometer data associated with either the highest or lowest vehicle speed was found.
Start from first stop	The vehicle was at rest prior to accelerating and then involved in a collision. The frame associated with vehicle motion following this stop was used in conjunction with the impact frame. The accelerometer data was first used to find the time at which the vehicle first comes to rest. Then, the first time point following that at which the vehicle was moving is determined to be the time associated with the start from first stop.
Hard braking (> 0.2 g)	There was a defined spike in the vehicle's accelerometer pulse associated with deceleration that occurred either prior to or after the collision. The time point in the accelerometer data associated with vehicle braking exceeding 0.2 g was found.
Vehicle in reverse	Visual confirmation of impact was not possible given that the available video footage was for the forward-facing camera only. For this situation, the frame at which the vehicle began to reverse and the frame in which the vehicle came to rest were identified. In these instances, the maximum speed observed in the accelerometer data during this time window (i.e., the time of reversal) was taken to be the estimate for vehicle impact speed.
Last frame	The collision occurred near the end of the video and no specific vehicle kinematics could be ascertained (e.g., vehicle did not come to rest before end of video). The number of video frames between collision and the end of the video were used to determine the time of impact, and thus the vehicle's speed at impact.

While most collision events were frontal impacts, some involved engagement with side vehicle structures instead of the front bumper structure. To account for decreased engagement between the pedestrian and vehicle during these side impacts, a correction factor - representing a decrease in the impulse experienced by the pedestrian - was applied to the determined impact speed for these collisions based on previous work. This correction factor was based on Neale et al.'s photogrammetric analysis of video recordings of pedestrian sideswipe and minor overlap impact events [20]. In their work, vehicle speed at impact was computed for each event and compared to the predicted vehicle impact speed based on measured pedestrian projection distance. Level of engagement with the vehicle was found to vary depending on the nature of the collision and was lower than would be expected in a frontal collision [21]. Correction factors to the vehicle impact speed for these projection models were presented to account for the decreased impulse experienced by the pedestrian during the collision event. For this study, a scaling factor of 1.5 was applied for collisions involving side contact to account for this decrease in engagement (i.e., a side collision at 15 mph would be modeled as if it were a 10 mph frontal collision).

Injury Severity Assessment

This study relied on previously published injury risk curves by Lubbe et al. to translate the computed impact speed to a probability of injury based on severity of injury as defined by the 2015 revision of the Abbreviated Injury Scale (AIS) [22]. The AIS is an internationally recognized scale that scores injuries, considering "energy dissipation, tissue damage, treatment, impairment, and quality of life [22]." Lubbe et al. developed an injury risk function relating vehicle closing speed and pedestrian age to AIS2+, AIS3+, and fatal injury outcomes for frontal collisions involving pedestrians based on data from the German In-Depth Accident Study (GIDAS) [23]. The dataset used to develop the injury risk functions only consisted of collisions involving passenger vehicles; accordingly, vehicle mass/weight for the vehicles included in the SmartDrive dataset as part of this study was not considered. Lubbe et al.'s study considered pedestrians aged 15 and older. An average risk curve was fit using logistic regression based on the weighted distribution of pedestrians age 15+ in the Crash Report Sampling System (CRSS) to simplify evaluation of injury risk to only be dependent on speed. It should be noted that pedestrian speed was not considered as part of this analysis as it was assumed that the pedestrian's motion would not be expected to contribute substantially to the injury risk. Accordingly, vehicle speed at impact (v) was used for injury risk assessment instead of closing speed. These relationships are summarized in Equations 5, 6, and 7.

$$p(AIS2+) = 1/(1 + e^{1.824 - 0.060*v}) \qquad \text{Equation (5)}$$

$$p(AIS3+) = 1/(1 + e^{4.257 - 0.073*v}) \qquad \text{Equation (6)}$$

$$p(Fatal) = 1/(1 + e^{7.000 - 0.087*v}) \qquad \text{Equation (7)}$$

RESULTS

In general, most collisions in this dataset (34 out of 42) involved frontal vehicle structures (Figure 2). This is consistent with previous research of field crash data, which has shown that the frontal collision mode is the most common and most injurious [23]. The overall crash rate for this dataset was 0.63 collisions per million miles.

| 12 | 11 | 11 |

Front Axle

4
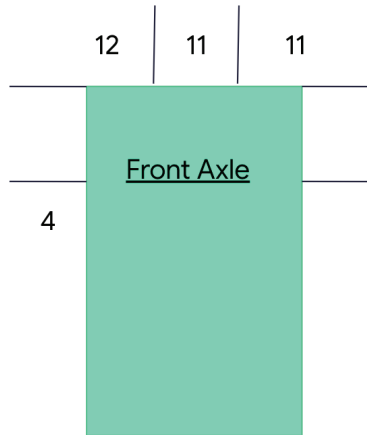
*2 sideswipes and 1
rear collision as well

Figure 2. Distribution of collision counts by impact location on vehicle

Vehicle impact speeds into the pedestrians varied from 1.5 mph to 38 mph. More than half of all events had an impact speed less than 10 mph and nearly all (38 out of 42) events had an impact speed less than 20 mph (Figures 3 and 4). The pedestrian collision events were associated with a wide range of MAIS2+ injury risk probabilities, from as low as 12% up to 85%. The majority of events were associated with an MAIS3+ injury risk probability below 10%, with only 5 events exceeding 10% and 2 exceeding 50% MAIS3+ injury risk (Figure 3). Almost all events were associated with a very low probability of fatal injury (Figure 4). Summed MAIS2+, MAIS3+, and fatal injury risk for this dataset totaled approximately 14, 3, and 0.5, respectively. In other words, given objective injury

outcome data for the pedestrians involved in these collisions, it would be expected that approximately 14 would sustain MAIS2+ injuries, approximately 3 would sustain MAIS3+ injuries, and approximately 0.5 would sustain fatal injuries. These expected injury outcomes may also be calculated as a measure of mileage in order to more accurately compare across datasets. For this dataset, we would expect to see a moderate or greater injury (MAIS2+) every 4.6 million miles, a serious or greater injury (MAIS3+) every 20 million miles, and a fatal injury (MAIS5+) every 128 million miles.

Figure 3. Distribution of events and MAIS3+ injury risk as a function of impact speed. Nearly all events were associated with an impact speed of less than 20 mph.

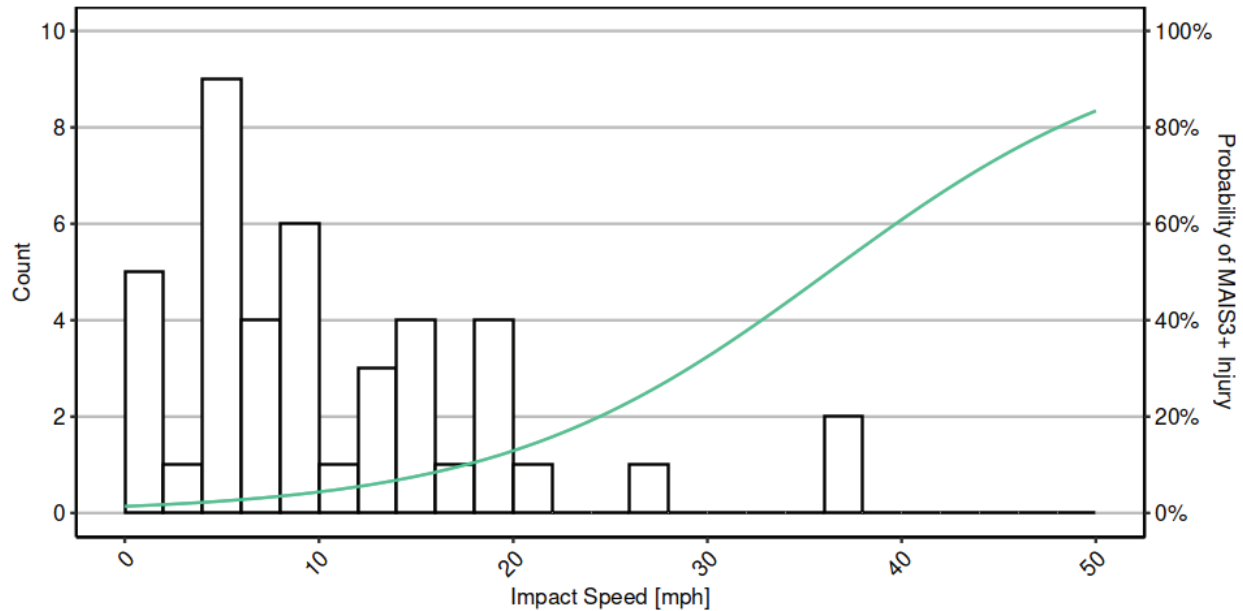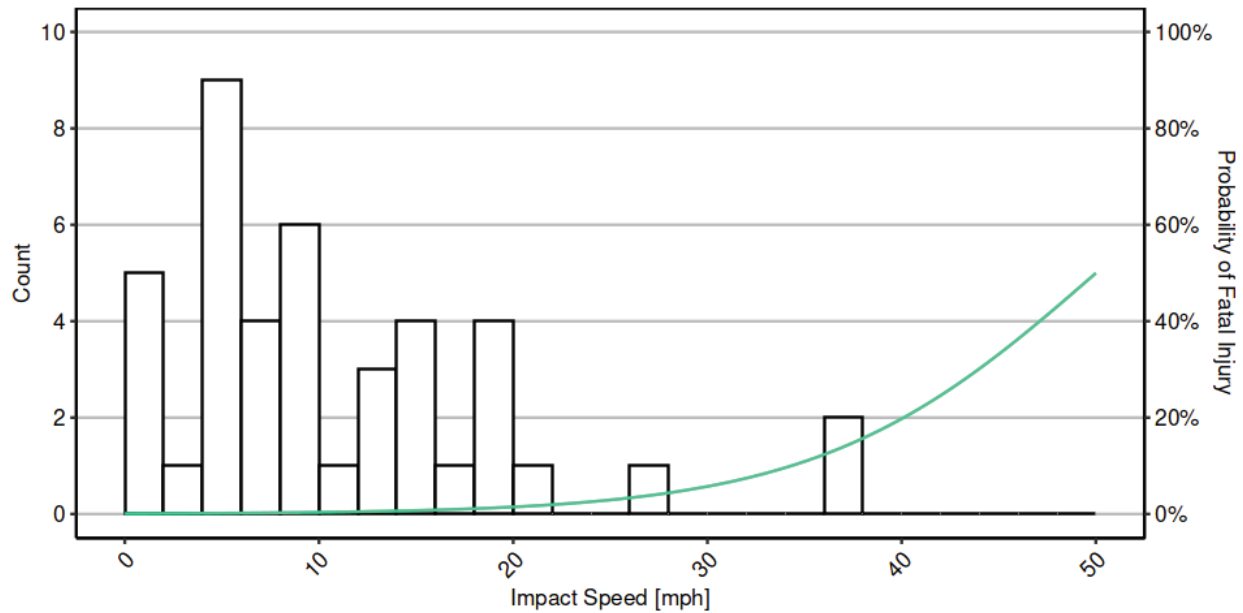**Figure 4. Distribution of events and fatal injury risk as a function of impact speed. Nearly all events were associated with a fatal injury risk probability near zero.**

Impact speed was also observed to vary by vehicle turning behavior. Many of the collision events in this representative dataset occurred at an intersection, and of those events, left and right turning was frequently observed.

A wide range of vehicle impact speeds was observed for situations in which the vehicle was traveling straight prior to the collision (Figure 5). In general, the act of turning prior to the collision led to lower traveling speeds, and accordingly, generally lower impact speeds. Additionally, narrower speed windows were observed when the vehicle was turning. Specifically, impact speeds associated with the vehicle making a right turn were all below 10 mph, while impact speeds associated with the vehicle making a left turn ranged from below 10 mph to over 20 mph (Figure 5).
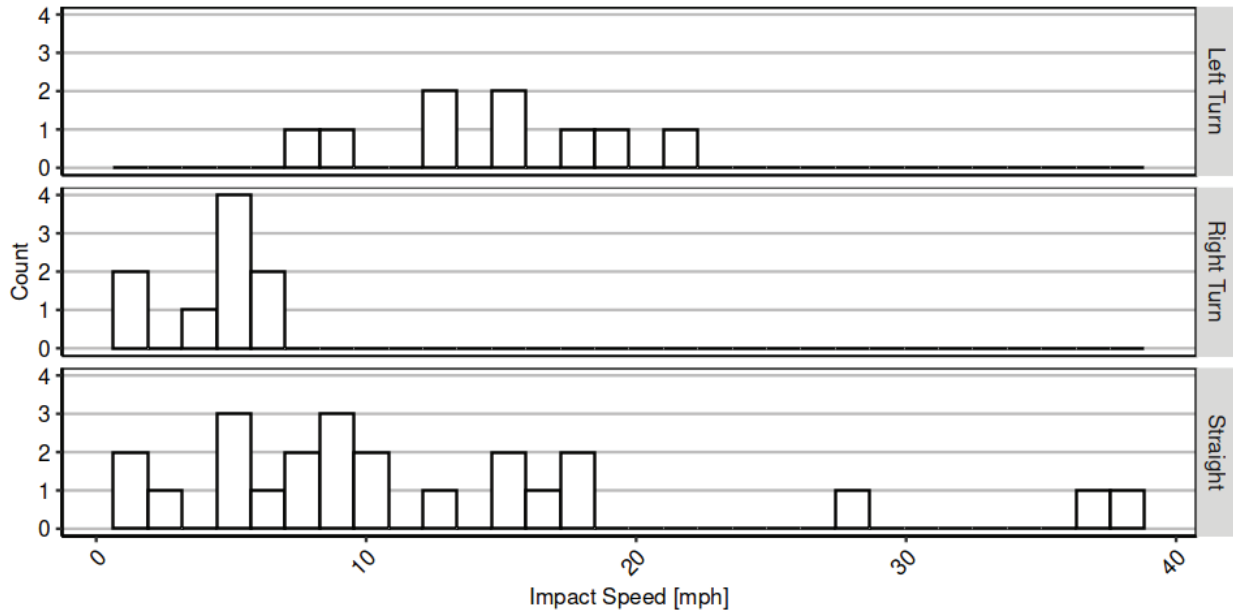
Figure 5. Distribution of events as a function of impact speed by vehicle travel behavior at the time of collision.

Pedestrian knock-down risk was also explored. Using the available collision video, only collisions with known impact speeds and knock pedestrian knock-down status were included as part of this analysis (i.e., cases where the video cut off or the pedestrian was out of frame after the collision event were excluded). Leveraging the assigned knock-over status based on review of the collision videos, a logistic regression model was developed to estimate risk of pedestrian knock-over as a function of collision speed. A 10% risk of knockdown was observed to occur at 2.8 mph (Figure 6). It should also be noted that in collisions with impact speeds above 10 mph, all pedestrians were knocked over.

Figure 6. Pedestrian knock-over risk as a function of impact speed. Events were evaluated binarily, as knock-over (1, 100%) or no knock-over (0, 0%).

DISCUSSION

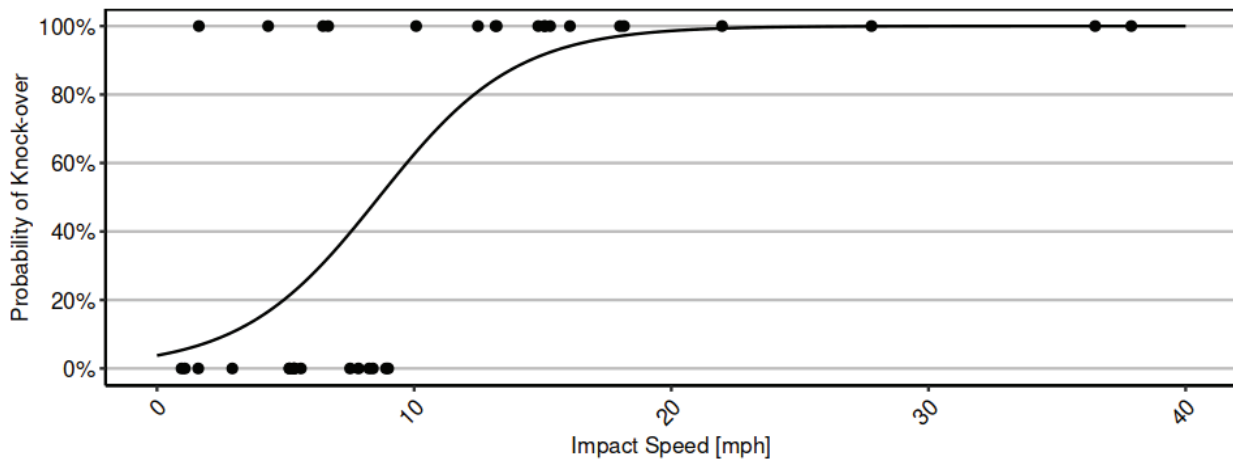Using the dash cam video and sensor data, impact speed was successfully extracted for all 42 pedestrian impact events considered in this study. Nearly all the events involved collision with the front portion of the vehicle, which enabled the impact to be readily identified and associated to the imputed vehicle speed. The outcome of this analysis is a representative dataset of collisions with corresponding injury from surface streets in Los Angeles, California.

In general, the number of injured persons in collisions may be lowered through reduction in the number of collisions, reduction in the severity of the collisions, and/or reduction in the injury risk associated with a given collision severity [24]. The present study offers insight into the severity of existing collisions and the predicted injury risk associated with them. One challenge in evaluating ADS technology is that retrospective safety benefits using in-field driving are typically established using historical crash outcomes, where a decrease in injury outcomes is used as evidence of safety impact [25-29]. Injuries, however, are relatively rare, which makes any statistical assertions using high severity outcomes alone require an extreme number of miles (e.g., billions of miles to prove a reduction in fatal injury outcomes) [30-31].

Injury outcomes are rare, but the conditions for creating those outcomes are considerably more frequent. Scanlon et al. (2021 and 2022) showed it was not uncommon for serious or greater (MAIS3+) injury risk to be below 25% in reconstructed cases where a fatality was observed [32-33]. This is illustrative of the probabilistic nature of injuries, where the conditions for injuries to occur are more common than the occurrence of the injury itself. Looking at the current study, although it comprises only 66 million miles worth of driving, several events had serious or greater (MAIS3+) injury risk over 10%. As an alternative to measuring serious injury, or worse, outcomes, measuring the frequency of the high severity potential conditions can be used as an early signal when evaluating safety benefits. For example, ISO 26262 uses the "S" severity grading scale using 10% risk of various AIS level probabilities (MAIS 1+, 3+, 5+) to bucket events according to injury risk in functional safety applications [34]. Relying on this probabilistic injury risk, rather than the occurrence of the injury, should theoretically provide earlier evidence of what safety impact is being achieved. These individual event injury risk predictions may be additionally leveraged by summing across all events to determine some measure of the overall expected injury outcome rate. Using this approach, the cumulative injury risk is being assessed, where one event with 50% probability of injury is treated equally as five events with a 10% probability of injury. This has previously been done in the field of automotive safety and sports head impact research [35-41] Scanlon 2017, Scanlon 2016]. As stated above, for the pedestrians involved in the collisions in this dataset, it would be expected that approximately 3 would sustain serious or greater injury (MAIS3+) injuries or that a similar injury would be expected to occur every 20 million miles of driving. These mileage-adjusted injury rates would be the metrics of interest when comparing human driving data with simulated or real collision data for autonomous vehicles in order to determine relative driving performance or in comparing across different ODDs.

Overall, the impact speeds were observed to follow a multimodal distribution (Figure 3). Controlling for turning behavior substantially limited outcome severity magnitude and variability, which clearly indicates the influence of turning on collision impact speed and, accordingly, injury risk. In most cases where vehicles were making right turns from a stop and did not accelerate to speed prior to engaging with a pedestrian; conversely, vehicles making left turns often engaged with the pedestrian when they were nearly complete with the left turn, after having traveled a greater distance and thus having a greater opportunity to achieve higher vehicle speed at impact. These observations are consistent with vehicle-to-vehicle intersection collisions in the United States, where impact speeds are dependent on turning behavior and stopping behavior [35, 39, 42-43]. Turning while traveling through intersections (without coming to a complete or rolling stop) notably features a general slowing prior to the turn with a generally constant speed during travel through the intersection.

For this dataset, there was a larger proportion of events associated with impact speeds between 5 and 10 mph than between 0 and 5 mph. This sort of distribution is also observed in intersection cross-traffic, where a severity risk "cliff" exists at the borderline of a small overlap strike and a near-miss (an analogous example of this risk cliff would be stepping in front of a moving train). It is also believed that low severity impacts are more easily avoidable by pedestrians. Although not explicitly examined in the current study, postural changes and evasive action were found to limit engagement between the pedestrian and vehicle at lower speeds. Several cases in this dataset included

instances of pedestrian adjustment to avoid or mitigate energy transfer during the collision, which was commonly observed as a rapid juke away from the approaching vehicle sometimes with outstretched arms that engaged the forward structures of the vehicle. This sort of complexity when developing injury risk curves is not commonly captured in the absence of first hand video footage. Additionally, these events are subject to underreporting given that the maneuvering can serve to prevent and mitigate a potential injury. Previous research reviewing video of pedestrian-to-vehicle collision events has shown that nearly two-thirds of pedestrians take avoidance action prior to the collision event [44]. This observed pedestrian avoidance action clearly plays a role in the level of engagement and potential injury risk for pedestrian collisions. Incorporation of this feature into the severity evaluation of observed collisions should be explored.

Review of the collision videos highlighted the effect of factors such as pedestrian age and pre-impact posture as also likely playing a role in pedestrian knock-down. At these lower speeds in which the pedestrians were knocked down, injury would primarily be expected to occur due to falling from standing height to the ground rather than from engaging with vehicle structures. An in-depth review of 100 pedestrian-to-vehicle collision in Paris, France showed that contact with the ground was the source of injury for over a quarter of all impacts with impact speeds less than 31 mph (50 kph) and more than half of all impacts with speeds below 18.6 mph (30 kph) [4].

Limitations
There are several limitations of this work that should be noted. Firstly, there were differences in sampling frequency for the GPS, accelerometers, and camera such that the original data were not synchronized. Corrections and temporal shifts were applied to the data to minimize error in computed impact speeds as part of the collision reconstruction. Secondly, pedestrian speed was not considered as part of this analysis; however, nearly all impacts involved a perpendicular collision between a vehicle and a pedestrian, and the pedestrian's motion would not be expected to contribute substantially to the injury risk.

There are also some notable limitations with the utilized injury risk model that may influence the accuracy of any individual risk estimation. First, only frontal collisions are considered. Use of this function for side impacts and rear collisions may result in some unquantified deviation from actual risk. Second, this data was developed using German crash data from 1999 to 2020. Differences in the composition of this fleet with respect to the current United States fleet may lead to some unquantified accuracy deviations. Third, for a case to be included in the dataset, the pedestrian must be suspected of having experienced some injury. It is common for police-reported pedestrian data to almost always have an associated pedestrian injury, so this data requirement is unsurprising. Still, collisions without an injury are not considered, resulting in data censoring and low-end risk offsets.

CONCLUSIONS

Assessing injury severity for collisions involving VRUs is highly impactful for the continued development of traffic safety, including ADAS, ADS, and roadway design. Using naturalistic VRU collision data collected from dashboard cameras, a methodology for assessing event severity by pairing accelerometer and GPS data with video to compute impact speed was presented. This is the first known analysis of pedestrian severity distributions using a naturalistic US database. The methods presented in this study may be applied to larger datasets or other sensing systems to enable further ODD-specific modeling of the current crash population.

REFERENCES

[1] National Center for Statistics and Analysis. (2021). Pedestrians: 2019 data (Traffic Safety Facts. Report No. DOT HS 813 079). National Highway Traffic Safety Administration.
[2] Martin, J. L., & Wu, D. (2018). Pedestrian fatality and impact speed squared: Cloglog modeling from French national data. *Traffic injury prevention*, 19(1), 94-101.
[3] European Commission (2021) Road safety thematic report – Pedestrians. European Road Safety Observatory. Brussels, European Commission, Directorate General for Transport.
[4] Guillaume, A., Hermitte, T., Hervé, V., & Fricheteau, R. (2015). Car or ground: which causes more pedestrian injuries. In *24th International Technical Conference Enhanced Safety Vehicle*.
[5] Davis, G. A. (2001). Relating severity of pedestrian injury to impact speed in vehicle-pedestrian crashes: Simple threshold model. *Transportation research record*, 1773(1), 108-113.

[6] Niebuhr, T., Junge, M., & Achmus, S. (2013). Pedestrian injury risk functions based on contour lines of equal injury severity using real world pedestrian/passenger-car accident data. *Annals of advances in automotive medicine*, 57, 145.

[7] Richards, D. C. (2010). Relationship between speed and risk of fatal injury: pedestrians and car occupants. Department for Transport: London.

[8] Rosén, E., & Sander, U. (2009). Pedestrian fatality risk as a function of car impact speed. *Accident analysis & prevention*, 41(3), 536-542.

[9] Saadé, J., Cuny, S., Labrousse, M., Song, E., Chauvel, C., & Chrétien, P. (2020). Pedestrian injuries and vehicles-related risk factors in car-to-pedestrian frontal collisions. In *Proceedings of the 2020 IRCOBI Conference* (pp. 278-289). Munich: IRCOBI.

[10] Tefft, B. C. (2011). Impact speed and a pedestrian's risk of severe injury or death. AAA Foundation for Traffic Safety.

[11] Otte, D., Jänsch, M., & Haasper, C. (2012). Injury protection and accident causation parameters for vulnerable road users based on German In-Depth Accident Study GIDAS. *Accident analysis & prevention*, 44(1), 149-153.

[12] Badea-Romero, A., & Lenard, J. (2013). Source of head injury for pedestrians and pedal cyclists: Striking vehicle or road?. *Accident analysis & prevention*, 50, 1140-1150.

[13] Fredriksson, R., Rosén, E., & Kullgren, A. (2010). Priorities of pedestrian protection—a real-life study of severe injuries and car sources. *Accident analysis & prevention*, 42(6), 1672-1681.

[14] Mallory, A., Fredriksson, R., Rosén, E., & Donnelly, B. (2012). Pedestrian injuries by source: serious and disabling injuries in US and European cases. In *Annals of Advances in Automotive Medicine/Annual Scientific Conference* (Vol. 56, p. 13).

[15] Chidester, A. B., & Isenberg, R. A. (2001). The pedestrian crash data study. In *Proceedings: International Technical Conference on the Enhanced Safety of Vehicles* (Vol. 2001, pp. 12-p). National Highway Traffic Safety Administration.

[16] Chung, Y. (2018). Injury severity analysis in taxi-pedestrian crashes: An application of reconstructed crash data using a vehicle black box. *Accident analysis & prevention*, 111, 345-353.

[17] *Phoenix*. Waymo. Retrieved December 5, 2022, from https://waymo.com/phx/

[18] *Waypoint - the official waymo blog: Taking our next step in the city by the Bay*. Waypoint – The official Waymo blog. (2022, March 30). Retrieved December 5, 2022, from
https://blog.waymo.com/2022/03/taking-our-next-step-in-city-by-bay.html

[19] US Census Bureau. (2010). 2010 TIGER/Line® Shapefiles Technical Documentation.

[20] Neale, W. T., Danaher, D., Donaldson, A., & Smith, T. (2021). Pedestrian Impact Analysis of Side-Swipe and Minor Overlap Conditions. *SAE Technical Paper*, 01-0881.

[21] Toor, A., & Araszewski, M. (2003). Theoretical vs. empirical solutions for vehicle/pedestrian collisions. *SAE transactions*, 853-865.

[22] Association for the Advancement of Automotive Medicine. (2016). The Abbreviated Injury Scale: 2015 Revision. Chicago, IL: AAAM.

[23] Lubbe, N., Wu, Y., & Jeppsson, H. (2022). Safe speeds: fatality and injury risks of pedestrians, cyclists, motorcyclists, and car drivers impacting the front of another passenger car as a function of closing speed and age. *Traffic Safety Research*, 2.

[24] Kullgren, A. (2008). Dose-response models and EDR data for assessment of injury risk and effectiveness of safety systems. In *Proc of Int. IRCOBI Conf., Bern, Switzerland* (pp. 3-14).

[25] Blower, D., & Woodrooffe, J. (2013). *Real-World Safety Effect of Roll Stability Control* (No. 2013-01-2392). SAE Technical Paper.

[26] Cicchino, J. B. (2017). Effectiveness of forward collision warning and autonomous emergency braking systems in reducing front-to-rear crash rates. *Accident analysis & prevention*, 99, 142-152.

[27] Isaksson-Hellman, I., & Lindman, M. (2015). Real-world performance of city safety based on Swedish insurance data. In *24th international technical conference on the enhanced safety of vehicles (ESV)* (Vol. 8, pp. 15-0121).

[28] Partnership for Analytics Research in Traffic Safety (2022). *Real-world Effectiveness of Model Year 2015–2020 Advanced Driver Assistance Systems*. The MITRE Corporation.

[29] Riexinger, L., Sherony, R., & Gabler, H. (2019). *Has Electronic Stability Control Reduced Rollover Crashes?* (No.2019-01-1022). SAE Technical Paper.

[30] Kalra, N., & Paddock, S. M. (2016). Driving to safety: How many miles of driving would it take to demonstrate autonomous vehicle reliability?. *Transportation Research Part A: Policy and Practice*, 94, 182-193.

[31] Lindman, M., Isaksson-Hellman, I., & Strandroth, J. (2017). Basic numbers needed to understand the traffic safety effect of automated cars. In *Proceedings of the 2017 IRCOBI Conference* (pp. 1-12).

[32] Scanlon, J. M., Kusano, K. D., Daniel, T., Alderson, C., Ogle, A., & Victor, T. (2021). Waymo simulated driving behavior in reconstructed fatal crashes within an autonomous vehicle operating domain. *Accident Analysis & Prevention*, 163, 106454.

[33] Scanlon J. M., Kusano, K. D., Engstrom, J., & Victor, T. (2022). Collision Avoidance Effectiveness of an Automated Driving System Using a Human Driver Behavior Reference Model in Reconstructed Fatal Collisions.

[34] International Organization for Standardization. (2018). 26262-3: 2018. Road vehicles—Functional safety—Part 3: Concept phase.

[35] Bareiss, M., Scanlon, J., Sherony, R., & Gabler, H. C. (2019). Crash and injury prevention estimates for intersection driver assistance systems in left turn across path/opposite direction crashes in the United States. *Traffic injury prevention*, 20(sup1), S133-S138.

[36] Campolettano, E. T., Gellner, R. A., Sproule, D. W., Begonia, M. T., & Rowson, S. (2020). Quantifying youth football helmet performance: assessing linear and rotational head acceleration. *Annals of biomedical engineering*, *48*(6), 1640-1650.

[37] Kusano, K. D., & Gabler, H. C. (2012). Safety benefits of forward collision warning, brake assist, and autonomous braking systems in rear-end collisions. *IEEE Transactions on Intelligent Transportation Systems*, *13*(4), 1546-1555.

[38] Scanlon, J. M., Kusano, K. D., & Gabler, H. C. (2016). Lane departure warning and prevention systems in the US vehicle fleet: Influence of roadway characteristics on potential safety benefits. *Transportation Research Record*, *2559*(1), 17-23.

[39] Scanlon, J. M., Sherony, R., & Gabler, H. C. (2017). Injury mitigation estimates for an intersection driver assistance system in straight crossing path crashes in the United States. *Traffic injury prevention*, 18(sup1), S9-S17.

[40] Stemper, B. D., Shah, A. S., Harezlak, J., Rowson, S., Mihalik, J. P., Duma, S. M., et al. (2019). Comparison of head impact exposure between concussed football athletes and matched controls: evidence for a possible second mechanism of sport-related concussion. *Annals of biomedical engineering*, *47*(10), 2057-2072.

[41] Urban, J. E., Davenport, E. M., Golman, A. J., Maldjian, J. A., Whitlow, C. T., Powers, A. K., & Stitzel, J. D. (2013). Head impact exposure in youth football: high school ages 14 to 18 years and cumulative impact analysis. *Annals of biomedical engineering*, *41*(12), 2474-2487.

[42] Scanlon, J. M., Sherony, R., & Gabler, H. C. (2017). Models of driver acceleration behavior prior to real-world intersection crashes. *IEEE Transactions on intelligent transportation systems*, 19(3), 774-786.

[43] Scanlon, J. M. (2017). *Evaluating the Potential of an Intersection Driver Assistance System to Prevent US Intersection Crashes* (Doctoral dissertation, Virginia Tech).

[44] Han, Y., Li, Q., He, W., Wan, F., Wang, B., & Mizuno, K. (2017). Analysis of vulnerable road user kinematics before/during/after vehicle collisions based on video records. In *IRCOBI Conference, Antwerp, Belgium* (pp. 13-15).

THE KNOWLEDGE FOR TOMORROW'S ROAD SAFETY BASES ON HARMONISED DATA - THE GLOBAL SAFETY DATABASE DOES ITS CONTRIBUTION

Johann Ziegler
Institute for Traffic Accident Research at Dresden University of Technology (VUFO)
Germany

Michael Düring
Germany

Michael Wagner
Germany

Paper Number 23-0086

ABSTRACT

Road traffic accidents remain to be a leading cause of death worldwide with nearly 1.3 million fatalities each year (WHO Global status report on road safety 2018) [1]. To develop safety systems according to real-world challenges, harmonized information is needed. Therefore, vehicle and road traffic safety experts are constantly looking for real-world data to answer the open challenges and to ultimately reach the "Vision Zero".

Numerous data on road traffic accidents exist and can be split into national and in-depth databases. The latter are characterized by a significantly lower number of cases then the national databases but a substantially higher level of detail and enable a microscopic view on the accident scenario.

By using in-depth databases, new safety systems may be developed and validated. The results of analyses are extrapolated to assess the impact on road safety for a specific country, continent or even for the whole world. However, it is not always obvious which database is suitable for which type of development approach or extrapolation.

The Global Safety Database (GSD) [2] solves this issue by offering access to a one of its kind up-to-date worldwide collection of road traffic accident statistics and database on a meta-data level. In addition to the objective evaluation of databases by matching them to research questions, the GSD also provides knowledge on the representativeness of each database. In order to identify similarities and differences in road safety within the countries, the latest publication of the Global Status Report on Road Safety from 2018 [1] is used to develop a clustering methodology. The goal of this method is to point out the possibilities and limitations of transferring information from the initial countries to other areas of interest.

The core of the investigation is the clustering methodology, which generates derivatives on countries or regions with similar road safety standards. The objective matching algorithm within the GSD helps to find the necessary information for the qualitative assessment of representativeness. Once the representative database within a country is identified, the clustering results are used to determine which countries represent the chosen database.

As the clustering relies on the latest Global Status Report from 2018 (and even partly from 2016), more recent data on road safety is desirable to narrow the spread to a steadily growing GSD. For a more integrated road safety approach, the GSD is also prepared to cover more topics related to road safety e.g., infrastructure or medicine. Additionally, an extension of the qualitative assessment of representativeness to a quantitative is more robust.

The clustering may be used to find derivations to the initial country and to transfer the results from these to the target countries by similarities in road traffic safety. From a global perspective, the GSD is one essential tool to push forth the worldwide harmonisation of traffic accident statistics and databases. Knowing what really happens on the roads by putting together everything we know empowers the data-driven development of safety systems and thus brings us one step closer to reach a road system without casualties – fulfilling the Vision Zero.

RESEARCH OBJECTIVE

Within the research and development on road safety, numerous interdisciplinary aspects are considered, particularly in the field of vehicle and traffic safety. The relevant issues of assisted, connected, and automated driving and the further development of passive and integral safety systems require reliable data sources. The heterogeneous traffic and accident situations in different countries and continents require taking data sources from numerous countries/regions into account. However, it is not always obvious which data source is suitable for what kind of research question or development approach.

The overall goal of the GSD is to provide a unified meta database that contains necessary information required for research and development departments on a meta based level (explicitly no raw data) for several countries. The database is designed dynamically on a platform that allows changes in the data sources to be effective immediately.

One of the main tasks is a detailed investigation on international data sources in the field of traffic and vehicle safety. This includes, but is not limited to, national road accident statistics based on police accident data as well as highly detailed investigations in smaller regions (so-called in-depth data sources).

In addition to the development of the meta database, a questionnaire is established and used to check the applicability of the developed meta database for specific questions regarding road safety. The questions are reformulated using variables which are necessary to answer the questions. An objective assessment of the meta database and the questionnaire requires developing a matching process. The aim of this matching process is to calculate the percentage of necessary variables covered in the various data sources for each question. The results of the matching process are collected in a result matrix within the GSD.

The result matrix offers a possibility for an objective assessment of data sources and provides the opportunity for data providers to improve their data quantity and data quality. Furthermore, the meta database can act as a platform to bring several data providers from different countries together and to encourage the global harmonisation of traffic accident data sources. For this purpose, a usage and management system are set up to improve and control data quality and quantity. Furthermore, it puts forth the search on new data providers and road safety experts.

In addition to the development of the database structure and user administration, the representativeness of individual data sources is examined and compared with the country-specific accident figures and investigation methods. The developed clustering procedure supports the process of searching for representatives in regions or for individual countries. The data analysis of the meta database is intended to show specificities within the data sources.

The GSD platform act as a tool to promote the global harmonisation of accident data and statistics for support the acceleration future research and development processes.

METHODS AND DATA SOURCES

Conception of the meta database
The basis for the conception of the meta database within GSD is the database structure of the interdisciplinary German In-Depth Accident Study (GIDAS) [3], one of the world's leading accident research projects. The meta database contains high-level information about the data sources and a content-related part in which available information is inventoried. Each part comprises several tables that are linked by primary keys.

The database not only contains information on the parameters and contents available in a data source, but also meta data that directly determine the suitability of the data source for certain research questions or the reliability of statements derived from it. An example of this is the representativeness of a data source, which is an elementary aspect for the usability and evaluation of data sources.

Further parameters are dedicated to the investigation methods as well as access options and costs to provide GSD users an overview of potential access paths in addition to an assessment of the usability of the content. For the derivation of exposure variables or basic figures, country-specific key figures are stored, e.g. the number of traffic acci-

dents per year, information on demographics, vehicle fleet, and infrastructure. Content-related aspects comprise tables for the accident itself, involved participants, persons, and their injuries.

Search for data sources

The investigation of data sources for road traffic accidents is specific for national databases on the one hand side and in-depth databases on the other. Regardless of the origin of the data (national or in-depth databases), the researched databases or statistics for the GSD are designated as data sources and the developed database as meta database (*Figure 1*).
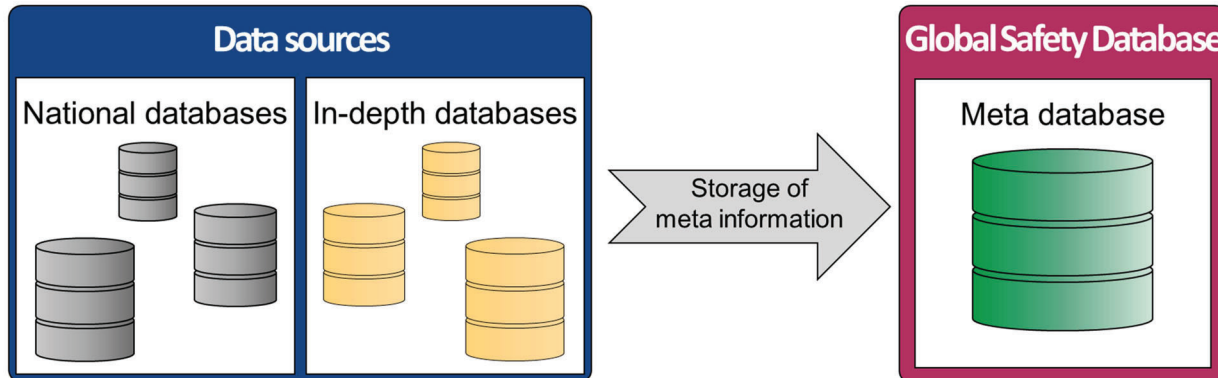

Figure 1. Scheme of the wording within the GSD

The so-called national data sources are based on data collected by the police, which consist of a large number of investigated accidents and give a macroscopic view of accident scenario. The use of a police reported data source on a national level allows a national coverage of the accident scenario and the acquisition of numerous cases.

The two main objectives of the police investigation and the national data sources is the collection of general accident-related data to gather evidence for prosecution and assessing the infrastructure safety. In-dept data sources take a different approach, in which the data providers primarily want to investigate how the accident happened without focusing on evidence subsequent prosecution.

In comparison to the national data sources, in-depth data sources are mainly characterised by a smaller number of cases, but usually by a higher level of detail in the investigation of road traffic accidents. This allows a microscopic view on the accident scenario. In contrast to the police reported accidents, the accidents of the in-depth data sources are usually investigated by accident researchers and medical experts.

The investigation for data source is based on a process that has be defined within the GSD. Figure 2 shows the process with all phases for contacting data providers and data immigration into the GSD.

Figure 2. Overview research process within GSD

Methodology of the objective assessment

A key idea of the project is being able to objectively assessment the quality of existing data sources in the GSD. A metric for evaluating the quality is defined with the suitability of the data sources for answering current and future research questions, also with a view to a practical application of the meta database.

For the object assessment of the meta database, the membering companies of the Research Association of Automotive Technology e.V. (FAT e.V.) were asked to collect questions relevant to the field of design, development, and evaluation of road safety measures. This collection of questions resulted in a questionnaire with more than 190 questions, of which 120 are research questions with content and the rest are questions about the characteristics and meta data of the researched data sources. The GSD user group has the possible to add new questions to the catalogue, which leads to a permanent growth and specification of the questionnaire.

The research questions are subsequently analyzed semantically in order to create a mapping of the content associated with the question to the variables of the meta database. The requirements for the data source contents are thus defined for each question, which are stored in binary codes at the parameter level.

Due to the basic binary coding structure of information, the linkage between questions and provided information in the meta database is based on the expertise of the user of the GSD. After translating, each "QUESTION_ID" with its coded variables is matched to each "SOURCE_ID" and its variables (Table 1).

Table 1.
Example of the questionnaire and meta database content

QUESTIONNAIRE

QUESTION_ID	VARIABLE_1	VARIABLE_2	VARIABLE_3	VARIABLE_4
1	1	1	0	1
2	0	0	0	1
3	1	1	1	1

META DATABASE

SOURCE_ID	VARIABLE_1	VARIABLE_2	VARIABLE_3	VARIABLE_4
1	1	0	1	1
2	1	1	1	1
3	0	1	0	1

The content of the result matrix indicates the percentage of the "SOURCE_ID" variables that match the necessary variables to answer the question. The result matrix (Table 2) is structured as follows:

- "QUESTION_ID" as row and

- the "SOURCE_ID" as column

A complete match between one "SOURCE_ID" and one question results in a value of 100 % (green box).

Table 2.
Example of the questionnaire and meta database content

RESULT MATRIX

QUESTION_ID	SOURCE_ID_1	SOURCE_ID_2	SOURCE_ID_3
1	2/3 = 66 %	3/3 = 100 %	2/3 = 66 %
2	2/2 = 100 %	2/2 = 100 %	1/2 = 50 %
3	3/4 = 75 %	4/4 = 100 %	2/4 = 50 %

In addition to the result matrix, the analysis of the data sources and questions as well as the matching process supports to identify important variables and labels, needed for current and future research questions. The analysing process described provides the opportunity for data providers to improve their data quantity and quality.

It should also be noted that an assessment completeness and plausibility of the actual (accident) data does not take place. This quality check and the decision whether a data source is used for an analysis even if the percentage value is low lies in the responsibility of the experienced users.

Assessment of representativeness
The representativeness is defined diversely, depending on the scientific mission and the goal to be aimed for. Within the GSD, the representativeness is defined by two key aspects:

- the existence of a "suitable" sample plan, and

- the unbiased chance of any accident to be part of data base.

A data source is representative if it is possible to draw conclusions from a sample to the totality, i.e. when certain elements of the totality have the same chance of being part of the sample. Therefore, the official road traffic accident statistics or national data sources collected by the police form the totality and represent the road accident scenario for a country or region. The sample of an in-depth data source corresponds to accident investigations in a certain region, which may also be investigated by the police, but are mostly carried out by in-depth collection units, which do not include all police-recorded accidents.

The assessment of representativeness can be determined with the statistics from official authorities as well as from the in-depth database via a quantitative methodology. The GSD with its "no raw data"-policy enables just a qualitative assessment of the in-depth data sources. For this purpose, a collection of variables is extracted from the GSD and compared to the national and the in-depth data sources of each country. The variable set can be chosen according to requirements of the analyses.

The methodology for the qualitative assessment is based on comparing the predefined variables between the national data source and the in-depth data source. In this process, it is queried whether a variable is present or not. If a variable is present in both types of data sources, it may be possible to use this variable for a representativeness assessment of the in-depth data source to the national statistics. The values within the variables are not considered in this qualitative method.

In addition to the qualitative assessment of representativeness, the data providers are also interviewed regarding the representativeness of their databases. These information as well as the result of the qualitative assessment form the variable representativeness within the GSD.

The variable "representativeness" in the GSD is defined by these parameters:

> 1 - representative for country (official statistics) without weighting
>
> 2 - representativeness possible (weighting necessary)
>
> 3 - not representative
>
> 999999 - unknown

Clustering methodology

The assessment methodology for the representativeness is used to compare national and in-depth data sources within a country. We investigate the feasibility of clustering by comparing and analyzing similarities and differences in road safety between two or more countries.

The main objective of the cluster analysis is to find out which countries have the closest similarity to a country selected for the analyses (target country) based on road safety standards. But it is not intended to carry out a full clustering calculation. The basis of the clustering method within the GSD is a simple comparison with rank assignments.

The clustering is carried out according to the following safety standards (description/category/unit) in Table 3.

Table 3.
Safety standards by category and unit

Safety standards	Category	Unit
Population density	A	[inhabitants / km²]
Gross Nation Income	B	[US dollars per capita]
Fatality rate I	C	[road deaths per 1 Mio. inhabitants]
Fatalities by road user	D	[percentage]
Vehicle rate	E	[vehicles per 1 Mio. Inhabitants]
Distribution of reg. vehicles	F	[percentage]
Fatality rate II	G	[road deaths per 1 Mio. vehicles]
Safety standards in traffic	H	[speed limitation, belt usage, helmet law]

The basis of the road safety standard is the latest WHO global status report on road safety for 2018 [1]. In total, 175 countries are mentioned in der WHO report, which are considered in the clustering process within this project. Not every country contains full information to all road safety standards. The boundary conditions for data collection by the WHO are mentioned in the report and can be found there.

In order to identify the countries with the closest similarity to regions or other countries, a ranking system is developed. A methodology checks within the safety standards which country is closest to the target region or country. The relative ratio between challenging country and target country/region identifies the deviations. The countries with the closest distance to the target earn the highest scores. The score depends on the number of countries to be compared. The average score of all safety standards results in the final rank for each challenged country. The highest average score gets the ranking position 1 and is closest to the target country.

The example of the Scandinavian countries shows which country is the closest to Norway (NOR) by using four of eight safety standards (Table 4). Depending on the three chosen safety standards, Sweden (SWE) is the closest to Norway. By using all categories of safety standards, Sweden is also the closest country to Norway.

Table 4.
Example of the clustering methodology for the Scandinavian countries

	Category: A		Score	Category: C		Score	Category: E		Score	Ø SCORE	RANK
NOR	14.1			26.31			730,307				
SWE	23.3	+65%	3	26.54	+1%	4	582,606	-20%	4	3,7	**1**
DNK	137.0	+871%	1	38.58	+47%	3	532,275	-27%	3	2,3	**3**
FIN	16.4	+16%	4	46.85	+78%	2	940,142	+29%	2	2,7	**2**
ISL	0.4	-97%	2	583.12	+2116%	1	7,673,373	+951%	1	1,3	**4**

The clustering process not only map which country is most similar to the target country. It also offers the possibility to find out which country within a region most closely represents the region. For this purpose, all countries of the chosen region are combined, and the average values of the respective safety standards is calculated based on the country-specific individual values. As an example, for Northern Europe and the Scandinavian countries, Sweden is the representative for this region after the clustering calculation.

RESULTS

Content of the meta database
In the two project phases commissioned by the FAT, 17 countries are researched in detail by national and in-depth data sources. In total, 52 data sources are found, where the half of the total is distributed between national and in-depth data sources (Table 5).

Table 5.
Number and type of data sources searched by country

Countries	Number of national data sources	Number of in-depth data sources
Australia	3	3
Brazil	1	1
China	0	2
Czechia	1	1
Denmark	2	-
France	1	1
Germany	3	9
Greece	1	1
India	1	1
Indonesia	2	0
Japan	1	1
Nigeria	2	0
Norway	1	1
Russia	1	0
South Africa	1	0
Sweden	1	2
USA	4	3
TOTAL	**26**	**26**

Additional information on other countries is recorded in the GSD fact sheet. In total the GSD contains 40 countries, where at least one national data source or one in-depth data source is mentioned. Currently, 103 individual data sources are inventoried.

Evaluation of the representativeness

For the qualitative assessment of the representativeness, a collection of variables is extracted from the GSD and compared for the national as well as for the in-depth data sources for each chosen country. The variable set can be chosen according to requirements of the analyses. Within this project, the following variables from the GSD were selected for the qualitative assessment (Table 6). These variables can be used for the general description of an accident.

Table 6.
Variables set from the GSD for the qualitative assessment of the representativeness

Variable description	Variable GSD	Classification
Accident month	ACCMONTH	
Weekday	WDAY	
Daytime	DAYTIME	
Accident location	LOCATION	Accident data
Maximum accident severity	ACCSEVERITY	
Accident type	ACCTYPE	
Number of participants	NR_PARTICIPANTS	

Due to a lack of information provided by the data provider or due non-collection of data some countries (e.g., Germany, Greece, France, Czech Republic, USA, Brazil, Australia) have better preconditions than other countries (e.g., Sweden, India, Norway, Japan). Consequently, the qualitative assessment is only carried out for the first seven mentioned countries (Table 7). For the methodological example, only one in-depth data source per country has been compared with the national database.

Table 7.
Example for the qualitative assessment of national data sources and In-Dept data sources

Country	Type of database	ACCMONTH	WDAY	DAYTIME	LOCATION	ACCSEVERITY	ACCTYPE	NR_PARTICIPANTS	Total	Share of Matches
GERMANY	National data source	1	1	1	1	1	1	1	7	
	In-depth data source	1	1	1	1	1	1	1	7	7/7 = **100%**
GREECE	National data source	1	1	1	1	1	1	1	7	
	In-depth data source	1	1	1	1	1	1	1	7	7/7 = **100%**
FRANCE	National data source	1	1	1	1	1	1	1	7	
	In-depth data source	0	0	0	1	1	1	1	4	4/7 = **57%**
CZECH REPUBLIC	National data source	1	1	1	1	1	1	0	6	
	In-depth data source	1	1	1	1	1	1	1	7	6/7 = **85%**
USA	National data source	1	1	1	1	1	1	1	7	
	In-depth data source	1	1	1	1	1	1	1	7	7/7 = **100%**
BRAZIL	National data source	1	1	1	1	1	1	0	6	
	In-depth data source	1	1	1	1	1	1	1	7	6/7 = **85%**
AUSTRALIA	National data source	1	1	1	1	1	1	0	6	
	In-depth data source	1	1	1	1	1	1	1	7	6/7 = **85%**

The qualitative assessment of Table 6 indicate some in-depth data sources with potential on representative statements to the official statistic. However, it depends on which set of variables is chosen for the comparison. For example, the in-depth data source in Brazil shows with 85% of the chosen variable potential for representative statements on the entire Brazilian accident scenario. Whereby a weighting process within the in-depth data source to the official statistic is recommended based on the selection of variables.

Clustering of the countries
In-depth databases on road traffic accidents are not provided in every country in the world. This leads to the idea of using the already known in-depth data sources to make statements about countries or regions with similar road safety standards as the origin country with in-depth data source.

According to the clustering method developed, the Table 8 shows which bordering countries and countries by continent are most similar to the selected countries.

Table 8.
Bordering countries and countries by continent with the closest similarity to the country selection

Country	Bordering country	Continent
GERMANY	Austria	Spain
GREECE	Bulgaria	Cyprus
FRANCE	Belgium	Slovenia
CZECH REPUBLIC	Poland	Slovenia
USA	Canada	Canada
BRAZIL	Suriname	Suriname
AUSTRALIA	New Zealand	New Zealand

The countries with the closest similarity to the country of origin give a possible indication of which countries could be served by the data sources. The developed clustering method is a rough comparison of static key factor, whereby mentalities and country-specific behaviours are not considered.

Objective evaluation of the data sources
The result of the objective evaluation of the meta database is the result matrix. This dynamic table is calculated automatically and continuously after every change or adjustment in the meta database or in the questionnaire. Finally, the content of this matrix indicates for each data source the proportion of variables that correspond to the variables necessary to answer the research question.

Figure 3 shows in a cross comparison of seven selected data sources how many of the 120 research questions can be answered completely or to what percentage. The seven data sources are based on the countries from Table 8. In order to preserve the data protection of the data provider and avoid distortion of competition, no countries or data sources are named in the Figure 3.

With the data source from "Country I", for example, 30 of the research questions included in the GSD questionnaire can be answered completely.
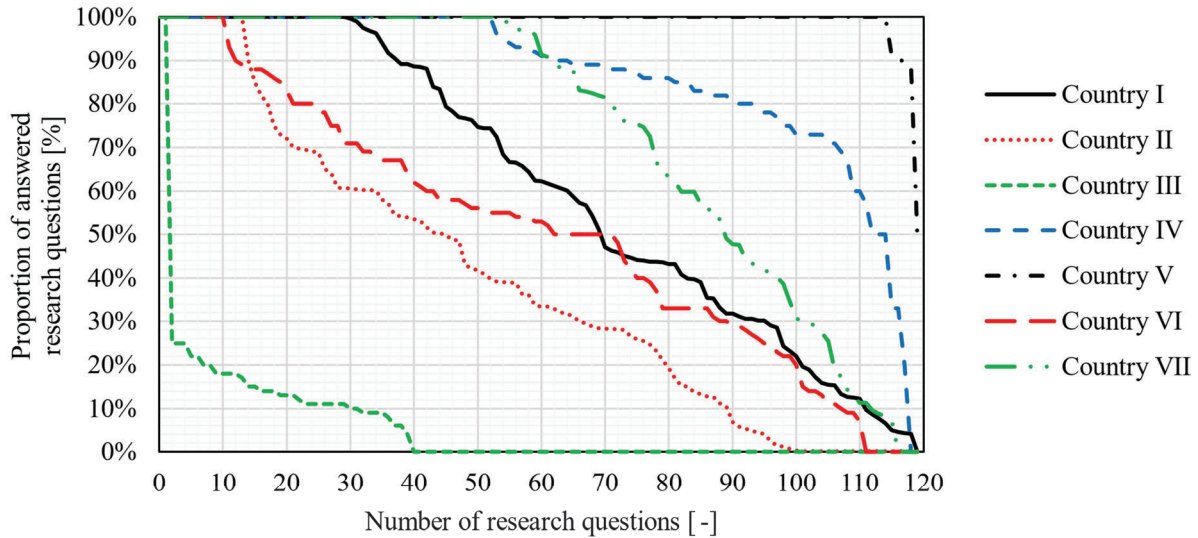
Figure 3. Visualization of the usability of selected data sources for answering the research questions stored in the GSD

DISCUSSION AND LIMITATIONS

The challenging task of storing meta data from several data sources around world from different data providers in a uniform database structure was successfully completed. The exchange of information between the GSD working group and the data providers is essential. Each data provider has different descriptions or meanings of variables and their collection. By this information the GSD working group have to decide which variables in the GSD match to the information of the data providers. The best scenario is when the data provider directly enters its meta data into the GSD.

The current questionnaire within the GSD and the evaluation of the suitability data sources is mainly based on research questions from R&D departments of automotive companies. For a more integrated road safety approach, the GSD is also prepared to cover more topics related to road safety e.g., infrastructure or medicine as well as the GSD questionnaire could be expanded to include questions from legislative bodies, authorities, associations, universities, or consumer protection organizations.

For a solid argumentation for future developments in road safety, up-to-date data is mandatory. The current basis of the clustering is the latest Global Status Report from 2018 [1] with data partly from 2016, whereby some of these data calculated and extrapolated by WHO. For a meaningful comparison, more recent data on road safety is desirable to narrow the spread to a steadily growing GSD. Current influences (e.g., covid pandemic, climate change, energy transition) can rarely be considered.

Additionally, an extension of the qualitative assessment of representativeness to a quantitative would be more robust. The GSD working group provides the methodology and framework for the quantitative assessment of representativeness, but on basis of the meta data stored in the GSD only a qualitative assessment is feasible.

In order to guarantee the data quality of the GSD, a steering committee (SC) is established. Every change that is made by authorised GSD users in the meta database is recorded in an integrated change log and will lead in a review. SC members are responsible for reviewing these changes. Each review is held according to the two-man rule, where disagreements can be escalated to the head of the SC. The SC is still in the process of being set up and the group of GSD experts will constantly looking for new SC members with expertise on accident statistics and databases worldwide.

CONCLUSION AND OUTLOOK

The Global Safety Database aims to investigate, inventory and objectively evaluate numerous accident data sources from different countries all over the world. Thus, it provides data for top relevant questions of todays and tomorrows road safety. For this purpose, a meta database is designed and filled with data sources of different kinds and origins. The subsequent objective evaluation is based on a matching process, which matches the content of current research questions of a questionnaire with the availability of variables in each data source. The result is stored in a so-called result matrix that shows the availability of necessary variables per data source for each and every research question.

An innovative methodology for clustering is used in order to identify countries or regions which data may be used to be transferred to other countries with similarities evaluating the road safety factors. Therefore, the representativeness of data sources especially of in-depth data sources is an essential aspect as knowledge of one country or region may accelerate the road safety improvement in other regions of the world as well.

As the GSD comprises only meta data, representative statements may also only be formulated on a qualitative level. The GSD is designed to only store meta data of data sources. This meta data is not sufficient for a qualitative assessment which requires raw data. Within the GSD, a qualitative assessment has been co-developed to show the possibilities how representativeness could be assessed with raw data if it is accessible.

In order to support the development process, the GSD is meant to be used by everyone, regardless of the position or organisation. [4] The GSD is freely accessible and the data quality as well as user management is ensured by the voluntarily voted Steering Committee.

From a global perspective, the GSD is one essential tool to push forth the worldwide harmonisation of traffic accident statistics and databases. The GSD is designed to be an ongoing meta database as well as questionnaire that engages its users by sharing information on global data sources for road traffic accidents and upcoming research questions for road safety. Thus, a community of experts may be formed and grow steadily. Furthermore, the GSD aims to support the increasingly data-driven vehicle development process by greatly reducing the effort finding required and suitable data sources to answer the top relevant research and development questions. This novel community is a key puzzle piece for enabling right developments and decision for future generations of safety measures, regulations, and systems. Thus, a Vision Zero with no road traffic casualties is getting closer and closer.

REFERENCES

[1]   **World Health Organization**. "Global status report on road safety 2018" Geneva: World Health Organization; 2018; Licence: CC BY-NC-SA 3.0 IGO; ISBN 978-92-4-156568-4

[2]   **Ziegler, J.; Liers, H.; Chanove, A.; Pohle, M**. "Objective assessment of database quality for use in the automotive research and development process". FAT publication series 343, Berlin, 2021

[3]   **The Research Association of Automotive Technology (FAT), Federal Highway Institute of Germany (BASt).** "German In-Depth Accident Study (GIDAS)". [Online] [Cited: December 08, 2022.] www.gidas.org.

[4]   **Global Safety Database** [Online] [Cited: December, 2022.] https://www.global-safety-database.com/

THE PREVALENCE AND PROFILE OF SPEEDING IN VEHICLE CRASHES USING EVENT DATA RECORDERS

Sam Doecke
Giulio Ponte
Martin Elsegood
Centre for Automotive Safety Research, University of Adelaide
Australia

ABSTRACT

Travelling at a speed above the speed limit is commonly known as speeding. Prior studies examining the prevalence and profile of speeding in Australia (and other countries) have used data from various sources, including speed enforcement data, speed measurement surveys, self-report studies, and naturalistic studies. Attempts have been made to determine the prevalence of speeding in crashes using police reports, but these have conflated inappropriate speed for the conditions with speeding. The objective of the present study was to use data from event data recorders (EDRs) that record pre-crash speed to determine the prevalence and profile of speeding in crashes that occur in South Australia. Data from the Centre for Automotive Safety Research's Event Data Recorder database (CASR-EDR) was used in the analysis. Separate analyses were conducted for all bullet vehicles (n=319) and for those travelling at a free, or self-selected, speed (n=160). It was found that 27% of bullet vehicles involved in the crash sample were speeding. The most common category of speeding was 1-5 km/h above the speed limit, but 6% of bullet vehicles were found to be speeding by more than 20 km/h prior to their crash. When only free speed vehicles were considered the percentage of vehicles speeding rose to 39%. Speeding was found to be more prevalent in crashes where the bullet vehicle was driven by a young driver, a driver with a provisional license, or the vehicle was black, red, or grey in colour. Speeding was also most prevalent in crashes that occurred on a weekend night, on a curve, at a mid-block location, on a local road, in regional areas, on a wet road, in low-speed zones, and in single vehicle crashes. These findings reinforce the need to reduce the prevalence of speeding through means such as education, enforcement, road design or vehicle technology. Young drivers should be a particular focus of efforts to reduce speeding. The findings can also provide some guidance on where enforcement activities should be further focussed.

INTRODUCTION

Speed is one important part of the Safe System approach to road safety which recognises the need for safe interactions between people, roads, vehicles and speed [1]. As the speed at which a vehicle is travelling increases so does the risk of being involved in an injury crash [2-4] and the risk of a crash resulting in serious or fatal injuries [5]. To balance this increase in risk against the need for mobility, jurisdictions set speed limits on roads that state the maximum speed at which a vehicle may legally travel on that road.

There are many factors that authorities may consider when setting speed limits. In Australia, speed limits are meant to be set based on the functional hierarchy and physical characteristics of the road, and should reflect individual and collective safety risk to road users as well as considering amenity and mobility [6-7]. However, other factors, such as local politics, may still play a role [8].

Although it is illegal, it remains relatively common for drivers to exceed the speed limit, commonly known as speeding [9]. Measurements or estimates of the prevalence and profile of speeding in Australia (and other countries) have come from a variety of sources.

Speed Enforcement and Speed Surveys
One of the main sources of data on the prevalence of speeding is from measurement of vehicle speeds at a given location or section of road, logged for either enforcement purposes or for speed measurement surveys conducted for research. Speed measurement devices may also record the vehicle registration, which allows matching to vehicle and driver details to provide a profile of the driver characteristics in addition to road characteristics recorded by the operators of the speed measurement devices.

Alavi *et al.* [10] analysed a sample of about 350,000 speed measurements from mobile speed enforcement cameras in Victoria. They excluded data recorded when traffic flow was particularly low or high for a given location, which may have excluded peak or late-night / early-morning periods. They found that 9.5% of drivers

captured in their sample exceeded the speed limit, and most speeders (95%) were speeding by 1 to 10 km/h over the posted speed limit. They also found that drivers in rural areas were 1.85 times more likely to speed at any specific time of the year compared to metropolitan areas (11% compared to 6% for metropolitan drivers). When considering speed zone, they found that the highest level of speeding occurred in 40 km/h speed zones, where 47% of drivers in metropolitan areas exceeded the speed limit, followed by 50 km/h (23% regional, 21% metropolitan) and 60 km/h speed zones (12% regional, 10% metropolitan). The lowest speeding rates in metropolitan areas were 80 km/h speed zones (3%) whereas the lowest speeding rates in regional areas were 90 km/h speed zones (5%).

In South Australia, annual speed surveys are conducted at more than 100 sites using pneumatic tubes to measure speed and headway. These speed surveys were conducted at sites with speed zones ranging from 50 to 110 km/h and found that speeding varied according to location (metropolitan or rural) and speed zone [9]. In 2018, speeding was most prevalent on metropolitan 50 km/h collector roads (37%), rural 100 km/h roads (35%), rural 50 km/h roads (26%) and rural 80 km/h roads (24%), for any driver exceeding the speed limit by any amount. Rural 100 km/h and Adelaide 50 km/h roads also had the highest percentage of drivers exceeding the speed limit by 10 km/h or more, 7% and 5% respectively. These speed surveys also considered speeding for free-speed vehicles. Free-speed vehicles were defined as those having a headway gap of at least four seconds. The prevalence of speeding of free-speed vehicles were only marginally different from that of all vehicles on most roads, except 60 km/h metropolitan arterial roads (12% increased to 18%) and 80 km/h rural roads (24% increased to 29%).

Williams, Kyrychenko, & Retting [11] undertook speed surveys on roads in Northern Virginia (USA) with speed limits ranging from 40 mph to 55 mph (64 to 89 km/h). They recorded the speeds of "free-flowing" vehicles using a photoradar camera system and examined licensing details of the speeding drivers in their sample to gain further insight. Williams *et al.* [11] found that 28%, 29% and 15% of drivers in their sample exceeded the posted speed limit by 0-4, 5-9, and 10-14 mph respectively, while 5% of drivers exceeded the speed limit by more than 15 mph. However, Williams *et al.* [11] defined 'speeding' as travelling 15 mph (25 km/h) over the speed limit and at least 5 mph faster than 3 of the 4 vehicles around them, therefore only 3% of their sample met their operational definition of speeding. Their results indicated that their speeding drivers were younger and more likely to drive newer vehicles (and SUVs) and it was suggested that they were more likely to be male than female. Furthermore, their speeders had more traffic violations and on average had more crashes per year than their comparison group.

Self-Report Studies
Stephens *et al.* [12] conducted a community attitude survey on an age and sex representative sample of Australian drivers (excluding South Australia) to profile some aspects of speed behaviours. They found that males were more likely to speed by any amount compared to females, and speeding was least prevalent in low-speed zones (40 km/h) with prevalence increasing as speed limit increased. Most speeding was 1-5 km/h over the speed limit, with a higher proportion of 16–25 year olds reported driving 11 km/h or more over the speed limit.

Naturalistic Studies
Naturalistic studies can also reveal the characteristics of speeding drivers. Perez et al., [13], using objective data from the SHRP2 naturalistic driving study (conducted in various states of the US), found that male drivers were more likely to speed than females (Odds Ratio [OR] 1.1) and younger drivers were more likely to speed (OR 1.5) compared to older drivers (80+ years-old reference group). Speeding decreased across increasing age groups. Perez et al., [13] also found that the odds of speeding were larger at lower speed limits and speeding decreased with increasing speed limit; in 10-20 mph speed zones (16-32 km/h) the OR of speeding was 9.5 times than that in 60 mph (96 km/h) reference speed limit group.

Ellison & Greaves [14] used GPS data and follow-up survey data to evaluate prevalence and characteristics of speeding behaviours for drivers undertaking normal driving in the Australian state of New South Wales. They found that 20% of moving distance travelled was spent over the speed limit (by 1 km/h or more) and there was a small but significant number who frequently exceeded the speed limit by 10 km/h or more. They also found that males were more likely than females to speed in each age group (except in the 46-65 age group, where females sped more), and little difference was observed in the prevalence of speeding in the different age groups. Ellison & Greaves [14] also found that speeding was more prevalent on weekends (and at night) than weekdays, but weekday speeding was most prevalent in the mornings. Speeding was highest when the driver was the only occupant and decreased slightly as occupancy increased (to 3 occupants) but then increased again with more

occupants. Speeding was found to be highest by purpose of the trip for those traveling on vacation and commuting to work and lowest for education/childcare trips.

Crash Studies

Determining the prevalence and profile of speeding in crashes is more complex as the only way to ascertain objective speed in crashes was, historically, through crash reconstructions. Crash reconstructions require specialist knowledge, are labour intensive, and are typically conducted by police in Australia except for the most serious of crashes. Even crash reconstructions are limited in their ability to identify speeding due to uncertainties around identifying when the vehicle began to brake.

While routine police crash reports usually cannot objectively state whether speeding was a contributing factor in a particular crash, there have been attempts to try to identify speeding based on information in a police report. The Centre for Road Safety, Transport for NSW provide criteria whereby speed as a factor in crashes can be derived that is also used in other Australian jurisdictions [15]. This method identifies both inappropriate speed for the conditions and speeding but has been shown to lack both sensitivity and specificity if used to identify only speeding [16]. A similar issue exists in the US where speed related crashes are identified by police but inappropriate speed for the conditions and speeding are often conflated [17].

Aim of the Present Study

The increasing prevalence of vehicles with event data recorders (EDRs) in the fleet enables a new method of examining speeding in crashes. Studies have found that EDR speed data are accurate, with speed generally slightly underreported by around 1 km/h [18]. Doecke, Kloeden, & Paine [19] used EDR speed data to examine the prevalence of speeding in crashes in the US, concluding that speeding in crashes is far more prevalent than indicated by police reports. Doecke *et al.* [19] suggested that routine collection and use of EDR data would better represent the extent of speeding in crashes. The aim of the current study was to determine the prevalence and profile of speeding in South Australian crashes using EDR data.

METHOD

Data from the Centre for Automotive Safety Research's Event Data Recorder database (CASR-EDR) was used to examine the prevalence and profile of speeding in South Australia. The CASR-EDR database contains the largest set of EDR data from crashed vehicles in Australia. It includes vehicles that were legally too damaged to be repaired, or were deemed uneconomical to repair by an insurer. Data collection began in 2017 and is ongoing. It also contains data matched from several sources, such as police reports and a licensing and registration database. This means that it not only contains highly accurate speed data from crashed vehicles, but also contains a range of information that can be used to profile the characteristics of drivers, vehicles, and locations of crashes involving speeding. The CASR-EDR database had 639 records of EDR data collected between 2017 and 2021 that have been matched to police reports and other data sources.

Two variables in the CASR-EDR database were used to identify speeding, the travel speed of the vehicle and the speed limit. The travel speed of the vehicle in the CASR-EDR database is defined as the highest speed shown in the 2.5 to 5 seconds of pre-crash data recorded on the EDR. The speed limit is sourced from the matched police report. By comparing the travel speed from the EDR to the speed limit, speeding in crashes was identified.

The CASR-EDR database has been found to be representative of police reported crashes in South Australia in terms of area, speed limit, and crash type [20]. Crash severity in the CASR-EDR database is skewed toward higher severity crashes, most likely due to EDR devices not recording data from very minor crashes. It should also be noted that the sample is limited to vehicles supported by the Bosch CDR tool in Australia. This limits the sample to vehicles manufactured after about 2004. It also results in the makes of vehicle that have been supported by the Bosch CDR tool for the entire duration of the CASR-EDR database's data collection (e.g. Toyotas, Holdens, Jeeps) being over-represented in the sample, the makes that have been supported for some of the duration of data collection (e.g. Mitsubishi, Subaru, BMW) being under-represented, and some makes not being represented at all (e.g. Hyundai, KIA).

Crashes in the CASR-EDR database that occurred between 2017 and 2021 were included in the analysis if they contained speed data from a bullet vehicle. A bullet vehicle is defined in the CASR-EDR database using the movements of the vehicles as described in the police report. Bullet vehicles were vehicles that generally had

right of way (if travelling through an intersection). For crashes where a vehicle was performing a turning manoeuvre across traffic, the bullet vehicle was the through vehicle. In rear-end crashes, the rear-most vehicle was the bullet vehicle. For single vehicle crashes, the crashed vehicle was always classified as the bullet vehicle. In head-on crashes and side-swipe crashes, both vehicles were classified as bullet vehicles. There were 319 crashes identified in the CASR-EDR database as having speed data and being from a bullet vehicle.

The prevalence and profile of speeding free-speed vehicles was also examined. Free, or self-selected, speed could not be determined in terms of a time headway from EDR data, as is done in speed surveys using pneumatic tubes (e.g. [9]). Instead, the CASR-EDR database classifies free-speed according to what is deduced from the EDR data and the police report. To be considered a free-speed vehicle, the vehicle must not have been:
- involved in a rear end crash
- performing a turning manoeuvre
- accelerating from a stationary position
- performing an illegal manoeuvre
- travelling through work zones
- operated by a driver who had a medical episode or fatigued prior to their crash

The focus of the free-speed criteria in the CASR-EDR database was to minimise false positives (misclassification as free-speed). However, it is acknowledged that this comes at the expense of false negatives (misclassification as not free-speed). There were 160 vehicles that were classified as free-speed vehicles.

Prior traffic offences committed by the drivers were also included in the analysis of free-speed vehicles. This data was sourced from a licensing and registration database of offences committed within South Australia. The offences were expressed as the number of offences per three years of licensure to attempt to account for driving exposure.

RESULTS

It was found that 27% of bullet vehicles involved in the crashes were speeding (Table 1). The most common category of speeding was 1-5 km/h above the speed limit (9% of vehicles), but 6% of bullet vehicles were found to be speeding by more than 20 km/h prior to their crash. When only free speed vehicles were considered (Table 2) the percentage of vehicles speeding rose to 39%.

Table 1 and 2 also show the prevalence and category of speeding by the characteristics of the driver, while Figures 1 and 2 provide the prevalence and category of speeding by age and sex. Tables 1 and 2 show that speeding was more prevalent among younger drivers, particularly when only free-speed vehicles were considered, but there was little difference between the sexes. However, Figures 1 and 2 reveal that there were differences by sex for 16-24 year olds and those 65 and older, although these differences were not statistically significant. Tables 1 and 2 also show the prevalence of speeding according to the driver's alcohol test result, the level of license, and the location of residence. Speeding was more prevalent among drivers who had a positive alcohol test result, especially high-level speeding, but the statistical significance of this could not be tested. Speeding was also more prevalent amongst drivers on a provisional license than amongst those on a full license. Drivers that resided in regional areas had different patterns of speeding than those from the major city. For free-speed vehicles (Table 2), speeding drivers who live in a major city tended to speed by 10 km/h or less, while those in inner regional areas tended to speed by more than 10 km/h.

Table 2 displays speeding prevalence by number of prior speeding offences per year of licensure, and by all driving offences per year of licensure. Speeding was least prevalent amongst drivers that had a speeding offence but had less than 1 per 3 years of licensure. This pattern was also evident when all driving offences were considered, but neither result was statistically significant.

Table 1.
Speeding prevalence by driver characteristics and speeding category for all bullet vehicles

Driver Char.	Category	Count	Total speeding		Chi squared test results		Speeding category (km/h)							
							1-5		6-10		11-20		21+	
			No.	%	χ²	p	No.	%	No.	%	No.	%	No.	%
Age	16 - 24	75	27	36%	18.5	<0.001	9	12%	7	9%	4	5%	7	9%
	25 - 39	96	35	36%			12	13%	10	10%	6	6%	7	7%
	40 - 64	110	19	17%			7	6%	3	3%	7	6%	2	2%
	≥65	34	3	9%			2	6%	1	3%	0	0%	0	0%
Sex	Male	183	51	28%	0.3	0.570	17	9%	14	8%	11	6%	9	5%
	Female	132	33	25%			13	10%	7	5%	6	5%	7	5%
Alcohol*	Positive	7	5	71%	NA	NA	1	14%	0	0%	1	14%	3	43%
	Negative	241	65	27%			27	11%	18	7%	12	5%	8	3%
	Not tested	67	14	21%			2	3%	3	4%	4	6%	5	7%
Licence	Full	274	67	24%	7.0	0.008	25	9%	16	6%	15	5%	11	4%
	Provisional	38	17	45%			5	13%	5	13%	2	5%	5	13%
	Learners	3	0	0%			0	0%	0	0%	0	0%	0	0%
Location of residence	Major Cities	262	67	26%	1.2	0.264	25	10%	19	7%	12	5%	11	4%
	Regional	48	16	33%			5	10%	2	6%	4	8%	5	10%
	Unknown	5	1	20%	NA	NA	0	0%	0	0%	1	20%	0	0%
Total		**315**	**84**	**27%**			**30**	**9%**	**21**	**7%**	**17**	**5%**	**16**	**5%**

Note: Four drivers had unknown data for all driver characteristics.
* Positive means above the legal limit for that driver, which in most cases is a BAC of 0.05, but is 0.00 for drivers with a provisional license, and bus, truck and taxi drivers.
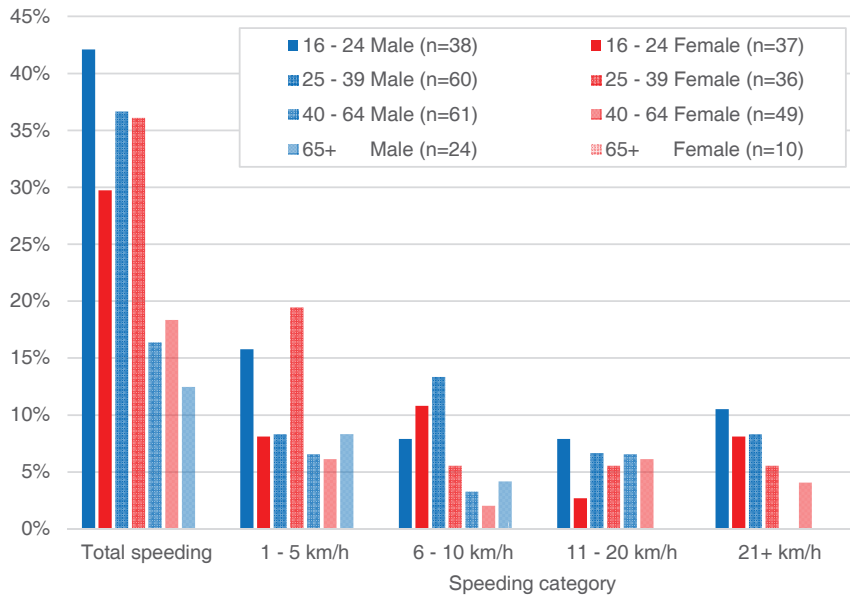
Table 2.
Speeding prevalence by driver characteristics and speeding category for free-speed vehicles

Driver Char.	Category	Count	Total speeding		Chi squared test results		Speeding category (km/h)							
							1-5		6-10		11-20		21+	
			No.	%	χ²	p	No.	%	No.	%	No.	%	No.	%
Age	16 - 24	33	20	61%	15.2	0.002	6	18%	5	15%	3	9%	6	18%
	25 - 39	50	24	48%			8	16%	6	12%	5	10%	5	10%
	40 - 64	62	15	24%			6	10%	3	5%	4	6%	2	3%
	≥65	13	3	23%			2	15%	1	8%	0	0%	0	0%
Sex	Male	94	38	40%	0.1	0.712	13	14%	10	11%	8	9%	7	7%
	Female	64	24	38%			9	14%	5	8%	4	6%	6	9%
Alcohol*	Positive	6	5	83%	NA	NA	1	17%	0	0%	1	17%	3	50%
	Negative	120	44	37%			19	16%	13	11%	6	5%	6	5%
	Not tested	32	13	41%			2	6%	2	6%	5	16%	4	13%
Licence	Full	138	49	36%	6.4	0.012	19	14%	11	8%	11	8%	8	6%
	Provisional	20	13	65%			3	15%	4	20%	1	5%	5	25%
Place of residence	Major Cities	126	50	40%	0.1	0.821	20	16%	13	10%	9	7%	8	6%
	Regional	32	12	37%			2	6%	2	6%	3	9%	5	16%
Previous speeding offences	None	49	21	43%	3.5	0.171	8	16%	6	12%	2	4%	5	10%
	<1 per 3 yrs	70	22	31%			8	11%	4	6%	4	6%	6	9%
	≥1 per 3 yrs	39	19	49%			6	15%	5	13%	6	15%	2	5%
Previous driving offences	None	37	17	46%	3.3	0.196	5	14%	6	16%	2	5%	4	11%
	<1 per 3 yrs	70	20	29%			10	14%	3	4%	4	69%	3	4%
	≥1 per 3 yrs	51	25	49%			7	14%	6	12%	6	12%	6	12%
Total		**158**	**62**	**39%**			**22**	**14%**	**15**	**9%**	**12**	**8%**	**13**	**8%**

Note: Two drivers had unknown data for all driver characteristics.
* Positive means above the legal limit for that driver, which in most cases is a BAC of 0.05, but is 0.00 for drivers with a provisional license, and bus, truck and taxi drivers.

Figure 1. Speeding prevalence by age, sex, and speeding category for all bullet vehicles.
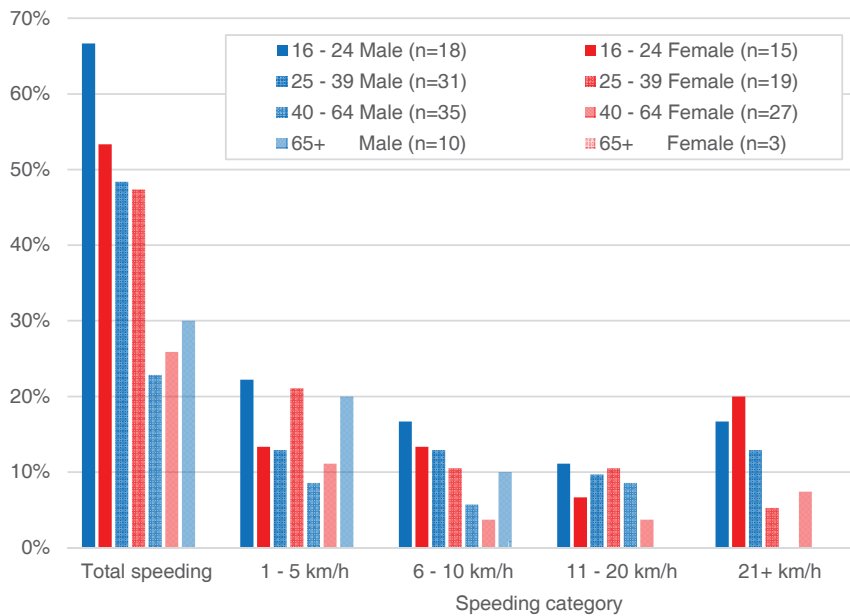

Figure 2. Speeding prevalence by age, sex, and speeding category for free-speed vehicles.

Table 3 shows the speeding prevalence of the bullet vehicles with respect to vehicle characteristics, and Table 4 shows the same data for free-speed vehicles. There was little difference in the prevalence of speeding between sedans and SUVs (including derivatives). Speeding was more prevalent amongst vehicles that were black, grey and red in colour. Speeding was also more prevalent among vehicles with a manual transmission and those with a sole occupant, but these results were not statistically significant. Newer vehicles (less than 5 years old) had lower speeding rates than older vehicles, but this was also not statistically significant.

Table 3.
Speeding prevalence by vehicle characteristics and speeding category for all bullet vehicles

Vehicle Char.	Category	Count	Total speeding		Chi squared test results		Speeding category (km/h)							
			No.	%	χ^2	p	1-5		6-10		11-20		21+	
							No.	%	No.	%	No.	%	No.	%
Body Type	Sedan type	235	64	27%	0.0	0.957	22	9%	14	6%	12	5%	16	7%
	SUV type	78	21	27%			8	10%	6	8%	5	6%	2	3%
	Van	6	1	17%	NA	NA	0	0%	1	17%	0	0%	0	0%
Transmission	Automatic	275	70	25%	2.3	0.130	26	9%	20	7%	12	4%	12	4%
	Manual	44	16	36%			4	9%	1	2%	5	11%	6	14%
Colour	Black	49	19	39%			7	14%	6	12%	3	6%	3	6%
	Grey	38	12	32%			6	16%	3	8%	2	5%	1	3%
	Red	36	12	33%	6.0	0.015	5	14%	1	3%	3	8%	3	8%
	Silver	57	13	23%			3	5%	3	5%	1	2%	6	11%
	White	99	21	21%			6	6%	6	6%	6	6%	3	3%
	Other	40	9	23%	NA	NA	3	8%	2	5%	2	5%	2	5%
Number of occupants	Sole driver	245	71	29%	2.2	0.139	24	10%	16	7%	15	6%	16	7%
	Multiple occupants	74	15	20%			6	8%	5	7%	2	3%	2	3%
Vehicle age	0 to 4 years	106	23	22%			9	8%	4	4%	7	7%	3	3%
	5 to 9 years	137	42	31%	2.5	0.292	13	9%	14	10%	7	5%	8	6%
	≥ 10 years	76	21	28%			8	11%	3	4%	3	4%	7	9%
Total		319	86	27%			30	9%	21	7%	17	5%	18	6%

Table 4.
Speeding prevalence by vehicle characteristics and speeding category for free-speed vehicles

Vehicle Char.	Category	Count	Total speeding		Chi squared test results		Speeding category (km/h)							
			No.	%	χ^2	p	1-5		6-10		11-20		21+	
							No.	%	No.	%	No.	%	No.	%
Body Type	Sedan type	119	48	40%	0.0	0.939	17	14%	10	8%	9	8%	12	10%
	SUV type	39	16	41%			5	13%	5	13%	3	8%	3	8%
	Vans	2	0	0%	NA	NA	0	0%	0	0%	0	0%	0	0%
Transmission	Automatic	131	51	39%	0.3	0.558	19	15%	14	11%	9	7%	9	7%
	Manual	29	13	45%			3	10%	1	3%	3	10%	6	21%
Colour	Black	24	12	50%			6	25%	3	13%	0	0%	3	13%
	Grey	17	9	53%			4	24%	2	12%	2	12%	1	6%
	Red	24	10	42%	2.3	0.133	4	17%	1	4%	3	13%	2	8%
	Silver	31	10	32%			2	6%	3	10%	1	3%	4	13%
	White	43	16	37%			4	9%	5	12%	4	9%	3	7%
	Other	21	7	33%	NA	NA	2	10%	1	5%	2	10%	2	10%
Number of occupants	Sole driver	116	51	44%	2.8	0.096	18	16%	10	9%	11	9%	12	10%
	Multiple	44	13	30%			4	9%	5	11%	1	2%	3	7%
Vehicle age	0 to 4 years	50	16	32%			6	12%	2	4%	5	10%	3	6%
	5 to 9 years	72	31	43%	2.0	0.373	9	13%	10	14%	5	7%	7	10%
	≥ 10 years	38	17	45%			7	18%	3	8%	2	5%	5	13%
Total		160	64	40%			22	14%	15	9%	12	8%	15	9%

The prevalence of speeding according to characteristics of the crashes are shown in Tables 5 and 6 for all bullet vehicles and free-speed vehicles, respectively. Speeding was more prevalent in crashes that occurred at night and on the weekend, in regional areas, on curves, at midblock locations, and on a wet road. Speeding was most prevalent on local roads and least prevalent on arterial roads. In terms of speed limit, speeding was most prevalent on roads with a speed limit of 50 km/h or less and least prevalent on roads with speed limits of 60 km/h. Speeding was also far more prevalent in single vehicle and side swipe crashes than any other crash type.

Table 5.
Speeding rates according to crash characteristics and speeding category for all bullet vehicles

Crash Char.	Category	Count	Total speeding		Chi squared test results		Speeding category (km/h)							
							1-5		6-10		11-20		21+	
			No.	%	χ^2	p	No.	%	No.	%	No.	%	No.	%
Time and day	**Weekday day**	213	47	22%	13.2	0.004	20	9%	13	6%	7	3%	7	3%
	Weekend day	22	8	36%			2	9%	1	5%	2	9%	3	14%
	Weekday night	58	17	29%			6	10%	6	10%	4	7%	1	2%
	Weekend night	26	14	54%			2	8%	1	4%	4	15%	7	27%
Area	**Major Cities**	265	65	25%	4.7	0.030	24	9%	17	6%	12	5%	12	5%
	Regional	54	21	39%			6	11%	4	7%	5	9%	6	11%
Road curvature	**Curved**	33	17	52%	11.3	0.001	5	15%	4	12%	4	12%	4	12%
	Straight	286	69	24%			25	9%	17	6%	13	5%	14	5%
Intersection	**Mid-block**	200	66	33%	10.6	0.031	22	11%	15	8%	15	8%	14	7%
	Cross Road	47	9	19%			3	6%	2	4%	2	4%	2	4%
	T-Junction	55	8	15%			4	7%	3	5%	0	0%	1	2%
	Roundabout	9	1	11%			0	0%	0	0%	0	0%	1	11%
	Other	8	2	25%			1	13%	1	13%	0	0%	0	0%
Road class	**Freeway**	23	8	35%	14.9	0.002	4	17%	1	4%	2	9%	1	4%
	Arterial	159	30	19%			11	7%	8	5%	7	4%	4	3%
	Collector	89	26	29%			10	11%	8	9%	5	6%	3	3%
	Local	48	22	46%			5	10%	4	8%	3	6%	10	21%
Speed zone (km/h)	**≤ 50**	75	33	44%	16.3	0.001	8	11%	8	11%	6	8%	11	15%
	60	163	31	19%			11	7%	9	6%	5	3%	6	4%
	70 - 90	48	13	27%			8	17%	2	4%	3	6%	0	0%
	100 - 110	33	9	27%			3	9%	2	6%	3	9%	1	3%
Crash type	**Head on**	12	3	25%	23.3	<0.001	2	17%	0	0%	1	8%	0	0%
	Rear end	90	19	21%			8	9%	6	7%	4	4%	1	1%
	R. turn/angle	96	15	16%			8	8%	5	5%	2	2%	0	0%
	Side swipe	16	6	38%			3	19%	2	13%	1	6%	0	0%
	Single vehicle	86	39	45%			9	10%	6	7%	8	9%	16	19%
	Other	19	4	21%	NA	NA	0	0%	2	11%	1	5%	1	5%
Road conditions	**Dry**	277	23	25%	3.0	0.084	23	8%	21	8%	14	5%	12	4%
	Wet	42	7	38%			7	17%	0	0%	3	7%	6	14%
Total		**319**	**30**	**27%**			**30**	**9%**	**21**	**7%**	**17**	**5%**	**18**	**6%**

Day is defined as 6:00 to 19:59, Night is defined as 20:00 to 5:59.

Area is defined according to the Australian Statistical Geography Standard Remoteness Structure. Regional includes the categories; inner regional, outer regional, remote, and very remote.

Table 6.
Speeding rates according to crash characteristics and speeding category for free-speed bullet vehicles

Crash Char.	Category	Count	Total speeding		Chi squared test results		Speeding category (km/h)							
							1-5		6-10		11-20		21+	
			No.	%	χ²	p	No.	%	No.	%	No.	%	No.	%
Time and day	Weekday day	100	32	32%			14	14%	9	9%	4	4%	5	5%
	Weekend day	14	7	50%			2	14%	0	0%	1	7%	4	29%
	Weekday night	30	13	43%	11.6	0.009	4	13%	5	17%	3	10%	1	3%
	Weekend night	16	12	75%			2	13%	1	6%	4	25%	5	31%
Area	Major Cities	124	46	37%	1.9	0.164	17	14%	12	10%	8	6%	9	7%
	Regional	36	18	50%			5	14%	3	8%	4	11%	6	17%
Road curvature	Curved	21	15	71%	9.9	0.002	4	19%	3	14%	4	19%	4	19%
	Straight	139	49	35%			18	13%	12	9%	8	6%	11	8%
Intersection	Mid-block	80	46	58%			14	18%	10	13%	10	13%	12	15%
	Cross Road	32	8	25%	19.6	<0.001	3	9%	2	6%	2	6%	1	3%
	T-Junction	43	9	21%			4	9%	3	7%	0	0%	2	5%
	Roundabout	1	0	0%	NA	NA	0	0%	0	0%	0	0%	0	0%
	Other	4	1	25%	NA	NA	1	25%	0	0%	0	0%	0	0%
Road class	Freeway	16	7	44%			3	19%	1	6%	2	13%	1	6%
	Arterial	65	17	26%	10.7	0.014	7	11%	6	9%	2	3%	2	3%
	Collector	45	20	44%			8	18%	4	9%	5	11%	3	7%
	Local	34	20	59%			4	12%	4	12%	3	9%	9	26%
Speed zone (km/h)	≤ 50	39	24	62%			5	13%	7	18%	3	8%	9	23%
	60	75	23	31%	10.5	0.015	10	13%	5	7%	3	4%	5	7%
	70 - 90	23	8	35%			4	17%	1	4%	3	13%	0	0%
	100 - 110	23	9	39%			3	13%	2	9%	3	13%	1	4%
Crash type	Head on	10	3	30%			2	20%	0	0%	1	10%	0	0%
	R. turn / angle	72	16	22%	26.0	<0.001	8	11%	5	7%	2	3%	1	1%
	Side swipe	9	6	67%			3	33%	2	22%	1	11%	0	0%
	Single vehicle	54	35	65%			9	17%	6	11%	7	13%	13	24%
	Other	15	4	27%	NA	NA	0	0%	2	13%	1	7%	1	7%
Road surface conditions	Dry	139	50	36%	7.2	0.007	16	12%	15	11%	9	6%	10	7%
	Wet	21	14	67%			6	29%	0	0%	3	14%	5	24%
Total		**160**	**64**	**40%**			**22**	**14%**	**15**	**9%**	**12**	**8%**	**15**	**9%**

Day is defined as 6:00 to 19:59, Night is defined as 20:00 to 5:59.
Area is defined according to the Australian Statistical Geography Standard Remoteness Structure. Regional includes the categories; inner regional, outer regional, remote, and very remote.

DISCUSSION

This study used EDR data matched to police reports and a licensing database to examine the prevalence of speeding in crashes in South Australia. It also produced a profile of the driver, vehicle and crash characteristics of crashes where the bullet vehicles and free-speed vehicles were speeding. Speeding was also broken down into different categories of speeding to provide further detail related to the prevalence and profile of speeding in South Australia.

When interpreting the results, it is important to bear in mind that they do not necessarily reflect the prevalence of speeding under normal traffic conditions. For a vehicle to be included in the sample it had to have been involved in a crash. The prevalence of vehicles speeding in a crash with a certain characteristic is a function of the prevalence of vehicles speeding with that characteristic, and the relationship between speed and crash risk for that characteristic. For example, the crash risk of driving on a wet road or around a curve may be more

sensitive to driving above the speed limit than driving on a dry or straight road. It should not be concluded that speeding is more prevalent on curves or wet conditions based on the results.

Limitations

Several limitations with police report and traffic offence data should be noted. Data from police reports should not be assumed to be 100% reliable. Kloeden, Linke and Ponte [21] found that South Australian police reports on injury crashes attended by police were at least 92% for the variables used in the present analysis, but this may be reduced for non-injury crashes that police do not necessarily attend. The traffic offence database only contains offences committed within South Australia, and may therefore not reflect the overall driving history for drivers who have spent a considerable amount of their time driving in other states.

As detailed in the method, the sample is limited to crashed vehicles that could have their EDR data downloaded using the Bosch CDR tool. This limited the sample to vehicles manufactured from about 2004 onwards, and has resulted in certain makes of vehicle being over-represented. The exclusion of older vehicles may have had an impact on the overall prevalence of speeding found in the results. Older vehicles are generally thought to be driven by younger drivers due to affordability, but a US study showed that drivers aged over 65 also drive older vehicles than the middle aged [22]. It is therefore unclear what effect this may have had on the results, as it may have excluded some young drivers, who are the most likely to be speeding in a crash, and some old drivers who are least likely to be speeding. Particular makes were over-represented and this would influence the results if speeding varied between makes. This seems unlikely as the two most common vehicle makes in the sample, Holden and Toyota, have a wide range of models to appeal to various market segments and demographics.

Comparisons to prior research

The age of drivers that were more likely to have been speeding prior to a crash in the present study is largely consistent with prior research that obtained data on speeding drivers from other sources. The naturalistic study by Perez *et al.* [13] and the study by Williams, Kyrychenko & Retting [11] based on enforcement data, and the study by Stephens *et al.* [12] based on self-reported speeding behaviours, all found that speeding was more prevalent amongst younger drivers. However, the findings of the present study with regard to sex was not consistent with prior research. The same prior studies that examined speeding outside of the context of a crash [11-13] found that speeding was more prevalent amongst males drivers, but in the present study males involved in crashes had very similar prevalence of speeding to females. While the present study did show some differences between young (16-24 year old) males and young females, and males and females aged over 65, the sample size precluded these differences from being statistically significant when disaggregated to this level.

Speeding, and especially high-level speeding, was more prevalent in crashes on roads with a low-speed limit. This is consistent with studies that measured speeding objectively, be it through enforcement data [10], speed surveys [9], or naturalistic studies [13]. However, it is inconsistent with the study by Stephens *et al.* [12] that used self-reported data. This may suggest that drivers that self-report their speeding behaviour are less aware of their speeding in low-speed zones, or that speeding in low-speed zones is less socially acceptable and therefore less likely to be self-reported. The increased speeding in crashes in low-speed zones may be a result of the perceived risk of being caught on such roads being low, as these tend to be local metropolitan roads that have less enforcement. It may also point to a lack of credibility of these speed limits in the minds of some drivers, which can be related to compliance [23].

Speeding in crashes was more common in regional areas than in the major city areas. This is consistent with Alavi *et al.* [10]. Like speeding on low-speed local roads, this may be related to a low perceived chance of being caught by enforcement activities.

A prior study looking at speeding survey data found that speeding drivers had a higher number of traffic violations [11]. The present study found that drivers involved in speeding crashes were more likely to have either no speeding or no traffic offences, or more than 1 per 3 years of licensure, but this result was not statistically significant.

Newstead & D'Elia [24] found that black, grey and red were some of the colours that had an increased risk of being involved in a crash, with blue, green and silver also being associated with higher crash risk. The current work suggests that at least some of this increased crash risk for black, red and grey vehicles is due to the fact that they are more likely to be speeding. However, it should be noted that the sample size of the present analysis only allowed for the most common colours to be examined.

Williams, Kyrychenko & Retting [11] found that newer vehicles and SUVs were more likely to be speeding, but this was not reflected in the present study. This may be due to differences between the types of drivers of such vehicles in Australia and the US.

Generalisability

The generalisability of the results may vary between the different characteristics being considered. The results related to driver characteristics are most likely applicable to many other jurisdictions and countries as they are unlikely to be cultural to South Australia. The region of the drivers' homes may be uniquely related to South Australia's geography and the perception of the risk of being caught for speeding in these different regions. With respect to crash characteristics, the results for road curvature, intersection type, and road surface condition are likely to be widely applicable. However, the way in which the area, road class, and speed zones are classified may vary between jurisdictions and countries in a manner that reduces the generalisability of these results. It is unclear how generalisable the results related to crash type are as classification may vary between regions. The degree of generalisability of the results relating to vehicle characteristics will also depend on consistency in classification.

CONCLUSIONS

It was found that 27% of bullet vehicles involved in crashes in South Australia were speeding. The most common category of speeding was 1-5 km/h above the speed limit, but 6% of bullet vehicles were found to be speeding by more than 20 km/h prior to their crash. When only free speed vehicles were considered the percentage of vehicles speeding rose to 39%. Speeding was found to be more prevalent in crashes where the bullet vehicle was driven by a young driver, a driver with a provisional license, or the vehicle was black, red, or grey in colour. Speeding was also most prevalent in crashes that occurred on a weekend night, on a curve, at a mid-block location, on a local road, in regional areas, on a wet road, in low-speed zones, and in single vehicle crashes.

These findings reinforce the need to reduce the prevalence of speeding through means such as education, enforcement, road design or vehicle technology. Young drivers should be a particular focus of efforts to reduce speeding. The findings can also provide some guidance on where enforcement activities should be further focussed.

FUNDING

REFERENCES

[1] ITF (2016) *Zero Road Deaths and Serious Injuries: Leading a Paradigm Shift to a Safe System.* OECD Publishing, Paris. http://dx.doi.org/10.1787/9789282108055-en

[2] Kloeden, C. N., McLean, A. J., Moore, V. M., & Ponte, G. (1997). *Travelling speed and the risk of crash involvement. Volumes 1 and 2* (CR172). Canberra: Federal Office of Road Safety, Transport and Communications.

[3] Kloeden, C. N., Ponte, G., & McLean, A. J. (2001). *Travelling speed and the risk of crash involvement on rural roads* (CR204). Canberra: Australian Transport Safety Bureau.

[4] Fitzharris, M., Lenne´, M.G., Corben, B., Arundell, T.P., Peiris., S., Liu. S., Stephens., A., Fitzgerald, M., Judson, R., Bowman., D., Gabler, C., Morris, A., Tingvall., C. (2020) *ECIS Report 1: Overview and Analysis of Crash Types, Injury Outcomes and Contributing Factors.* Melbourne: Monash University Accident Research Centre.

[5] Doecke, S. D., Dutschke, J. K., Baldock, M. R. J., & Kloeden, C. N. (2021). Travel speed and the risk of serious injury in vehicle crashes. *Accident Analysis and Prevention, 161* (2021), 106359.

[6] Austroads (2021) Guide to Road Safety Part 3: Safe Speed.
https://austroads.com.au/publications/road-safety/agrs03

[7] Department of Planning, Transport and Infrastructure (2017) *Speed Limit Guideline for South Australia.* https://www.dpti.sa.gov.au/?a=338713

[8] McCarthy, M., Martin, P. (2017) *Speed limit cut: SA minister breaks ranks, Opposition promises reverse.* Accessed on 22/2/2022. https://www.abc.net.au/news/2017-10-05/sa-cabinet-minister-breaks-ranks-over-speed-limit-policy/9017580

[9] Kloeden CN, Woolley JE (2020) *Vehicle speeds in South Australia 2018.* (CASR155) Centre for Automotive Safety Research, Adelaide.

[10] Alavi, H., Keleher, S., Nieuwesteeg, M. (2014). *Quantifying the contribution of low-level speeding to trauma in Victoria.* Australasian Road Safety Research Policing Education Conference. 2014, Melbourne, Victoria, Australia.

[11] Williams, A. F., Kyrychenko, S. Y., Retting, R.A. (2006). Characteristics of speeders. *Journal of Safety Research 37* (2006) 227-232.

[12] Stephens, A.N., Nieuwesteeg, M., Page-Smith. J., Fitzharris, M. (2017). Self-reported speed compliance and attitudes towards speeding in a representative sample of drivers in Australia. *Accident Analysis and Prevention 103* (2017) 56–64.

[13] Perez, M.A., Sears, E., Valente, J.Y., Huang, W., Sudweeks, J. (2021) Factors modifying the likelihood of speeding behaviors based on naturalistic driving data. *Accident Analysis and Prevention 159* (2021) 106267.

[14] Ellison, A.B & Greaves, S. (2010) *Driver Characteristics and Speeding Behaviour* Australasian Transport Research Forum. https://www.australasiantransportresearchforum.org.au/sites/default/files/2010_Ellison_Fifer_Greaves.pdf

[15] Centre for Road Safety, Transport for NSW (2020). *Road traffic crashes in New South Wales: Statistical Statement for the year ended 31 December 2019.* https://roadsafety.transport.nsw.gov.au/downloads/crashstats2019.pdf

[16] Doecke, S. D., & Kloeden, C. N. (2014). The accuracy of determining speeding directly from mass crash data and using the NSW Centre for Road Safety method. *Journal of the Australasian College of Road Safety, 25*(1), 35-41.

[17] Fitzpatrick, C.D., Rakasi, S & Knodler Jr., M.A. (2017) An investigation of the speeding-related crash designation through crash narrative reviews sampled via logistic regression. *Accident Analysis and Prevention 98* (2017) 57-63.

[18] Bortles, W., Biever, W., Carter, N., and Smith, C., (2016) *A Compendium of Passenger Vehicle Event Data Recorder Literature and Analysis of Validation Studies.* SAE Technical Paper 2016-01-1497, doi:10.4271/2016-01-1497.

[19] Doecke SD, Kloeden CN, Paine M (2019) *Speeding in crashes in the United States of America: A pilot study using event data recorder information from NASS-CDS.* 26th International Technical Conference on The Enhanced Safety of Vehicles, Eindhoven, The Netherlands, 10-13 June 2019.

[20] Elsegood, M. E., Doecke, S. D., & Ponte, G. (2021). *Collection and analysis of EDR data from crash-involved vehicles: 2020-21 summary report* (CASR188). Adelaide: Centre for Automotive Safety Research.

[21] Kloeden, C. N., Linke, B. J., & Ponte, G. (unpublished). *How accurate is the South Australian crash database in recording casualty crash details?* (CASR078). Adelaide: Centre for Automotive Safety Research.

[22] Metzger, K. B., Sartin, E., Foss, R. D., Joyce, N., & Curry, A. E. (2020). Vehicle safety characteristics in vulnerable driver populations. *Traffic injury prevention*, *21*(sup1), S54-S59.

[23] Yao, Y., Carsten, O., & Hibberd, D. (2020). Predicting compliance with speed limits using speed limit credibility perception and risk perception data. *Transportation research record, 2674*(9), 450-461.

[24] Newstead, S., & D'Elia, A. (2010). Does vehicle colour influence crash risk? *Safety science*, *48*(10), 1327-1338.

GENERATING REPRESENTATIVE TEST SCENARIOS:
THE FUSE FOR REPRESENTATIVITY (FUSE4REP) PROCESS MODEL FOR COLLECTING AND ANALYSING TRAFFIC OBSERVATION DATA

Maximilian Bäumler
Matthias Lehmann
Günther Prokop,
Chair of Automobile Engineering,
Technische Universität Dresden
Germany

ABSTRACT

Scenario-based testing is a pillar of assessing the effectiveness of automated driving systems (ADSs).
For data-driven scenario-based testing, representative traffic scenarios need to describe real road traffic situations in compressed form and, as such, cover normal driving along with critical and accident situations originating from different data sources. Nevertheless, in the choice of data sources, a conflict often arises between sample quality and depth of information. Police accident data (PD) covering accident situations, for example, represent a full survey and thus have high sample quality but low depth of information. However, for local video-based traffic observation (VO) data using drones and covering normal driving and critical situations, the opposite is true. Only the fusion of both sources of data using statistical matching can yield a representative, meaningful database able to generate representative test scenarios. For successful fusion, which requires as many relevant, shared features in both data sources as possible, the following question arises: How can VO data be collected by drones and analysed to create the maximum number of relevant, shared features with PD?

To answer that question, we used the Find–Unify–Synthesise–Evaluation (FUSE) for Representativity (FUSE4Rep) process model. We applied the first ("Find") and second ("Unify") step of this model to VO data and conducted drone-based VOs at two intersections in Dresden, Germany, to verify our results. We observed a three-way and a four-way intersection, both without traffic signals, for more than 27 h, following a fixed sample plan. To generate as many relevant information as possible, the drone pilots collected 122 variables for each observation (which we published in the ListDB Codebook) and the behavioural errors of road users, among other information. Next, we analysed the videos for traffic conflicts, which we classified according to the German accident type catalogue and matched with complementary information collected by the drone pilots. Last, we assessed the crash risk for the detected traffic conflicts using generalised extreme value (GEV) modelling. For example, accident type 211 was predicted as happening 1.3 times per year at the observed four-way intersection.

The process ultimately facilitated the preparation of VO data for fusion with PD. The orientation towards traffic conflicts, the matched behavioural errors and the estimated GEV allowed creating accident-relevant scenarios. Thus, the model applied to VO data marks an important step towards realising a representative test scenario database and, in turn, safe ADSs.

INTRODUCTION

Automated driving systems (ADSs), as an increasingly common part of road traffic today (Hohm, 2022), are designed to reduce the number of accidents and fatalities on the road and, as such, to play a significant role in making road traffic safer. To that end, ADSs first have to prove that they can drive more safely than attentive human drivers (Bergmann, 2022). One way to test ADSs for the safety of their intended functionality and thus safe driving is scenario-based testing, which entails using scenarios derived from real-world data (Nalic *et al.*, 2020), including naturalistic driving studies, police accident data (PD) and video-based traffic observations (VOs) using drones (Bock *et al.*, 2019; Nalic *et al.*, 2020). At best, real-world data sources cover all road traffic in the ADSs' operational design domain (ODD) and thus represent the ODD of road traffic (Lehmann *et al.*, 2019). Ideally, those data sources should also have the same depth of information needed to derive test scenarios.

However, the continuous collection of real-world data in all ODDs in which ADS are slated to operate is cost-intensive and technically complex. Beyond that, real-world data sources vary in the content of their information. Although PD represent entire regions or countries, they encompass information accessible only to police officers. Given that restriction, dynamic information about parties involved in accidents is not collected. By contrast, VOs afford a microscopic perspective on the dynamic behaviour of road users but are often spatially and temporally limited available.

In response to those setbacks, Bäumler and Prokop (2022) have proposed creating representative, information-rich databases for deriving test scenarios by fusing various real-world data sources. For instance, PD from Germany can be fused with data from local VOs, assuming that they belong to one unobserved, superordinate population (Bäumler *et al.*, 2020). In that case, dynamic information about road users (e.g. trajectory, speed and acceleration) can be assigned to the corresponding PD.

Given a common, unobserved, superordinate population, the quality of fusing two data sources depends primarily on the overlapping information between the sources—for instance, in the form of common variables (D'Orazio, Di Zio and Scanu, 2006). The more variables that coincide, the higher the probability of achieving good data fusion results (Rässler, 2002; D'Orazio, Di Zio and Scanu, 2006). For that reason, data collection should consider unifying information between the sources to be fused. However, regarding the fusion of, for example, German PD and VO data, changes in the nationwide standardised data collected by police are achievable only in the long term. Thus, VOs should be geared towards collecting information and/or variables comparable to PD. To that end, with reference to a real-world case, this paper answers a specific research question: How can VO data be collected by drones and analysed to create the maximum number of relevant, shared features with PD?

To answer this question, we introduce and apply the Find–Unify–Synthesise–Evaluation (FUSE) for Representativity (FUSE4Rep) process model (Bäumler and Prokop, 2022) to collect and analyse VO data for subsequent data fusion.

In what follows, we first introduce the general idea of the FUSE4Rep process model and the resulting requirements for collecting VO data using drones. Next, we demonstrate how VOs are collected using drones and a mobile app that we developed, after which we analyse the data collected and derive additional common variables concerning PD. We close the paper with a discussion of our results and directions for future research.

BACKGROUND

The FUSE4Rep model (see Figure 1), developed by Bäumler and Prokop (2022), proposes a holistic approach for fusing PD with VO data. In contrast to alternative approaches (Erbsmehl *et al.*, 2017; Erbsmehl, Lich and Mallada, 2019; Krause, 2019), the FUSE4Rep model explicitly seeks to maximise overlapping information between both sources of data to be fused and, in the process, to ensure valid fusion using statistical procedures, specifically statistical matching. As shown in Figure 1, the FUSE4Rep model starts by determining the shared, unobserved, superordinate population between two data sources as well as identifying potential common information that can be collected and/or analysed in both sources. Second, the common information identified needs to be mined and unified to be comparable. Third, both prepared data sets are synthesised using statistical matching, a process detailed by Bäumler et al. (2020). Last, data fusion is evaluated using statistical indicators and, if available, real-world data.

In light of our research question, this paper focuses on the first and second step of the FUSE4Rep model: "Find" and "Unify". Thus, possible information shared by PD and VO data is identified and subsequently unified. In the following, we use the terms *crash* and *accident* synonymously.
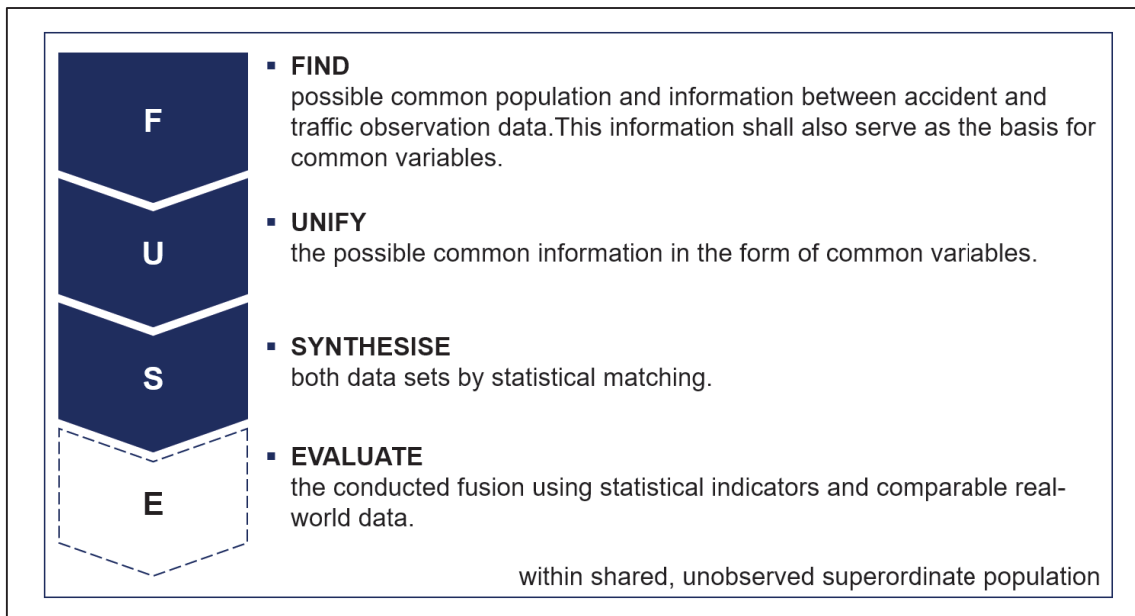
Figure 1. The four steps of the FUSE4Rep process model.

METHOD

This section describes our VOs, conducted to collect data to be fused with PD, and their subsequent analysis. Figure 2 shows the specific steps of the FUSE4Rep process model applied in this paper. In doing so, it anticipates that possible traffic conflicts, in the form of three-digit accident types (3AT), belong to the overlapping information within VOs and PD and should thus be collected and analysed.

1. Find the information to be collected:
(Meta) variables / Codebook

2. Find a data collection method:
Smartphone application

Find

3. Find the population to be observed:
Location and sample plan

4. Find the conflict situations theoretically possible:
3-digit-accident types

5. Unify by analysing the conflict situations happened:
3-digit-accident types

Unify

6. Unify by assessing crash risk:
Extreme value modelling (GEV)

Synthesise

Evaluate

within shared, unobserved superordinate population

Figure 2. The FUSE4Rep process model applied to VO data.

Step 1: Find
In this subsection, we introduce all of the necessary steps for collecting VO data within the first step, "Find", of the FUSE4Rep process model (see Figure 2).

Information to be collected
To ensure that the VO data collected can be fused with PD, they need to fulfil the following four requirements:

1. Coverage of information collected by the police and thus published in national statistics (Destatis, 2021), because the PD to be fused are German;

2. Consideration of the traffic safety causality model (see Figure 3; Tarko, 2019; Orsini *et al.*, 2021), which represents the emergence of crashes;

3. Consideration of the six-layer model for scenario description (Scholtes *et al.*, 2021), because the fused data set should ultimately support the generation of test scenarios; and

4. Information collected by one drone pilot equipped with corresponding measurement instruments to keep personnel costs low.

Based on the four requirements, we created a codebook containing 122 different variables to be identified during and after a VO. The ListDB Codebook, published as part of the "Leverage Information on Street Traffic (ListDB)" project, has been made publicly available.[1]

---

[1] The ListDB Codebook can be accessed at https://w3id.org/listdb/.

According to the adapted causality model of traffic conflicts and crashes displayed in Figure 3, every crash is preceded by a traffic conflict. However, because not every traffic conflict necessarily leads to a crash, every accident recorded by the police is based on a traffic conflict, which in Germany can be described with the help of the 3AT classification (Ortlepp and Butterwegge, 2016; Destatis, 2021). Specifically, a traffic conflict represented as a 3AT describes the simultaneous approach of road users to a point on the road where they may collide (Ortlepp and Butterwegge, 2016). At the same time, traffic conflicts can be recorded and video-based analysed (Polders and Brijs, 2018). Therefore, a possible link between PD and VO data lies in the uniform description of traffic conflicts in both data sources according to the 3AT classification. The causality model (Figure 3, left) also shows that a set of different factors (e.g. road- and weather-related factors) can influence traffic conflicts and, in turn, crashes (Tarko, 2020). Thus, those factors should also serve as links between PD and VO. In that context, the six-layer model (6LM) for describing test scenarios for assessing ADSs already covers all factors except human factors. Because the 6LM was taken into account in the design of the ListDB Codebook, we here detail the collection and presentation of traffic conflicts in connection with human factors in the Codebook and refer to the detailed online ListDB Codebook for information from the other layers and factors.
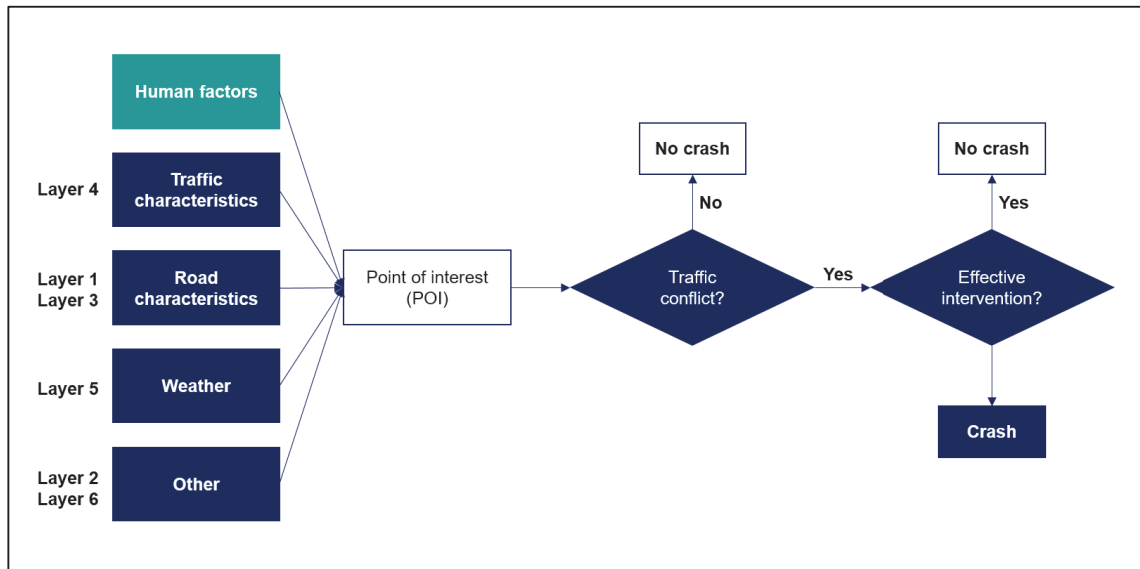
Figure 3. Causality model of traffic conflicts and crashes with assigned scenario layers, adapted from Tarko (2019) and Orsini et al. (2021).

In German PD, human factors primarily consist of drivers' behavioural errors, which can be assigned to different parties involved in accidents —namely, the primary contributor to the accident and other parties (Destatis, 2021). To each party, the police can assign up to three behavioural errors, including errors in observing the right of way, choice of speed or overtaking (Destatis, 2021). Therefore, it makes sense to adopt the police's categories of behavioural errors for VO data and assign them to observed traffic conflicts. However, the following challenges arise as a consequence:

1. **Limited detection of traffic conflicts:** Reliably detecting traffic conflicts in the recorded VO data needs to be possible. Test observations have shown that parking crashes, for example, are difficult to detect in VOs from the height at which drones fly (ca. 80 m) due to constraints in resolution and object detection. Traffic conflicts caused by unusual events, including ambulances with active blue lights, are also challenging to detect.

2. **Lack of ego-perspective:** Due to the missing ego-perspective of road users involved in traffic conflicts, the causes of behavioural errors, including visual obstacles, are challenging to detect and assess. Road users may also agree on the right of way at intersections, meaning that a seeming right-of-way error, especially when seen from the drone's bird's-eye view, may not in fact be one.

3. **Lack of personal information:** Drivers' behavioural errors, which affect drivers as people (e.g. excessive alcohol consumption and fatigue) are not detectable from the outside.

The first two challenges require a deep understanding of the traffic situation in question and its context, which cannot be achieved by analysing only the video data collected afterwards. However, the drone pilot

monitoring traffic situations during VOs can help to overcome those challenges. Therefore, we propose including the drone pilot in the detection of traffic conflicts and behavioural errors and linking it to real-time, drone-based video recording. That approach combines conflict techniques relying on human experts, so to speak, including parts of the "Swedish Traffic Conflict Technique" (Polders and Brijs, 2018), with automatic video analysis afterwards.

Nevertheless, because it is also difficult for drone pilots to recognise traffic conflicts, we introduced the concept of point of interest (POI), which generally precedes a potential traffic conflict (see Figure 3) and is easier for drone pilots to detect. As detailed in Table 1 in the Appendix, we differentiate four types of POIs:

1. **Single (1×):** One road user shows unusual behaviour or behavioural errors.

2. **Interaction (8×):** At least one road user reacts or should react to another road user. Interactions include the type of road user for interactions between a maximum of two users. Interactions with more than two users are multi-object interactions that do not specify the types of users.

3. **Predefined event (5×):** Predefined events are special and rare events (e.g. ambulances with active blue lights or slow-moving obstacles such as sweepers).

4. **Other (1×):** Everything that does not fit into the other three types is categorised as "Other".
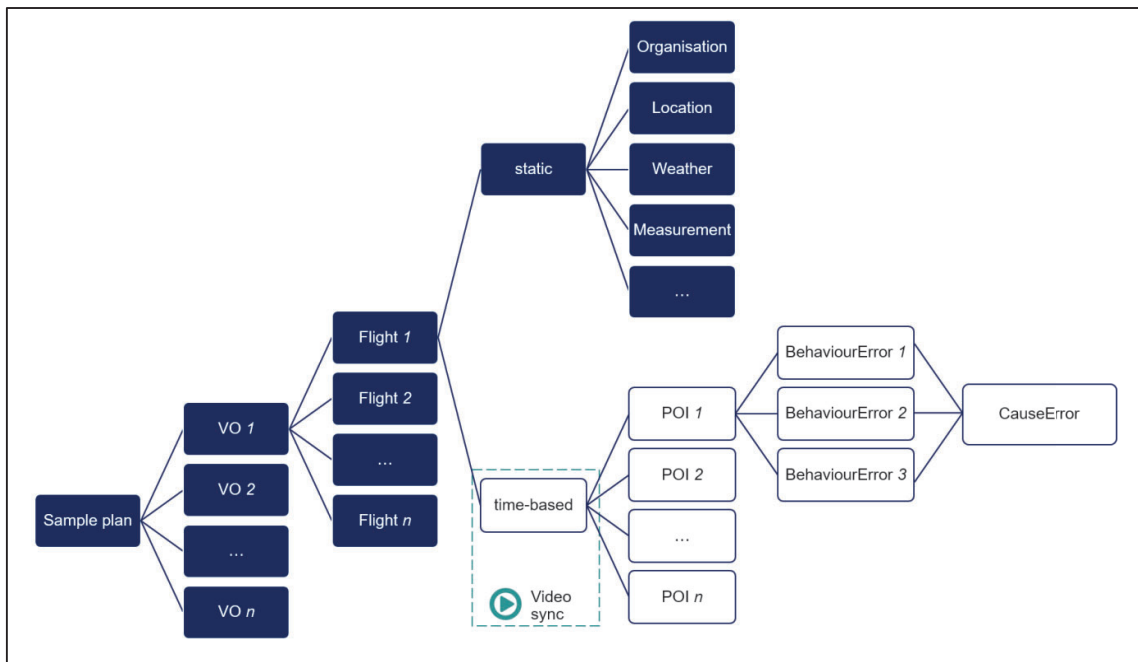
Figure 4. Relationships between sample plan, VOs, flights and identified variables.

For each POI that the drone pilot captures, three different behavioural errors can also be captured, along with one cause of the behavioural error (see Figure 4). Next, to overcome the third challenge, because the drone pilot can capture only behavioural errors that are visible to them, we have reduced possible behavioural errors in the PD (Destatis, 2021) to 11 major categories, including "PriorityError", "RoadUseError" and "DistanceError" (see Appendix, Table 5). The causes of such errors can be obstacles distracting the driver's sight (i.e. "VisualCause"), technical issues (i.e. "TechnicalCause") or weather-related issues (i.e. "EnvironmentalCause").

In general, every VO can consist of several drone flights, with the battery's capacity generally limiting flight times. There are also static and time-based variables for each flight. On the one hand, static variables (e.g. location, weather and measurement equipment) are considered to have stationary status during flights. For example, if the weather changes during a flight, then a new flight has to be started and the variable adjusted accordingly. As for time-based variables, on the other hand, to ensure the subsequent matching of POIs detected by a drone pilot with the traffic conflicts detected in subsequent video analysis, the timestamp of each detected POI is (manually) synchronised with that of the VO at the beginning of the recording (see Figure 4). Thus, POIs are treated as time-based variables, as shown in Figure 4.

Data collection tools

Aside from a video drone and thermometers,[2] the essential survey instrument is an Android smartphone with the ListDB app, which the drone pilot can use to record all static and time-based variables defined in the ListDB Codebook. Figure 5 (left) illustrates the POI screen visible to the drone pilot during video-recording. As shown, the drone pilot can collect all POIs displayed on the screen by clicking on the corresponding buttons. Whereas a short click records a POI and the corresponding timestamp (see Figure 5, bottom), a long click opens another screen showing all possible behavioural errors and causes. After selecting the road user showing the behavioural error, the drone pilot can select up to three errors and one cause. Upon completion, the screen closes, and the data are saved together with the POI and the timestamp.

Date	Time	POI	Error of…	BehaviouralError 1	BehaviouralError 2	BehaviouralErrror 3	CauseError
20221123	130735	Videostart					
20221123	131020	VehicleVehicle	Vehicle	PriorityError	SpeedError	OvertakingError	VisualObstacle
20221123	131240	VehicleCycle	Cycle	PassedPriority	/	/	/
20221123	132010	Videoend					
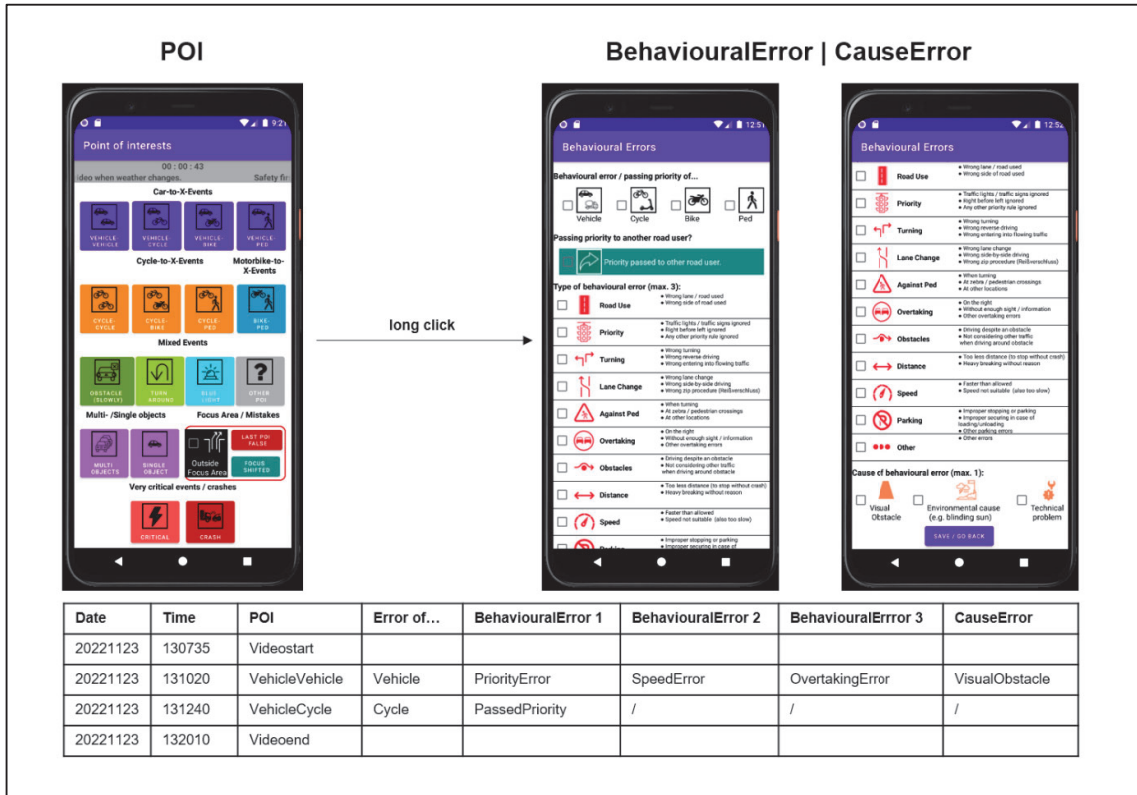
Figure 5. ListDB App v0.3.2.4 – Screenshot of the POI and behavioural error screens. The table illustrates the format in which the information is stored.

---

[2] The video drone used was the DJI Mini 2, which offers video recording with a resolution of 3.840×2.160 pixels and a sampling rate of 29.97 frames per second.

Population to be observed

A shared, unobserved, superordinate population is a prerequisite for successfully fusing PD and VO data. For that reason, VOs have to target a population intersecting with the PD. Generally, a population and samples drawn from it should be described factually, spatially and temporally (Gabler and Häder, 2015; Lehmann *et al.*, 2019). From a factual perspective, the common population can be formed by all traffic conflicts at the examined locations, in which case traffic conflicts can be regarded as the binding element between PD and VOs (see Figure 3). Based on the factual component of the population, selecting locations where traffic conflicts are known to occur makes sense as a means to determine the spatial component of the population. Indeed, the conflicts need to have occurred in locations where accidents have already happened. Thus, we selected two intersections in Dresden, Germany, for VO, where five relevant crashes occurred between 1 January 2005 and 31 December 2021: a three-way intersection called "Tharandter Straße/ Frankenbergstraße" and a four-way intersection called "Dorfhainer Straße/Kohlenstraße" (see Figure 7).[3] Both intersections are located within the city and therefore have a speed limit of 50 km/h on the priority road. From the temporal perspective, it would make sense to have a permanent VO in place to record all traffic conflicts at the selected intersections. However, because the availability and number of survey personnel, as well as the research's budget, did not allow such monitoring, we defined a 3-month period in which the VO had to occur. As shown in Figure 6, June, July and August constituted the period chosen for VOs, as they are relatively accident-prone months in Dresden from 2017 to 2021 that usually have good weather conditions. Statistics of traffic accidents in Dresden (Figure 6) also illustrate that the occurrence of accidents does not depend on the day of the week; thus, all weekdays can be treated equally in the VO, though the weekend has to be excluded due to the limited availability of staff. Regarding the exact recording times, the following boundary conditions were used to confine continuous VO during all weekdays in the three selected months:

1. **Daylight recording:** Video recordings at night are impossible with the drones used.

2. **Good weather conditions:** The drones cannot fly in strong winds (>21 km/h), rain or snow.

3. **Limited flight time:** The average drone flight time is 20–25 min per battery charge. With the equipment available, about 90 min of recording at a time can be achieved.

4. **Limited access:** The responsible air traffic control authority has to inspect and approve each flight.

5. **Limited personnel budget:** The weekly working time of the two employed drone pilots cannot exceed nine hours incl. arrival and departure as well as data transfer.

Thus, it is necessary to develop a sampling plan to cover the targeted population, one able to ensure that every traffic conflict has the same odds of being considered in the sample and thus guarantee the random selection of traffic conflicts (Bischoff, 1995; Pfeiffer, 2006; Lehmann *et al.*, 2019). The requirements for the sampling plan were therefore:

1. **Fixed time slots:** Fixed time slots have to be considered for recording and covering accident-prone daylight hours. Each time slot can last 90 min maximum.

2. **Equal distribution of time slots:** Each time slot has to be observed once per month at each intersection. All time slots have to be observed the same number of times.

3. **Equal distribution of weekdays:** The time slots have to be evenly distributed across the weekdays. A time slot may only be observed again on the same day of the week when the other weekdays have already been fulfilled.

4. **Flexibility:** The drone pilot has to be free to choose the day of surveying with the given sampling requirements, because the weather conditions have to be suitable, and the flight permit has to be granted.

After analysing the statistics of accidents by hour of occurrence (see Figure 6), we defined four 90-min time slots distributed over the course of a day with daylight as follows:

1. **Time slot 1:** 7:30 a.m. to 9:00 a.m.

2. **Time slot 2:** 10:00 a.m. to 11:30 a.m.

3. **Time slot 3:** 1:00 p.m. to 2:30 p.m.

---

[3] In-house accident data begin on 1 January 2005. Accidents had to involve two cars, not involve a party under the influence of drugs or alcohol, not involve a trailer and be of accident type 2 (turning), 3 (turning in or crossing), or 6 (longitudinal traffic).

4. **Time slot 4:** 3:30 p.m. to 5:00 p.m.
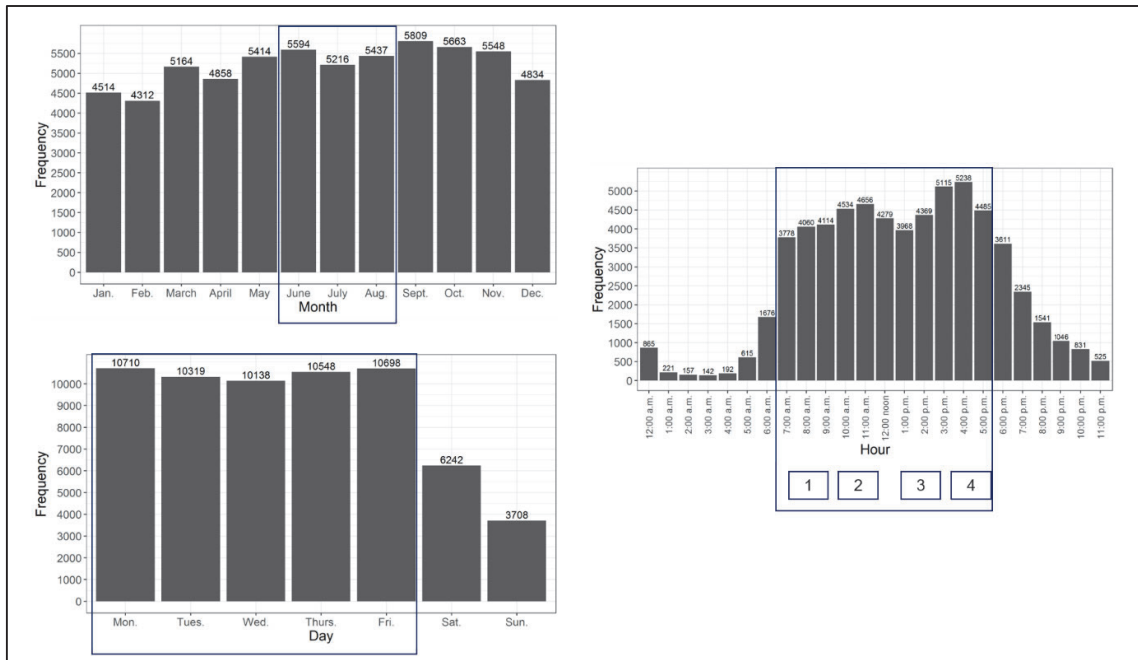
Figure 6. Road traffic accidents in Dresden, 2017–2021. All crashes involved no more than two parties.

Taken together, those boundary conditions and the derived sampling plan slightly changed the target population compared with the desired one (see Table 1). The most significant deviation was that the actual targeted population represented only traffic conflicts in good weather during daylight hours and the defined time slots.

Table 1.
Comparison of the desired and real target population for VOs.

	Factual	**Spatial**	**Temporal**
Desired target population	All traffic conflicts in any weather condition, regardless of daylight	Dresden, Tharandter Straße/Frankenbergstraße	Total period from 1 June to 31 August 2022
Actual target population	Traffic conflicts in good weather conditions during daylight hours	Dresden, Dorfhainer Straße/Kohlenstraße	Within the four time slots defined, from 1 June to 31 August 2022

Theoretically possible conflict situations

The FUSE4Rep process model will be applied to generate test scenarios for car specific ADSs in the first stage (Bäumler and Prokop, 2022). However, because subsequent video analysis cannot be used to mine pedestrian and bicycle trajectories reliably, we have focused on detecting traffic conflicts between two cars. At the same time, because the traffic conflicts should affect ADSs in their ODDs, we have not considered traffic conflicts involving only one road user—for example, veering off the road to the right due to the driver's carelessness. We have also not considered parking and animal-related traffic conflicts. Figure 7 illustrates the remaining 3ATs that can theoretically occur at the observed intersections, all 27 of which represent one of four accident types—(2) turning, (3) turning in or crossing, (6) longitudinal traffic, and (7) other (Ortlepp and Butterwegge, 2016)—defined as follows:

2. **Turning:** Conflicts between a road user turning and another road user coming from the same or opposite direction;

3. **Turning in or crossing:** Conflicts between a road user who is turning or crossing but obliged to wait for another road user with the right of way;

6. **Longitudinal traffic:** Conflicts between road users moving in the same or opposite direction; and

7. **Other:** Conflicts that cannot be classified into any other category.

Figure 7 also displays traffic conflicts that do not apply to the three-way intersection observed—namely, the blue-coloured traffic conflicts 215, 301, 321, 602, 612 and 651—and that, of the five crashes observed at either intersection, only the 3ATs 201, 211, 302 and 601 were represented.
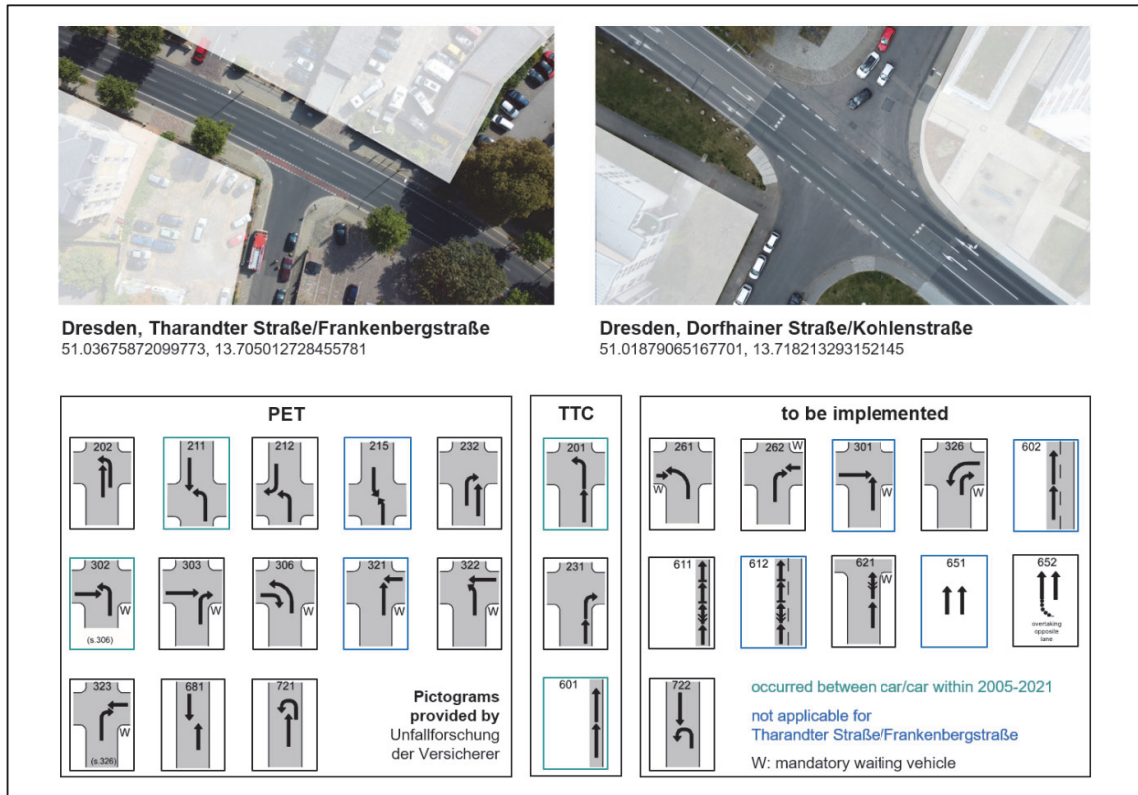
Figure 7. Intersections observed from a height of approximately 80 m with theoretically possible and implemented three-digit accident types.

Step 2: Unify

In what follows, we introduce all steps necessary for analysing VO data in the second step, "Unify", of the FUSE4Rep process model (see Figure 2).

Trajectory mining

Our drone-based observations each delivered a video file, from which certain information about the dynamic behaviour and properties of the road users and their interactions has to be extracted. Such information encompasses:

- Properties of road users

  ○ Object type (i.e. car, van, truck, biker, cyclist and pedestrian)

  ○ (Transit) manoeuvres (i.e. turn right, turn left and go straight)

  ○ Kinematics (i.e. velocity, acceleration, location and manoeuvre-specific development over time)

- Interactions with other road users

  ○ Surrogate safety measures (SSM), including time to collision (TTC; Hayward, 1972), and post-encroachment time (PET; Allen, Shin and Cooper, 1978)

Extracting that information from the video files requires the steps shown in Figure 8, all adapted from Khan *et al.* (2017). In preprocessing, all unnecessary parts of the recording (e.g. flight start) are removed, followed by image rectification required by the non-ideal parameters of the camera lens.
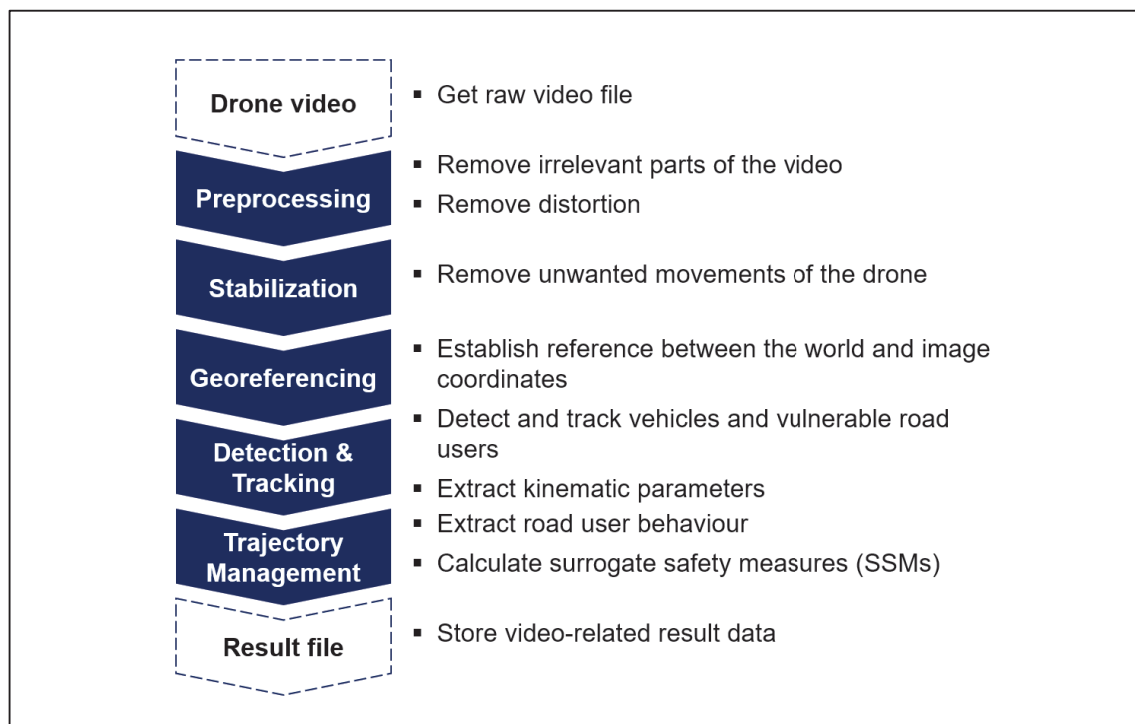
Figure 8. Steps of information extraction, adapted from Khan et al. (2017).

Before being analysed, the recordings have to be stabilised. When in operation, the drones are exposed to external influences from the wind that, despite each drone's internal control strategy, cause unwanted movements and thus changes in the recording angle relative to the ground (see Figure 9). For example, the detected vehicle in the red box in Figure 9 would be repositioned on the sensor due to such movements, which would give it a velocity (v) and acceleration (a) during detection that misrepresent reality. To overcome those movements, all video frames are mapped to a so-called base frame at the beginning of each recording. Once the recordings have been stabilised, the relationship between each

drone's coordinate system (x_{image}, y_{image}, see Figure 9) and a geodetic reference system—for example, WGS84 (United States - Defense Mapping Agency, 1987)—has to be established in order to be able to convert the kinematic parameters from pixel to metric units (Hackeloeer *et al.*, 2014). Next, the video data are prepared to allow the extraction of the required information. During detection, all objects of interest in the frames have to be detected so that the information between the frames can subsequently be merged into the tracking part. Correct detection is the only way to ensure that objects of interest are always clearly identifiable over time and to extract the kinematic parameters correctly. Last, in trajectory management, all required data about drivers' behaviour (e.g. manoeuvres) are derived and simple conflict situations measures (e.g. TTC) calculated.
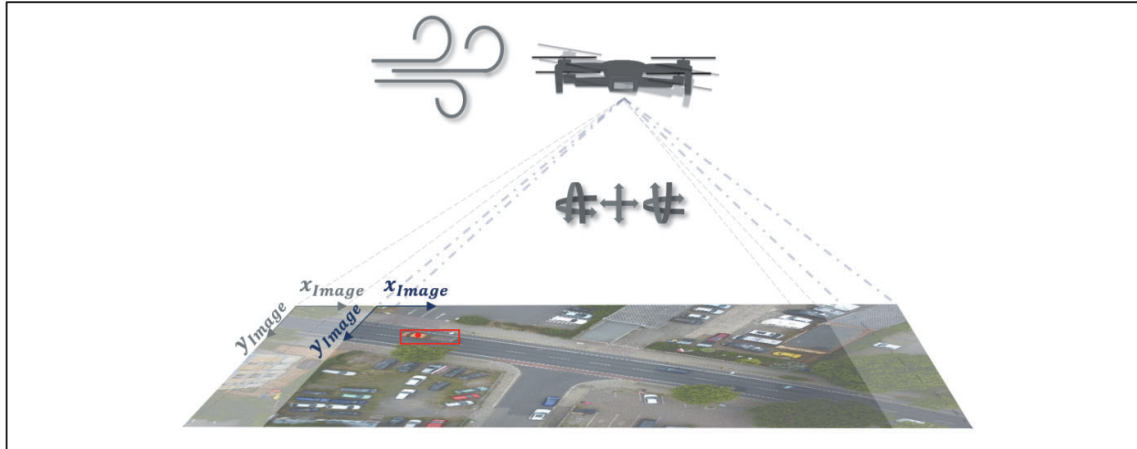
Figure 9. Drone movement due to external influences.

In video analysis, a wide variety of algorithms are needed to perform individual tasks. To that end, and to respond to shifting insights and requirements, a custom tool called "track in drone view" (tidv) has been developed, namely on a microkernel architecture (Richards and Ford, 2020). By outsourcing the individual tasks (e.g. keypoint detection as part of stabilisation) to plug-ins, different algorithms can be used, and the functionalities can be easily extended. The structure of tidv is outlined in Figure 10.
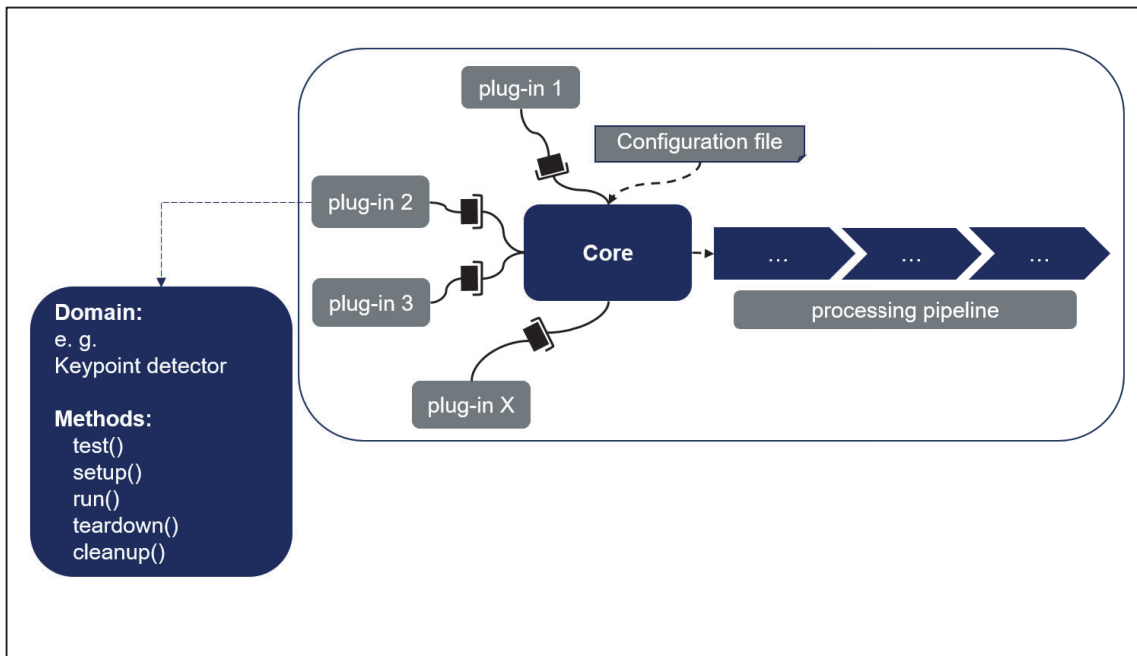
Figure 10. Track in drone view structure (tidv) and plug-in structure.

The core of tidv completely takes over the control and monitoring of the workflow processes. For its part, the workflow is defined via a configuration file written in YAML (Ben-Kiki, Evans and Ingerson,

2021) that can be created manually by the user or with the help of a graphical user interface. With reference to the processing steps, the processing pipeline is checked for consistency by the core before the plug-in's execution. Each plug-in follows a fixed structure (see Figure 10 left side), in which the associated domain is first defined, which determines the data interfaces because the data input and output formats are defined for each domain within tidv. A plug-in's five defined methods to be implemented are test, set-up, run, clean-up and teardown. First, *test* involves checking the behaviour and presence of the necessary data before the setup's execution. Second, *set-up* involves preparing the *run* method for its execution; for example, the necessary neural network weights have to be loaded such that the trained network is available. Third, *run*, occurring at the core of the plug-in, performs the task, after which *clean-up* involves eliminating data that are no longer needed. Last, *teardown* involves terminating the pipeline if an unexpected error occurs. In all, the plug-in's structure allows performing a modular, continuously expandable analysis of traffic observations using tidv.

Because the implementation of the plug-ins is beyond this paper's focus, we discuss only the two plug-ins that are essential in our work: one for recognising road users' manoeuvres, the other for calculating TTC. First, for manoeuvre recognition, the user defines gates on the base frame of the stabilised video (i.e. reference mapping frame for stabilisation), as shown in Figure 11, where white lines indicate the start and end of the junction arm and the black lines the start and end of the central intersection area. Thus, and as shown, the intersection is divided into respective arms and a central area. The start and end points of the trajectories in the defined areas can be used to determine the manoeuvre performed by the road user (i.e. turning right or left or driving straight), which is connected with the individual analysis of the dynamics and heading of the road users performed to extract manoeuvres inside the specified areas. By comparing the position within the areas, the current state of the intersection can also be determined (e.g. access to or departure from the intersection or passage of the central area).
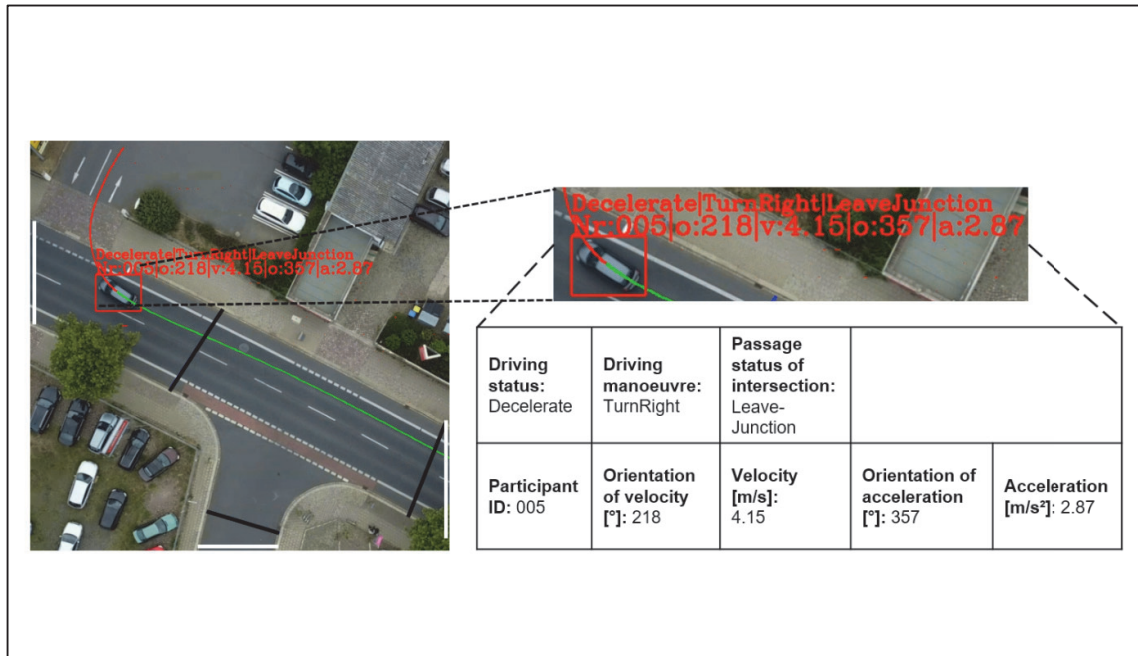
Figure 11. Analysis of a road user's manoeuvre.

To calculate TTC, the vehicles' geometries are first estimated entirely because the YOLOv4 detector (Bochkovskiy, Wang and Liao, 2020) uses only axis-aligned bounding boxes as outputs ("red box framing the vehicle in Figure 11"). The minimum size of the bounding box can be determined by rotating the image to estimate the size of the road users. The TTC for conflict situations, in which one car follows another car (i.e. situations corresponds to 3AT 601) can be calculated with Equation 1:

$$TTC_i(t) = \frac{\left(X_f(t) - X_l\right) - S_f}{v_f(t) - v_l(t)} \tag{1}$$

in which X is the vehicle position of the following (f) or leading vehicle (l) and v is the velocity of the vehicle and S the vehicle's length (Wang *et al.*, 2021).

By contrast, PET is calculated to determine the time elapsed between one road user leaving the potential collision zone (t_1) and another road user entering it (t_2). Following Allen, Shin and Cooper (1978), PET is defined as shown in Equation 2:

$$PET = t_2 - t_1 \qquad (2)$$

Last, as mentioned, processing a large amount of data with tidv was only partly possible owing to the hardware's limited capacity. Thus, commercial provider DataFromSky (DFS) supported video analysis.[4] Although we assumed that DFS's video-processing method was similar to our developed procedure, in the data obtained using DFS, TTC and PET had to be calculated using estimated vehicle dimensions (i.e. width and length).

Determining accident type

We next analysed all four 3ATs that resulted in at least one crash between 2005 and 2021 (see Figure 7). Beyond that, we selected 12 additional 3ATs, also listed in Figure 7, to be identified in the VO data. However, due to time constraints, we did not analyse the 12 other theoretically possible 3ATs listed in Figure 7.

Ascertaining a 3AT requires the correct manoeuver classification and SSM calculation. Building upon the mined trajectories, the process consists of seven steps, as shown in Figure 12, beginning with (1) taking a pair of trajectories t_i, t_j and (2) checking whether the road users belonging to the trajectories are visible in the video at the same time. If so, then (3) the corresponding manoeuvers m_i, m_j need to be obtained, including the manoeuver direction (e.g. turning left from B to C), at which time the directions depend on the location observed (e.g. a four-way intersection).
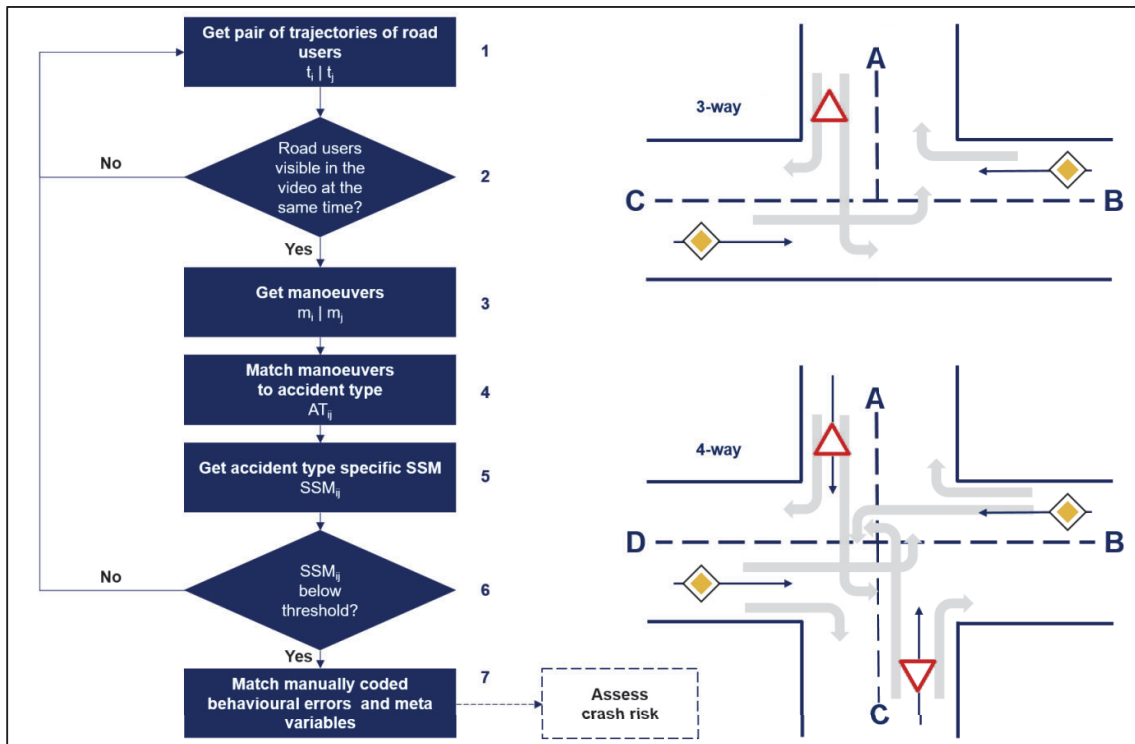
Figure 12. (Left) Determining accident type and (right) possible manoeuvres without turning around.

---

[4] www.ai.datafromsky.com/aerial

Next, (4) whether the combination of obtained manoeuvers matches a predefined 3AT AT_{ij} needs to be checked; for example, the manoeuver turning left from B to C and going straight from D to B could theoretically represent 3AT 211 (see Figure 7). After that, (5) the SSM_{ij} assigned to the previously determined AT_{ij} needs to be calculated. For 3AT 211, for instance, the PET is suitable for assessing conflicts between the two road users (see Figure 7). Once done, (6) whether the SSM_{ij} is in a predefined threshold needs to be determined in order to sort out irrelevant conflicts (e.g. $< 5s$ according to the length of the GIDAS pre-crash-matrix (Schubert, Erbsmehl and Hannawald, 2013)). Last, once the threshold is met, (7) the corresponding meta variables and manually coded behavioural errors can be matched to the determined AT_{ij} using the common timestamp (see Figure 5) between manual coding and the video-recording. As a result, the risk of a crash can be assessed.

Assessing the risk of a crash
Once the identified traffic conflicts were categorised according to the 3AT classification (see Figure 7), we examined the risk of a crash, or *crash risk*, of each 3AT to ensure that the 3AT populations obtained were relevant for fusion with PD. Because traffic conflicts can lead to crashes but do not have to (see Figure 3), we wanted to assess whether the detected traffic conflicts had at least an inherent risk of leading to a crash. If the risk was significantly greater than zero, then the traffic conflicts were suitable for subsequent fusion. Thus, we modelled crash risk using generalised extreme value (GEV) distributions (Zheng and Sayed, 2020) based on corresponding 3AT SSM distributions.

Zheng and Sayed (2020) have already predicted crash risk, R_C, for traffic conflicts in longitudinal traffic equivalent to 3AT 601 (see Figure 7), in which they used the modified TTC to assess conflicts and model the corresponding GEV distributions. For validation, in this paper we determine the crash risk for each 3AT, $R_{C,3AT}$, and predict the number of crashes, $N_{C,3AT}$, likely to occur in a year. Having a predicted number of crashes per year allows a comparison with PD within the scope of validation.

We applied the process from Coles (2013) and Zheng and Sayed (2020) to each of the observed locations (i.e. intersections without traffic signals) as follows:

1. **Extreme value determination:** Determining extreme values by data blocking, in which each detected traffic conflict represents a block represented by the corresponding SSM distribution (see Figure 13), and the SSM value from the block is taken to represent the maximum critical situation (i.e. SSM minimum);

2. **GEV modelling:** Estimating the corresponding GEV distribution $G_{3AT}(SSM)$ using maximum likelihood estimation,[5] particularly of the scale parameter σ, the location parameter μ and the shape parameter ξ;

3. **Risk calculation:** Making the corresponding SSM zero in the event of a crash, as shown in Equation 3;

$$R_{C,3AT} = G_{3AT}(0) = \begin{cases} exp\left\{-\left[1 + \xi_i\left(-\frac{\mu_i}{\sigma_i}\right)\right]^{-\frac{1}{\xi_i}}\right\}, & \xi \neq 0 \\ exp\left[-exp\left(\frac{\mu_i}{\sigma_i}\right)\right], & \xi = 0 \end{cases} \tag{3}$$

4. **Extrapolation:** Predicting the number of crashes for a year by extrapolating the location-dependent observation time t_l, as shown in Equation 4; and

$$N_{C,3AT}(T = 1\ year) = R_{C,3AT} * \frac{60[min]}{t_l[min]} * 24[hours] * 365[days] \tag{4}$$

---

[5] We used the function "fevd" from the R package extRemes (version 2.1).

5. **Validation:** Comparing the predicted $N_{C,3AT}$ with the corresponding PD.
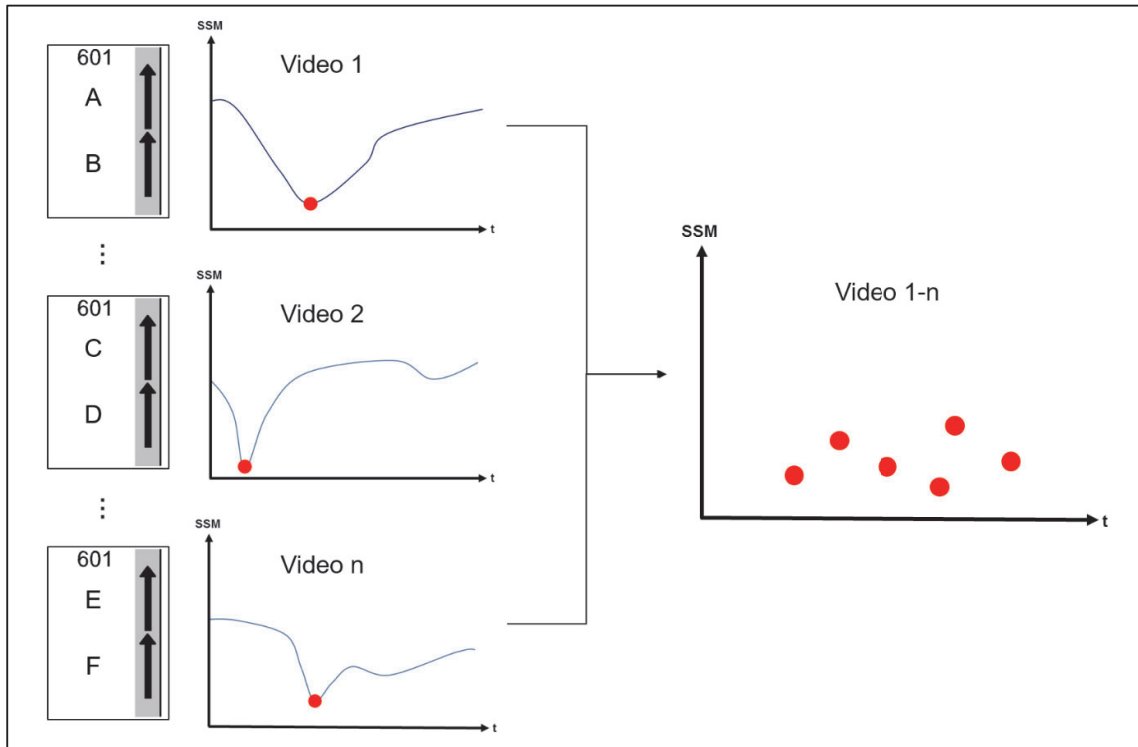
Figure 13. Determination of extreme values dependent on the 3AT.

RESULTS

Collected data

Table 2 introduces the data collected by two drone pilots: Pilot A and Pilot B. We assigned each pilot to one intersection depending on their route of approach to the intersection; Pilot A observed the three-way intersection for 790 min (13.2 h) and Pilot B the four-way intersection for 855 min (14.3 h), both in similar weather conditions. Among the results, Pilot A marked 2.4 times more POIs at the three-way intersection (i.e. 1827) than Pilot B at the four-way intersection (i.e. 774). Pilot A also marked eight near crashes and 241 POIs associated with behavioural errors, whereas Pilot B observed no near crashes and associated only 10 POIs with behavioural errors. At the same time, Pilot B associated 8 of 11 behavioural errors with visual causes (e.g. obstacles obstructing the drivers' view), whereas Pilot A recorded no such errors.

Table 2.
Overview of the data collected.

	Tharandter Straße / Frankenbergstraße	*Dorfhainer Straße / Kohlenstraße*
Drone pilot	A	B
Intersection type	3-way	4-way
Observation duration	1 June–31 August 2022	
Number of days observed	11	12
Recording time (in minutes)	790	855
Average temperature (in median °C)	21	22
Number of points of interest	1827	774
Number of crashes	0	0
Number of near crashes	8	0
Number of vehicle–vehicle interactions	1154	523
Number of behavioural errors	241	11
Number of vehicles with behavioural errors	175	11
Number of causes in total	0	8
Number of visual causes	0	8
Number of technical causes	0	0
Number of environmental causes	0	0
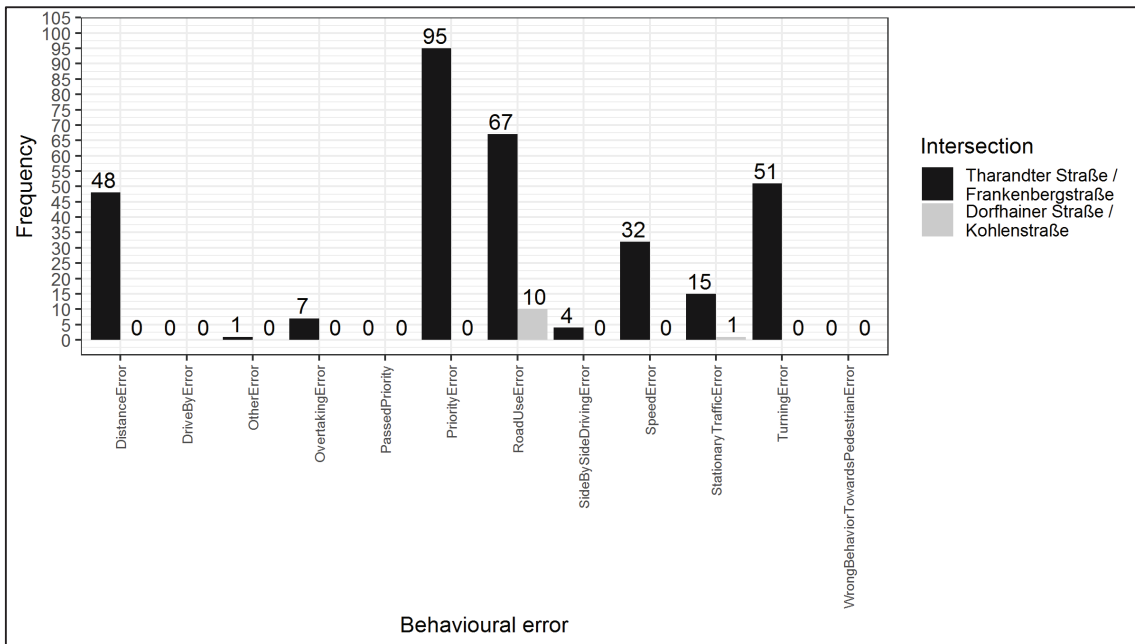
Figure 14. Type of behavioural errors.

Figure 14 highlights the different behavioural errors observed by the drone pilots. Overall, Pilot A observed nine types of errors at the three-way intersection, among which priority errors (95×), road use errors (67×) and turning errors (51×) were the most frequent. Meanwhile, Pilot B observed only two types of behavioural errors: 10 road use errors and one stationary traffic error. The aspect of "PassedPriority", meaning when a road user voluntarily gives up the right of way to another road user, was not logged during the observation and introduced only after the observation had ended; as we found this aspect to be important during the observation. Moreover, neither pilot observed the behavioural errors "DriveByError" or "WrongBehaviourTowardsPedestrianError".
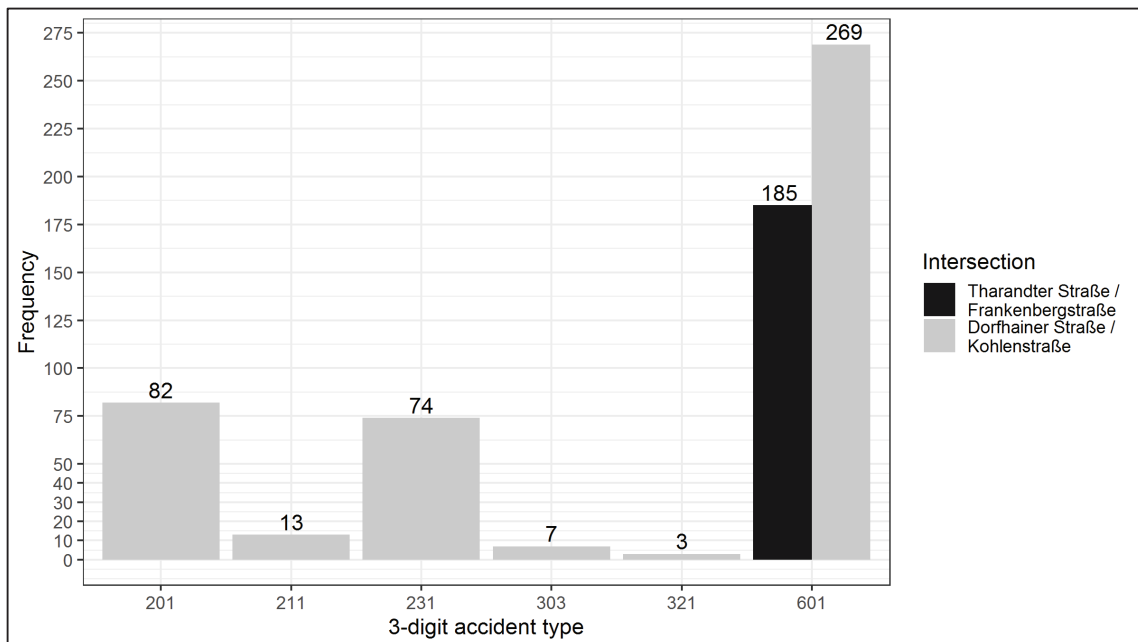
Figure 15. Detected conflict situations according to 3AT.

Determined conflict situations

Figure 15 introduces the automatically detected conflict situations between two cars, categorised according to the 3AT classification shown in Figure 7. Overall, 185 conflicts were detected at the three-way intersection, which represented 15.9% of all POIs marked by Pilot A, versus 448 conflicts detected at the four-way intersection, which represented more than 85.7% of the POIs marked by Pilot B. Remarkably, only 3AT 601 appeared in the three-way intersection, whereas that type and five additional 3ATs (i.e. 201, 211, 231, 303 and 321) appeared in the four-way intersection. Furthermore, as Table 3 reveals, only one type of behavioural error, "DistanceError", could be matched with the detected conflicts using the timestamp. An example of matching for DistanceError appears in Figure 16; although the white car with the red dot keeps a distance of 5.78 m while going 50 km/h, in Germany a distance of 15 m has to be maintained at that speed in urban areas (Autowelt, 2022). By comparison, the black car in the middle maintains a distance of 13.32 m, which is closer to the prescribed 15 m. The other behavioural errors listed in Figure 14 could not be assigned. Table 3 also introduces the conflict-related SSM distributions based on the extreme values revealed by data blocking. For example, 3AT 601, detected 178 times at the three-way intersection, had an extreme value distribution $G_{601}(TTC)$, with an average TTC of 1.53 s (median), a 25th percentile of 0.86 s and a 75th percentile of 2.25 s. To determine the extreme values, we removed SSM values less than 0.2 s if they did not lead to a crash, which was always the case. Therefore, the conflicts detected and the sample size, n, of the respective distributions differed (see Table 3). Beyond that, because the corresponding sample sizes for 3AT 601 (i.e. at the three-way intersection), 303 and 601 were quite small for GEV modelling, the distributions determined are not especially meaningful.

Table 3.
Detected conflict situations at the observed locations.

	No.	Frequency	3AT	Behavioural error	Cause	SSM	n (0.2 s > SSM < 5.0 s)	SSM [s] (25th percentile | median | 75th percentile)
Tharandter Straße/ Frankenbergstraße (3-way)	1	178×	601	/	/	TTC	178	0.86 | 1.53 | 2.25
	2	7×	601	Distance error	/	TTC	7	1.42 | 1.74 | 1.92
Dorfhainer Straße/ Kohlenstraße (4-way)	3	82×	201	/	/	TTC	27	0.86 | 1.08 | 1.60
	4	13×	211	/	/	PET	13	1.07 | 1.50 | 1.80
	5	74×	231	/	/	TTC	67	0.60 | 1.22 | 1.62
	6	7×	303	/	/	PET	7	2.20 | 2.64 | 2.64
	7	3×	321	/	/	PET	3	2.24 | 2.24 | 2.45
	8	269×	601	/	/	TTC	263	1.32 | 1.72 | 2.12
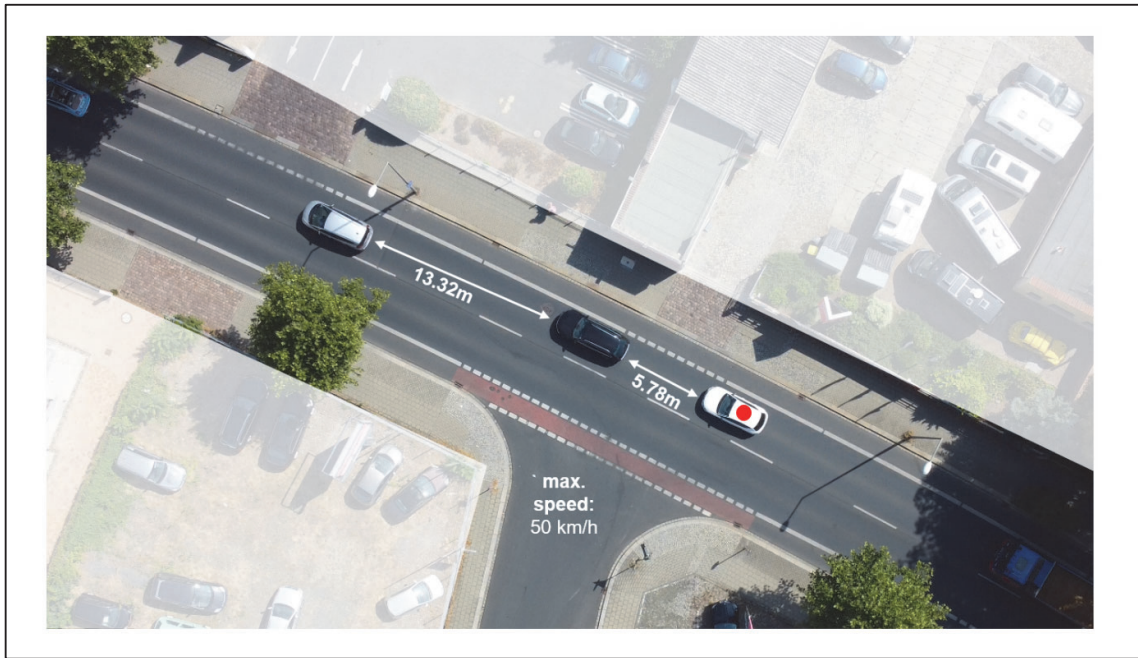
Figure 16. Manually coded distance error of car with red dot at Tharandter Straße/Frankenbergstraße.

Modelled crash risk

Table 4 lists the results of the modelled crash risk compared with official PD for the observed locations. Overall, the predicted number of crashes per year was rounded to 16 for the three-way intersection and to one for the four-way intersection. For the three-way intersection, the 3ATs 302 and 201, which led to crashes between 2005 and 2021, could not be predicted due to missing data (see Figure 15). As for the four-way intersection, the predicted results and official PD seem to coincide for 3AT 601; whereas 3AT 601 never led to a crash between 2005 and 2021, the predicted number of crashes was 0.012 and thus close to 0. The graphical analysis in Figure 17 (right) confirms that positive result, for the modelled distribution and empirically determined data coincide well. However, 3AT 211 occurred only once between 2005 and 2021 but was predicted to occur 1.3 times a year. At that rate, over 16 years, 3AT 211 would have occurred approximately 20 times, which is 20 times more than captured in the PD. Added to that, 3AT 601 also occurred only once between 2005 and 2021 at the three-way intersection but was predicted to occur 16 times a year, or 240 times more than in the PD across the 16-year period. Those results are confirmed in Figure 17 (left), which shows that the modelled and empirical distributions coincide poorly. In total, the predicted crash risks illustrate that the identified traffic conflicts according to the 3AT 601 for both intersections and the 3AT 211 have an inherent crash risk and seem suitable for subsequent fusion with PD.
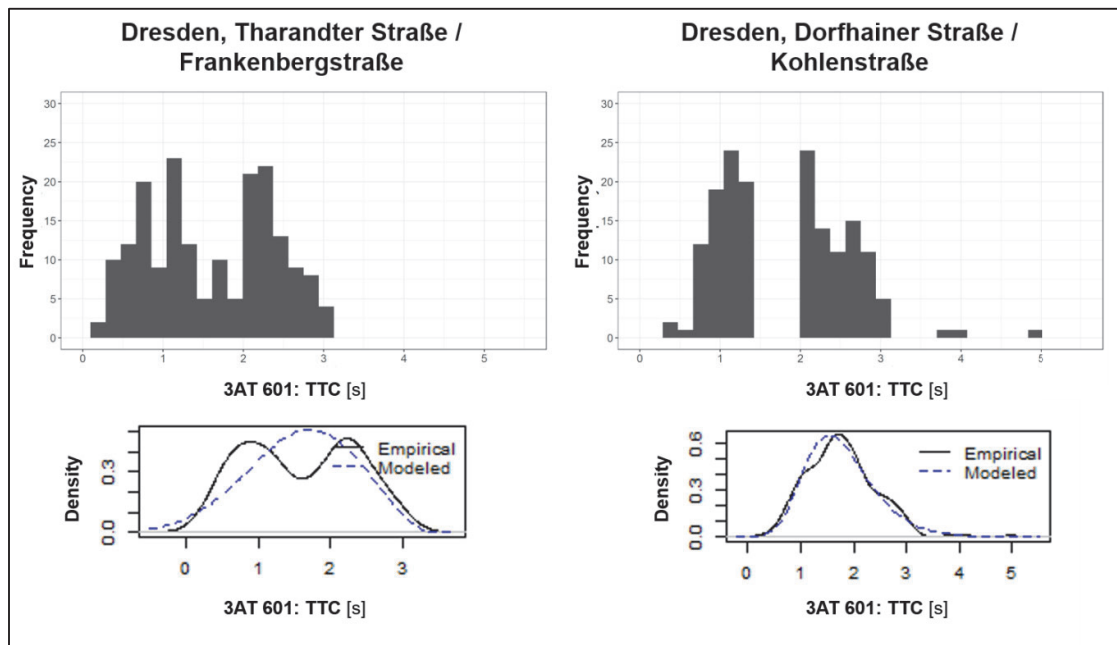
Figure 17. Histogram of TTC and GEV modelling results for 3AT 601.

Table 4.
Results of the modelled risk of a crash.

	3AT	Number of car–car crashes, 2005–2021	n	μ	σ	ξ	RC	Predicted crashes per year
Tharandter Straße / Frankenbergstraße (3-way)	601	1	185	1.363	0.788	−0.393	0.0237	15.74
	302	1			Not detected in traffic observation			
	201	2			Not detected in traffic observation			
Dorfhainer Straße/ Kohlenstraße (4-way)	601	0	263	1.491	0.564	−0.084	1.882e-05	0.012
	211	1	13	1.284	0.557	−0.249	0.0021	1.268

DISCUSSION

This paper reveals that the design of VO studies and the information to be collected during VOs should be planned to accommodate subsequent fusion with PD. By adopting the FUSE4Rep process model to VO using drones, we have demonstrated how to choose observation locations, derive sampling plans and collect relevant information, especially on behavioural errors. Along those lines, the sampling plan should be oriented towards an unobserved, superordinate population with overlap with the PD to be fused. The information to be collected should also coincide with information contained in the PD, information needed to describe test scenarios according to the 6LM and information derived from the adapted causality model of crashes. Due to space constraints, we have published only the information necessary for conducting drone-based VO in the ListDB Codebook. Even so, we have also shown how to mine trajectories efficiently, classify traffic conflicts according

to the 3AT classification and how to match the traffic conflicts with behavioural errors. Last, we have demonstrated how to assess the inherent crash risk of the identified traffic conflicts using extreme value theory.

The efficient, accurate interpretation of VO data and subsequent generation of test scenarios require combining human knowledge with automatic video analysis. While video analysis leveraging computer vision algorithms can help to mine road users' trajectories and detect traffic conflicts, it cannot contextualise the detected conflicts due to relying only on the drone's bird's-eye view. Even so, the drone pilot can help to detect barely visible parking crashes or behavioural errors, including informal agreements with other road users about yielding the right of way; identify causes of behavioural errors such as visual obstacles or technical problems; and note any major traffic-impacting events (e.g. football games in a nearby stadium that are not visible in the video-recording). Nevertheless, some of the information collected from pilots is highly subjective, especially when it concerns behavioural errors such as "DistanceError" or "SpeedError". Another challenge is the real-time synchronisation of points of interest and information collected by pilots with the traffic conflicts detected in the video-recordings made by drones. Especially at busy intersections, delays of only one or two seconds in the synchronisation can result in incorrect assignments, e.g. one second delay corresponds already to 13.8m distance travelled at a permitted speed of 50 km/h.

Categorizing traffic conflicts according to the 3AT classification leads to a good fit with PD according to the FUSE4Rep process model. At the same time, the approach detects only known constellations of traffic conflicts, whereas conflicts that do not fall into the 3AT classification cannot be sufficiently considered. Furthermore, the choice of the appropriate SSM determines the quality with which the conflict is described. For example, the TTC does not take acceleration behaviour into account.

GEV modelling allows analysing the inherent risk of traffic conflicts found separately according to 3AT classification and independently of other simulation methods such as stochastic traffic simulations (Siebke *et al.*, 2023). However, the modelled GEV distributions heavily depend on outliers and thus accurately calculated SSM values. Evaluating the data of the calculated SSMs has revealed that, especially at the three-way intersection, low values often result (e.g. TTC < 0.2 s), which typically precipitate crashes. A more detailed video analysis of traffic conflicts that stand out due to low TTC values suggests that the reason may be poorly fitting bounding boxes and, in turn, wrongly calculated vehicle dimensions. Figure 18 illustrates that problem; whereas the following car with ID 204 is very close to the leading car in front, a crash is highly unlikely because the vehicles do not overlap in their dimensions, and, thus, the following car could drive past. However, if the object detector incorrectly determines the vehicle dimensions and positions, then the TTC will be miscalculated. Furthermore, GEV modelling should be refined to take the overall scene embedding the traffic conflicts into account. For example, traffic flow can significantly affect the overall safety and crash risk at intersections (Oh, Washington and Choi, 2004), which can consequently affect the distribution of extreme values. A next step is therefore to include corresponding covariates in GEV modelling (Zheng and Sayed, 2020). Last, quantitative measures, including the coefficient of determination R^2 and the Akaike information criterion, to assess the quality of the GEV modelling, need to be introduced.
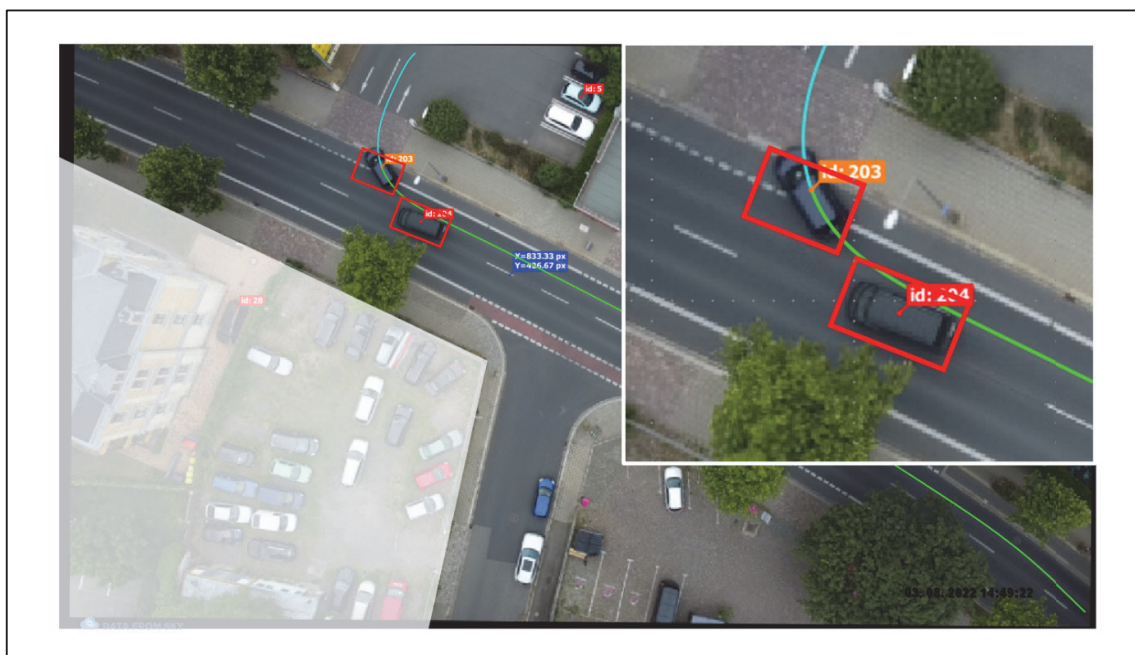
Figure 18. Traffic conflict detected with miscalculated TTC due to poorly fitting bounding boxes.

Limitations

In the data collected by the drone pilots, the unknown inter-rater reliability is a major limitation. Although both pilots received the same intensive training and supervision during observations, each pilot was assigned an observation site in which they specialise. Thus, the results of the pilots at the different survey locations were not compared with each other.

The validation of GEV modelling results using PD was also limited in its informative value. On the one hand, the number of accidents with five relevant crashes between 2005 and 2021 was quite small for comparison. On the other, the prediction referred to future traffic events, whereas the accident data referred to past traffic events.

For practitioners

Independent of applying the FUSE4Rep process model, practitioners can use the proposed process for conducting VO studies to collect and analyse data for use in generating test scenarios (Nalic *et al.*, 2020). As a result, practitioners can also transfer the information collected into corresponding OpenX formats (ASAM e.V., 2022) such as OpenScenario and OpenDrive. Practitioners can also improve the survey process by conducting drone pilot training that is more technical and aligned with the Swedish Traffic Conflict Technique (Polders and Brijs, 2018). Also, the mapping of the POIs in the ListDB app should be synchronised electronically in real time with the drone recoding. Additionally, the observation locations could be divided into spatial zones so that for each POI, spatial information is also available for matching with the conflicts detected by the video analysis.

For scientists

Scientists can directly use the proposed application of the FUSE4Rep process model for VO for data to fuse with German PD and derive representative test scenarios. In that process, scientists should also improve the calculation of SSM values, especially TTC; because conflicts in which one car follows another car ideally are only one part of the conflict situations, in which the TTC has to be determined. Thus, the calculation of TTC should be more generalised to be able to take angular situations into account for assessment as well. According to Laureshyn, Svensson and Hydén (2010) and Tarko (2019), generalised TTC calculation should be used to allow a possible collision angle between two road users. In addition, new object detectors should be used to directly detect rotated bounding boxes (e.g. Yang *et al.*, 2021) and thereby deliver more precise vehicle dimensions. Moreover, scientists should study how correcting factors of observation altitude (i.e. approx. 80 m above the ground) affects the determination of the position of objects (Kruber *et al.*, 2020) and might increase the accuracy of the entire video analysis. Last, scientists should investigate the additional automatic detection of behavioural errors and improve GEV modelling by taking appropriate covariates (e.g. traffic flow) into account.

CONCLUSION

Strictly applying the FUSE4Rep process model in collecting and analysing VO using drones supports the generation of representative test scenarios by applying data fusion. In that process, not only VO analysis but also study planning (e.g. sample plan) and the information to be collected need to be aligned in advance with the PD to be fused later on. In data collection, drone pilots can set observed traffic conflicts into context and record behavioural errors of road users, which then can be linked to the traffic conflicts. After that, GEV modelling can help to assess the inherent crash risk of the traffic conflicts identified.

Drone-based VOs for subsequent scenario generation are already publicly available as data sets about location-specific trajectories. Such data sets seldom follow a comprehensible sampling plan, and only a few metavariables are used to describe them. As our results show, it makes sense to embed the drone-based VOs in a systematic in-depth survey, which we describe using the 122 variables of the ListDB Codebook. In addition, the consistent alignment of the traffic conflict analysis with PD and the German 3AT classification can help to ensure that test scenarios can be found quickly and that fusion can be performed. We anticipate that only with the subsequent application of the FUSE4Rep process model will it become possible to find representative test scenarios for the evaluation of ADSs in the future.

ACKNOWLEDGEMENTS

supporting the video analysis. Our research was conducted within the MOTUS project (19FS2015A) and supported by the mFUND grant by Germany's Federal Ministry for Digital and Transport.

BIBLIOGRAPHY

Allen, B. L., Shin, B. T. and Cooper, P. J. (1978) 'Analysis of Traffic Conflicts and Collisions', pp. 67–74.

ASAM e.V. (2022) *ASAM Standards*. Available at: https://www.asam.net/standards/ (Accessed: 28 December 2022).

Autowelt, A. (2022) *Abstandsmessung - Wann bin ich zu dicht dran?* Available at: https://www.allianz-autowelt.de/bussgeld/abstandsmessung/# (Accessed: 28 December 2022).

Bäumler, M. *et al.* (2020) 'Use Information You Have Never Observed Together : Data Fusion as a Major Step Towards Realistic Test Scenarios', in *IEEE 23rd Intelligent Transportation Systems Conference (ITSC), Proceedings*, pp. 672–679. doi: 10.1109/ITSC45102.2020.9294649.

Bäumler, M. and Prokop, G. (2022) 'Validating automated driving systems by using scenario-based testing: The Fuse4Rep process model for scenario generation as part of the "Dresden Method"', *Zeitschrift für Verkehrssicherheit*, July, pp. 226–230. doi: 10.53184/ZVS3-2022-11.

Ben-Kiki, O., Evans, C. and Ingerson, B. (2021) *YAML Ain't Markup Language (YAML™) version 1.2. Revision 1.2.2 (2021-10-01)*. Available at: https://yaml.org/spec/1.2.2/ (Accessed: 28 December 2022).

Bergmann, L. T. (2022) 'Ethical Issues in Automated Driving—Opportunities, Dangers, and Obligations', *Studies in Computational Intelligence*. Springer Science and Business Media Deutschland GmbH, 980, pp. 99–121. doi: 10.1007/978-3-030-77726-5_5.

Bischoff, M. (1995) 'Zur Problematik der Repräsentativität in der empirischen Sozialforschung'. Bochum: Fakultät für Sozialwissenschaft, Ruhr-Universität Bochum.

Bochkovskiy, A., Wang, C.-Y. and Liao, H.-Y. M. (2020) 'YOLOv4: Optimal Speed and Accuracy of Object Detection', *arXiv preprint*.

Bock, J. *et al.* (2019) 'The inD Dataset: A Drone Dataset of Naturalistic Road User Trajectories at German Intersections', *arXiv preprint*. Available at: http://arxiv.org/abs/1911.07602.

Coles, S. (2004) *An Introduction to Statistical Modeling of Extreme Values*. 3rd edn. London: Springer-Verlag.

D'Orazio, M., Di Zio, M. and Scanu, M. (2006) *Statistical Matching: Theory and Practice*. Edited by R. M. Groves et al. West Sussex: John Wiley & Sons Ltd.

Destatis (2021) *Fachserie 8 Reihe 7: Verkehr (Verkehrsunfälle)*. Statistisches Bundesamt, Wiesbaden. Available at: https://www.destatis.de/DE/Themen/Gesellschaft-Umwelt/Verkehrsunfaelle/Publikationen/Downloads-Verkehrsunfaelle/verkehrsunfaelle-jahr-2080700217004.pdf?__blob=publicationFile.

Erbsmehl, C. *et al.* (2017) 'Analysis and Investigation Method for All Traffic Scenarios (AIMATS)'.

Erbsmehl, C., Lich, T. and Mallada, J. (2019) 'How to Link Accident Data and Road Traffic Measurements to Enable ADAS/AD Simulation?', *Journal of Mechanics Engineering and Automation*, 9(6), pp. 177–184. doi: 10.17265/2159-5275/2019.06.001.

Gabler, S. and Häder, S. (2015) *Stichproben in der Theorie (Version 1.1)*. (GESIS Survey Guidelines). Mannheim: GESIS - Leibniz-Institut für Sozialwissenschaften. doi: 10.15465/gesis-sg_009.

Hackeloeer, A. *et al.* (2014) 'Georeferencing : a review of methods and applications', *Annals of GIS*. Taylor & Francis, 20(1), pp. 61–69. doi: 10.1080/19475683.2013.868826.

Hayward, J. C. (1972) 'Near-Miss Determination Through Use Of A Scale of Danger', *Highway Research Board*, pp. 24–35. Available at: http://onlinepubs.trb.org/Onlinepubs/hrr/1972/384/384-004.pdf.

Hohm, A. (2022) 'The Second Wave of Automated Driving', *ATZ worldwide 2022*. Springer, 124(5), pp. 64–64. doi: 10.1007/S38311-022-0815-X.

Khan, M. A. *et al.* (2017) 'Unmanned Aerial Vehicle–Based Traffic Analysis: Methodological Framework for Automated Multivehicle Trajectory Extraction', *Transportation Research Record: Journal of the Transportation Research Board*, 2626, pp. 25–33.

Krause, S. (2019) 'Development of a database for the description and analysis of use cases for automated driving', *98th Annual Meeting of the Transportation Research Board (TRB 2019)*.

Kruber, F. *et al.* (2020) 'Vehicle position estimation with aerial imagery from unmanned aerial vehicles', in *2020 IEEE Intelligent Vehicles Symposium (IV)*. IEEE, pp. 2089–2096.

Laureshyn, A., Svensson, Å. and Hydén, C. (2010) 'Evaluation of traffic safety, based on micro-level behavioural data: Theoretical framework and first implementation', *Accident Analysis and Prevention*. Elsevier Ltd, 42(6), pp. 1637–1646. doi: 10.1016/j.aap.2010.03.021.

Lehmann, M. *et al.* (2019) 'Use of a criticality metric for assessment of critical traffic situations as part of SePIA', in Bargende, M. et al. (eds) *19. Internationales Stuttgarter Symposium: Automobil- und Motorentechnik*. Wiesbaden: Springer Vieweg, pp. 9–10. doi: 10.1007/978-3-658-16988-6.

Nalic, D. *et al.* (2020) 'Scenario Based Testing of Automated Driving Systems: A Literature Survey', in *Proceedings of the FISITA Web Congress 2020*.

Oh, J., Washington, S. and Choi, K. (2004) 'Development of Accident Prediction Models for Rural Highway Intersections', *Transportation Research Record: Journal of the Transportation Research Board*, 1897, pp. 18–27.

Orsini, F. *et al.* (2021) 'A conflict-based approach for real-time road safety analysis: Comparative evaluation with crash-based models', *Accident Analysis and Prevention*. Elsevier Ltd, 161(May), p. 106382. doi: 10.1016/j.aap.2021.106382.

Ortlepp, J. and Butterwegge, P. (2016) 'Unfalltypen-Katalog: Leitfaden zur Bestimmung des Unfalltyps'. Berlin: Gesamtverband der Deutschen Versicherungswirtschaft e.V. | Unfallforschung der Versicherer. Available at: https://www.udv.de/resource/blob/80022/89b4d80028aacf8cab649d3a3c6157a0/unfalltypenkatalog-data.pdf.

Pfeiffer, M. S. J. (2006) 'Statistical and Methodological Foundations of the GIDAS Accident Survey System', *2nd International Conference on ESAR „Expert Symposium on Accident Research"*, pp. 81–87.

Polders, E. and Brijs, T. (2018) *How to analyse accident causation? A handbook with focus on vulnerable road users*. (Deliverable 6.3). Horizon 2020 EC Project, InDeV. Hasselt, Belgium: Hasselt University.

Rässler, S. (2002) *Statistical Matching: A Frequentist Theory, Practical Applications, and Alternative Bayesian Approaches*. New York: Springer Science and Business Media New York.

Richards, M. and Ford, N. (2020) *Fundamentals of Software Architecture: An Engineering Approach*. O'Reilly Media.

Scholtes, M. *et al.* (2021) '6-Layer Model for a Structured Description and Categorization of Urban Traffic and Environment', *IEEE Access*, 9, pp. 59131–59147. doi: 10.1109/ACCESS.2021.3072739.

Schubert, A., Erbsmehl, C. and Hannawald, L. (2013) 'Stadardized pre-crash-scenarios in digital format on the basis of the VUFO simulation'.

Siebke, C. *et al.* (2023) 'Predicting the impact on road safety of an intersection AEB at urban intersections. Using a novel virtual test field for the assessment of conflict prevention between cyclists/pedelecs and cars', *Transportation Research Interdisciplinary Perspectives*. Elsevier Ltd, 17(June 2022), p. 100728. doi: 10.1016/j.trip.2022.100728.

Tarko, A. P. (2020) *Measuring Road Safety Using Surrogate Events*, *Measuring Road Safety with Surrogate Events*. Amsterdam: Elsevier Inc. doi: 10.1016/C2016-0-00255-3.

United States - Defense Mapping Agency (1987) 'Department of Defense World Geodetic System 1984: its definition and relationships with local geodetic systems', 8350.

Wang, C. *et al.* (2021) 'A review of surrogate safety measures and their applications in connected and automated vehicles safety modeling', *Accident Analysis and Prevention*. Elsevier Ltd, 157(April), p. 106157. doi: 10.1016/j.aap.2021.106157.

Yang, X. *et al.* (2021) 'R3Det: Refined Single-Stage Detector with Feature Refinement for Rotating Object', *Proceedings of the AAAI conference on artificial intelligence*, 35(4), pp. 3163–3171.

Zheng, L. and Sayed, T. (2020) 'A novel approach for real time crash prediction at signalized intersections', *Transportation Research Part C: Emerging Technologies*. Elsevier, 117, p. 102683. doi: 10.1016/j.trc.2020.102683.

APPENDIX

Table 5.
Excerpt from the official ListDB Codebook (https://w3id.org/listdb/) for video-based traffic observations (VO).

Category	Variable	Values	Explanation	Example
Time *(Static)*	**TimeStamp**	YYYYMMDD_HHMMSS	Start of VO	20221210_18512 0
	RecordingTime [minutes]	Integer	Duration of VO	25
	Weekday	Monday | Tuesday | Weekday | Thursday | Friday | Saturday | Sunday	/	Monday
	PublicHoliday	Yes | No | Unknown	/	Yes
Environment *(Static)*	**Temperature** [°C]	Integer	Outdoor temperature	15
	RoadCondition	Dry | Wet | Icy/Snow-covered | Slippery | Unknown	/	Dry
	RoadSurfaceTemperature [°C]	Integer	/	9
	Sunshine			No
	Rain			Light
	Fog	No | Light | Strong | Not applicable | Unknown	/	Strong
	Snow			No
	Wind			Light
	WindSpeed [km/h]	Integer	/	10
	Light	Day | Night | Not applicable	/	Day
Point of interest (POI) *(Time-based)*	**POI**	Crash | NearCrash | SpecialOperationVehicle | ObstacleOnRoad | VehicleVehicle | VehicleCycle | VehicleBike | VehiclePed | CycleCycle | CycleBike | CyclePed | BikePed | SingleObject | MultiObjects | TurnAround | Other	Detected POIs describing events or interactions saved with timestamp HHMMSS	VehicleCycle, 185230
	BehaviouralError	PassedPriority | RoadUseError | PriorityError | TurningError | SideBySideDrivingError | WrongBehaviourTowardsPedestrianError | OvertakingError | DriveByError | DistanceError | SpeedError | StationaryTrafficError | OtherError	Detected wrong behaviour in relation to a prior detected POI Road user showing the wrong behaviour is also recorded	Vehicle, PriorityError
	CauseError	VisualCause | EnvironmentalCause | TechnicalCause	Detected cause of wrong behaviour in relation to a previously detected POI	VisualCause
Special remarks *(Static)*	**Remarks**	String	Free text describing events affecting the traffic situation	Football game between 3 and 6 p.m. in the nearby stadium (stadium not visible in the video)

PEER REVIEW PAPER

This paper has been peer-reviewed and published in a special edition of Traffic Injury Prevention 24(S1), by Taylor & Francis Group. The complete paper will be available on the Traffic Injury Prevention website soon. To access ESV Peer-reviewed papers click the link below
https://www.tandfonline.com/toc/gcpi20/24/sup1?nav=tocList

APPLICATION OF A MODIFIED INTEGRATED SAFETY CHAIN USING IN-DEPTH CRASH DATA TO IDENTIFY FACTORS ASSOCIATED WITH SERIOUS INJURY CRASHES: A METHOD TO PRIORITISE CURRENTLY AVAILABLE ACTIVE SAFETY SYSTEMS AND TO IDENTIFY NEW OPPORTUNITIES TO ADVANCE VEHICLE SAFETY.

Michael Fitzharris
Mike Lenné
Sara Liu
Tandy Pok Arundell
Sujanie Peiris
Accident Research Centre, Monash University
Australia

Bruce Corben
Corben Consulting
Australia

Claes Tingvall
Accident Research Centre, Monash University
Australia

Chalmers University of Technology
Sweden

ÅFRY
Sweden

Diana Bowman
Arizona State University
United States of America

Andrew Morris
Loughborough University
United Kingdom

Paper Number 23-0156

ABSTRACT

Recognising the ambition of Vision Zero, vehicle safety will play a critical role in reducing the number of road users seriously injured globally. The objective of this research, therefore, was to identify currently available and required future countermeasures that will lead to the elimination of serious injury. To meet this objective a systematic approach to the analysis of in-depth crash data using case-by-case analysis linking contributing factors to safety countermeasures was developed.

In-depth crash investigation data collected as part of the MUARC-TAC Enhanced Crash Investigation Study (ECIS) was used. 400 drivers (MAIS 3+: 47%) admitted to a major trauma centre in Victoria, Australia, were included. Data sources included: driver or next-of-kin/family interview, ambulance and medical records, and police data. Vehicle and scene analysis was undertaken. Crashes were reconstructed using HVE and PC-Crash. EDR data was accessed where available.

Using a modified version of Tingvall's Integrated Safety Chain, contributing factors and safety countermeasures across the 10-phase crash chain were examined using a case-by-case approach. Contributing factors were those associated with crash occurrence and injury severity. An countermeasure library was established with each of the 278 countermeasures linked to a specific contributing factor. Countermeasures included those focussed on the driver, passive and active vehicle safety systems, road infrastructure and post-crash response. The efficacy and time-horizon of each was assessed and estimated for future active safety systems. All applicable countermeasures for each crash and injured driver were identified; these were considered to be sensitive to the countermeasure effect.

Driver distraction (48.8%), sudden sickness (10.0%), drowsy driving (24.5%), and impaired driving (19.8%) resulted in lane departure and cross-path vehicle movements; this, combined with low proportion of driver pre-crash braking (55%, 1.3 s) and exceeding the speed limit (27.0%) demonstrates the need for intervening safety systems (e.g., ISA, AEB). Intervening systems to correct lane deviations and intersection entry are also required.

The findings highlight the importance of in-depth data in establishing the use case for existing but relatively new systems as well as the identification of system capability limits in addressing current crash scenarios. These crash scenarios represent development opportunities for new standalone active safety systems. However, for full safety benefits to be realised, and to address the full range of driver performance and impairments, next generation systems that are fully integrated with one another are required (e.g., AEB + driver monitoring systems, DMS). Occupant status monitoring, on-board sensors, V2I and V2V enabled technologies linked to chassis control systems will be central to the future safety architecture of the vehicle.

The findings are relevant to passenger vehicle crashes where at least one driver was seriously injured and admitted to hospital. Other limitations associated with the sample and data collection methods must also be considered.

The analysis method represents a powerful approach to analyse in-depth crash data and to understand crash causation, injury occurrence and applicable countermeasures. Adoption of this method using other datasets is recommended so that the full range of countermeasure needs across jurisdictions and other road user groups can be understood.

INTRODUCTION

The use of crash data — whether it be large-scale administrative datasets based on police reports or in-depth investigation of a sample of crashes — to inform the development, selection, and implementation of safety countermeasures has a long history.[1, 2] The systematic analysis of crashes and adoption of an evidence-based approach to countermeasure implementation has translated to fewer traffic-crash related deaths, at least on a per-capita basis, in many jurisdictions.[1,2] Nonetheless, it remains the case that approximately 1.35 million people are killed and tens of millions are injured each year on the worlds roads.[3].

Frameworks for the analysis of crashes and the identification of safety countermeasures

A number of frameworks and approaches to the analysis of crashes and systematic identification of road safety countermeasures exist. These are briefly outlined below given their relevant to the present study.

The 3 E's of road safety. As early as 1923 road safety countermeasure opportunities were seen through the lens of education, enforcement and engineering; these are commonly referred to as the 3 E's of road safety.[4] Proposed by Harvey, this characterisation of the primary elements of safety, as described by Groeger in 2011, dominated road safety thinking for decades.[4] While succinctly defining the prospects for intervention. Groeger argued that a narrow interpretation of the original three E's limited the scope of each and their potential contribution to road safety. For instance, education was seen as having solely a driver skill-based learning focus and enforcement was undertaken by police to ensure drivers complied with the road rules; engineering was broader in that it included road design and quality (i.e., surface, geometry) as well as improvements in occupant protection, vehicle build quality and reliability. With advances in technology and the increasing inter- and interdisciplinarity required to achieve improvements in road safety, Groeger argued that the 3 E's can continue to remain a useful way of conceptualising road safety measures so long as a broader view of their application was adopted; Groeger did however identify four additional potential contributors to safety, these being exposure, emergency response, examining for competence, and evaluation.[4] Collectively, these 3 + 4 E's capture the range of measures across the road safety cycle. What the 3 E model did not do, however, was to highlight the interdependencies across the elements in what is today considered a systems-based approach.

Following this, it is notable that the dominant paradigm in road safety for many decades was a focus on driver behaviour as a means of reducing the number of people killed in crashes.[5,6] This was driven by the perspective that drivers were almost always responsible for crashes, a point lamented by Haddon.[7,8] Whether this stemmed from a narrow view of the analysis of crash factors and/or a narrow application of the original 3 E's is unknown.

The Haddon Matrix Taking key learnings from aviation safety and impact biomechanics, Haddon transformed road safety by arguing that greater focus ought to be given to 'crash packaging' and energy control, given the relationship of the latter to injury severity; this same concept forms the basis of modern occupant protection strategies and underpins *Vision Zero* and the *Safe System* approach.

In defining the *Haddon Matrix* [7,9], Haddon also argued for the objective study of crashes where the causes of injury and safety measures (i.e., countermeasures) were identified, rather than viewing crashes, or 'accidents' as commonly referred to, as 'chance' events. The systematic analysis of crash data was central to this objective. To facilitate this analysis, the *Haddon Matrix* (Figure 1) identified three factors in the road transport system (humans/driver, vehicle, environment) and three phases (pre-crash, crash, post-crash) in the sequence of events leading to injury, where '…causal factors are active and countermeasures can be undertaken' [7, p.1434]. While Haddon placed emphasis on energy management and injury control, post-crash care including rehabilitation and addressing driver-related factors – including broader person-based risk factors – were also seen to be important.

PHASE		FACTORS		
		HUMAN	VEHICLES AND EQUIPMENT	ENVIRONMENT
Pre-crash	Crash prevention	Information Attitudes Impairment Police enforcement	Roadworthiness Lighting Braking Handling Speed management	Road design and road layout Speed limits Pedestrian facilities
Crash	Injury prevention during the crash	Use of restraints Impairment	Occupant restraints Other safety devices Crash-protective design	Crash-protective roadside objects
Post-crash	Life sustaining	First-aid skill Access to medics	Ease of access Fire risk	Rescue facilities Congestion

Figure 1. An example of the Haddon Matrix with selected countermeasures.[1]

The influence of the *Haddon Matrix* on crash analysis and road safety cannot be overstated. Through the *Haddon Matrix*, Haddon provided the basis for the systematic analysis of crashes and the means to operationalise a preventative, population-based approach to preventing road trauma. Of particular note is that Haddon proposed two matrices, the first being the factors associated with crash events and injury, and the second being ways to address these factors. Haddon went further and suggested mathematical modelling to assess intervention choices in a systematic way. While the countermeasures identified through this process could arguably be classified within the 3 E's, the greater specificity provided a more robust basis from which to prioritise road safety countermeasures and shape road safety policy. It is for these reasons that the *Haddon Matrix* was used as a key starting point for the analysis of crashes and countermeasures in the present study.

The Integrated Safety Chain While a number of other frameworks and crash analysis methods have emerged since the *Haddon Matrix*, including for instance, the *Road Trauma Chain* [10], KEMM-X [11], AcciMAP [12], DREAM, [13] arguably the most prominent crash sequence model was the *Integrated Safety Chain* (ISC) first outlined by Tingvall in 2008.[14] (Figure 2) and subsequently applied by Lie [15], Strandroth [16], Rizzi [17] and Sunnevång [18]. The ISC provides a framework for understanding the role that individual factors play in the crash sequence and how to best intervene. The influence of the ISC is driven by its operational links to *Vision Zero* [19,20,21] and the Multi-dimensional (SRA) Model of a Safe Road Transport System [22,23].

The ISC is a time-based model of the driving process where the pre-crash phase is divided into discrete sub-phases leading up to a crash (Figure 2). Requirements to access the road transport system are described, as is crash protection and post-crash emergency care. This overlaps with Haddon's pre-crash, crash and post-crash phases. The key point of difference is in the pre-crash phase and once driving has commenced. Having set requirements for accessing the road transport system in order to facilitate *Normal Driving* (i.e., seat-belt used, compliance with speed limit, sober), and once the trip has commenced, the pre-crash phase is divided into three distinct phases where the intervention urgency escalates if the driver does not respond to *Normal Driving*. The intervention objective is to return a driver to the *Normal Driving* phase as quickly as possible.
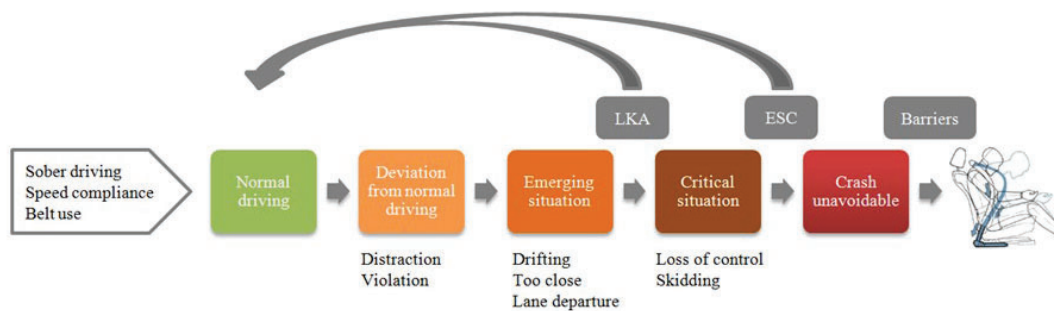
Note: Arrows indicating a return to normal driving due to the influence of specific countermeasures; Lane Keep Assist [LKA] and Electronic Stability Control [ESC] shown as specific examples). Barriers shown as an energy management intervention in the crash phase.

Figure 2. The Integrated Safety Chain [14, 15, 16]

In addition to road user access requirement, measures to support and sustain *Normal Driving* include infrastructure and enforcement measures, as well as vehicle-based active safety systems. Indeed, the ISC is especially well suited to identifying relevant active safety measures given the emergence of new vehicle technologies that shape driver and/or vehicle response aimed at crash prevention, injury mitigation, or both. Indeed, it was this blurring of system functionality across the driver, vehicle and road environment across the pre-crash, crash, and post-crash phase [24] that transformed vehicle safety from 'passive' occupant protection crashworthiness measures toward dynamic

integrated safety systems that linked driver responses to the vehicle, linked the vehicle to the road environment, better prepared the driver for the crash through optimisation of the drivers seating position, and automatically called emergency services post-crash. These systems gave rise to the idea that vehicle safety countermeasures could be placed on a timeline from the seconds to milliseconds before the crash, during the crash itself, and after the crash. It can be observed that as one moves closer to the crash the burden of preventing the crash moves further away from the driver toward the vehicle and infrastructure solutions.

For completeness, the prevention of serious injury once a crash occurs is the exclusive domain of passive vehicle safety measures and energy-control infrastructure measures; these sit within the crash phase of the ISC. This includes setting speed limits in line with the limits of protection offered by vehicles and foreseeable crash types given the road environment due to its link to impact speed. While emergency response is noted in Tingvall's original ISC [14], a distinct post-crash response phase was added by Rizzi, who also represented the ISC in a vertical manner.[17]

In addition to being a time-based model of the crash sequence, the ISC explicitly brings together primary prevention (i.e., crash prevention) and secondary prevention (i.e., injury mitigation) into a sequential and integrated model. With discrete phases, the ISC permits determination of where each risk factor sits within the crash sequence, and by extension, where specific countermeasures apply. To do so however requires a detailed understanding crash occurrence and injury severity risk factors in real-world crashes; for this reason, data collected using in-depth methods is ideal for this purpose.

The present study

The present study is set within the context of a broader *Enhanced Crash Investigation Study (*ECIS). The ECIS had two goals: 1. to identify the factors associated with serious injury crashes, and 2. to identify crash prevention measures and measures that would be effective in preventing occupants of vehicles being seriously injured once a crash occurs. The ECIS examined, in-depth, the crashes of 400 drivers admitted to a major trauma centre in Victoria, Australia.

The objective of this research paper is to demonstrate the application of an expanded ISC using defined crash scenarios to 1. prioritise currently available active safety systems, and 2. to identify opportunities to advance vehicle safety.

METHODS

Data

Crashes included in the ECIS program were those where a driver of a passenger vehicle was injured and admitted to one of two adult trauma centres in Melbourne, Australia (i.e., The Alfred Hospital; The Royal Melbourne Hospital).

Injured drivers, or their Next-of-Kin for the most seriously injured drivers, were required to give informed consent for participation in the study. The study was approved by The Alfred Hospital Research Ethics Committee (HREC, Project: 249-14), The Royal Melbourne Hospital HREC (Project: 249-14), and the Monash University HREC (CF14/2329-2014001254).

In total, 400 injured drivers were enrolled to the study (67% consent rate). Enrolled drivers were aged 18 – 93 years, 55% were male, and 37% of crashes occurred in non-metropolitan, regional areas of Victoria. These drivers were involved in 393 crashes, with two drivers injured in 7 crashes enrolled to the study. In total, these crashes involved 923 people, 18 of which died (in 17 crashes) and 547 people were hospitalised.

Comprehensive details of the crash were obtained. This included interviews with the involved driver, medical records, police reports, inspection of the vehicle, inspection of the scene and full crash reconstruction. Injuries were coded using the Abbreviated Injury Scale [25], with 'serious injury' being defined as a driver having sustained an AIS 3 or higher injury, referred to as MAIS 3+; injured drivers are referred to as MAIS 1+ injured drivers. The reader is referred to ECIS Reports 1,2,3, and 4 for detail [26,27,28,29].

Development of the expanded ISC for use in the ECIS program

Following Tingvall and others, a modified version of the ISC was created for use in the ECIS program. This forms the basis of the analysis of the ECIS data report here. The original ISC was modified after significant development work, including a review of conceptual models and application of the original ISC using ECIS case data across a series of workshops [28].

The modified version of the ISC used in the ECIS program is presented in Figure 2.

PHASE	DEFINITION AND INTERVENTION APPROACH	INTERVENTION GOAL
1. Threats to Normal Driving	• Driver (D), Vehicle (V), and Road Infrastructure/Environment (E) factors detrimental to *Normal Driving*, including factors that pre-dispose a driver to a crash or act to negatively impact driver ability to respond and avoid a crash. • D: intoxication and/or use of illicit drugs, abuse of prescribed medication; medical/health condition; experiential factors (new licence, presence of peers), offence/crash history; V: vehicle condition/roadworthiness including tyre tread and lighting systems; E: signage, road geometry, latent (in-built) risk by design. • The goal is to eliminate the presence or manage the influence of these threats.	**Measures to address human, vehicle & road environment factors detrimental to *Normal Driving***
2. Normal (Routine) Driving	• *Normal Driving* is characterised by the control of the vehicle by a driver in a manner that is responsive to the road environment, surrounding traffic and other road users such that a trip is successfully completed as planned and without conflict/incident. *Normal Driving* includes compliance with traffic laws. • Per the *Safe Driver* element of the *SRA Model of a Safe Road Transport System*[22,23], the prerequisites for *Normal Driving* are: seat belt worn (i.e., use of protective equipment); driving within the speed limit; non-use (handling) of mobile phone; BAC within limit for licence class; no illicit drugs used or abuse/non-prescribed use of benzodiazepines and/or opioid-based analgesics; no excessive drowsiness.	**Measures to promote and return a driver to *Normal Driving***
3. Deviation from Normal Driving	• Driver (human) factors causing a shift from *Normal Driving*. In addition to the prerequisites of *Normal Driving* not being met (excluding impairment factors present prior to the commencement of driving (Phase 1: Threats), the driver/vehicle deviates from a safe travel path due to driver performance failure(s) (e.g., error), the effect of health and driver state factors, and/or non-compliant behaviour; these factors can result in a failure to recognise roadway cues and the presence of other road users/objects resulting in an *Emerging Situation* if not corrected. • Intervention approach: provide information and support (includes warning).	
4. Emerging Situation	• Vehicle is in a position sufficiently beyond *Deviation from Normal Driving* to be a direct threat to the driver (and other road users) if left uncorrected. • Movement depends on crash type: midblock/lane departure involves a drift/deviation/move from travel lane; intersection: lack of proper response to traffic control signal and/or on-coming vehicle. • Intervention approach: warning and intervention in driving.	
5. Critical Situation	• Crash event is imminent due to non-response or ineffective response to the threat of the *Emerging Situation*. • Trajectory of vehicle: in-path of other road user, entered shoulder/off-roadway, non-response to stationary vehicle. • Intervention approach: immediate and active correction.	
6. Crash Unavoidable	• Crash is imminent with the time-to-collision (and vehicle trajectory) so short as to make the crash unavoidable. • Intervention approach: preparation for the crash with a viewing of controlling the level of crash energy and optimising vehicle safety systems to minimise crash energy and preparing the driver/vehicle safety systems for impact.	**Energy reduction and injury mitigation measures**
7. CRASH	• Injury mitigation through the effective control and management of crash energy. • Intervention approach: measures aimed at vehicle crashworthiness and road engineering solutions to manage impact speed, energy transfer, and energy dissipation. Includes measures to prevent secondary impacts, the prevention of vehicle rollover events and/or impacts with non-frangible roadside objects.	**Injury mitigation measures/energy dissipation**
8. Ambulance & Hospital Care	• Emphasis is on systems, processes, and training to enable an optimal outcome for the injured driver to be achieved. • Intervention approach: stabilisation, extrication and transport of the injured driver and the provision of rapid and efficacious trauma care in the hospital setting.	**Immediate post-crash emergency care, retrieval, and acute hospital trauma care**
9. Rehabilitation, Recovery, Injury/other Insurance	• Care and access to services following acute treatment for injuries. • Intervention approach: processes and programs to facilitate recovery and achievement of optimal health, function, and re-integration to everyday life post-crash and beyond the hospital setting.	**Rehabilitation, supported recovery and community integration**
10. Crash Data Systems	• Vehicle (on-board) data systems to capture critical pre-crash and in-crash data, enabling understanding of crash circumstances, occupant injury risk factors and effects of safety systems. Data collected via in-depth crash investigation. • Integrated administrative crash data, emergency service and hospital-based data systems required to monitor system performance and monitoring of road trauma. • Required for the development of road safety strategy and action plans.	**Fitment, access, collection, and reporting**

Figure 3. The expanded Integrated Safety Chain adopted in the ECIS program [26,27]

Formulation of crash types/scenarios

Recognising that countermeasures will differ across crash types and according to specific vehicle movements, eleven (11) crash scenarios were identified (Appendix, Table A.1). Broadly, these were defined as Lane Departure crashes, Across Path crashes, Rear Impact crashes, and 'Other'; this latter category were characterized by complex vehicle movements that did not fall within the three principal crash types. Within each principal crash type, sub-types were also defined. For Across Path crashes, a further split was created based on the presence/absence of traffic lights.

Risk factor identification and countermeasure library

Comprehensive data collection forms were created for use in the study. These included a Driver Interview form, including a truncated form where Next-of-Kin consent was required, a Vehicle Inspection form, and a Scene Inspection form. An *ECIS Contributing Factors Form* was also created; this was largely structured on the *Haddon Matrix,* informed by known risk factors based on the road safety literature and ECIS Investigator team expertise. In completing the *ECIS Contributing Factors Form* all available information was used. A distinction was made between the presence of a particular factor and whether it contributed to the crash and/or injury.

As stated, risk factors – also referred to as contributing factors – were aligned with a specific phase of the modified ISC. In a separate exercise, all possible countermeasures (278) associated with each contributing factor were identified, including future measures; this represents the countermeasure library. This was made possible through the input of an expert group where 40 cases were analysed individually using the integrated safety chain, while an additional 56 cases were individually discussed and countermeasure opportunities identified in 16 multi-disciplinary panels.

Each identified countermeasure was assessed for its likely efficacy in addressing the contributing factor given. A scale of low (<20%), medium (20% - 50%), and high (50%+) was adopted. This assessment was based on a number of parameters, including its function and technical limits (i.e., operational boundaries), effectiveness studies published in the research literature and technical reports/manuals, as well as expert opinion. For countermeasures not presently available and where no formal evaluations were available, expert opinion was used in the context of the crash scenario; while estimates of efficacy are given, these technologies will require testing and field evaluations to be undertaken.

For each crash, countermeasure applicability was assessed independently of one another, and no consideration was given to cost-effectiveness or other policy implementation considerations.

A countermeasure availability time horizon for each countermeasure was identified. For countermeasures under development, a short-term (within 5-years) or medium-term (> 5 years) availability time horizon was estimated based on best available information.

Countermeasure categories, based on their action and point of effect, were also defined [29]; these are not considered here for the sake of brevity.

Analysis approach and primary analysis outcome

Using the crash categories, a case-by-case analysis using the modified ISC and associated decision rules on risk factors and aligned countermeasures was performed.

The primary analysis outcome of interest was the proportion of serious injury crashes where each contributing factor is present and each associated countermeasure is applicable to the crash. Whether the crash was 'sensitive' to the countermeasure was based on the function and technical performance specifications of the countermeasure being considered.

RESULTS

The analysis of contributing factors highlights a broad array of driver, vehicle and road infrastructure factors that contributed to the occurrence of crashes and their severity. Driver distraction (48.8%), sudden sickness (10.0%), drowsy driving (24.5%), and impaired driving (19.8%; alcohol: 11.3%; illicit drugs: 12.8%) resulted in lane departure, cross-path vehicle movements and collisions with parked vehicles, fixed objects and rear impact crashes.

Driver performance failures also included looked but failed to see errors (20.3%), failure to detect parked vehicle/objects at roadway (4.3%), driving too close (7.8%), as well as non-compliance with traffic signals and directional yield signs (20.5%). Non-compliance with seat belt use was 6.8%.

The data also indicated that in only 55% of crashes did drivers apply the brakes, and when they did the time was short resulting in a small percentage reduction in vehicle speed at impact. Further, analysis indicated that in 27% of crashes, one (or more) of the involved driver(s) were exceeding the speed limit.

In addition to driver-based factors, infrastructure-related factors (e.g., pavement surface 6.3%) and vehicle-related factors (e.g., tyre condition, 4.8%) were also evident as contributing factors.

Linking these contributing factors back to the pre-crash phases of the modified ISC (Figure 3) and with reference to the established countermeasure library, a broad range of countermeasures are available either now (Table 1) or could be available in the future (Table 2) were identified.

From an implementation perspective, ideally priority is given to high efficacy countermeasures that are applicable to a high proportion of serious injury crashes. Notably, high efficacy measures are intervening technologies, while medium and low efficacy measures are generally warning systems that are dependent on drivers responding accordingly. However, from a technology acceptance perspective, warning-based systems may be preferable for many drivers. It is likely that the acceptability of intervening technologies among driver will evolve over time as systems as the safety and convenience benefits become clear.

It is also evident from Table 2 that a large number of countermeasure opportunities exist. These are either new systems entirely or are more advanced, intervening technologies than what are currently available. In some instances, significant research and development work would be required to bring these technologies to the vehicle fleet.

Table 1.

Identified (select) currently available countermeasures and the proportion of serious injury crashes to which they are applicable

System / countermeasure	Contributing Factor being addressed	Applicable serious injury crashes (%)		ISC Phase	Efficacy	Horizon
		MAIS 1+	MAIS 3+			
Intelligent Speed Assist (ISA) (intervening, retrofitted)	Traffic offence, within last 12-months	24.8%	23.4%	1	High	Now
Alcohol interlock	Impairing influence alcohol	11.3%	13.8%	1	High	Now
Seat belt reminder (SBR) systems (advisory)	Seat belt not worn	6.8%	7.4%	3-5	Medium	Now
Speed assistance - manual speed limiter	Non-compliance with posted speed limit	27.0%	36.2%	3-5	Low	Now
Speed assistance – speed sign recognition & warning	Non-compliance with posted speed limit	27.0%	36.2%	3-5	Medium	Now
Intelligent Speed Assist (ISA) (advisory)	Non-compliance with posted speed limit	27.0%	36.2%	3-5	Medium	Now
– Intelligent Speed Assist (ISA) (intervening)	Non-compliance with posted speed limit	27.0%	36.2%	3-5	High	Now
Attention Assist (warning)	Driver Inattention (all forms including driver state and sudden sickness)	66.8%	68.6%	3-5	Low	Now

System / countermeasure	Contributing Factor being addressed	Applicable serious injury crashes (%) MAIS 1+	MAIS 3+	ISC Phase	Efficacy	Horizon
Attention Assist (warning)	Inattention – distraction inside/outside of vehicle/phone use	48.8%	50.0%	3-5	Low	Now
	Drowsy driving	24.5%	26.6%	3-5	Low	Now
Advanced vehicle lighting systems (DRL / auto high beam / adaptive headlights)	Looked but failed to see vehicle or hazard / object (i.e., other road users, object)	13.5%	12.8%	3-5	Medium	Now
Object detection (including night vision assist & 360° surround view monitor with Head-Up Display (HUD)	Failure to detect parked vehicle / objects on side of roadway	4.3%	1.1%	3-5	High	Now
Braking systems – EBA fitment	Braking system fitted to crash-involved vehicle sub-optimal	78.5%	85.6%	3-5	High	Now
Braking systems – ABS fitment	Braking system fitted to crash-involved vehicle sub-optimal	48.5%	53.2%	3-5	High	Now
Braking systems – EBD fitment	Braking system fitted to crash-involved vehicle sub-optimal	74.0%	79.8%	3-5	High	Now
Forward collision warning (FCW, camera, radar, LiDAR)	On collision trajectory	67.0%	64.4%	4-5	Medium	Now
Autonomous Emergency Braking (AEB) – includes consideration of subtypes (e.g., junction AEB, high-speed AEB)	On collision trajectory	67.0%	64.4%	5	High	Now
Lane departure warning	Vehicle deviated (departed) from lane / beyond centre of lane	47.3%	53.7%	3-5	Medium	Now
Automated Lane Keep Assist (ALKS): intervening for oncoming traffic crash mitigation	Vehicle deviated (departed) from lane / beyond centre of lane	47.3%	53.7%	3-5	High	Now
Electronic Stability Control (ESC)	Loss of control causing departure from lane (i.e., out of control, not overtaking)	15.5%	15.4%	3-5	Medium	Now

System / countermeasure	Contributing Factor being addressed	Applicable serious injury crashes (%)		ISC Phase	Efficacy	Horizon
		MAIS 1+	MAIS 3+			
Traffic light alert (advisory, V2I)	Apparent failure to see / recognise /obey traffic signs at intersection	8.3%	7.4%	3-5	Medium	Now
Traffic sign display (in-vehicle)	Apparent failure to see / recognise /obey traffic signs at intersection	11.5%	12.2%	3-5	Medium	Now
Cross Traffic Alert (collision warning)	Enter intersection across path of vehicle [crash types F, H; refer Appendix]	19.3%	20.2%	3-5	Medium	Now
Turn Assist (collision) warning (intersections) / Right turn crash warning (in intersection and turning)	Turn across path of oncoming vehicle in intersection [crash type G; refer Appendix]	10.8%	8.0%	3-5	Medium	Now

Table 2.

Identified (select) likely available countermeasures in the short-term (within 5-years) and medium term (beyond 5 years), and the proportion of serious injury crashes to which they are applicable

System / countermeasure	Contributing Factor being addressed	Applicable serious injury crashes (%) MAIS 1+	MAIS 3+	ISC Phase	Efficacy	Horizon
Vehicle ignition technology (e.g., smart key)	Driver experience, indicated by driver behaviours and vehicle control.	8.0%	8.0%	1	Medium	Short-term
	Traffic offence, within last 12-months	36.0%	32.4%	1	Medium	Short-term
Telematics fitment and on-going monitoring as licensing requirement	Driver experience, indicated by driver behaviours and vehicle control.	8.0%	8.0%	1	Medium	Short-term
	Crash history – involved in injury crash last 5-years	11.0%	8.0%	1	Medium	Short-term
	Traffic offence, within last 12-months	36.0%	32.4%	1	Medium	Short-term
Vehicle ignition technology (e.g., smart key)	Driver experience, indicated by driver behaviours and vehicle control.	8.0%	8.0%	1	Medium	Short-term
	Traffic offence, within last 12-months	36.0%	32.4%	1	Medium	Short-term
	Inattention – distraction inside/outside of vehicle	45.0%	45.2%	3-5	High	Short-term
Passive alcohol sensor (warning)	Impairing influence alcohol	11.3%	13.8%	1	Medium	Medium-term
Passive alcohol sensor with interlock (intervening)	Impairing influence alcohol	11.3%	13.8%	1	High	Medium-term
Drug interlock (intervening) via passive detection	Impairing influence illicit drugs	12.8%	17.6%	1	High	Medium-term
Tyre pressure monitoring system (TPMS)	Underinflation of tyres	4.5%	5.3%	1	Medium	Short-term
Tread warning	Poor type condition/low tread	4.8%	5.9%	1	Medium	Medium-term
Co-operative ITS enabled warning systems including speed advisory	Pavement surface having a negative impact on vehicle stability and friction	6.3%	5.3%	1	Medium	Medium-term
	Pavement surface conditions having a negative impact on vehicle stability due to foreign substances on road	4.5%	4.3%	1	Medium	Medium-term
Congestion alert (V2V / V2I enabled)	Dynamic, congested high volume traffic environment	7.5%	5.3%	1	Medium	Medium-term

System / countermeasure	Contributing Factor being addressed	Applicable serious injury crashes (%)		ISC Phase	Efficacy	Horizon
		MAIS 1+	MAIS 3+			
Seat belt reminder (SBR) systems (intervening)	Seat belt not worn	6.8%	7.4%	3-5	High	Short-term
Attention assist (warn) / Driver monitoring system (camera-based)	Driver Inattention (all forms including driver state and sudden sickness)	66.8%	68.6%	3-5	Medium	Short-term
	Inattention – distraction inside/outside of vehicle/phone use	48.8%	50.0%	3-5	Medium	Short-term
	Drowsy driving	24.5%	26.6%	3-5	Medium	Short-term
Attention assist (intervening with steer assist) / Driver monitoring system (camera-based)	Driver Inattention (all forms including driver state and sudden sickness)	66.8%	68.6%	3-5	High	Short-term
	Drowsy driving	24.5%	26.6%	3-5	High	Short-term
	Sudden sickness	10.0%	9.0%	3-5	High	Short-term
Attention Assist via DMS / OSM with vehicle takeover (steer, park) for a non-responsive driver)	Drowsy driving/asleep	11.0%	13.3%	3-5	High	Medium-term
	Sudden sickness	10.0%	9.0%	3-5	High	Medium-term
Intervening Headway / Following Distance System	Unsafe margin / follow too close	7.8%	4.8%	5	High	Short-term
Adaptive cruise control (ACC) [with Stop-Go & Traffic Jam Assist plus Steer / Collision Evade Assist]	Cruise control active and apparent failure to respond to intersection / correct lane deviation	2.8%	2.7%	3-5	Medium	Medium-term
Disengage cruise control linked to Attention Assist, using DMS / OSM	Cruise control active and assessed to be contributing factor for crash event and/or associated with injury severity	2.8%	2.7%	3-5	High	Medium-term
Autonomous Emergency Steer / Collision Evade Assist	On collision trajectory	67.0%	64.4%	5	High	Medium-term

System / countermeasure	Contributing Factor being addressed	Applicable serious injury crashes (%) MAIS 1+	MAIS 3+	ISC Phase	Efficacy	Horizon
Autonomous Emergency Steer / Collision Evade Assist linked to DMS/OSM for non-responsive drivers	On collision trajectory	10.0%	10.6%	5	High	Medium-term
Emergency Lane Keep Assist (ELKS) to manage non-responsive drivers (intervening, linked to DMS/OSM)	Vehicle deviated (departed) from lane / beyond centre of lane	15.0%	17.0%	3-5	High	Medium-term
Active Brake Assist with cross-traffic function / Junction AEB (optimised with sensor based on V2V)	Enter intersection across path of vehicle [crash types F, H; refer Appendix]	19.3%	20.2%	3-5	High	Short-term
Intelligent Traffic Light Assist (haptic feedback of accelerator pushback + braking, V2V / V2I)	Driver failed to obey a red light at intersection, entered	8.3%	7.4%	3-5	High	Medium-term
Brake-hold with roll warning	Drift / roll into intersection (from stationary)	0.8%	1.6%	3-5	Medium	Medium-term
Autobrake – forward (linked to DMS-OSM for non-responsive drivers)	Drift / roll into intersection (from stationary)	0.8%	1.6%	3-5	High	Medium-term

While a range of passive vehicle safety measures were identified as being applicable to the serious injury crash sample, these were not the focus of this paper. These measures relate to Phase 6 (*Crash Unavoidable*) (e.g., pre-safe) and Phase 7 (*Crash*)(e.g., airbags; crashworthiness indicated by NCAP star-rating; impact speed relative to vehicle safety) of the modified ISC. Here it is worth noting the AEB has both a collision avoidance function and if successful the driver can return to *Normal Driving* from a *Critical Situation,* otherwise AEB can play a role in injury mitigation by reducing the impact speed where the time-to-collision allows (Phase 7, crash). As none of the vehicles involved in the crashes examined has AEB fitted, AEB was considered applicable to 67% of all serious injury crashes in the sample; however, to bring the impact speed with the safety design window of the vehicle given its NCAP star rating, AEB would be applicable to 43% of crashes.

The role of post-crash notification technology and on-board vehicle data systems are important to note. Due to the severity and location of a subset of crashes, eCALL/AECS technology must be considered to be a vital safety technology, particularly as timely treatment is critical to survival following injury. While technically applicable to all of the crashes in the sample as all required emergency care, based on crash location, road type and traffic volume, eCALL/AECS would be applicable to 43% of crashes. Taking an even narrower perspective, eCALL/AECS would be highly applicable to 5.5% of serious injury crashes where the delayed notification of emergency medical services and/or difficulty in locating the crash was apparent.

On-board vehicle data systems, including Event Data Recorders (EDR) and Data Storage Systems for Automated Driving (DSSAD), are an essential crash investigation and research tool. The data collected by these systems will be essential in evaluating driver engagement, the efficacy of both active and passive safety systems, and more broadly, assessing the influence of road safety policies over time. The global adoption of regulations concerning the fitment, data points, and access of these systems is essential. It is worth noting that within the ECIS sample, EDR data was available and accessible in only 9.8% of ECIS driver vehicles.

DISCUSSION

Using recently collected crash data, this paper set out to demonstrate the application of an expanded form of the Integrated Safety Chain (ISC) using pre-defined crash type scenarios to identify the potential of currently available active safety systems to reduce serious injury crashes. A further objective was to identify crash-relevant technologies not currently available but likely to be of value given the observed range of driver behaviours and associated vehicle movements pre-crash. The primary analysis outcome was the proportion of hospitalisation crashes where each currently available or future identified countermeasure would be applicable.

As a starting point, modifications were made to Tingvall's original ISC [14], in addition to those made by other researchers [15-18]. Expansions to the ISC included the addition of a number of phases in the crash sequence, specifically as they relate to *Threats to Normal Driving* and further splitting the *Post-crash phase* into two distinct phases. A final phase, *Crash Data Systems* was added given the value of on-board data collection systems. Further innovations included defining crash and injury relevant contributing factors that align to each crash phase, defining the intervention approach specific to each crash phase, and the formulation of relevant decision-making heuristics. A conceptual and operational definition of *Normal Driving* was also articulated. The basic principles of Tingvall's ISC remain the same however, these being that each phase represents an intervention opportunity to promote safe driving or to protect occupants from serious injury in the event of a crash.

Analysis of the ECIS serious injury crash data highlighted the broad range of factors that contribute to both crash occurrence and injury severity, once a crash occurs. By making explicit the nature of *Threats to Normal Driving*, it is evident that there are a range of driver, vehicle and road infrastructure factors that need to be addressed, even before a driver enters the vehicle to commence their trip. Intervening safety systems play a key role in addressing these threats. The need for systems that monitor occupant status and impairments are clear.

As described, drivers shift from *Normal Driving* due to performance failures (e.g., error), the effect of health and driver state factors, and intentional or unintentional non-compliance with relevant road laws. These deviations cascade into *Emerging Situations* and *Critical Situations* that are characterised by the vehicle moving toward, and ultimately a position of conflict, with another vehicle, road user or fixed object. Active safety systems can play key role in addressing these shifts from *Normal Driving,* from warning drivers through to intervening when drivers fail to respond accordingly. A range of active safety measures in the form of Advanced Driver Assistance Systems (ADAS) were identified. It is likely that convergence of multiple active safety systems will provide the most benefit in the future. For example, occupant status or driver state monitoring linked to braking systems and cross-traffic alerting systems offer immense promise in preventing inattentive drivers from entering intersections into the path of other vehicles, pedestrians and cyclists, for instance. The efficacy of such systems will be further enhanced through vehicle-to-vehicle (V2V) and vehicle-to-infrastructure (V2I) communication technologies.

Application of the modified ISC also highlights the need for advanced post-crash, automated response systems in the form of eCALL / Accident Emergency Call System (AECS). Similarly, there is a key role for the universal fitment of crash data collection systems, including Event Data Records and Data Storage Systems for Automated Driving (DSSAD).

While recognising the prior work of other researchers that have use the ISC, the analysis method presented in this paper represents a powerful approach to analyse in-depth crash data and to understand crash causation, injury occurrence and applicable countermeasures. This work differed from earlier work by using an expanded crash sequence model across the full range of serious injury crash scenarios. Adoption of this method using other datasets is recommended so that the full range of countermeasure needs across jurisdictions and other road user groups can be understood.

Limitations

There are a number of assumptions and limitations that need to be considered when interpreting and applying the findings presented in this paper. First, the study examines passenger vehicle crashes where at least one involved driver was admitted to hospital for at least 24 hours. While drivers included in the study were age 18-93 and approximately half were female, the sample is biased toward MAIS 3+ injury crashes (47%).

Second, crashes were those that occurred in Victoria, Australia, in the 2014 – 2016 period. While vehicle turnover is slow, at approximately 2 – 3% per annum, the entry of newer vehicles due to attrition through vehicle age or

crash-involvement may impact the proportion of crashes to which the fitment particular vehicle safety systems would be relevant. The extent to which the impact of COVID-19 will impact this vehicle replenishment rate is currently unknown. This is relevant to understanding the proportion of the crash population that has the potential to be influenced by vehicle safety systems.

Third, it is also noted that while the crash reconstruction process and attribution of contributing factors was conducted in a systematic manner with multiple checks and balances, it is recognised that the interpretation is that of the ECIS Crash Investigation team and ECIS Program Investigators.

For a full exposition of the limitations of the ECIS program and impacts on interpretation, the reader is referred to available reports [26,26,27,28].

CONCLUSIONS

Using a modified crash sequence model, this paper highlights the significant potential of active vehicle safety systems in reducing serious injury road trauma. The findings can be used to promote the uptake and adoption of these systems through government and fleet road safety action plans, as well as being useful in informing consumers on the protective role of these technologies in preventing crashes, mitigating serious injury, and in promoting timely emergency care once a crash occurs. In addition, the findings can be used to promote targeted investment in research and development of new vehicle technologies. From a conceptual perspective, the modified ISC when linked with specific crash scenarios offers a viable systematic method to analyse crashes across the entire crash sequence, from before drivers enter the vehicle through to recovery from the crash.

Finally, it is important to note that other non-vehicle related countermeasures that were identified as being applicable to these crashes. These countermeasures included driver-based measures and infrastructure-based measures. While not included in this paper for reasons of space and the focus on active safety systems, addressing the range of risk factors through implementation of these measures remains critical, as is the need to implement countermeasures at each part of the crash sequence. Doing so is necessary as each countermeasure addresses a specific risk factor that exerts its influence at a particular part of the ISC, and no single countermeasure is 100% effective 100% of the time.

ACKNOWLEDGEMENT

REFERENCES

[1]   Peden M, Scurfield R, Sleet D, Mohan D, Hyder AA, Jarawan E, et al. (Eds.). World Report on road traffic injury prevention. Geneva: World Health Organisation; 2004.

[2]   Shinar D. Traffic Safety and Human Behavior: Second Edition. UK: Emerald Publishing Limited; 2017.

[3]   World Health Organisation. Global status report on road safety 2018. Geneva: World Health Organization; 2018.

[4]   Groeger JA. Chapter 1 - How Many E's in Road Safety? In: Porter BE, editor. Handbook of Traffic Psychology. San Diego: Academic Press; 2011. p. 3-12.

[5]   Muir C, Johnston IR, Howard E. Evolution of a holistic systems approach to planning and managing road safety: the Victorian case study, 1970–2015. Injury Prevention. 2018;24(Suppl 1):i19-i24.

[6]   Johnston I. Beyond "best practice" road safety thinking and systems management – A case for culture change research. Safety Science. 2010;48(9):1175-81.

[7]   Haddon W Jr. The changing approach to the epidemiology, prevention, and amelioration of trauma: the transition to approaches etiologically rather than descriptively based. American Journal of Public Health. 1968;58(8):1431-38.

[8]   Haddon W, Jr. On the escape of tigers: an ecologic note. American Journal of Public Health. 1970;60(12):2229-34.

[9]   Haddon W Jr. A logical framework for categorizing highway safety phenomena and activity. Journal of Trauma. 1972;12(3):193-207.

[10]   Cameron MH. Vehicle crashworthiness ratings, preliminary report. Monash University Accident Research Centre; 1990, cited in Cameron MH. Statistical evaluation of road trauma countermeasures. Clayton: Monash University; 2000.

[11] Corben B., Senserrick T., Cameron M., Rechnitzer G. Development of the Visionary Research Model – application to the car / pedestrian conflict, Report 229. Clayton: Monash University Accident Research Centre; 2004.

[12] Salmon PM, Cornelissen M, Trotter MJ. Systems-based accident analysis methods: A comparison of AcciMap, HFACS, and STAMP. Safety Science. 2012;50(4):1158-70.

[13] Thomas P, Morris A, Talbot R, Fagerlind H. Identifying the causes of road crashes in Europe. Annals of Advances in Automotive Medicine. 2013;57:13-22.

[14] Tingvall C. Distraction from the view of governmental policy making. Subsection of the chapter: Government and Industry Perspectives on Driver Distraction. In: Regan M, Lee J, Young K, editors. Driver distraction: Theory, effects, and mitigation. Melbourne: CRC Press; 2008.

[15] Lie A. Managing traffic safety: an approach to the evaluation of new vehicle systems. Stockholm, Sweden: Karolinska Institute; 2012.

[16] Strandroth J, Sternlund S, Tingvall C, Johansson R, Rizzi M, Kullgren A. A new method to evaluate future impact of vehicle safety technology in Sweden. Stapp Car Crash Journal. 2012;56:497-509.

[17] Rizzi M, Strandroth J, Tingvall C. The effectiveness of antilock brake systems on motorcycles in reducing real-life crashes and injuries. Traffic Injury Prevention. 2009;10(5):479-87.

[18] Sunnevång C. Characteristics of nearside car crashes – an integrated approach to side impact safety. Umeå, Sweden: Umeå University 2016.

[19] Tingvall C. The Zero Vision a road transport system free from serious health losses. In: von Holst H, Nygren Å, Thord R, editors. Transportation, Traffic Safety and Health — The New Mobility: First International Conference. Brussels, Belgium: Springer Berlin Heidelberg; 1995, Published 1997. p. 37-57.

[20] Tingvall C, Lie A. The implications of the Zero Vision on biomechanical research International Research Council on the Biomechanics of Injury (IRCOBI); Dublin; 1996.

[21] Tingvall C. The Swedish 'Vision Zero' and how parliamentary approval was obtained. Road Safety Research, Policing and Education Conference; Wellington, New Zealand; 1998.

[22] Tingvall C, Lie A, Johansson R. Traffic Safety in Planning - A Multidimensional Model for the Zero Vision. In: von Holst H, Nygren Å, Andersson ÅE, editors. Transportation, Traffic Safety and Health — Man and Machine: Second International Conference. Brussels, Belgium: Springer Berlin Heidelberg; 1996, Published 2000. p. 61-9.

[23] Stigson H. A Safe Road Transport System - Factors Influencing Injury Outcome for Car Occupants. Stockholm Sweden: Karolinska Institute; 2009. The SRA Model of a Safe Road Transport System operationalises the Vision Zero Multi-Dimensional Model for Safe Travel.

[24] Kanianthra, J. Re-inventing safety: Do technologies offer opportunities for meeting future safety needs? SAE Technical Paper 2006-21-0009; 2006.

[25] Association for the Advancement of Automotive Medicine (AAAM). Abbreviated Injury Scale (AIS) 2005 – Update 2008. Chicago: AAAM; 2015.

[26] Fitzharris MP, Corben B, Lenné MG, Pok Arundell T, Peiris S, Liu S, Stephens A, Fitzgerald M, Judson R, Bowman DM, Gabler HC, Morris A, Tingvall, C. Overview and analysis of serious injury crashes – crash types, injury outcomes and contributing factors, ECIS Report 1. Monash University Accident Research Centre, Report 346; Clayton; 2022.

[27] Fitzharris MP, Corben B, Lenné MG, Peiris S, Pok Arundell T, Gabler HC, Liu S, Stephens A, Bowman DM, Morris A, Tingvall C. Speed, crash risk and injury severity, ECIS Report 2. Monash University Accident Research Centre, Report 344; Clayton; 2022.

[28] Fitzharris MP, Corben B, Lenné MG, Liu S, Peiris S, Pok Arundell T, Stephens A, Bowman DM, Morris A, Tingvall C. Understanding contributing factors for serious injury crashes using crash chain analysis, ECIS Report 3. Monash University Accident Research Centre, Report 345; Clayton; 2022.

[29] Fitzharris MP, Pok Arundell T, Corben B, Lenné MG, Liu S, Peiris S, Stephens A, Bowman DM, Morris A, Tingvall C. Identification of countermeasures to address serious injury crashes, ECIS Report 4. Monash University Accident Research Centre, Report 346; Clayton; 2022.

APPENDICES
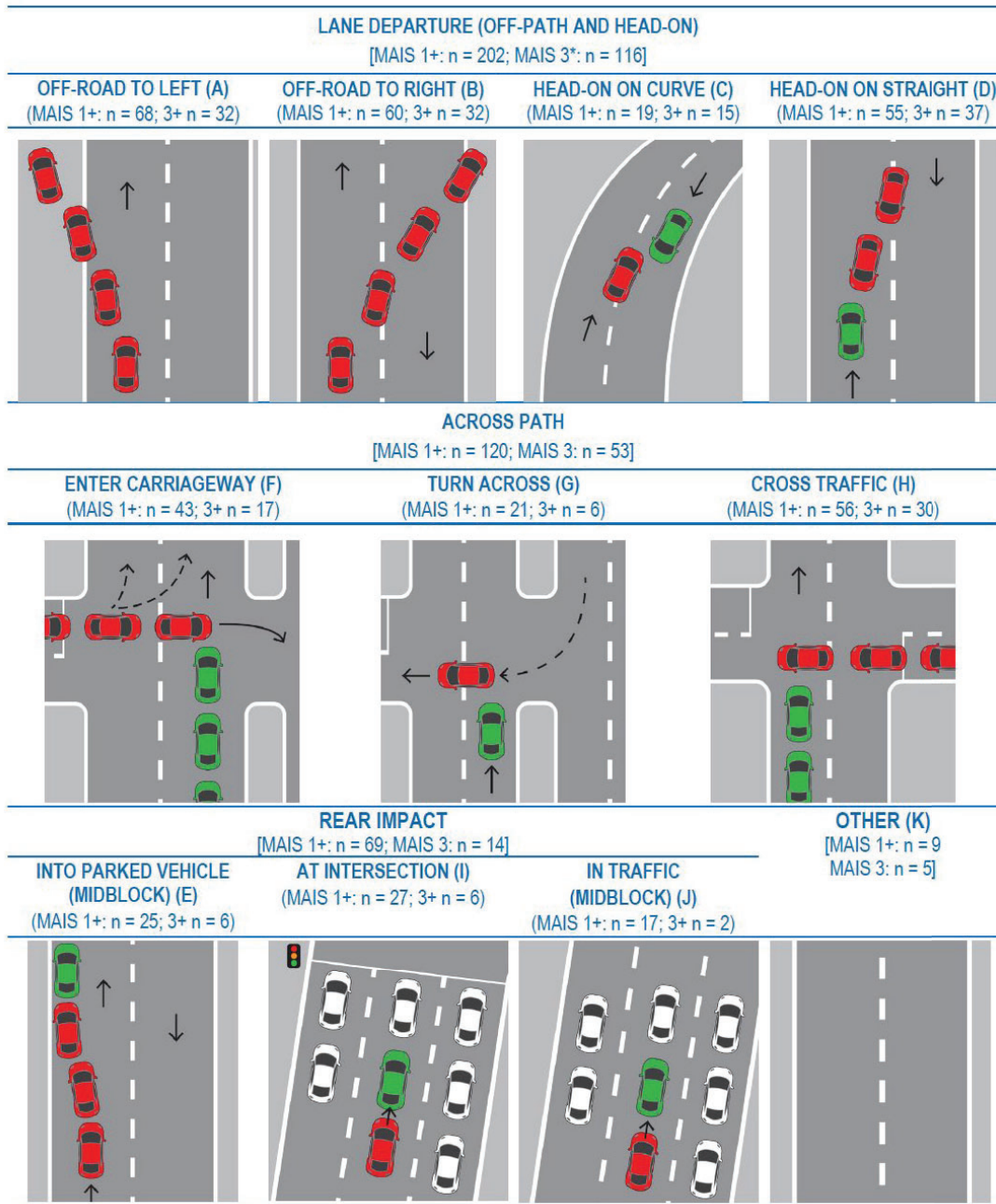
Figure A.1   Defined crash types and number of injured ECIS case drivers

Key: Vehicle (red): signifies the critical pre-crash vehicle movement; Vehicle (green): signifies that vehicle travelling in its normal path (or is stationary, rear impact - parked) and involved in the crash; Vehicle (white): vehicle (stationary or moving) in proximity of rear-impact crash but not involved. The ECIS driver can be the occupant of either of the crash-involved vehicles in each of the crash type scenarios. Note: * 3+ refers to MAIS 3+ injury severity. (letter) denotes crash type identifier.

OBSERVATION-BASED PEDESTRIAN SCENARIO EXTRACTION FOR VIRTUAL TESTING

Martin Schachner[1], Nadezda Kirillova[2,4], Fabian Weißenbacher[1], Bernd Schneider[1], Horst Possegger[2], Horst Bischof[2], Arno Eichberger[3], Zoltan Ferenc Magosi[3], Jan Dobberstein[5], Thomas Lich[6], Martin Kirchengast[7], Marcus Hennecke[8] and Corina Klug[1]

[1]Vehicle Safety Institute, Graz University of Technology, Austria
[2]Institute of Computer Graphics and Vision, Graz University of Technology, Austria
[3]Institute for Automotive Engineering, Graz University of Technology, Austria
[4]Christian Doppler Laboratory for Semantic 3D Computer Vision, Austria
[5]Mercedes Benz AG, Germany
[6]Robert Bosch GmbH, Germany
[7]AVL List GmbH, Austria
[8]Infineon Technologies Austria AG, Austria

Paper Number 23-0167

Abstract

An overall reduction of pedestrian-vehicle collisions is expected with the market penetration of Advanced Driver Assistant System (ADAS) and autonomous driving (AD) functions. The performance of ADAS is commonly evaluated through virtual scenario-based testing. Hence, scenario catalogs that represent realistic pedestrian-vehicle interactions are needed.

This study shows an approach to automatically extract pedestrian-vehicle scenarios at a selected road intersection, which was observed with a dual-lens stationary observation system. A deep learning-based visual perception pipeline was implemented to reconstruct road user trajectories via state-of-the-art object detection, visual multi-object tracking and object re-identification models. These models were trained and fine-tuned on a manually annotated, diverse dataset, randomly sampled from recordings over multiple weeks. All models were evaluated using common performance metrics. Additionally, localization precision of reconstructed trajectories was assessed using georeferenced ground truth measurements conducted at the intersection. The visual perception pipeline was applied on selected video data and extracted trajectories converted according to the openSCENARIO standard, including a virtual representation of the selected road intersection. The compiled scenarios were further simulated with the openPASS framework.

The results show that pedestrians and vehicles were tracked with high accuracy (Multiple Object Tracking Accuracy $> 83.2\%$) and trajectories were reconstructed with a mean deviation of 0.9 m for pedestrians and vehicle paths with a deviation of 0.68 (SD 0.5) m. The observation system allowed both the obtaining of typical pathways and also speed profiles. An exemplary reconstructed scenario was successfully resimulated in the openPASS framework.

The described approach is promising and can be used to create new scenario catalogs for scenario-based assessments in line with the openSCENARIO standard. Furthermore, the viewpoint of the observation system allows the reconstruction of pedestrian attributes including poses, age or gender, which, alongside an analysis of the recorded pathways and speed profiles with respect to influencing factors, is a focus of ongoing research.

1 INTRODUCTION

Every 5th road user killed in Europe is a pedestrian [11]. To counteract this trend, partner protection by other road users is an issue of great importance. ADAS and AD functions, such as Forward Collision Warning (FWC), Autonomous Emergency Braking (AEB), evasive steering or combinations of these are promising technologies to decrease the number of pedestrian accidents or at least to reduce collision speeds [23, 40], which has a positive effect on pedestrian's injury risks [38]. Scenario-based evaluation is a commonly used method to assess the effectiveness of ADAS for pedestrian safety. The creation of scenario catalogs, consisting of critical pedestrian-vehicle interactions is a major challenge. This effects on the one hand the scenario representation, but also the usage of appropriate data sources. The representation requires a domain-specific scenario description language (SDL), which needs to be in line and interpretable by the underlying simulation environment. A commonly used SDL is openSCENARIO [1], which requires a model of the scenery and the integration of the dynamic entities through storyboards. In order to fill those storyboards, reconstructed real-world accidents can be used according to [8, 16]. In addition to the fact, that accidents are rare events [22], leading to small sample sizes, the pedestrian movement prior to a collision can only be reconstructed with great difficulty and is thus often simplified, *i.e.* assumed to be constant. To compensate this drawback more data on pedestrian behavior and movement is needed.

Camera-based traffic observations are a promising alternative to complement missing information and benefit from new deep learning approaches for automatic scene reconstruction, capable to detect (*e.g.* [20, 34]) and track objects (multiple object tracking (MOT)) over multiple video frames (*e.g.* [48, 51]). Scene reconstruction can therefore be used to better understand the pedestrian behavior in the pre-crash phase [39, 26] but also to derive entire scenario catalogs [50, 4], which incorporate information of the entire scenery, *i.e.* not only of the conflict partners.

There are a variety of different pedestrian observation datasets recorded for specific application purposes. Datasets that record pedestrian movements from a static observation point, *e.g.* [2], mostly serve as benchmarks for tracking algorithms and usually do not provide interaction with other road users, *i.e.* vehicles. Datasets recorded from a vehicle centered view, as shown in [13, 45, 7] have the drawback that trajectories are only recorded over a relatively short time horizon. The datasets published by [50, 4] record pedestrian-vehicle interactions with drones, which make difficult any further determining of pedestrian attributes, such as *i.e.* age [5] or distractions [42, 19], which have an impact on pedestrian behavior. Thus, a trade-off between the level of detail and the overall observability of the scenery must be ensured to provide the necessary details for reconstructing pedestrian-vehicle interactions.

The objective of this study is to present a framework to automatically derive pedestrian-vehicle scenarios capable of integration in common traffic simulation frameworks from a camera-based observation system.

2 METHOD

For automatic extraction of pedestrian and vehicle trajectories, state-of-the-art computer vision algorithms, consisting of deep learning-based visual MOT and image classification models, are combined to a visual perception pipeline. Different datasets were generated in order to enhance the performance

of existing tracking and classification models, but also to evaluate the accuracy of reconstructed trajectories. The traffic observation and the newly generated datasets build the first part of this section, while road network modelling and the visual perception pipeline for trajectory reconstruction build the second part. Details on the simulation of selected reconstructed scenarios complete this section. The overall approach of this and the interplay of the different parts is shown in Figure 1.
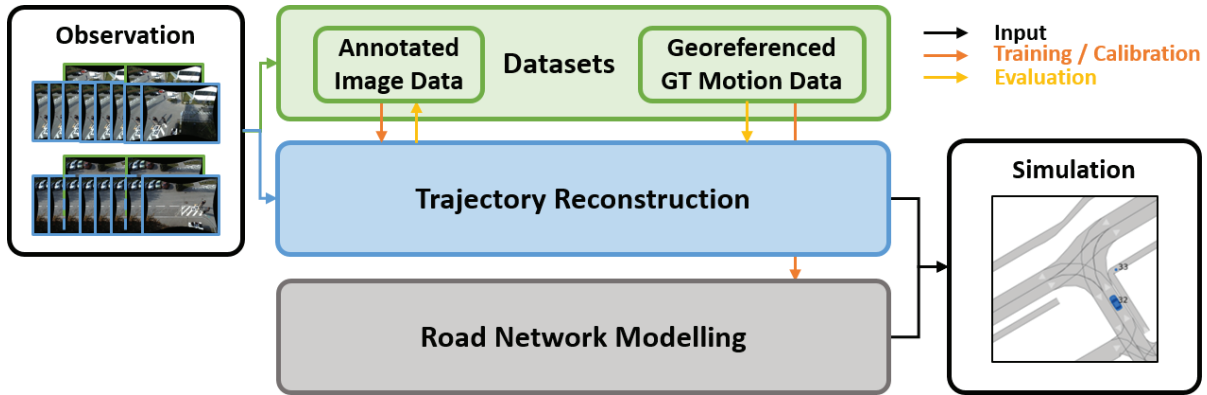
Figure 1. Outline and interplay of different components for automatic scenario extraction with a camera-based traffic observations system. The dataflow among different components is highlighted through arrows. Recorded data from the *observation system* is the input for the *trajectory reconstruction* process (blue frames), selected images (green frames) are combined into *datasets* to enhance (Training/Calibration, orange arrow) and quantify the reconstruction accuracy (Evaluation, yellow arrow). Reconstructed trajectories were aligned with the *road network* (grey) and incorporated in a *simulation* environment (black arrow).

2.1 Camera-based Observation

A robust system was developed for camera-based observation, which enables continuous data extraction even under extreme weather and temperature conditions. As shown in Figure 2, it consists of an Industrial Personal Computer (IPC) inside of a robust control cabinet, on which a dual-lens camera and a long-term evolution (LTE) antenna are mounted. The combined field of view (FOV) of the dual-lens camera thus allows recording of almost $180°$, shown in Figure 3.

The camera-based observation system was installed at an intersection of two private service roads, forming a T-junction, at the campus Inffeldgasse of Graz University of Technology. At the observation point, the traffic operates in accordance with the Austrian road traffic regulations, which implies right-hand driving and giving priority to the right at intersections. A speed limit of max. 20 km/h applies within the area. Furthermore, ground markings and road signs give information about towing zones as well as other prohibitions or bans. Sight obstructions, caused by parked vehicles as well as a large-scale art installation (a frame structure spanning the road), lead to a potential threat for pedestrians and potentially to interesting and frequent interactions with vehicles.

In order to record the intersection appropriately with the camera-based observation system, it was mounted at the frame structure of the art installation at a height of approximately 5 m, as shown in Figure 2. The cameras were aligned accordingly to best observe the events at the road intersection, which is shown in Figure 3.

Since the projection of 3D real world information onto a 2D image discards metric information, the dual-lens camera must be properly calibrated to allow recovering of 3D units from image-based

3

measurements. To this end, the system was calibrated intrinsically (using the calibration target and framework from [12], which extends [6]) which allows image rectification, *i.e.* to correct the inaccuracies caused by the inherent distortion of the optical lenses (which is most notable at the image border). To align the rectified camera images with a common World Coordinate System (WCS) denoted as O_W, *i.e.* extrinsic calibration, the AprilTag [36] framework was used. These calibration markers can be robustly detected outdoors and yield a sufficiently low pose estimation error. In particular, the translation and rotation errors over 20 consecutive video frames are $\leq 1.5\,\text{mm}$ and $\leq 0.1°$, respectively. In this study the WCS was calibrated in such a manner that an XY-plane is placed on the ground (*i.e.* at $Z = 0$), and the Z-axis is pointing up, see Figure 3.
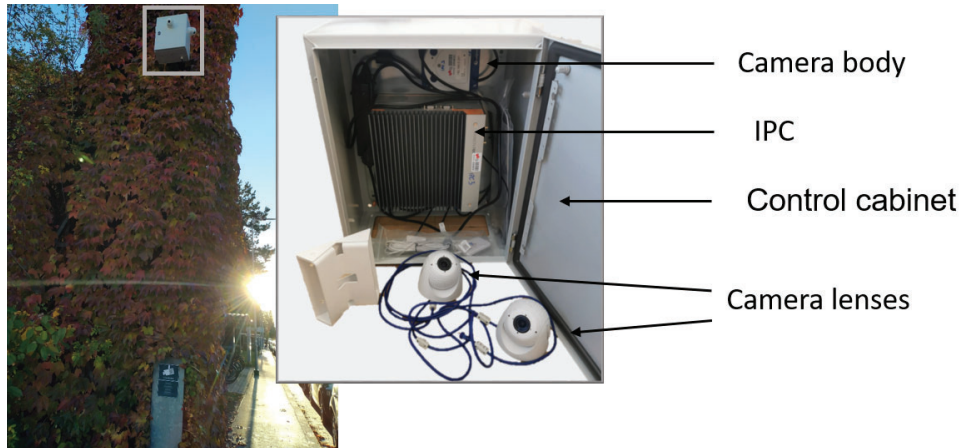
Figure 2. Mounted observation system at campus Inffeldgasse. The left image shows the observation system mounted at the art installation at the selected intersection. A sign informs pedestrians about the project and the legal basis of data collection. The right image shows the main components of the observation system, which consists of an IPC, connected to a Mobotix S16B camera body and the two camera lenses. An LTE antenna is mounted on the side of the control cabinet.
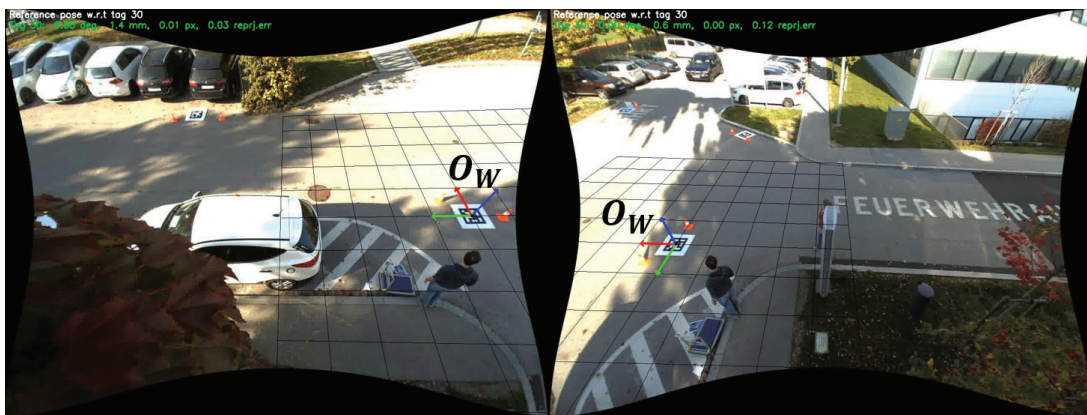
Figure 3. Left and right FOV of the installed observation system at the selected intersection. The extrinsic camera calibration defines the WCS O_W, which is illustrated via arrows pointing along the major axes (red: X-axis, green: Y-axis, blue: Z-axis).

4

2.2 Datasets

The camera placement of the observation system allows recording of the events at the selected intersection, but it does not resemble the viewing angle of publicly available datasets. Thus, the object detection, tracking and re-identification models had to be properly adjusted via finetuning. For this, we collected a sufficiently diverse image dataset. In addition to the collected image data, dedicated experiments were performed, in which georeferenced locations of vehicles and pedestrians were measured. This data was used to evaluate the accuracy of the trajectory reconstruction process.

2.2.1 Image Data

In order to generate a suitable dataset for fine-tuning and performance evaluation of a MOT algorithm, a dataset consisting of 10,800 frames was created from the recorded videos at the observation point. Each frame was manually annotated using the CVAT tool [43], where each annotation consists of an object's bounding box, as well as other relevant attributes, such as age category, gender, personal mobility device (scooter, bicycle, *etc.*) and potential distractions caused by smartphones or headphones. One part of the dataset, consisting of 7,200 frames, acts as training, the other as evaluation data. Due to the demographic conditions at the selected intersection, some attributes and objects are underrepresented, when sampling uniformly from the sample images (*e.g.* children, adolescents). To cope with this issue, particular interesting samples have been searched manually.

2.2.2 Ground Truth Motion Data

For estimating the accuracy of the trajectory reconstruction process, geolocations of pedestrians and vehicles were measured within dedicated tests. The geolocations were measured in both cases with an inertial navigation system (INS), using the Global Positioning System (GPS). Going forward, this measured data will be denoted as ground truth (GT) motion data. The temporal synchronization between video and the GT motion data was established through timestamps, associated to each video frame and the measurement, respectively.

Pedestrian The measurements of pedestrian GT motion data were designed to further allow for estimating the accuracy of the camera projection with respect to the WCS. For measuring the GT motion data, the INS (type: OxTS RT3000 v2 [30]) was mounted on a trolley. In order to be able to identify the INS in the recorded video frames using the AprilTag [36] framework, the trolley was equipped with a calibration tag, offset relative to the INS (in the reference frame of the measurement trolley). The INS base station was placed near the measurement area, with a sufficient distance to surrounding buildings that could have shielded the GPS signal and thereby could have introduced additional uncertainties. The developed measurement setup is shown in Figure 4.

In the experiment, the trolley was moved in the scene in such a way that it was visible in the video recordings. By this means the area of interest was covered by a grid of measurements with a spacing of about 1 m, resulting in around 200 distinct georeferenced measurement positions. Each position was captured for approximately 10 s, during which the trolley remained stationary. This made it easier to extract the particular image point and the corresponding GT position data. For the further usage, the position data of each measurement position was time-averaged to reduce measurement noise.

Vehicle For recording GT vehicle motion data, a dedicated test vehicle has been adapted to the needs of this investigation. Figure 5 sketches the vehicle setup schematically. Its setup consists of
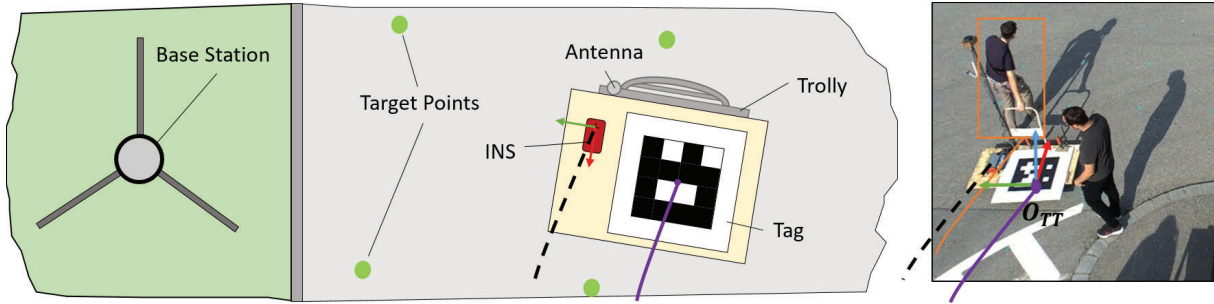
Figure 4. Schematic representation of the measurement setup installed on the movable trolley. The trolley was equipped with a calibration tag, the INS and its GPS antenna. Illustrated are the measured GPS track (black dashed), as well as the projected tag position (purple) and the trajectory resulting from the tracked operator (orange).

a data acquisition unit (DAU) (type: dspace AUTERA autobox operated by Intempora RT-MAPS 4 data acquisition software) which collects and synchronizes data from different sensor sources. A combination of accurate GPS-RTK (type: Novatel OEM 6, corrected by APOS service) and intertial measurement unit (IMU) (type: Genesys ADMA-III) is used to record trajectories and dynamic driving states (position angle, speeds, acceleration *etc.*). This is complemented by a Light Detection and Ranging (LiDAR) sensor (type: OUSTER OS1-128) which operates with a resolution of 128 x 1024 at 10 Hz and triggers the recording of the installed camera system (type: IDS - UI-5240CP with TAMRON M118FM08 lens).

Within the experiment the test vehicle was driven through the intersection several times, covering all dedicated routes given by the road network, as shown in Figure 6. The test drives were made in the speed range foreseen for the intersection. Further, recordings include typical interactions with other road users, especially pedestrians, in which the driver gives right of way and vice versa.
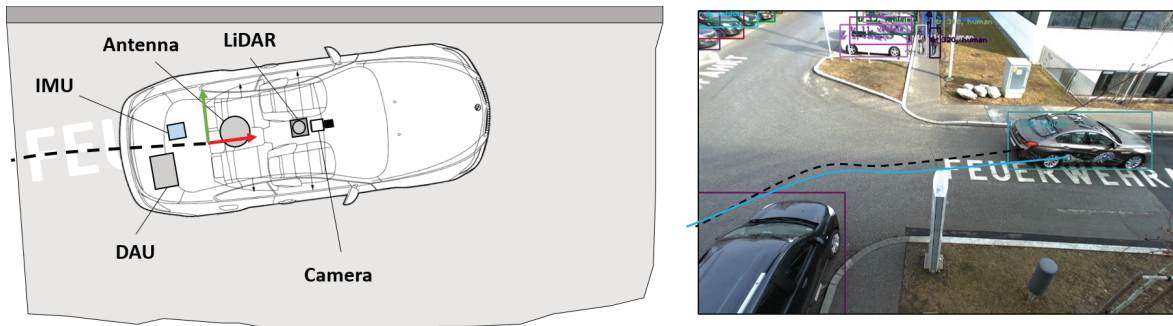
Figure 5. Schematic representation of the measurement setup installed in the test vehicle. The vehicle was equipped with a DAU, an IMU for measuring geolocation as well as a LiDAR sensor and a camera system. Shown are the GPS track (black dashed) that was measured in the conducted test and the projected trajectory resulting from the scenario reconstruction (blue).

2.3 Road Network Modelling

The static environment of the selected observation point (discussed in Section 2.1) serves as a basis for the agent simulations and have been digitized such that they are in line with the specifications of

the openSCENARIO [1] standard. In the following the 3D scene representation is explained as well as its alignment with the reconstructed trajectories in WCS.

2.3.1 3D Scene Representation

For the modelling, freely available, high quality geographic data of the selected intersection was used. This includes the direct proximity to the mounted observation system within the observation (*e.g.* intersection, crosswalks, etc.) as well as the adjacent road network within a radius of about 100 m. Orthophotos, retrieved from [15], as well as surface and terrain information, retrieved from [14], were used as data sources. As a pre-processing step, both data sources were merged and processed with QGIS [32]. For the creation of the 3D scenes, RoadRunner [29] was used. The construction of the road network, including sidewalks, was done manually, based on orthophotos of the observation point. The resulting 2D road network was supplied with terrain information and exported as an openDRIVE file. A visualization of the resulting 3D openDRIVE road network is shown in Figure 6.
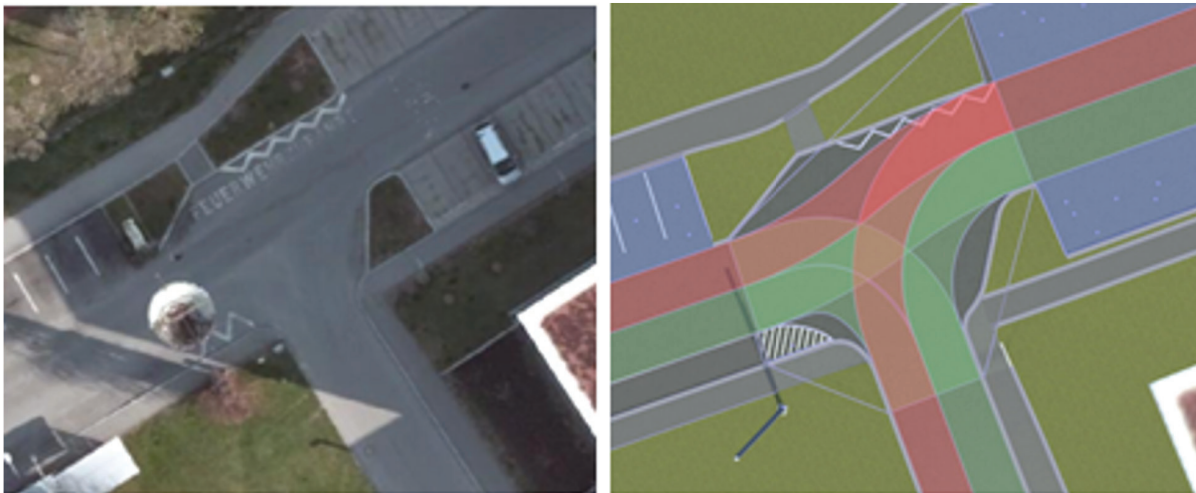
Figure 6. Modelling of the Inffeldgasse observation site. In the left image the orthophoto of the intersection area is shown. In the right image a 3D model of the observation point including the overlay of the openDRIVE network and the driveable routes.

2.3.2 Coordinate System Alignment

As described in Section 2.1, the WCS O_W is determined by the extrinsic camera calibration, which is used to recover 3D information of the road users, *i.e.* projecting trajectories to the ground plane. Reconstructed trajectories need to be transformed from the WCS to the OpenDRIVE Coordinate System (OCS) O_{OD} in order to obtain the representation of the trajectory in openSCENARIO. This OCS is bound to the georeferenced openDRIVE representation of the scene and therefore its coordinate axes are aligned to the cardinal directions following the east-north-up (ENU) convention.

GT motion data from the trolley measurements was used to determine the transformation T_{W2OD} between WCS and OCS. Therefore a third, intermediary coordinate system (ICS) O_I was defined by a reference tag at a selected measurement location I. Through the georeferenced position and orientation of I, the transformation of O_I relative to O_{OD} is known. Further, the transformation from O_I to O_W can be computed using the AprilTag framework. T_{W2OD} is thus defined by chaining these

transformations. It should be noted that only the Z-rotation angle (heading) of I was used, since pitch and roll angle were both relatively small, and their influence on the X/Y position was thus deemed negligible (< 5 cm).

2.4 Trajectory Reconstruction

The implemented visual perception pipeline for automated trajectory reconstruction consists of four building blocks, as shown in Figure 7. The central part includes the MOT algorithm, which localizes the road users, *i.e. pedestrians* and *vehicles*, throughout video frames while maintaining their identitys (IDs). Tracked road users in image coordinates then have to be mapped to the scenery representation (ground plane (WCS) and further to OCS), which forms the second part of the pipeline. To obtain consistent trajectory IDs across the partially overlapping FOVs of the dual-lens camera, the third step is to match corresponding road user trajectories across both FOVs. Finally, a post-processing step suppresses potential measurement noise from the reconstructed trajectories.
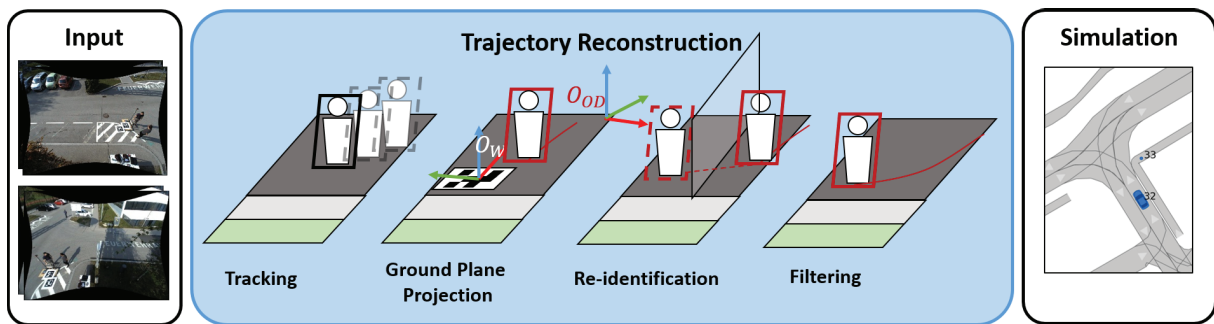
Figure 7. Schematic representation of the visual perception pipeline for trajectory reconstruction. The input frames from the cameras' FOVs are processed by the four building blocks, *multiple object tracking*, *ground plane projection*, *re-identification* and *trajectory filtering*.

2.4.1 Multiple Object Tracking-by-Detection

The MOT algorithm used follows *the tracking-by-detection paradigm* and provides a favorable balance between high accuracy and low run-time. It leverages a state-of-the-art single-stage object detector, *i.e.* YOLOv5 [20, 34], which generates object hypotheses in the form of bounding boxes (*i.e.* rectangular regions which likely contain an object) per frame. These object hypotheses are then temporally linked to object trajectories via an implemented multi-class capable extension of the Deep-SORT [48] MOT algorithm. For improved robustness, the standard appearance feature estimation in DeepSORT was replaced by the re-identification model OSNet [51], which performs favorably for varying object sizes and is thus more suitable for deployment in this study's observation scenario.

The output of the tracking step is a sequence of bounding boxes for each road user k over time t, *i.e.*

$$\mathbf{O}^{(k)} = \left(O_{t_{init}}^{(k)}, \dots, O_{t_{end}}^{(k)} \right), \tag{1}$$

where a bounding box $O_t^{(k)} = (x_t^{(k)}, y_t^{(k)}, w_t^{(k)}, h_t^{(k)})$ is defined by its top-left corner coordinates, width and height, respectively. All units are in pixels. The set of all estimated trajectories is denoted as

$$\mathcal{O} = \{\mathbf{O}^{(k)}\}_{k \in [1, \dots, N]}, \tag{2}$$

8

where N is the number of all detected road users.

2.4.2 Ground Plane Coordinates from Image-based Measurements

The image-based bounding box trajectories $\mathcal{O}$ need to be projected into the WCS to obtain 2D road user trajectories. For the projection, the widespread *central perspective projection* model (*pinhole camera*) is assumed, which follows the collinearity principle, *i.e.* each real-world point is projected along a straight line through the projection center (the camera's optical center) onto the image plane [18]. Using both intrinsic and extrinsic calibration of the camera, a homography (projective collineation) can be derived which allows mapping image coordinates onto a reference plane in the world coordinate system. Since the object foot points can be easily estimated from the image-based detection results, the world ground plane was chosen at $z = 0$ as reference plane for this projection.

In particular, given an object's bounding box $O_t^{(k)}$, we leverage the scene geometry given by the extrinsic calibration to compute the object's *orientation vector*. This allows accurate location of the *foot* (bottom) and *head* (top) points of the road user by intersecting the orientation vector with the edges of the corresponding bounding box, as illustrated in the left and middle image of Figure 8, the right image shows exemplary trajectories superimposed on a bird's eye view image. To obtain the corresponding location in OCS $\mathbf{x}_t^{(k)} = (x_t^{(k)}, y_t^{(k)}, 0)$ (measured in mm), the derived *foot* points are projected onto the world ground plane, *i.e.* WCS representation and further transformed to the OCS, as described in 2.3.2. Thus, the reconstructed trajectory signal $\mathbf{x}^{(k)}$ of a road user k is

$$\mathbf{x}^{(k)} = \left(\mathbf{x}_{t_{init}}^{(k)}, \ldots, \mathbf{x}_{t_{end}}^{(k)} \right). \tag{3}$$

In order to represent the road user movements within openSCENARIO, the reconstructed trajectory $\mathbf{x}^{(k)}$ is further filtered as described in 2.4.4,
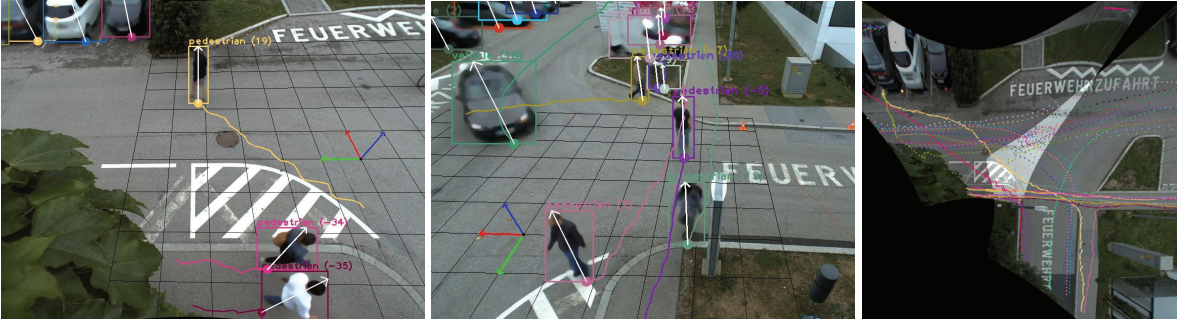
Figure 8. Multi-object multi-class tracking visualization with object *orientation vector* estimation and road user's *foot point* derivation. The colors of the bounding boxes and trajectories correspond to the object's instance ID. The right image shows exemplary trajectories after projecting image-based localization results onto the world's ground plane. The bird's eye view image was obtained by projecting the camera image pair onto the same plane.

2.4.3 View-consistent Trajectory IDs via Re-identification

The observation system uses two partially overlapping FOVs to cover a larger area of the road intersection. To obtain the most accurate localization results, tracking-by-detection is performed in each FOV independently. For consistent trajectory IDs throughout the *two-stream* scene, a road user re-identification approach is applied to establish correspondences between them in different FOVs. The

method reuses the appearance features already extracted by the OSNet re-identification model from the tracking step (as discussed in Section 2.4.1) which allows saving computational resources. For each road user, a feature gallery for 60 video frames, which is 5 seconds by recording at 12 fps, is kept and used in the following feature matching step. To predict an object transition between the two FOVs, temporal and spatial information is used in the same coordinate system, *i.e.* per frame coordinates projected onto the world ground plane (see Section 2.4.2). Thus, when a new road user is detected in the current FOV, and its real-world trajectory lies in the area of the second FOV, the feature galleries of these objects are matched across both FOVs and assigned a consistent trajectory ID upon finding correspondences in the galleries.

2.4.4 Velocity Estimation through Trajectory Filtering

The output of the previous steps consists of time-dependent trajectory signal $\mathbf{x}^{(k)}$ in the OCS reference frame (see Equation (3)). Due to the nature of the tracking algorithm (see Section 2.4.1 and 2.4.2), velocity information is not provided explicitly, and the position estimates are related to the bounding box of the objects, which introduces additional measurement noise. In order to retrieve meaningful trajectories and velocity profiles of the tracked road users, a constant acceleration Kalman filter [21] followed by a Rauch-Tung-Striebel (RTS) smoother [33] is applied on the trajectory signal $\mathbf{x}^{(k)}$. This approach benefits from improving $\mathbf{x}^{(k)}$, while yielding an estimate for the tracked object's velocity $\dot{\mathbf{x}}^{(k)}$ and acceleration $\ddot{\mathbf{x}}^{(k)}$. The chosen Kalman filter models the X and Y-component of the object's motion independently using position, velocity and acceleration as state variables. The acceleration may change between time steps, based on a discrete white noise model, where the amount of change is controlled by the estimated maximum jerk ($\dot{a}$) of the tracked object. The attached RTS smoother exploits the fact that $\mathbf{x}^{(k)}$ is already known for the whole trajectory when running the filter operation.

When setting up the filter, it was assumed that the measurement noise and the covariance of the position state variable can be estimated with the position accuracy of the tracking algorithm, Δx. Further it has been assumed that the maximum absolute values for velocity and acceleration, v_{max} and a_{max} respectively, can be used to estimate the covariances of the corresponding state variables as $\sigma_v^2 \approx (v_{max}/3)^2$ and $\sigma_a^2 \approx (a_{max}/3)^2$ [24].

2.5 *Reconstruction Accuracy Estimation*

For the accuracy evaluation of the trajectory reconstruction process, the georeferenced GT trajectories $\hat{\mathbf{x}}^{(k)}$ were compared with the reconstructed $\mathbf{x}^{(k)}$. As a pre-processing step, the measured data had to be aligned and time-synchronized for the setups, *i.e.* the reconstructed trajectories, as described in Section 2.4, had to be linearly interpolated, resulting in a sampling frequency of 100 Hz. Since each $\hat{\mathbf{x}}^{(k)}$ is accompanied by its timestamps, they were used to extract the corresponding frames from the video material. For time ranges in which the GT motion has been recorded in the vicinity of the selected intersection, the video recordings where searched for a tracked object $O_t^{(k)}$ (vehicle, pedestrian), which corresponds to the georeferenced GT motion data. To extract $\mathbf{x}^{(k)}$, the trajectory reconstruction process as described in Section 2.4 has been applied. At this point, it should be mentioned, that for the recordings with the measurement trolley (see Section 2.2.2), two different signals have been retrieved. Sequences, in which the trolley and operator moved in unison offered the opportunity to test the reconstruction process in the wild, *i.e.* on a pedestrian $\mathbf{x}^{(k)}$ as compared to an idealized object $\tilde{\mathbf{x}}^{(k)}$, *i.e.* the center of the tracking tag. This setup is particularly helpful for investigating how bounding box related effects affected the tracked trajectory of the pedestrian, since the tag is tracked with high accuracy and its image position is clearly defined.

Additionally, $\tilde{\mathbf{x}}^{(k)}$ was used to test and tune the performance of the Kalman Filter that was subsequently used to smooth reconstructed trajectories and provided velocity estimates, as discussed in Section 2.4.4.

2.6 *Pedestrian-Vehicle Scenario Simulation using openPASS*

The specifics are described in the following for simulating the observed scenarios in the simulation platform openPASS [47, 9]. Originally, the term openPASS formed a backronym for "Open Platform for the Assessment of Safety Systems". It has since been expanded beyond the scope of safety alone, and extends to the assessment of any kind of ADAS and AD function, using the standards OpenDRIVE, OpenSCENRIO and OpenSimulationInterface. In line with this, the simulation aims to provide vehicle and pedestrian agents that are modelled through system definitions and follow model-based design approaches. The agents are therefore composed by motion dynamics models and may consist of interconnected subsystems, such as ADAS functions. openPASS requires a certain information flow and thus files necessary to perform a simulation study. Besides meta information for the simulation (provided in *SimulationConfig*) and the agent models (*ProfilesCatalog*, *SystemConfigs*), which have to be passed, peculiarities of the scenario description and the properties of the pedestrian and the vehicle agent should be summarized in short form.

Scenario Description using OpenSCENARIO   The scenario file describes the traffic situation following the OpenSCENARIO standard [1]. The scenery used was modelled in Section 2.3 and was incorporated into the scenario via its corresponding openDRIVE description. The storyboard, indicating the interplay of road users and the temporal development of the scene has been modelled in accordance to the openPASS PreCrash Matrix (PCM) use case. The behavior is therefore composed as a *FollowTrajectoryAction*, which consists of the trajectory description, sampled with 100 Hz. The same method of trajectory interpolation as described in 2.4 has been used. Furthermore, the scenario file includes a link to a *ProfilesCatalog*, which describes the underlying algorithmic models of the spawned road users.

Pedestrian Agent   The pedestrian agent is relatively simple. Prescribed trajectories that are continuous in their velocities and accelerations are defined as a *FollowTrajectoryAction* in the Scenario file. The internal implementation of a trajectory follower forces the pedestrian agent to move to the defined position in time.

Vehicle Agent   The vehicle agent is similar to the model used in [40]. The target trajectory is described by the *FollowTrajectoryAction*, defined for each simulated agent in the storyboard of the scenario file. This given target trajectory is passed to a *route control algorithm*, which controls brake, throttle and steering signals based on the deviation between the actual and target state. This behavioral model affects the dynamics of the two-track model and the dynamics of the chassis, which simulate the suspension of the vehicle due to inertia forces.

3   RESULTS

The first the results of the described methodology are presented in the following. The main focus is on the accuracy of the trajectory reconstruction process. Since this visual perception pipeline is

significantly influenced by the MOT, its performance has been assessed separately. Further, the reconstructed trajectories have been assessed as described in Section 2.5. This section is complemented with first simulation results, which were generated by using the derived scenario in openPASS.

3.1 Multiple Object Tracking-by-Detection

Since MOT is a complex task consisting of detection, localization and association, multiple metrics should be considered to evaluate the performance of a multi-class multi-object tracking-by-detection approach. We employ the widely adopted multiple object tracking accuracy (MOTA) [3], identification F_1 score (IDF_1) [37] and trajectory quality [25] measures. Since it has recently been shown by [28] that these measures are often biased towards specific components of a tracking system (*e.g.* CLEAR-MOT focuses on detection and localization, while IDF1 focuses on association), we additionally report the results in terms of higher order tracking accuracy (HOTA) [28], which explicitly addresses these biases of existing measures.

The results of the quantitative multi-class multi-object tracking-by-detection evaluation are shown in Table 1. The tracking performance for both pedestrian and vehicle classes achieves high MOTA rates, *i.e.* 83.24% and 92.50%, respectively. Moreover, for the pedestrian class, which is the most important class due to their high vulnerability, the IDF_1 and HOTA scores are also at state-of-the-art levels, *i.e.* 89.39% and 70.61%, respectively. The lower IDF_1 score for the vehicle class can be mostly attributed to identity switches at parking area (visible at the top border of the right FOV). There, vehicle detections are significantly more unstable due to the high degree of occlusions, *i.e.* both the traffic sign, as well as other parked vehicles occlude distant cars which leads to frequent detection failures. Consequently, this causes identity switches for the occluded cars. As this only affects the cars parked at the far end of the camera's FOV, it does not impede the performance of our system to extract trajectories of moving and interacting road users.

Object class	GT_{det}	$TP_{det}^{\uparrow}$	$FN_{det}^{\downarrow}$	$FP_{det}^{\downarrow}$	$IDF1^{\uparrow}$	$MOTA^{\uparrow}$	$IDsw^{\downarrow}$	GT_{traj}	$MT_{traj}^{\uparrow}$	$PT_{traj}^{\uparrow}$	$ML_{traj}^{\downarrow}$	$HOTA^{\uparrow}$
Pedestrian	3634	3180	454	156	89.39%	83.24%	4	41	26	13	2	70.61%
Vehicle	30496	30098	398	1887	44.46%	92.50%	3	88	87	1	0	56.85%

Table 1. Quantitative results of the multiple class multiple object tracking-by-detection method on our image data. GT_{det}, TP_{det}, FN_{det} and FP_{det} - the numbers of ground truth, true positive, false negative and false positive detections, respectively; IDF_1 - tracking Identification or association accuracy score; MOTA - multiple object tracking accuracy; IDsw - the number of trajectory ID switches; GT_{traj}, MT_{traj}, PT_{traj} and ML_{traj} - the numbers of ground truth, mostly tracked, partly tracked and mostly lost trajectories, respectively; HOTA - higher order tracking accuracy. $\uparrow$ and $\downarrow$ denote that higher/lower values correspond to better performance.

3.2 Reconstruction Accuracy

In general, it is hard to evaluate the similarity of two trajectories. One of the most commonly used approaches is the calculation of spatial distances between temporal corresponding points, also referred as lock-step Euclidean distance (LSED) Eu, as well as the calculation of the dynamic time warping (DTW), which is well suited to compare paths [46]. Since the trajectories used for the accuracy evaluation have different lengths, the mean μ_{Eu} and μ_{dtw} as well as the standard deviation σ_{Eu} and σ_{dtw} over all considered point pairs have been used for comparison. Besides a path reconstruction, it is essential to obtain accurate speed profiles of the road users. For the comparison of the speed profiles resulting from the trajectories, the cross-correlation $\rho_{\hat{v},v}^{(k)}$ between $\hat{\mathbf{v}}^{(k)}$ and $\mathbf{v}^{(k)}$ was used and an mean correlation μ_ρ calculated.

The deviation by means of the DTW, are promising and circumvent those effects by comparing paths.

3.2.1 Optimum

The tracked tag positions of all measurement positions (see Section 2.2.2) were mapped into the OCS separately for each FOV using the approach presented in Section 2.3.2 and compared against the recorded GPS measurements (also mapped into the OCS). The resulting deviations in the XY-plane of the OCS are plotted in Figures 9 and 10. For the left FOV, we were able to reconstruct the tracked tag positions with a mean absolute error (MAE) of 0.2 m, a median deviation of 0.14 m and a maximum absolute error of 0.63 m.

For the right FOV, we achieved a MAE of 0.17 m and a median deviation of 0.1 m. The maximum absolute error was higher with 0.95 m, but this can generally be attributed to outliers, since for approximately 95 % of all measured positions, the absolute deviation is actually ≤ 0.3 m. These outliers correspond to measurement positions that lay far from the camera and close to the edge of the image (as shown in the right pane of Figure 10) where the lens distortion is highest, thus making them especially susceptible for re-projection errors.
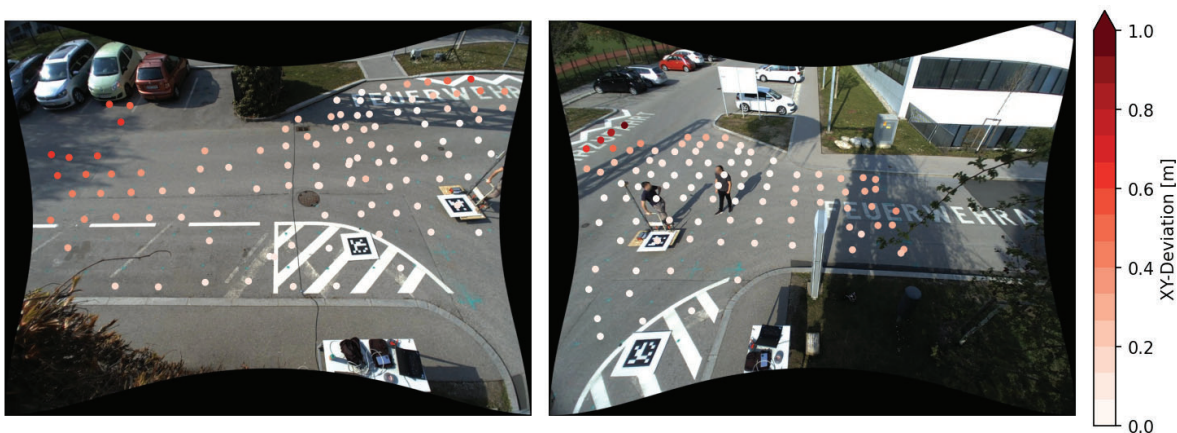
Figure 9. Reconstruction accuracy of the tag position overlaid on camera views. The left and right images show the deviations between GPS measurements and the tracked tag position (transformed via T_{W2OD}) for the left and right FOV respectively.

3.2.2 Pedestrian

Reconstructed trajectories were compared against the recorded ground-truth trajectories for 25 shared movement sequences of the measurement tag and trolley operator (pedestrian). It was found that the measurement tag position was reconstructed with a mean LSED of 0.2 m, which was in line with the optimal reconstruction accuracy of 0.17 m to 0.20 m that was established using static targets (see Section 3.2.1). The positional accuracy of the operator trajectories, in contrast, was significantly lower with an average LSED of 0.9 m and with maximum absolute errors reaching as high as 2.5 m compared to 1.0 m for the tag trajectories. The poorer performance for the operator trajectory can be explained to a great extent, as the effect of the distance between the operator and the measurement tag, which introduces a systematic error that could not be corrected during the analysis. For the
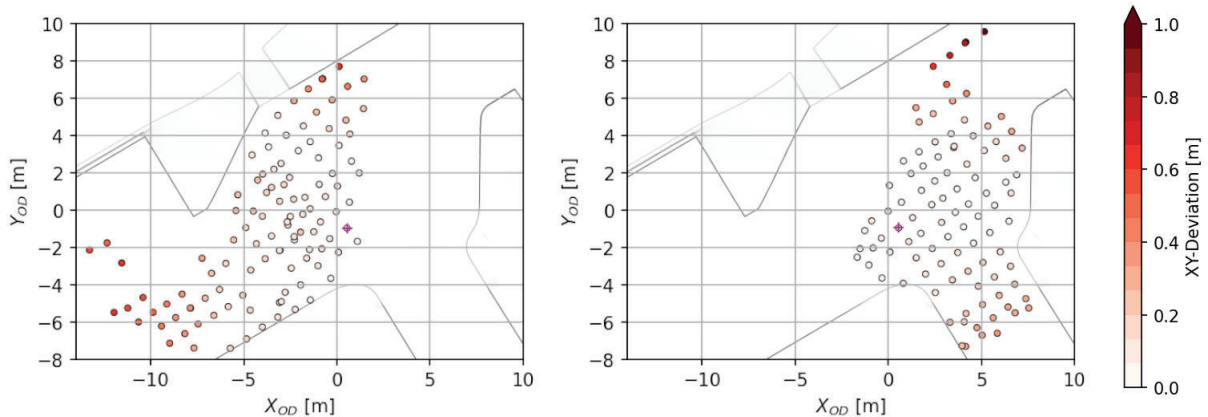
Figure 10. Reconstruction accuracy of tag position overlaid on road borders. The left and the right images show the deviations between GPS measurements and the tracked tag position (transformed via T_{W2OD}) for left and right FOV respectively. The position of the intermediary coordinate system is marked with a magenta cross.

comparison of velocities, the offset between operator and tag should have had less of an impact, assuming that it stayed approximately constant. On examining the calculated velocity accuracies, this has been the case: the LSED of the operator velocities was higher than that of the tag velocities, 0.27 m/s for operator versus 0.07 m/s for the tag, but the relative difference between these values was smaller than between the corresponding positional LSEDs. This can also be seen in Table 2, which summarizes the position and velocity accuracy statistics.

Figure 11 gives a qualitative comparison between tracked and reconstructed trajectories of reference tag and trolley operator for a selection of analyzed movement sequences. It can be seen that the recorded operator trajectory was significantly noisier than the tag trajectory, underscoring the need for Kalman filtering when confronted with realistic data. The Kalman filter was designed to filter out the high-frequency noise in the pedestrian tracking data, which is most apparent in the trajectories for sequences 10, 12, 23 and 24. This noise is generated by oscillations in the bounding box, and is most likely caused by foot movement and the pedestrian's legs being partially occluded by the measurement trolley. As can be seen from the right side of Figure 11, the filter generally succeeded in removing this type of noise.

| | Position | | Velocity | | |
Data source	$\mu_{Eu}\ [m]$	$Eu_{\max}\ [m]$	$\mu_{Eu}\ [m/s]$	$Eu_{\max}\ [m/s]$	μ_ρ
Optimal (tag)	0.2	1.0	0.07	0.7	0.97
in the wild (pedestrian)	0.9	2.5	0.27	2.2	0.77

Table 2. Quantitative results of the pedestrian trajectory reconstruction accuracy. μ_{Eu} - mean LSED, $Eu_{\max}$ - maxmium LSED, μ_ρ - mean velocity profile correlation

3.2.3 Vehicle

A total of 18 reconstructed trajectories were compared with their georeferenced GT measurement. The average LSED showed a reconstruction accuracy of 1.391 ($\pm$ 0.77) m and the DTW 0.675 ($\pm$ 0.51) m. Vehicle speed could be reconstructed with a MAE of 0.34 ($\pm$ 0.38) m/s. Reconstructed and
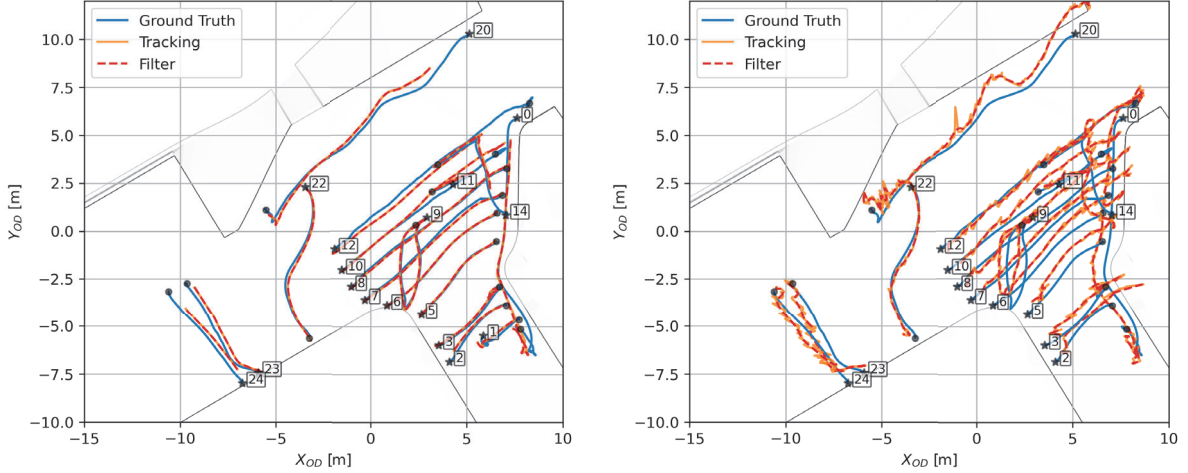
Figure 11. Qualitative comparison between reconstructed trajectories (red dashed lines) and geo-referenced ground-truth data (blue) for selected movement intervals. Left: trajectories based on the measurement tag. Right: trajectories of the person that operated the measurement trolley. The beginning and end of all sequences is marked by star and circle symbols, respectively. Best viewed on screen.

measured velocities showed a correlation of about 0.94 on average. The high deviation by means of LSED can be reasoned by the determination of the vehicle's representative point, which is a function of the bounding box. Therefore a systematic error in the distance between the GPS measured point and the reconstructed point effects the result. The deviation by means of DTW are however promising and circumvent those effects by evaluating path similarity. Furthermore, these results have been divided by means of the six different paths, which could possibly be taken by a vehicle on the basis of the road layout. The obtained results per path are provided in Table 3, selected trajectories per path are shown in Figure 12.

Scenario	Nr	Nr Points	μ_{Eu} $[m]$	$\sigma_{Eu}[m]$	μ_{dtw} $[m]$	$\sigma_{dtw}[m]$	$Eu_{\max}[m]$	μ_ρ
1-2	5	4944	1.406	0.518	0.54	0.414	2.425	0.974
1-3	4	4805	1.324	1.013	0.894	0.521	3.203	0.945
2-1	4	3335	1.079	0.475	0.383	0.305	2.378	0.884
2-3	2	1080	1.252	0.309	0.57	0.379	1.543	0.939
3-1	3	3040	1.911	0.799	0.841	0.627	3.289	0.941
3-2	3	1265	1.284	0.688	0.837	0.463	2.792	0.967
all	21	18469	1.391	0.767	0.675	0.511	3.289	0.942

Table 3. Quantitative results of the vehicle trajectory reconstruction accuracy. Results have been subdivided into different scenarios, based on the paths. μ_{Eu} - Mean LSED, σ_{Eu} - standard deviation of LSED, μ_{dtw} - Mean DTW, σ_{dtw} - standard deviation of DTW $DTW_{\max}$ - Maximum DTW, μ_ρ - mean velocity profile correlation

3.3 Simulating a Pedestrian-Vehicle Scenario

The openSCENARIO files, resulting from the reconstruction of the dedicated test drives were used as input for the simulation environment openPASS. An example for the simulated scenario is shown in Figure 13.

15
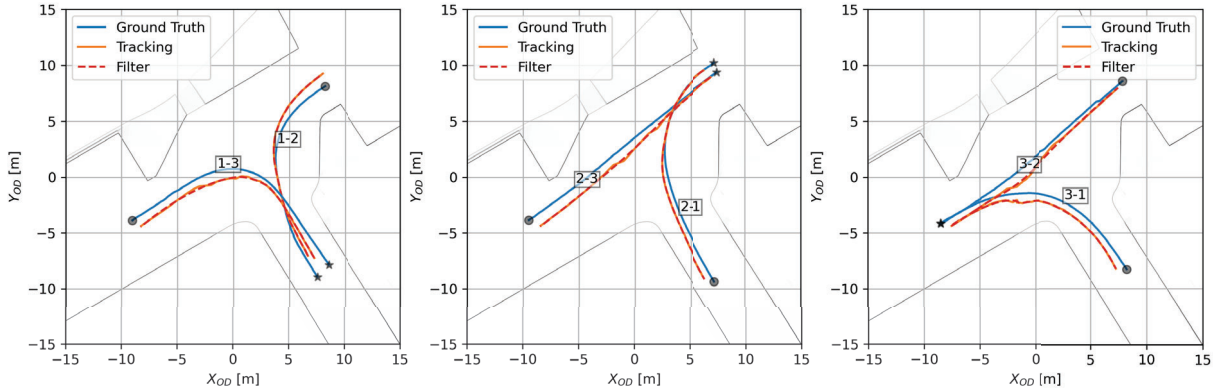
Figure 12. Qualitative comparison between the reconstructed trajectories (dashed line) and the geo-referenced GT motion data (solid lines). The left subfigure shows vehicle trajectories starting from road section 1, the middle from road section 2, and the right from road section 3, respectively.

4 DISCUSSION

In this paper a workflow has been established to extract pedestrian-vehicle scenarios from camera-based observation system, suitable to the virtual assessment of ADAS.

4.1 Traffic Observation and Visual Perception Pipeline

Due to the internal service roads at the observation point chosen in this study there are frequent interactions between vehicles and pedestrians. However, at this particular point, accident with personal injuries have not been recorded in recent years, which can be explained mainly by the speed limit. The extension to observation points in public space as in [50, 4], would complement the scenario catalog as it results in other scenario configurations. Recordings of road sections with a higher speed limit, *i.e.* 50 km/h, regulated and unregulated crosswalks, or interactions with public transportation would be of additional value. In order to further quantify scenario relevance, it would be necessary to evaluate complexity and criticality based on common metrics such as traffic densities, or time to collision (TTC). Further observation points would be needed to underpin the results and to better understand intersection specific differences. The deliberate camera placement and viewpoint choices differs significantly from previous studies [49, 50, 4], and allows a higher level of detail which is useful to further increase the realism of the scenario description, especially with respect to road user interactions. In addition to the approach shown for to extracting road user trajectories automatically, the close-up observations will allow future work to investigate pedestrian attributes and even include realistic pedestrian postures [39] in simulation environments such as Car Learning to Act (CARLA) [10].

A realistic assessment of integrated safety systems should take into account the initial posture of a vulnerable road user (VRU) prior to a crash, as it can influence the accident kinematics and the resulting crash severities. Having the capability of reconstructing realistic postures of VRUs in critical situations, as described in [39, 26], and transferring them into a simulation environment could therefore enable more realistic virtual testing of integrated safety systems.

Furthermore, it should be noted that the presented trajectory reconstruction process could be applied to other observation points with relative ease. The adaptions required for this mainly concern two parts of the visual perception pipeline, namely tracking and ground plane projection and there in
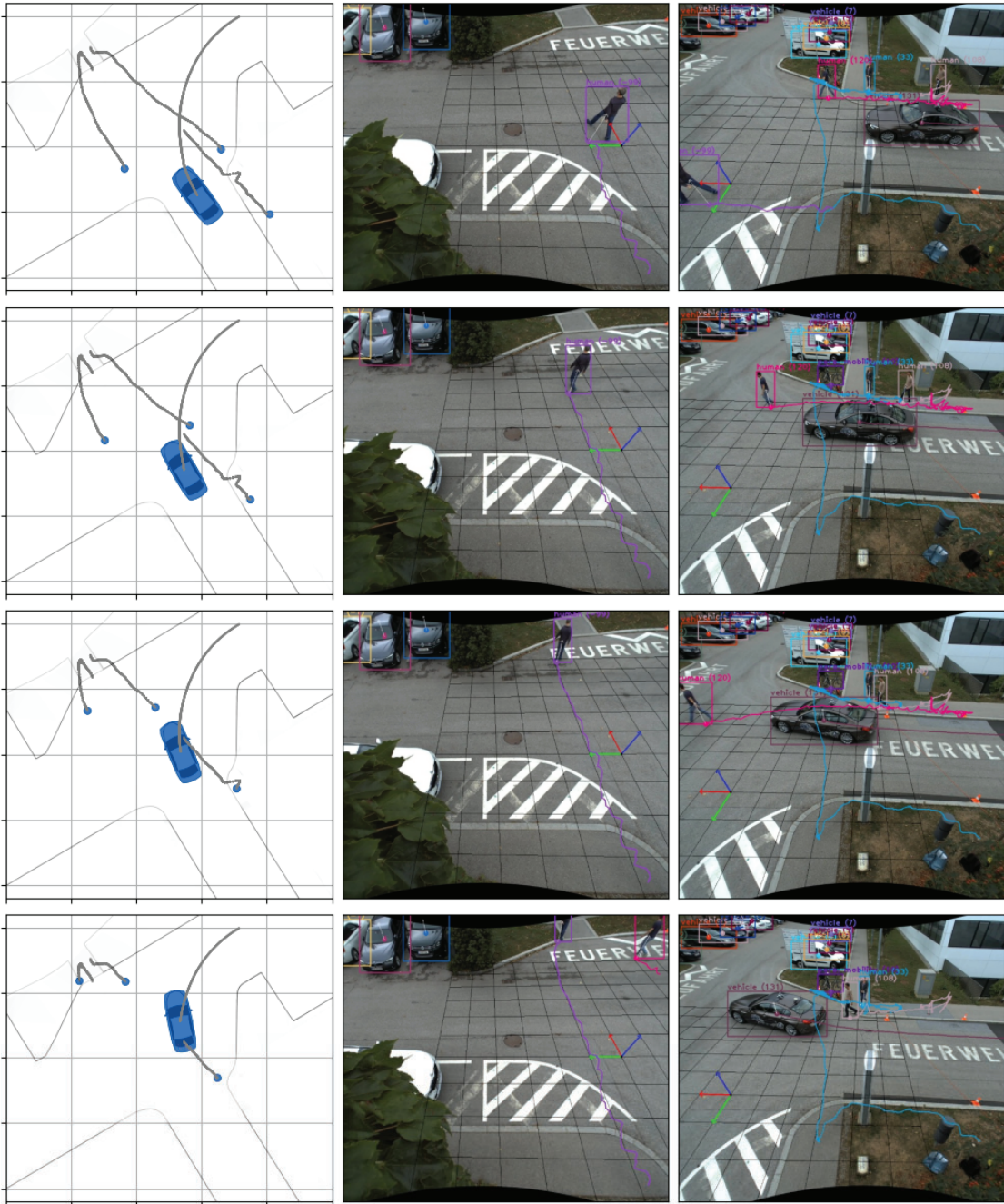
Figure 13. Visualisation of the scenario simulated in openPASS, alongside the corresponding video frames of the observation system, including the results of the MOT. Frames where taken at simulation time 0, 2, 4 and 6 seconds.

particular, the coordinate system alignment. The MOT algorithms can be adapted to other observation points, by adding additional training data and for the coordinate system alignment only one pair of corresponding GPS measurement and tag orientation/position measurement would be required to calculate the transformation T_{W2OD}.

4.2 Trajectory Reconstruction Accuracy

The performance of the trajectory reconstruction via perception pipeline, described in Section 2.4 depends on multiple factors. A central aspect of this is the correct operation of the MOT. The MOT performance shown in this paper is on state-of-the-art level, which could be quantified with common performance metrics. For the creation of a scenario catalog, the remaining misclassifications and ID switches play a minor role since they could be compensated in a post-processing step. A possible approach would be additional temporal and spatial sanity checks, *e.g.* checking if the start and end point of the trajectory are outside the observed area defined in Section 3.2.3. Overall, it can be assumed that the trajectories filtered in this way represent only a small subset of all reconstructed trajectories, and do not have a greater impact on the overall scenario distribution at this intersection. As expected, the highest reconstruction accuracy is reached near the center of each FOV. Furthermore, the road surface at the observation location in our study was highly uneven and thus, often violates the underlying assumptions of the central perspective projection model that the ground plane should be located at $z = 0$ for all locations in the observed image. The reconstruction accuracy is thus expected to improve notably when deployed at other observation points, where this assumption on the ground plane holds.

The investigation on vehicle trajectory accuracy estimation as presented in Section 3.2.3 shows a systematic deviation in the reconstructed path. The path reconstruction might be further improved by taking the distance to the image center into account, as well as the road network information, *i.e.* lane types, dedicated for specific road users. Apart from the general limits of reconstruction accuracy, as determined in Section 3.2.1, the representative vehicle point used for ground plane projection could possibly be enhanced, as shown by [44]. In our case, the representative point is a function of the bounding box size and is therefore of limited accuracy in the area where the vehicle is only partly visible, *i.e.* in the overlap of the cameras' FOVs. This transition affects both the reconstruction of the path as well as the reconstructed velocity. Since the path is currently reconstructed by spline interpolation, targeted smoothing by weighting the points with respect to the their WCS location could possibly enhance the results. For the velocity reconstruction, the effect is compensated by a mean filter, which could further be improved by using enhanced sensor fusion techniques.

Overall, the reconstructed trajectories were sufficiently accurate to permit realistic modelling as demonstrated by the low deviations in the specifically conducted accuracy estimation measurements and in the simulation.

4.3 Simulation

At the current stage only single scenarios were re-simulated. Nevertheless, the reconstructed trajectories could be lift the concrete scenario description to logical actions as shown in [35]. Logical scenarios, which are capable to model the entire traffic, can then be used for scenario-based assessment of ADAS, via stochastic simulations [40]. In general, traffic simulations include the dynamics and behavior of traffic participants (vehicles, pedestrians, *etc.*), the road network, environmental conditions (lighting, weather) and sensors like cameras, LiDARs, and Radio Detection and Ranging (Radars) [31]. The vehicle's sensors and the related perception algorithms for object detection and tracking provide essential input data for the ADAS that is being tested. Hence, modeling sensor capabilities and deficiencies with sufficient accuracy is thus a matter of the utmost importance for obtaining realistic simulation results. Different fidelity levels are required depending on which ADAS development process phase the sensor model is applied to. In early stages, where the focus lies on control or planning algorithm design, it is common to use models which provide object list outputs (see *e.g.* [27]),

i.e. sensor and perception are encapsulated in one model. Later on, when also the in-vehicle perception software is tested, sensor models which provide raw data output (*e.g.* LiDAR point clouds [17]) are applied. An overview of various sensor model types and their underlying principles is given in [41].

5 CONCLUSIONS

The exemplary application of a newly developed workflow to bridge the gap between observed real-world pedestrian scenarios and scenarios in traffic simulations used for the assessment of active pedestrian protection systems was showcased within this paper. It was possible to simulate the observed scenarios with the simulation framework openPASS. The developed method and recorded data sets show great potential for future work and will support the development of more realistic virtual pedestrian scenarios and therefore a more realistic effectiveness assessment of ADAS in the future.

REFERENCES

[1] ASSOCIATION FOR STANDARDIZATION OF AUTOMATION AND MEASURING SYSTEMS (ASAM). Openscenario®, 2022.

[2] BENFOLD, B., AND REID, I. Stable multi-target tracking in real-time surveillance video. In *CVPR 2011* (2011), pp. 3457–3464.

[3] BERNARDIN, K., AND STIEFELHAGEN, R. Evaluating multiple object tracking performance: The CLEAR MOT metrics. *European Association for Signal Processing (EURASIP) Journal on Image and Video Processing* (2008).

[4] BOCK, J., KRAJEWSKI, R., MOERS, T., RUNDE, S., VATER, L., AND ECKSTEIN, L. The inD Dataset: A Drone Dataset of Naturalistic Road User Trajectories at German Intersections. In *2020 IEEE Intelligent Vehicles Symposium (IV)* (2020), pp. 1929–1934.

[5] BOHANNON, R. W. Comfortable and maximum walking speed of adults aged 20-79 years: reference values and determinants. *Age and ageing 26*, 1 (1997), 15–19.

[6] BOUGUET, J.-Y. Camera calibration toolbox for MATLAB., 2013.

[7] CAESAR, H., BANKITI, V., LANG, A. H., VORA, S., LIONG, V. E., XU, Q., KRISHNAN, A., PAN, Y., BALDAN, G., AND BEIJBOM, O. nuScenes: A Multimodal Dataset for Autonomous Driving. In *2020 IEEE/CVF Conference on Computer Vision and Pattern Recognition (CVPR)* (2020), pp. 11618–11628.

[8] DETWILLER, M., AND GABLER, H. C. Potential Reduction in Pedestrian Collisions with an Autonomous Vehicle. In *The 25th ESV Conference Proceedings* (2017), NHTSA, Ed., ESV Conference Proceedings, NHTSA, pp. 1–8.

[9] DOBBERSTEIN, J., BAKKER, J., WANG, L., VOGT, T., DÜRING, M., STARK, L., GAINEY, J., PRAHL, A., MUELLER, R., AND BLONDELLE, G. The Eclipse Working Group openPASS – an Open Source Approach to Safety Impact Assessment Via Simulation. In *The 25th ESV Conference Proceedings* (2017), NHTSA.

[10] DOSOVITSKIY, A., ROS, G., CODEVILLA, F., LÓPEZ, A., AND KOLTUN, V. Carla: An open urban driving simulator, 2017.

[11] EUROPEAN COMMISSION. *Road safety thematic report - Fatigue*. European Road Safety Observatory, Brussels, European Commission, Directorate General for Transport, 2021.

[12] FERSTL, D., REINBACHER, C., RIEGLER, G., RÜTHER, M., AND BISCHOF, H. Learning Depth Calibration of Time-of-Flight Cameras. In *BMVC* (2015).

[13] GEIGER, A., LENZ, P., AND URTASUN, R. Are we ready for autonomous driving? The KITTI vision benchmark suite. In *2012 IEEE Conference on Computer Vision and Pattern Recognition* (2012), pp. 3354–3361.

[14] GIS STEIERMARK. Airborne laserscanning-basierende höhendaten, 2021.

[15] GIS STEIERMARK. Digitaler atlas, 2022.

[16] GRUBER, M., KOLK, H., KLUG, C., TOMASCH, E., FEIST, F., SCHNEIDER, A., AND ROTH, F. The effect of P-AEB system parameters on the effectiveness for real world pedestrian accidents. In *The 26th ESV Conference Proceedings* (2019), NHTSA.

[17] HANKE, T., SCHAERMANN, A., GEIGER, M., WEILER, K., HIRSENKORN, N., RAUCH, A., SCHNEIDER, S.-A., AND BIEBL, E. Generation and validation of virtual point cloud data for automated driving systems. In *2017 IEEE 20th International Conference on Intelligent Transportation Systems (ITSC)* (2017), pp. 1–6.

[18] HARTLEY, R., AND ZISSERMAN, A. *Multiple View Geometry in Computer Vision*, 2 ed. Cambridge University Press, 2004.

[19] JIANG, K., LING, F., FENG, Z., MA, C., KUMFER, W., SHAO, C., AND WANG, K. Effects of mobile phone distraction on pedestrians' crossing behavior and visual attention allocation at a signalized intersection: An outdoor experimental study. *Accident Analysis & Prevention 115* (jun 2018), 170–177.

[20] JOCHER, G., STOKEN, A., CHAURASIA, A., BOROVEC, J., NANOCODE012, TAOXIE, KWON, Y., MICHAEL, K., CHANGYU, L., FANG, J., V, A., LAUGHING, TKIANAI, YXNONG, SKALSKI, P., HOGAN, A., NADAR, J., IMYHXY, MAMMANA, L., ALEXWANG1900, FATI, C., MONTES, D., HAJEK, J., DIACONU, L., MINH, M. T., MARC, ALBINXAVI, FATIH, OLEG, AND WANGHAOYANG0106. ultralytics/yolov5: v6.0 - YOLOv5n 'Nano' models, Roboflow integration, TensorFlow export, OpenCV DNN support, oct 2021.

[21] KALMAN, R. E. A New Approach to Linear Filtering and Prediction Problems. *Journal of Basic Engineering 82*, 1 (03 1960), 35–45.

[22] KALRA, N., AND PADDOCK, S. M. Driving to safety: How many miles of driving would it take to demonstrate autonomous vehicle reliability? *Transportation Research Part A: Policy and Practice 94* (2016), 182–193.

[23] KOVACEVA, J., BÁLINT, A., SCHINDLER, R., AND SCHNEIDER, A. Safety benefit assessment of autonomous emergency braking and steering systems for the protection of cyclists and pedestrians based on a combination of computer simulation and real-world test results. *Accident Analysis & Prevention 136* (2020), 105352.

[24] LABBE, R. Kalman and bayesian filters in python, 2022.

[25] LI, Y., HUANG, C., AND NEVATIA, R. Learning to Associate: HybridBoosted Multi-Target Tracker for Crowded Scene. In *CVPR* (2009).

[26] LICH, T., MÖNNICH, J., SCHMIDT, D., AND VOSS, M. Preparation of an ai based real-time injury risk index estimation by deriving vru behavior from video-documented crashes. In *airbag 2022, 15th International Symposium and Exhibition on Sophisticated Car Safety Systems* (2022), Fraunhofer Institute for Chemical Technology ICT, pp. V20–19.

[27] LINNHOFF, C., ROSENBERGER, P., AND WINNER, H. Refining object-based lidar sensor modeling — challenging ray tracing as the magic bullet. *IEEE Sensors Journal 21*, 21 (2021), 24238–24245.

[28] LUITEN, J., OSEP, A., DENDORFER, P., TORR, P., GEIGER, A., LEAL-TAIXÉ, L., AND LEIBE, B. HOTA: A higher order metric for evaluating multi-object tracking. *International Journal of Computer Vision 129*, 2 (2020), 548–578.

[29] MATLAB. Roadrunner (r2022b), 2022.

[30] OXFORD TECHNICAL SOLUTIONS. User manual - rt3000 v3 and rt500 models, 2022.

[31] PAGE, Y., FAHRENKROG, F., FIORENTINO, A., GWEHENBERGER, J., HELMER, T., LINDMAN, M., OP DEN CAMP, O., VAN ROOIJ, L., PUCH, S., FRÄNZLE, M., SANDER, U., AND WIMMER, P. A Comprehensive and Harmonized Method for Assessing the Effectiveness of Advanced Driver Assistance Systems by Virtual Simulation: The P.E.A.R.S. Initiative. In *The 24th ESV Conference Proceedings* (2015), NHTSA.

[32] QGIS DEVELOPMENT TEAM. Qgis geographic information system, 2022.

[33] RAUCH, H. E., TUNG, F., AND STRIEBEL, C. T. Maximum likelihood estimates of linear dynamic systems. *AIAA Journal 3*, 8 (1965), 1445–1450.

[34] REDMON, J., AND FARHADI, A. Yolo9000: Better, faster, stronger. In *2017 IEEE Conference on Computer Vision and Pattern Recognition (CVPR)* (2017), pp. 6517–6525.

[35] REICHENBÄCHER, C., RASCH, M., KAYATAS, Z., WIRTHMÜLLER, F., HIPP, J., DANG, T., AND BRINGMANN, O. Identifying scenarios in field data to enable validation of highly automated driving systems. In *Proceedings of the 8th International Conference on Vehicle Technology and Intelligent Transport Systems* (2022), SCITEPRESS - Science and Technology Publications.

[36] RICHARDSON, A., STROM, J., AND OLSON, E. AprilCal: Assisted and repeatable camera calibration. In *IROS* (2013).

[37] RISTANI, E., SOLERA, F., ZOU, R., CUCCHIARA, R., AND TOMASI, C. Performance Measures and a Dataset for Multi-Target, Multi-Camera Tracking. In *ECCV Workshop* (2016).

[38] ROSÉN, E., AND SANDER, U. Pedestrian fatality risk as a function of car impact speed. *Accident Analysis & Prevention 41*, 3 (2009), 536–542.

[39] SCHACHNER, M., SCHNEIDER, B., KLUG, C., AND SINZ, W. Extracting Quantitative Descriptions of Pedestrian Pre-crash Postures from Real-world AccidentVideos. In *2020 IRCOBI Conference Proceedings - International Research Council on the Biomechanics of Injury* (2020), IRCOBI, pp. 231–249.

[40] SCHACHNER, M., SINZ, W., THOMSON, R., AND KLUG, C. Development and evaluation of potential accident scenarios involving pedestrians and AEB-equipped vehicles to demonstrate the efficiency of an enhanced open-source simulation framework. *Accident Analysis & Prevention 148* (2020).

[41] SCHLAGER, B., MUCKENHUBER, S., SCHMIDT, S., HOLZER, H., ROTT, R., MAIER, F. M., SAAD, K., KIRCHENGAST, M., STETTINGER, G., WATZENIG, D., AND RUEBSAM, J. State-of-the-art sensor models for virtual testing of advanced driver assistance systems/autonomous driving functions. *SAE International Journal of Connected and Automated Vehicles 3*, 3 (oct 2020), 233–261.

[42] SCHWEBEL, D. C., STAVRINOS, D., BYINGTON, K. W., DAVIS, T., O'NEAL, E. E., AND DE JONG, D. Distraction and pedestrian safety: How talking on the phone, texting, and listening to music impact crossing the street. *Accident Analysis & Prevention 45* (mar 2012), 266–271.

[43] SEKACHEV, B., MANOVICH, N., ZHILTSOV, M., ZHAVORONKOV, A., KALININ, D., HOFF, B., TOSMANOV, KRUCHININ, D., ZANKEVICH, A., DMITRIYSIDNEV, MARKELOV, M., JOHANNES222, CHENUET, M., A ANDRE, TELENACHOS, MELNIKOV, A., KIM, J., ILOUZ, L., GLAZOV, N., PRIYA4607, TEHRANI, R., JEONG, S., SKUBRIEV, V., YONEKURA, S., VUGIA TRUONG, ZLIANG7, LIZHMING, AND TRUONG, T. opencv/cvat: v1.1.0, 2020.

[44] SEONG, S., SONG, J., YOON, D., KIM, J., AND CHOI, J. Determination of vehicle trajectory through optimization of vehicle bounding boxes using a convolutional neural network. *Sensors 19*, 19 (2019), 4263.

[45] SUN, P., KRETZSCHMAR, H., DOTIWALLA, X., CHOUARD, A., PATNAIK, V., TSUI, P., GUO, J., ZHOU, Y., CHAI, Y., CAINE, B., ET AL. Scalability in perception for autonomous driving: Waymo open dataset. In *Proceedings of the IEEE/CVF Conference on Computer Vision and Pattern Recognition* (2020), pp. 2446–2454.

[46] TAO, Y., BOTH, A., SILVEIRA, R. I., BUCHIN, K., SIJBEN, S., PURVES, R. S., LAUBE, P., PENG, D., TOOHEY, K., AND DUCKHAM, M. A comparative analysis of trajectory similarity measures. *GIScience & Remote Sensing 58*, 5 (2021), 643–669.

[47] WANG, L., VOGT, T., DOBBERSTEIN, J., BAKKER, J., JUNG, O., HELMER, T., AND KATES, R. Multi-functional open-source simulation platform for development and functional validation of adas and automated driving. In *Fahrerassistenzsysteme 2016*. Springer, 2018, pp. 135–148.

[48] WOJKE, N., BEWLEY, A., AND PAULUS, D. Simple online and realtime tracking with a deep association metric. In *2017 IEEE International Conference on Image Processing (ICIP)* (2017), pp. 3645–3649.

[49] YANG, D., LI, L., REDMILL, K., AND ÖZGÜNER, U. Top-view Trajectories: A Pedestrian Dataset of Vehicle-Crowd Interaction from Controlled Experiments and Crowded Campus. In *2019 IEEE Intelligent Vehicles Symposium (IV)* (2019), pp. 899–904.

[50] ZHAN, W., SUN, L., WANG, D., SHI, H., CLAUSSE, A., NAUMANN, M., KÜMMERLE, J., KÖNIGSHOF, H., STILLER, C., DE LA FORTELLE, A., AND TOMIZUKA, M. INTERACTION Dataset: An INTERnational, Adversarial and Cooperative moTION Dataset in Interactive Driving Scenarios with Semantic Maps. *arXiv:1910.03088 [cs, eess]* (2019).

[51] ZHOU, K., YANG, Y., CAVALLARO, A., AND XIANG, T. Omni-scale feature learning for person re-identification. In *2019 IEEE/CVF International Conference on Computer Vision (ICCV)* (2019), pp. 3701–3711.

IN-DEPTH ACCIDENT STUDY ON D-CALL NET VEHICLES
BY MEDICAL ENGINEERING COLLABORATION

Toru Kiuchi

Institute for Traffic Accident Research and Data Analysis

Ayumi Shinohara

Ministry of Land, Infrastructure, Transport and Tourism

Hirotoshi Ishikawa

Helicopter Emergency Medical Service Network

Japan

ABSTRACT

D-Call Net, which Japan was the first country in the world to implement for practical use, is an extremely unique advanced automatic collision notification system in which a helicopter emergency medical service (HEMS) with a doctor and a nurse on board is requested by a vehicle involved in a collision. Six years have passed since the start of a pilot operation and four years since the start of a commercial operation, and more than twenty cases have been reported in which D-Call Net has activated HEMS and transported drivers or passengers to trauma centers. Since 2018, the Ministry of Economy, Trade and Industry (METI) has been supporting the international standardization activities of the injury estimation algorithm used in D-Call Net. Based on the newly established Japanese Industrial Standard (JIS) D0889 [1], ISO standardization activities are continuing to develop the technical specification under ISO TC22/SC36/WG7.

On the other hand, from FY2021, the Ministry of Land, Infrastructure, Transport and Tourism initiated the "D-Call Net In-Depth Accident Study" in which experts in emergency medicine and automotive engineering collaborate to establish an accident database for developing safer vehicles, replacing the previous "Medical Engineering Collaborative In-Depth Accident Study".

Institute for Traffic Accident Research and Data Analysis (ITARDA) has been in charge of both ISO standardization activities and the accident studies. This paper provides an executive summary of ITARDA's D-Call Net In-Depth Accident Study for FY2021. A total of twenty-one collisions were investigated during the study period, and several characteristic collisions were selected and detailed among them. The consideration of ΔV recorded by EDR, the time saving effect of D-Call Net and the evaluation of the algorithm according to the ISO technical specification are also discussed.

INTRODCTION

In Japan, the Automatic Collision Notification system, HELPNET, had been in service since 2000, automatically transmitting the collision location and other information to the Answering Point in the event of a collision such as airbag deployment, and transferring the information to Fire Head-quarters for prompt EMS activities.

The newly developed D-Call Net was a further enhancement of HELPNET, and its additional functions included automatic transmission of vehicle information such as severity and direction of collision, belt use and others to the Answering Point, as well as collision location. The system also uses the algorithm [2, 3] to estimate the probability of fatal or serious injury to the driver and front passenger. The estimated results are transmitted in real-time to the trauma center with HEMS, enabling an early decision to dispatch a helicopter or a rapid car, and significantly shortening the time until the start of treatment by a medical doctor. (See Figure 1)
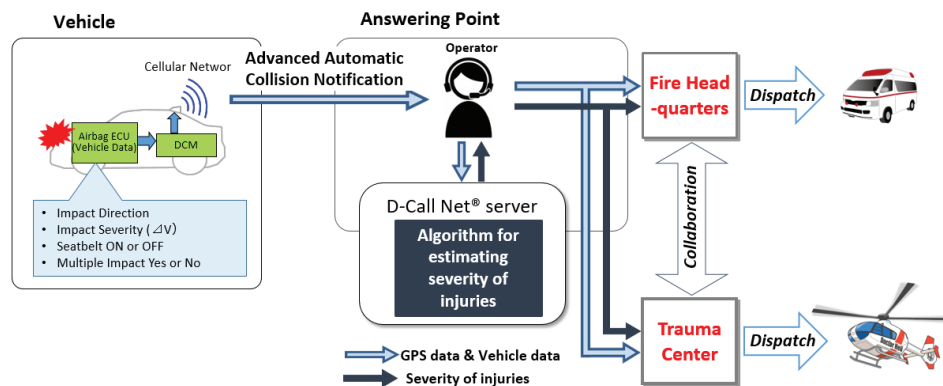
Figure 1. Outline of D-Call Net

In November 2015, Toyota Motor Corporation and Honda Motor Corporation together with HEM-Net had started a pilot operation of D-Call Net, and commercial operation had begun in April 2018 [4]. Subsequently, in 2019, Nissan Motor Corporation and Mazda Motor Corporation began selling vehicles equipped with D-Call Net, and in 2020, Subaru Corporation also began selling vehicles equipped with D-Call Net. In HEMS, a medical doctor and a nurse are trying to shorten the contact time with traffic accident victims with a strong desire to save lives.

ITARDA had been conducting the "Medical Engineering Collaborative In-Depth Accident Study" for vehicle safety as a research commissioned by MLIT, in order to obtain basic data for vehicle safety measures. The study was conducted by setting up a "Study Group for Detailed Investigation and Analysis of Traffic Accidents by Medical Engineering Collaboration" consisting of academic experts, medical professionals, researchers from traffic safety-related research institutes and engineers from vehicle manufacturers. The committee members could access the accident data. Some members wished to make free use of the accident data, but such free use was never approved because accident data was specific information under the Road Traffic Law. As a consequent, this committee closed its activities in FY2020.

On the other hand, the injury estimation algorithm used in D-Call Net had been registered as JIS D0889, and its evaluation was ongoing, but the number of accident cases to compare the estimated injury level with the actual injury level has never been sufficient. Therefore, in place of the medical and engineering collaborating in-depth accident study by FY2020, a new research project had been initiated to establish the all-Japan investigating structure and to accumulate accident data as a database, in cooperation with automobile manufacturers that produce vehicles equipped with D-Call Net.

At previous ESV conferences, Toyota Motor Corporation had made presentations on D-Call Net [5, 6], but this time, ITARDA introduces the recent study in all-Japan collaboration.

METHOD

Joint Research Consortium

The objective of this study is to prepare basic data for the investigation and collection of D-Call Net accident cases for continuous evaluation on D-Call Net effectiveness and operations, as well as to establish accident database in cooperation with medical and engineering. Although there had been no collaboration with MLIT for the previous study [7], MLIT proposed the establishment of a "Joint Research Consortium" centered on ITARDA in which MLIT would support the research and all manufacturers of vehicles equipped with D-Call Net would provide information of collision notification to ITARDA to establish the accident database. (See Figure 2)
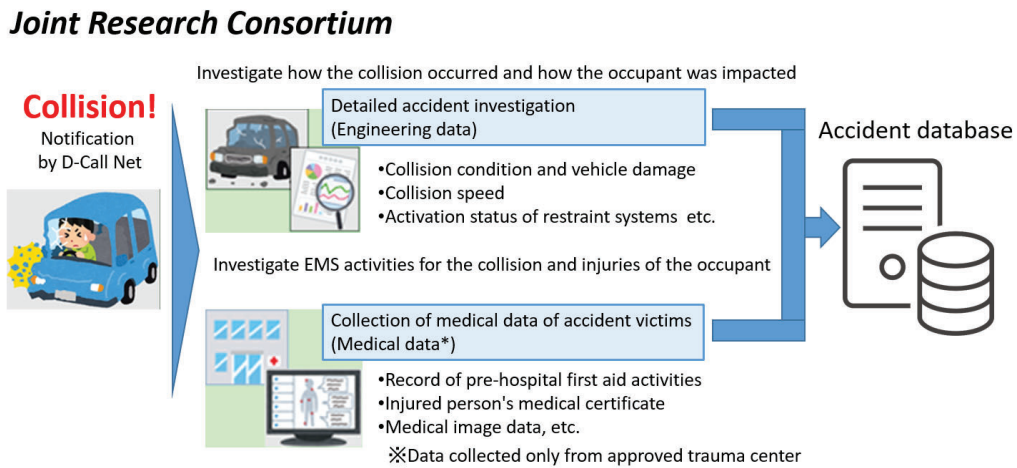
Figure 2. MLIT's medical and engineering collaborated accident database

The structure of the whole joint research is shown below, and the number of HEMSs subject to this research was sixty-one trauma centers and fifty-three helicopters in forty-four prefectures, as of the end of July 2022. Five manufacturers that currently provide vehicles with D-Call Net and National Research Institute of Police Science (NRIPS) were also participating in the joint research. (See Figure 3)
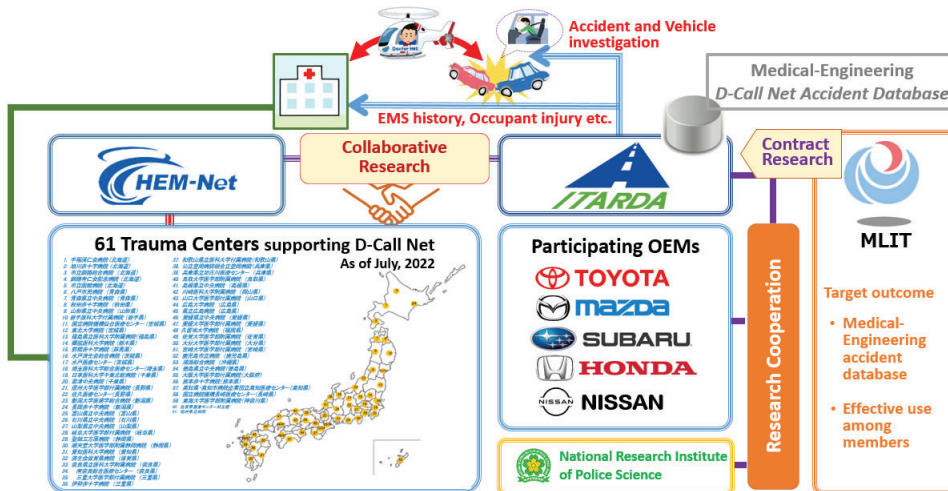
Figure 3. ITARDA's collaborative research project in all-Japan

Procedure of D-Call Net Accident Investigation

The basic premise of the in-depth accident study conducted by ITARDA is to obtain consent from the parties (often drivers) involved in a traffic accident before starting the in-depth investigation. Therefore, in the D-Call Net study as well, it is a prerequisite to obtain consent from the drivers of vehicles equipped with the D-Call Net and other related parties. Since collisions involving D-Call Net-equipped vehicles occur nationwide in Japan, coordination with the National Police Agency (NPA) and prefectural police headquarters was essential in order to obtain information on the subject accident cases. When ITARDA is notified of the occurrence of D-Call Net case, ITARDA informs the date, time, and location to NPA. NPA provided ITARDA with the contact information of the police headquarters in the relevant prefecture. Based on this information, ITARDA contacts the police headquarter with the jurisdiction, explains the circumstances of the accident investigation and obtains information on the driver involved in the collision from the police officer in charge of the case. ITARDA then contacts the driver directly and obtains his consent to the in-depth accident investigation.

RESULTS

Overview of Accident Cases Investigated

In the first year's joint research on D-Call Net accident investigations, the results of twenty-one cases that occurred from January to December, 2021 were investigated with the consent of the drivers involved, including cases in which HEMS or Rapid Car was dispatched, are summarized below.
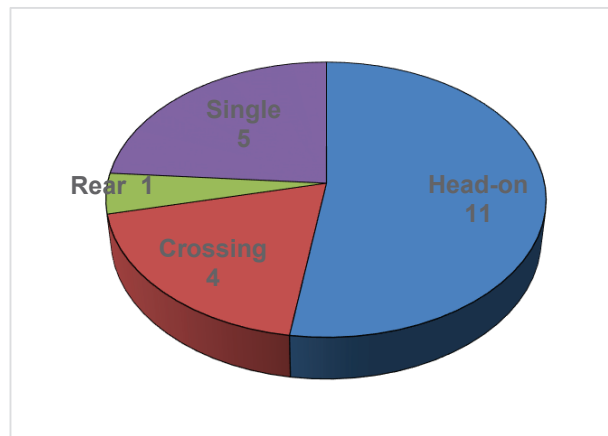
Figure 4. Collision types of 21 D-Call Net accidents investigated.

The distribution of collision types for the twenty-one vehicles equipped with D-Call Net was shown. Among them, eleven vehicles were head-on collisions, four were crossing collisions, and one was a rear-end collision with the other vehicle. In addition, there were five single vehicle collisions, mostly frontal collisions. (See Figure 4)

The plots of "delta V" versus "Predicted injury probabilities" for 24 occupants (twenty-one drivers and three front passengers) on the twenty-one vehicles were shown. Each plot was classified by the actual level of injury revealed by investigations, such as Severe, Minor or No injury and Unknown, as color-coded. (See Figure 5)
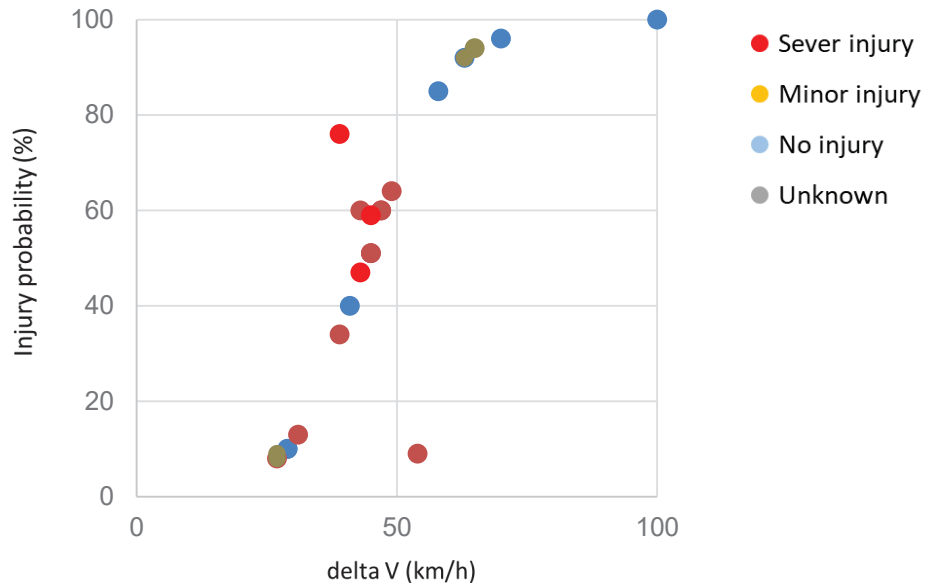
Figure 5. Injury outcomes of twenty-four occupants

Representative Examples of Distinctive Cases
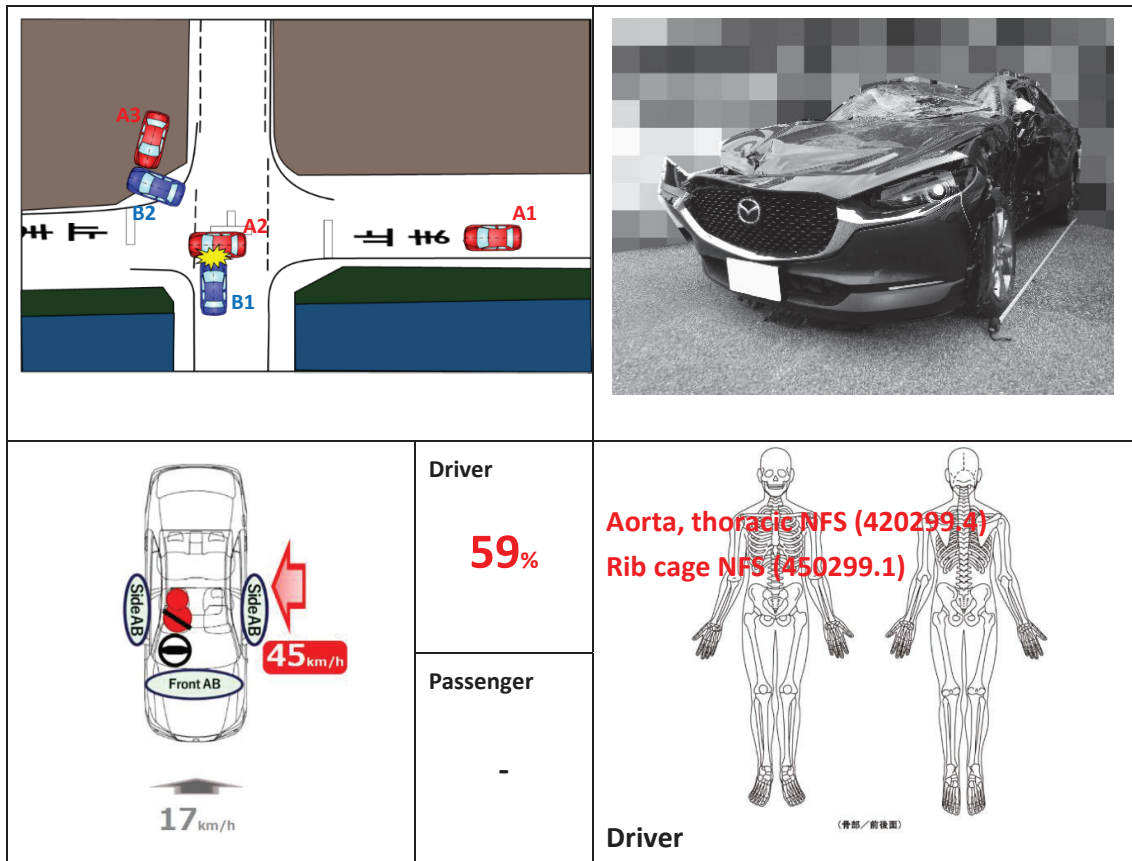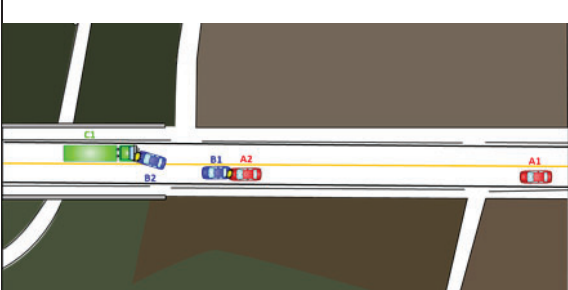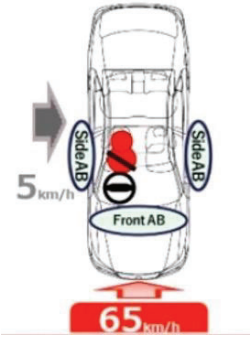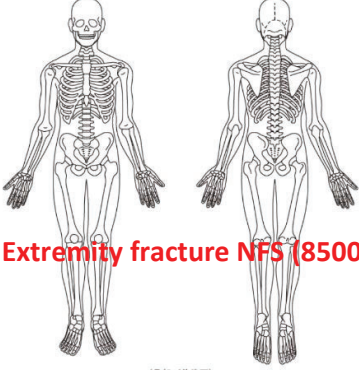
Figure 6. Accident summary of Case No. 1

This collision occurred in Shiga prefecture in the morning. A passenger car "A" was traveling on a single road along a canal. When it entered an intersection with a stop sign without stopping, it collided with a passenger car "B" proceeding from the left side of the crossing road and finally caused rollover off the road. The fatal or severe injury probability was 59%, and HEMS was activated. As the driver's severe injury was estimated, the actual driver's injuries were traumatic aortic rupture (420299.4) and rib fracture (450299.1) according to medical information provided by the trauma center [8]. In spite of far-side impact to passenger's side, a large deformation was observed on the door of driver's side, which may have been caused by a secondary impact with a guardrail at the intersection. Furthermore, the roof was also severely deformed due to rollover, and not enough survival space for the driver was secured. During both side impacts and roll over, the driver sustained serious chest injuries.

In this case, the early start of treatment by HEMS was effective, however it took 25 minutes from the time the trauma center became aware of the collision until the HEMS took off. Then, the time-saving effect of the D-Call Net could not be confirmed. Since no information was provided by the trauma center, the cause of this delay until take-off remained unclear, but the HEMS was most likely requested by the EMS team after arrival at the scene. For HEMS activated cases, it is important to improve collaboration between trauma centers and ITARDA so that they can provide information not only on the time lapse but also on the circumstances of the incident.

CASE No.2: Severe frontal impact   Rapid car was dispatched by D-Call Net

	Driver	
	94%	Lower Extremity fracture NFS (850099.9)
	Passenger	
	-	**Driver** (carried to another Trauma Center)

Figure 7. Accident summary of Case No. 2

This collisions occurred in Chiba prefecture at night. A compact passenger car "B" equipped with D-Call Net was proceeding on a road with one lane in each direction, and was waiting for oncoming vehicles to pass in order to turn right into an off-road facility. A following standard freight vehicle "A" collided against the rear of the car "B". As the result, it was pushed forward and moved into the oncoming lane, where it collided head-on with a large freight vehicle "C", proceeding straight ahead in the opposite direction. The predicted fatal or severe injury probability was as high as 94%. Because it was beyond the time period for HEMS operations, the Rapid Car (doctor car) was dispatched instead.

On the car "B", there were two occupants with seatbelt in rear seats, and they sustained severe injuries and were transported to the trauma center. Both of them sustained serious injuries to the abdomen and lumbar spine, but the causes of those injuries were most likely the seat belt (lap belt area). Another factor that may have contributed to their injuries was the fact that the car "B" was collided rear-ended by the vehicle "A" first and their upper bodies were tilted backward and that it collided head-on by the vehicle "C" shortly after the first impact. The occupant on the left rear seat suffered a head injury from the secondary impact against the front seat back resulted in a less severe lumbar spine injury than the occupant on the right. (See Figure 8)

Figure 8. Deformation of other vehicles

Case No.3: Severe front impact against object
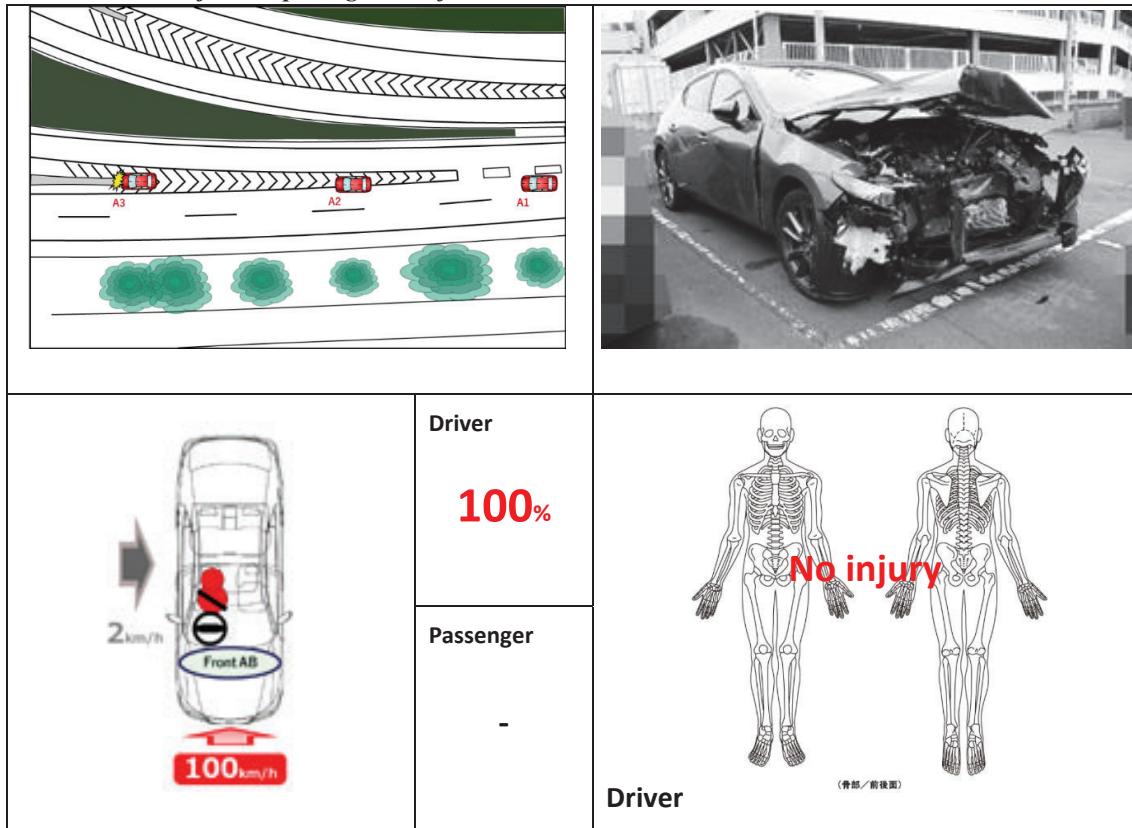
Figure 9. Accident summary of Case No. 3

This collision occurred at a junction of expressway in Tochigi prefecture late at night. The probability of fatal or severe injury of the driver was 100%, but no HEMS was activated because of the unavailability of night flights. An in-depth accident investigation was conducted with the driver's consent and the results revealed that it was an extremely rare case in which the driver was uninjured, regardless of the 100% probability of fatal or serious injury. Although there have been many over triage cases in the past investigations, this was the first case in which the driver was uninjured even at 100% probability. Hence, it is also addressed in this paper.

The investigation of the accident site revealed that the vehicle "A" collided head-on with a crash-impact absorber located at the junction of the main line and the off-ramp on the expressway, and the driver was presumed to have been uninjured because the structure effectively absorbed the vehicle impact energy, the cabin deformation was minimal and the restraint system was functioning, etc. The deformed absorber at this accident spot and a similar crash impact absorber without deformation are shown below (See Figure 10).

Observation of the vehicle involved in the accident revealed that the passenger compartment remained intact, and there was no significant setback of the steering wheel. In addition, the driver's airbag and knee airbag also deployed and all restraint systems functioned as intended. These facts were believed to have contributed to the driver's non-injury.

Deformed absorber at accident spot

Undeformed absorber elsewhere

Figure 10. Deformed and Undeformed absorber

DISCUSSION

Regarding the second case, the HEMS base trauma center provided a timeline of EMS events (See Table 1). The fact that the rapid car was dispatched prior to the arrival of the EMS ambulance at the accident spot indicated that the rapid car was activated by D-Call Net alert only, not by the on-scene request from the EMS team. A time saving effect of twenty-two minutes was confirmed. Then, this is a typical case in which the D-Call Net functioned effectively to activate the rapid car.

The driver of the car "B" was transported to another trauma center (detailed injury information was not obtained), and the two rear seat passengers of the car "B" were transported by ambulances to the trauma center. If the helicopter had been able to fly at night, one of the two seriously injured rear seat passengers would have been transported by HEMS and fundamental treatment could be initiated early. Nighttime flight of HEMS is considered to be one of the future issues.

Table 1.

Time lapse of the emergency medical event
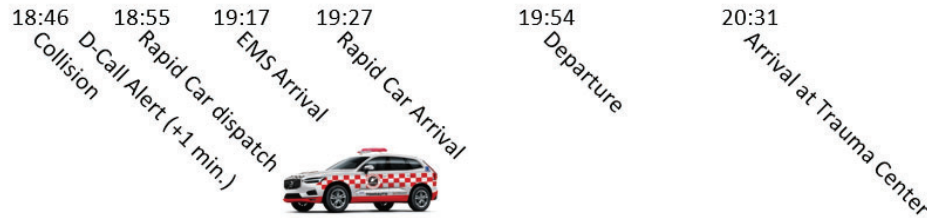
Using the validating methodology with reference to ISO DTS 4654 (Road vehicles – Advanced automatic collision notification (AACN) systems – Methodology for creating and validating algorithms for injury level prediction) which is still in development at the task force under ISO TC22/SC36/WG 7 (Traffic accident analysis methodology), the evaluation of the injury prediction algorithm used for D-Call Net was carried out. Seventeen drivers and three front passengers had their actual injury levels in this study, except for four unknowns. The "Confusion Matrix" proposed by ISO DTS 4654 is shown. (See Table 2)

Table 2.

Confusion Matrix for the prediction in this study

		Estimated injury level	
		Fatal or Sever (+)	Minor or No (-)
Actual injury level	Fatal or Sever (+)	**True Positive 3**	False Negative 0 (Under triage)
	Minor or No (-)	False Positive 17 (Over triage)	True Negative 0

- In case of normalization against actual classes,

$$OTR = FP / (FP + TN) \qquad \text{Equation (1)}$$

Then, OTR = 1.0

- In case of normalization against predicted classes,

$$OTR = FP / (FP + TP) \qquad \text{Equation (2)}$$

Then, OTR = 0.85

There is no "True Negative" case in the table. D-Call Net vehicle manufacturers participating in this joint research tend to provide ITARDA with information on collisions with high injury probabilities. Then, the bias of the sampling to focus on cases where HEMS might be dispatched resulted that there is no case predicted minor or no injury. During this study period, the threshold of predicting fatal or severe injury provability was 5% or more. All cases investigated by ITARDA had probabilities from 8% to 100%. Therefore, no "True Negative" case was investigated. Separating this in-depth study, manufacturers are strongly expected to accumulate and analyze all D-Call Net notifications that ITARDA is not able to know about.

An Event Data Recorder of the investigated vehicle with D-Call Net was often retrieved. The EDR of the third case vehicle was also retrieved. The vehicle speed at time of collision was 128 km/h and the maximum delta V was -140 km/h. According to the wave form of the delta V values decreased almost linearly and the values at time of 200 msec. was recorded as -110 km/h and at time of 250 msec. as -132 km/h, unfortunately, the waveform itself was not allowed to be included in the paper.

The delta V received at the answering point was 100 km/h and fatal or severe injury provability was calculated as 100 %. The driver experienced the deceleration as around 15 Gs during the collision against an absorbing structure for over 250 msec. The restraint system was activated properly and the driver was not injured at any body region. In this case, the algorithm used by D-Call Net itself never failed to predict injury probability. Regarding delta V value, the condition experienced by the driver was statistically resulted fatal or severe injury. About 50 % over triage rate is approved in D-Call Net and this case should be one example of the unique over triage case.

At present, very few trauma centers activate their HEMS based on D-Call Net alert only. Therefore, there is a desire to broaden the scheme of immediate dispatch by D-Call Net alert only. However, ITARDA's longstanding experiences from D-Call Net accident investigations suggest that deep consideration might be required for it.

CONCLUSION

From FY2021, ITARDA carried out the joint research commissioned by MLIT, which was started in place of the previous in-depth accident investigation by medical-engineering collaboration. The objectives of this joint research was to evaluate the D-Call Net effectiveness, system itself and operations, and to investigate and collect D-Call Net accident cases in cooperation with vehicle manufacturers and trauma centers with HEMS.

In the first year, in cooperation with the Japan Automobile Manufacturers Association (JAMA), we concluded agreements with all manufacturers of vehicles equipped with D-Call Net such as Toyota Motor Corporation, Mazda Motor Corporation, Subaru Corporation, Honda Motor Corporation and Nissan Motor Corporation. The all-Japan D-Call Net in-depth accident investigation structure had made it possible to receive a large amount of alert information. With the support of NPA, each information was referred to prefectural police headquarters, and with the consent of the drivers involved, twenty-one in-depth accident investigations were completed.

The twenty-one drivers and three front seat passengers on the twenty-one vehicles were examined, comparing predicted injury probabilities and actual injury outcomes. The results were: three True Positive cases, No "True Negative" case, seventeen "False Positive" (Over Triage) cases, and no "False Negative" case. The absence of "True Negative" and "False Negative" cases is due to the fact that accident cases estimated to be less than 5% were not investigated in this study.

FUTURE ISSUES

In order to understand the time-saving effect of D-Call Net, it is essential to know the time lapse of the emergency medical events in each case, as the second case. Currently, however, only a limited number of cooperating trauma center with HEMS were able to provide the time lapse information to ITARDA.

To solve this problem, ITARDA, in cooperation with HEM-Net, proposed the additional tag for D-Call Net cases to the HEMS registry at the 28th Annual Meeting of Japanese Society for Aeromedical Services held in Kumamoto, and is currently coordinating with the registry secretariat. ITARDA plans to start providing support to the registry office for the tagging in the next fiscal year. In addition, ITARDA plans to establish a joint research with some trauma centers, subject to approval by the trauma center's ethical committee, for the purpose of providing various types of information when dispatching its HEMS.

REFERENCES

[1] Japan Industrial Standard JIS D0889 2020

[2] Tominaga S, Nishimoto T, Motomura U, Matsumoto H, Lubbe N, Kiuchi T. 2014 "Injury Prediction Algorithm for AACN based Japanese Road Accident Data" JSAE Annual Autumn Congress 20145822

[3] Nishimoto, T. 2017. "Serious injury prediction algorithm based on large-scale data and under-triage control." Accident Analysis and Prevention, 98, 266-276

[4] Toyota Motor Corporation Global Newsroom. 2018. "Advanced Automatic Collision Notification Service, D-Call Net, Expanded Nationwide." (https://newsroom.toyota.co.jp/en/corporate/22961893.html)

[5] Kiuchi, T., Motomura, T., et al. 2015. "Pilot study on advanced automatic collision notification and helicopter

emergency medical service system in japan" 24th ESV Conference Proceedings 15-0415

[6] Miyoshi, T., Nishimoto, T. et al. 2019 "Evaluation of threshold used by advanced automatic collision notification system for dispatching doctors to accident sites" 26th ESV Conference Proceedings 19-00179

[7] Kiuchi, T., Ishikawa, H., et al. 2018 "Study on D-Call Net accident cases for the pilot study using in-depth investigation." JSAE Annual Spring Congress 20185251

[8] Gennarelli, T., et al. 2005 "Abbreviated Injury Scale" Association for the Advancement of Automotive Medicine

THE CREATION AND APPLICATION OF HARMONIZED PRE-CRASH SCENARIOS FROM GLOBAL TRAFFIC ACCIDENT DATA

Henrik Liers
Marcus Petzold
Institute for Traffic Accident Research at Dresden University of Technology (VUFO)
Germany

Harald Feifel
Germany

Jörg Bakker
Asymptotic AI
Sweden

Ernst Tomasch
Graz University of Technology
Austria

ABSTRACT

The development and test of future Advanced Driver Assistance Systems (ADAS) and Autonomous Driving (AD) AD functions requires sophisticated data from pre-crash scenarios. As real-world traffic provides an infinite variety of scenarios and vehicles are usually sold in many markets, valuable simulation datasets from several countries seem indispensable. The paper describes how we combined the format of the Pre-Crash Matrix (PCM) with global accident data from IGLAD. The goal was to create harmonized pre-crash simulation files from real accidents coming from several countries/continents and to use them exemplarily within a field-of-view analysis for future ADAS.

The basic data source is the IGLAD database. Within the "Initiative for the Global Harmonization of Accident Data" (IGLAD) traffic safety researchers from Europe, North America, South America, Asia, and Australia bring together road accident data in a harmonized dataset. Each single accident is reconstructed and contains relevant information like vehicle data, injury severities, anthropometric data, and scaled sketches.

The PCM format describes the vehicle dynamics (trajectories) in a defined time before the collision. It is similar to the OpenX formats and contains relevant information about the road layout, markings, view obstacles, etc.

The paper describes the process of creating IGLAD-PCM data, including the establishment of requirements, the harmonization of country-specific characteristics, and the definition of quality features.

In 2022, IGLAD-PCM was released for the first time providing 200 pre-crash simulations from real accidents coming from seven countries on three continents. The paper presents descriptive statistics (e.g. accident characteristics, accident configurations, injury severities) from these cases and a comparison to the current IGLAD dataset (with approximately 9,400 accidents from 10 different countries). We provide an overview of relevant accident situations and country-specific characteristics for different regions of the world, e.g. US, India, China, Germany, France, Italy, etc.

The paper also highlights the benefit of PCM data as one essential source for data-driven system development. During the concept definition of safety systems, pre-crash trajectory data is used to derive the required functional behavior. First, the relative positions and orientations of other traffic opponents are the basis for defining the necessary sensor field-of-view in given accident scenarios. Second, the speed distributions of ego and opponent serve as key performance indicators for the vehicle actuation system. Here, a relevant accident scenario is discussed, and relevant regional differences analyzed.

The IGLAD-PCM forms a unique global dataset of pre-crash simulations based on reconstructed traffic accidents. Of course, case numbers are quite low at this early stage, but will increase annually by more than 200. Using the data can enhance the development of ADAS and AD functions and help to adjust systems towards country-specific characteristics.

We have demonstrated that the PCM allows to harmonize pre-crash data from different countries and still can cover regional specifics. As the PCM is an open data format, various scenario descriptions can easily be generated, and existing development tool chains can be supported. Thus, we believe that the PCM can serve as a standard format for data-driven system development and simulation.

RESEARCH QUESTION / OBJECTIVE

More than 10 years after its initiation, the IGLAD project database has firmly established itself as an in-depth data source for accident research and vehicle safety applications. More than 9,400 accidents from five continents have now found their way into the database. They all share a uniform coding, harmonized between the data providers, as well as a quality standard. With the current data, it is already possible to perform descriptive analyses of accidents and injuries in various countries.

Current developments in the field of vehicle and road safety are focusing on the topics of connected and automated driving. This requires complex development, testing, and validation processes, which in turn require suitable input data. For ADAS and AD functions, accident and traffic scenarios play a decisive role. These scenarios are usually stored in open formats and are mostly created generically. Rarely do they originate from real accidents.

In this paper we have addressed the question whether it is possible to transfer the originally heterogeneous accident data of different data providers into a uniform, open and usable scenario format. For this purpose, different actors from the IGLAD consortium have joined forces to establish respective tool chains, processes, and data exports to transfer the pre-crash phases of IGLAD accidents into the PCM format. The main goal is to continuously provide pre-crash / scenario data from IGLAD in future project phases. Initially, this will be in PCM format, with OpenX formats also being considered later.

METHODS AND DATA SOURCES

The IGLAD project
Since the last report at the ESV conference 2017 (1) there have been numerous changes in the IGLAD project and improvements to the data set. This paper describes one of the major changes, the introduction of the IGLAD-PCM data. But before diving into this new feature we want to give a short general overview and update on the status of the IGLAD project.

IGLAD is an international in-depth accident data project and consortium that was initiated by Daimler AG, ACEA and different research institutes and announced as a working group at the FIA Mobility Group in October 2010 (2) (3) (4). The goal of the group was to define a common in-depth accident data standard and provide a yearly data set that is created from international partners that are part of the consortium. The non-profit project is completely self-funded and offers its data to interested parties to be used for research purposes charging a moderate membership fee. The data includes information that is common to most in-depth accident studies, like:

- accident time, description, type, influencing factors, …

- participant type, vehicle data, reconstruction data, …

- occupant age, weight, gender, injury severity, …

- safety system types, activation, …

The codebook of the common in-depth accident data scheme is freely available on the web page of the project (5). Besides the data tables, the IGLAD database also includes a scaled sketch for each accident in a common vector format.

The IGLAD consortium currently consists of 24 members complemented by the chair and administrator from Chalmers University and the SAFER Vehicle and Traffic Safety Centre at Chalmers (6) in Sweden. The project will celebrate its 10th yearly data release in June 2023. The currently released 9th data set includes 9,425 cases in total contributed by 14 data providers located in North America, South America, Europe, Asia, and Australia. The data originates from 12 different countries: Australia (AU), Austria (AT), Brazil (BR), China (CN), Czech Republic (CZ), France (FR), Germany (DE), India (IN), Italy (IT), USA (US), Spain (SP), and Sweden (SE). New countries, data providers, and members are expected to join the project in the near future. The goal is to cover as many regions/countries of the world as possible.

IGLAD dataset

In principle, the compiled IGLAD data set contains only accidents with personal injuries. Only in the pilot phase (Phase I) the data providers exceptionally were allowed to include accidents with property damage. These accidents now account for only 0.5% of the total IGLAD dataset. By contrast, the much larger proportion of accidents was initially biased toward serious and fatal accidents. This results from the fact that some data providers obtain their original data from accident reports, which are preferably commissioned only for severe and fatal accidents. Other data collections are primarily focused on fatality accidents. Over the various IGLAD phases, intensive work was therefore carried out to detect and successively eliminate possible system-inherent or random biases in the data sets (for further explanations, see chapter Representativeness).

Figure 1 shows the maximum injury severities of the accidents in the current IGLAD data set (Phase IV / 2021) per country. Also included are the numbers of cases, which differ between 50 and 1,800. The background of these strong differences is that some countries or data providers have only provided data once, while other countries have provided data continuously each year since the beginning.
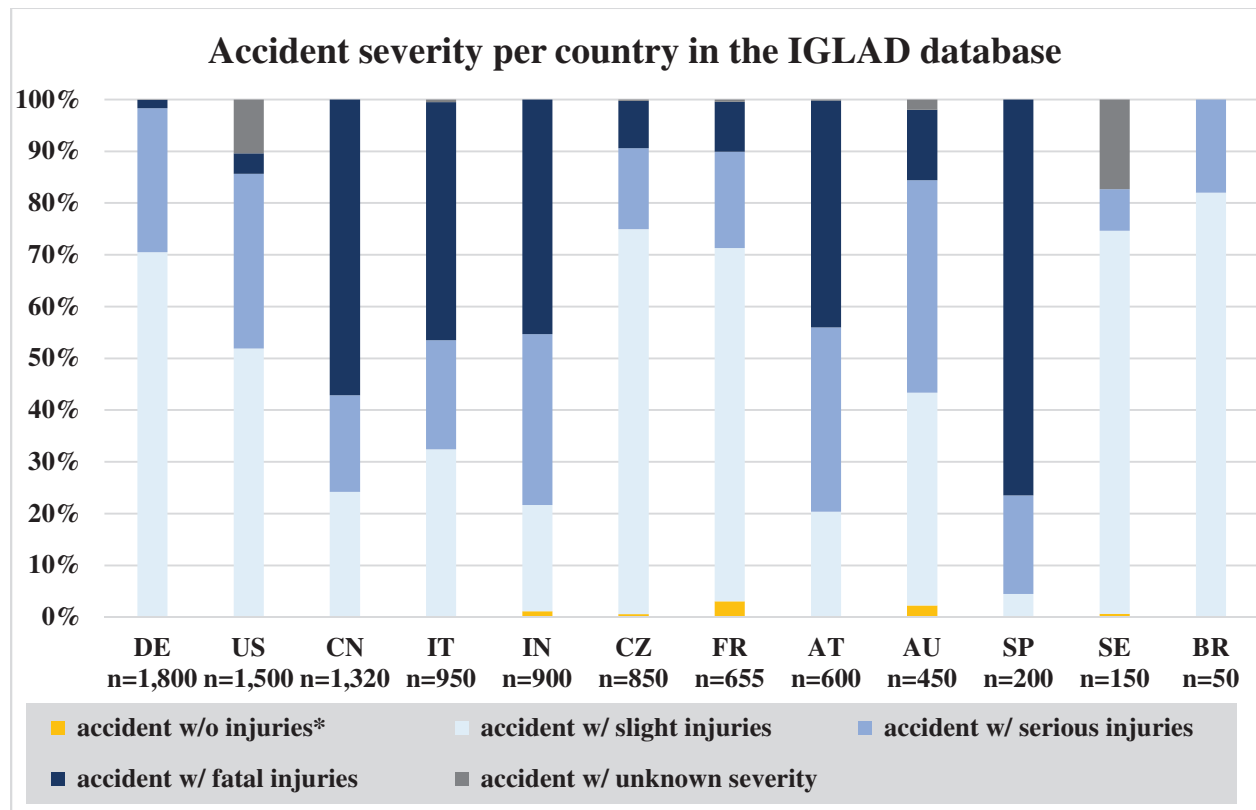
Figure 1. **Distribution of accident severity per country in the IGLAD database (Phase 4 / 2021).**

The diagram shows that among the regular data providers there are still some that deliver a comparatively high pro-portion of fatal accidents, e.g. China, Italy and India. On the other hand, many other data providers made some good progress and are now able to select accidents close to the national statistics to become representative gradually. A good example for this development is Austrian data, provided by TU Graz, see Figure 2.
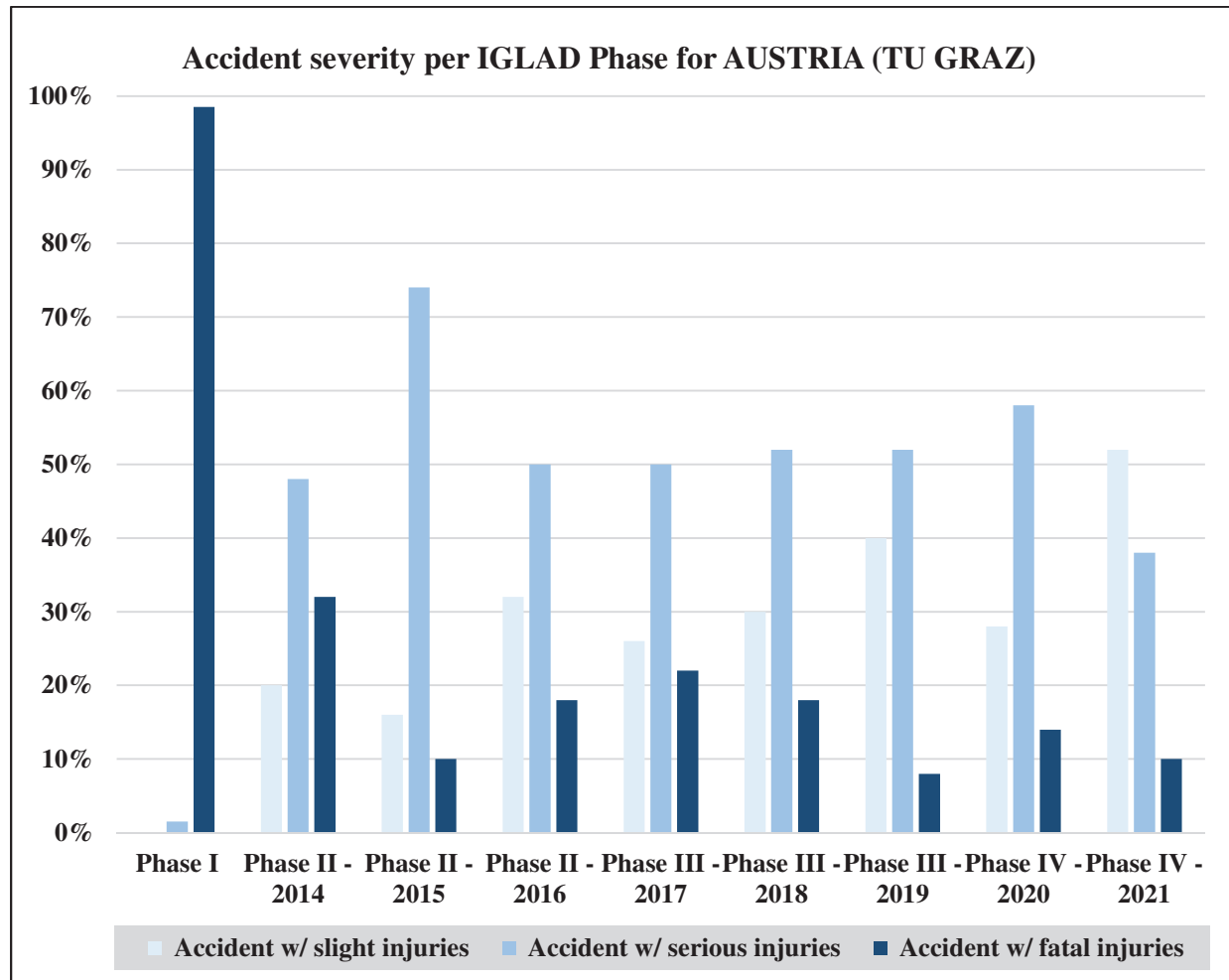
Figure 2. **Distribution of accident severity per IGLAD phase in Austrian cases (Data Provider: TU Graz).**

Although few data sources still have biases due to specific sampling criteria, the accidents in the IGLAD database cover all accident types and accident configurations. As an example, Figure 3 shows the distribution of main acci-dent types in the IGLAD cases per country. The main accident type describes the conflict/critical situation which resulted in the accident.

It can be seen that, although accident severities are quite different between many countries, the main accident types are rather similar, especially for countries in similar regions (e.g. Western Europe with AT, CZ, DE, FR, IT).
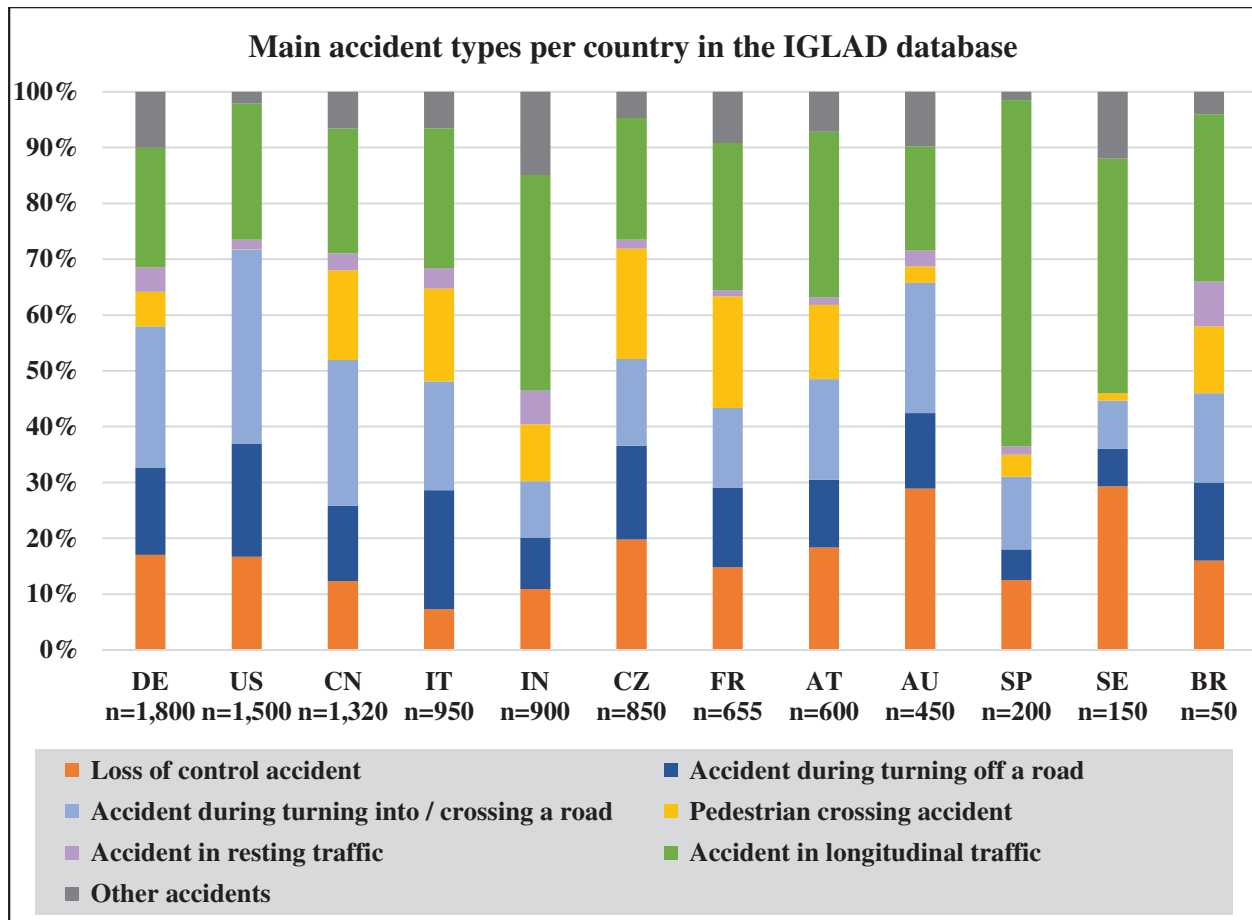
Figure 3. **Distribution of main accident types per country in the IGLAD database (Phase 4 / 2021).**

Representativeness

Even though most countries provide national statistics on road fatalities, injured road users, etc. no detailed data is given to collision characteristics, collision speeds, etc. (1) Thus, the basic idea of IGLAD was to establish an international in-depth database comprising more specific data from many countries as possible (1) (4). Due to the different investigation priorities or sampling criteria (e.g. focus on car accidents, vulnerable road users, fatalities, etc.) of the data providers, the data are possibly lacking of representativeness. However, there are only a few ways to compare data for representativeness such as global status report on road safety (7), annual statistics of the EU (8), or national statistics. Although the mode of transport is available in more detail (8) only few details are available in other documents (7) and these documents comprise fatal accidents only. Additional documents from national statistics might comprise more detailed data but are not available for everybody or written in the countries' language.

Bakker et al. (1) made an attempt to compare IGLAD data with national statistics. Data from IRTAD (International Traffic Safety Data and Analysis Group) were used (9). Unfortunately access to the IRTAD road safety database is limited to members and only selected variables for comparison. Thus, the main objective of the IGLAD Representativeness group was to provide a document available to every IGLAD member. A standardized template with specific variables was developed (Table 1) for the calculation of weighting factors of the IGLAD data for each participating country. Within a survey the data providers were asked if they could provide aggregated accident data of their national statistics or region. Finally, data from seven countries (AT, AU, CZ, DE, FR, IT, US) out of twelve are available. For the other countries no data were provided due to several reasons (time effort, resources, availability of actual data).

Table 1: Weighting variables

ACCIDENT LEVEL	CASUALTY LEVEL
Accident severity	*Age*
Month	*Gender*
Weekday	*Injury severity*
Time	*Participant type*
Road condition	
Road type	
Accident type	
Collision type	
Number of participants	

Not every single attribute of the variables in IGLAD corresponds to the attributes of the variables in the national statistics. Thus, the data provider had to aggregate either their attributes to the IGLAD attributes or the IGLAD attributes need aggregation to be comparable with national statistics. Most data providers could submit full cross tables for all variables distinguishing between minor, severe and fatal injuries for their countries. Some only could separate their data into fatal and non-fatal accidents but were able to provide these data for most of the variables requested. In Figure 4 a comparison of different age groups in IGLAD and the corresponding countries is given as an example how the data in the national statistics are represented in IGLAD. If both marks in the figure are superimposed, the data in IGLAD fully represents the national statistics.
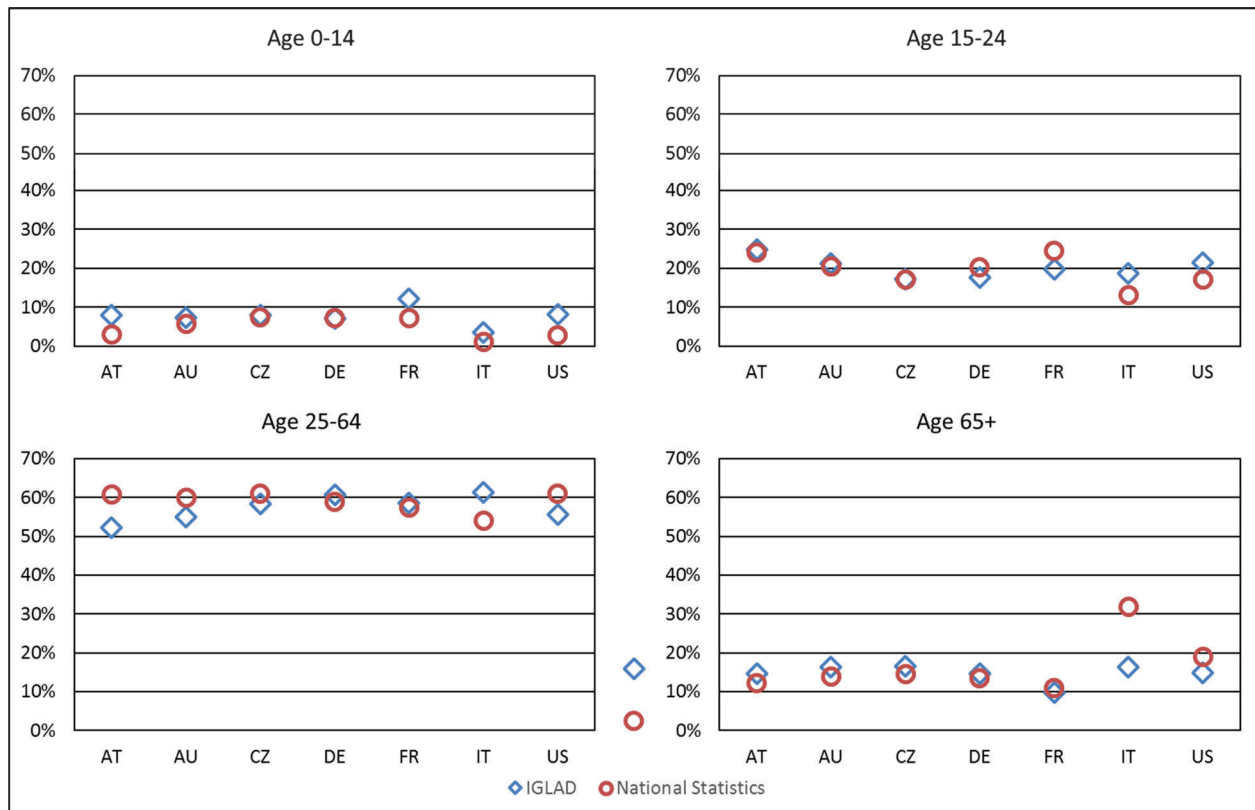
Figure 4. **Distribution of age groups in different countries in IGLAD compared to the national statistics.**

PCM (Pre-Crash-Matrix) Format

The sequence of accident events are often classified into three essential phases, the pre-crash phase, the in-crash phase and the post-crash phase. The vast majority of coded parameters in the IGLAD database is focusing on the in-crash phase (accident reconstruction) and passive safety aspects. However, for the evaluation of many safety systems or features the pre-crash phase is of particular interest. The assessment of the potential of sensor- or communication-based ADAS as well as AD functions can only be accomplished by a detailed analysis of the pre-crash phases of accidents (and incidents). Hence the necessity to analyze the early phase of accidents in detail arises.

Since its introduction in 2011, the Pre-Crash Matrix (PCM) format has offered the possibility to store and analyze information from the pre-crash phase of accidents (10). Until 2019, this format was not published and was used exclusively within the German In-Depth Accident Study (GIDAS) (11). Here, the time period of five seconds prior to the accident until the first collision (t0) was usually covered.

Since the revision and release of the format in 2019, there is also the possibility for any users to store and analyze data recordings of real driving situations (e.g. from Event Data Recorder (EDR), Naturalistic Driving Study (NDS), Field Operational Test (FOT), ...) in the format. The goal of the PCM format is to store accident and real driving data in a uniform, structured format in order to perform analyses and evaluations of time-dependent and driving dynamic variables. Furthermore, a detailed investigation of active safety systems has become possible.

The PCM format contains all relevant data to describe the pre-crash phase of an accident until the first collision. This includes the definition of the participants and their characteristics, the dynamic behavior of the participants as a time-series for at least five seconds prior to the accident, and the geometry of the traffic infrastructure. The following *Figure 5* shows the structure of the PCM format (12).
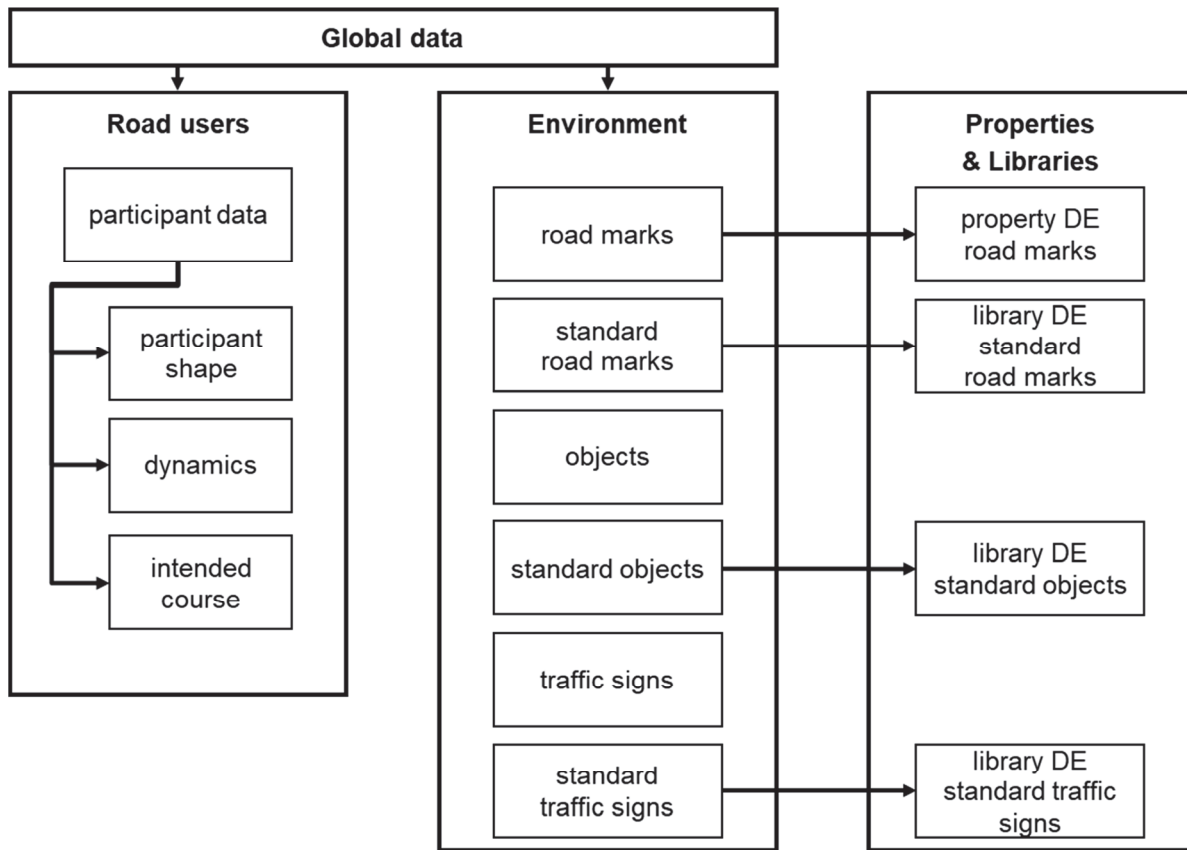
Figure 5. **Hierarchical structure of PCM (12).**

As can be seen in *Figure 5*, the PCM format consists of 15 different tables. These 15 tables can be roughly divided into the following categories: "Global data", "Road users", "Environment" and "Properties & Libraries". The table "Global data" provides general information of the accident / scenario, e.g. date and time and number of involved participants. The table "participant data" contains relevant variables to parameterize participants. This data can be used to model the geometry and further attributes. The table "participant shape" defines the geometrical shape for each participant by surfaces. Each surface contour is defined by points. Usually, simplified 2D/3D vehicle shapes are used within the PCM. Reducing the complexity of vehicle shapes increases the speed of simulation runs. However, it is also possible to realistically reproduce the vehicle contours in the PCM.

The table "dynamics" defines the global position of participants according to the global coordinate system as well as velocity and acceleration of the participants center of gravity (COG) according to the local COS at each time step of the simulation. The table "intended course" defines the course the participant initially intended to follow.

In the category "Environment" there are two basic approaches for defining objects. On the one hand, there are tables where information can be individually formatted (road marks, objects, traffic signs) and on the other hand tables which refer to a library (standard road marks, standard objects, standard traffic signs). The advantage of standard tables with the corresponding libraries is that they are defined only once and can be used for multiple cases, which saves storage space in the database. The PCM specification, explanations, and an example case can be found on the website of VUFO. (11)

Figure 6 shows an example visualization of a scenario in PCM format with Matlab.
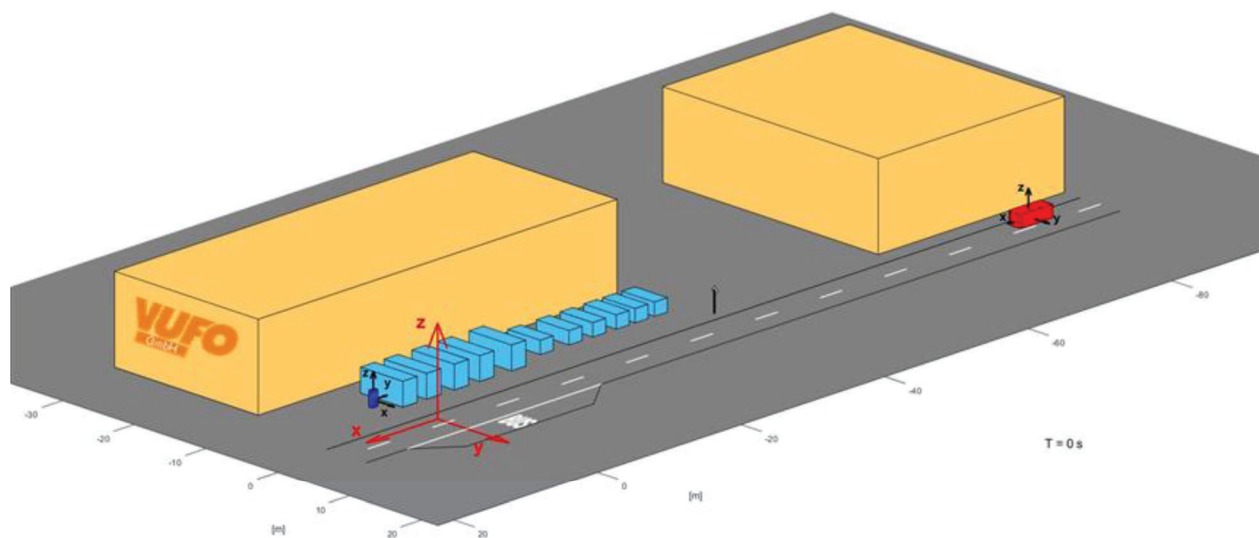
Figure 6. **Example visualization of a scenario in PCM format.**

With the PCM format, extensive user and application possibilities are thus available. In addition, it is freely available and independent of the data type. The simple structure allows easy access and understanding. However, two limitations of the PCM format specification should also be noted. Firstly, the environment has no logical information or metadata. This means that a participant has, for example, no direct information of the lane on which it is currently located. In addition, there is only one possibility of maneuver definition. In PCM format, all participants are defined by time-dependent trajectories of their center of gravity.

In order to visualize the data from the PCM format and also to perform a case by case analysis of quality as part of the creation of the IGLAD-PCM, VUFO has developed a PCM Viewer, which is shown in Figure 7.
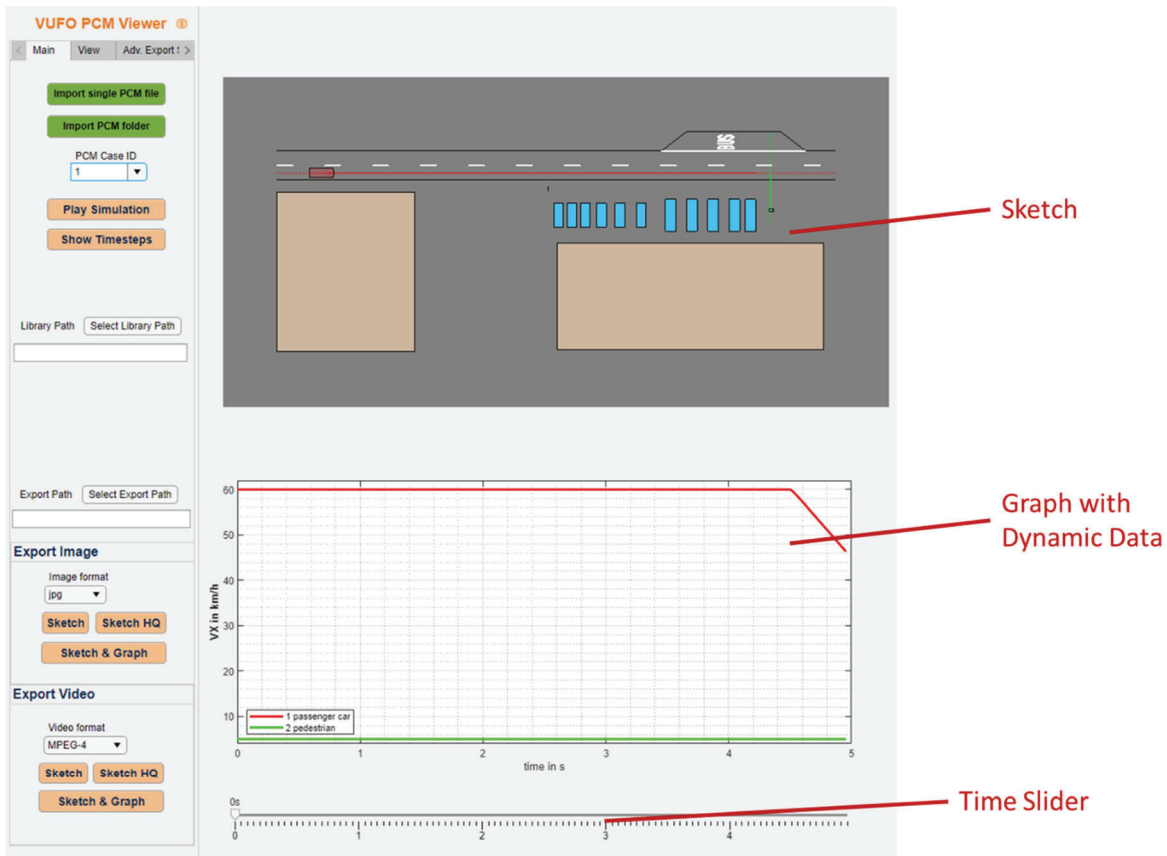
Figure 7. **GUI of PCM Viewer.**

The PCM Viewer GUI is separated in two areas, the "tabs-area" with different settings on the left and the "visualization area" on the right. To visualize the PCM either a video can be played with "Play Simulation" or the participants can be shown in timesteps every one second and at the last timestep with "Show Timesteps". To visualize a specific timestep, the time can be chosen on the time slider of the visualization panel.

Creation of IGLAD-PCM from Austrian (CEDATU) data

Graz University of Technology uses a fully retrospective accident data collection approach based on court cases (13). The court data includes police reports, accident sketches (not vectorized), pictures of the accident scene (road geometry, roadside information, road markings, etc.) and road users, witness reports, medical reports, etc. Graz University of Technology uses PC Crash for the accident reconstruction. A scaled bitmap of the accident site with the collision and rest positions, road layout is sufficient. However, a digital scaled sketch is not mandatory for this purpose. All functions included in PC Crash are sufficient to obtain an adequate overview of the accident situation including compiling videos.

For processing PCM, however, the accident sketches were digitized (vectorized) and layered based on the requirements of the PCM format. Digitization is done in PC Crash with the included drawing tools based on the accident sketch of the police. Appropriate layers were defined in a template to associate road marks, sight obstructions, vegetation, etc. with the PCM specifications.

For the translation of the dynamics the in-house tool X-RATE (Extended Effectiveness Rating of Advanced Driver Assistance Systems) was used. X-RATE was developed to assess the effectiveness of driver assistance systems or autonomous driven vehicles (14) (15) (16) (17). X-RATE interacts with PC Crash on a time-step basis using the OLE interface of PC Crash in a MATLAB environment. However, an additional function was necessary to include the processing of environmental data (roadside, road marks, etc.), participant data, and dynamics to create a complete PCM dataset.

Even though there is advise on how to position objects in the PCM manual, the orientation of objects in the PCM dataset was not plausible in some cases. In Figure 8 different orientations of road markings in the accident sketch and in the PCM data is given. The mistake could be either found in an incorrectly associated layer type, a wrong scaling factor or the rotation angle in an incorrect unit. Furthermore, artefacts are found in the PCM data which are not in the accident sketch (Figure 9). Whilst the position of road users is given in a global coordinate system, the velocities and accelerations are related to the local coordination system. This might lead to incorrect values. Specifically, if the road user negotiates a bend the velocity does not correspond to the acceleration. In Figure 10 on the left side the velocity in y-direction does not correspond to the acceleration. Approximately 0.8 s before the accident the acceleration increases but the velocity remains constant. In the x-direction no acceleration is observed and the velocity does not increase or decrease. The right picture shows correct values for both, the x-direction and the y-direction.
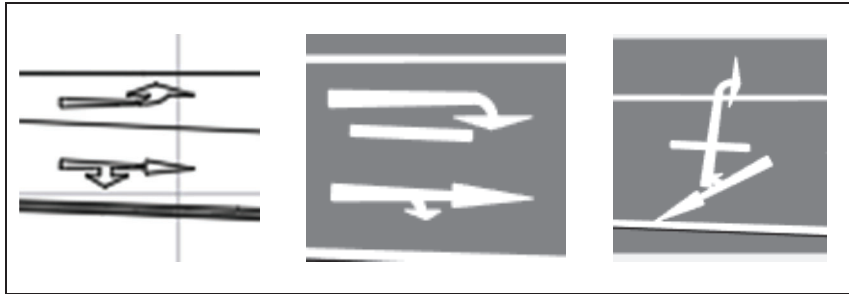
Figure 8. **Different orientation of standard road marks in the sketch (left) and in the PCM data (mid, right).**
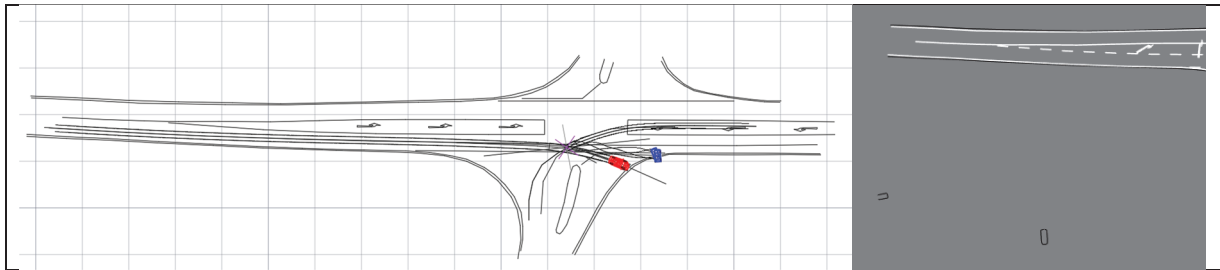
Figure 9. **Artefacts in the PCM data (right) which are not present in the accident sketch (left).**
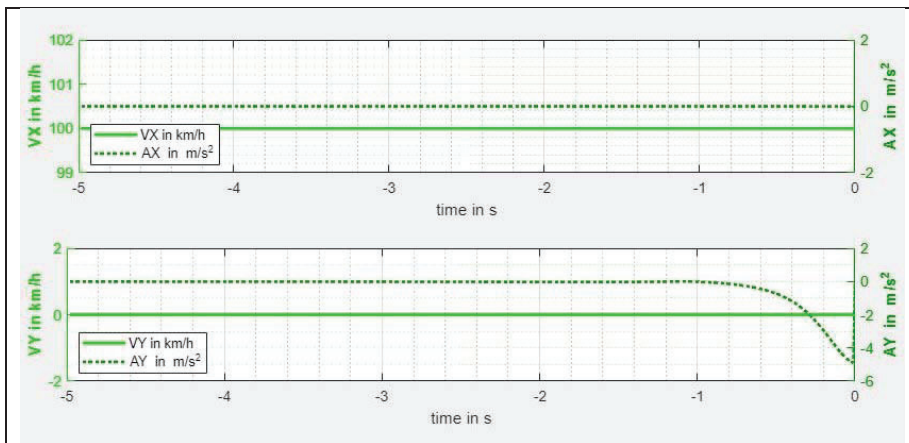
Figure 10. **Divergence between velocity and acceleration in y-direction**

The steps necessary to create a complete PCM dataset are either manually (draw vectorized sketches including the correct layers) or automatically (processing the sketches and dynamics). In the accident database CEDATU (Central Database for In-Depth Accident Study) of Graz University of Technology, the accident sketches are already created according to the PCM specifications on a regular basis. The effort to create a sketch according to PCM specifications compared to a simple vectorized accident sketch is not much higher. However, this manual related work leads to random errors e.g. incorrect object type and layer if the work is not carried out accurately.

Creation of IGLAD-PCM data from US (CISS) data

There are some differences that we want to outline in how the US IGLAD-PCM is generated compared to PCM data from other countries. The basis for creating the US IGLAD database and the PCM data set is the NHTSA CISS data (Crash Investigation Sampling System, see also (18). t is an in-depth data set and currently contains 3,000 – 4,000 accidents per year. Besides a complete reconstruction of each accident there are recordings of an EDR (Event Data Recorder; in the US usually named as *Crash Data Recorder / CDR*) available in most of the cases. They contain speeds, accelerations and other signals of a subset of the motorized participants at certain time intervals of the pre-crash phase. The PCM "dynamics" table that contains the kinematic information of each participant is generated using the data from the EDR of each involved vehicle. Additional checks are run to ensure that the resulting dynamics data is in line with the accident reconstruction in the IGLAD participant table which in turn is based on the CISS reconstruction data. Currently, the US PCM is the only IGLAD-PCM data set where the kinematic data is completely based on EDR so the process of creating it differs from that of the other IGLAD data providers which we will outline in more detail below.

When creating the US IGLAD-PCM the following four data sources are leveraged:

1. Accident and participant tables from IGLAD database: common accident and participant data which is imported from the core IGLAD and CISS database tables.

2. EDR data from the CISS database: measurements of different sensor inputs like velocity, acceleration and brake pedal activation typically starting five seconds before an event. Multiple events can be recorded.

3. Theodolite measurements stored in the CISS accident sketches: point coordinates of vehicle positions, road-, lane-markings, and object positions like signs and obstacles in 3D space, which are acquired by on-scene laser measurements using a theodolite and stored in FARO Blitz CAD sketch files.

4. Vehicle meshes stored in the CISS accident sketches: true to scale CAD meshes of the accident participant's exact vehicle model.

Based on these data sources a US IGLAD-PCM is created in five stages:

Stage 1. The general accident and participant information is re-coded to match the PCM "global data" and "participant data" tables.

Stage 2. The theodolite measurements are extracted from the CISS digital sketch of the accident scene. The CISS trajectory for each participant consists typically of a few points per participant that mark their positions during the pre- and post-collision phase including the collision point and the final rest. The PCM "dynamics" table is created by merging and enriching the trajectory points and the EDR data for each participant. First, the trajectory points need to be ordered and interpolated in a uniform manner. The trajectory curve of the US IGLAD-PCM is constructed using clothoid-splines as they tend to give the best fit for the vehicle's trajectory. Smooth tangent and curvature alignment between each clothoid-spline segment is achieved by using Hermite interpolation (19). With this enhanced representation of the participant's trajectory, the EDR data is complementing the geometric trajectory information and providing a speed and acceleration profile. This profile is mapped to the interpolated trajectory curve and the required values for the "dynamics" table are calculated for each simulation step along the trajectory of each vehicle up to the collision point. If more than one event is recorded before the primary collision in one of the participants EDR data a more sophisticated multi-segment mapping of the speed profile to the trajectory is applied.

Stage 3. The data for the "intended course" table of the PCM is calculated. Therefore, the trajectory needs to be extended beyond the collision point following an assessed intended course of the vehicle. This requires inserting new points into the CISS sketch by doing estimations based on the accident description and other information from the CISS database. These extra points are also interpolated and extend the already created clothoid-spline of the trajectory in a smooth manner without introducing unnatural accelerations. An example of the interpolated trajectory and intended course is shown in Figure 11.
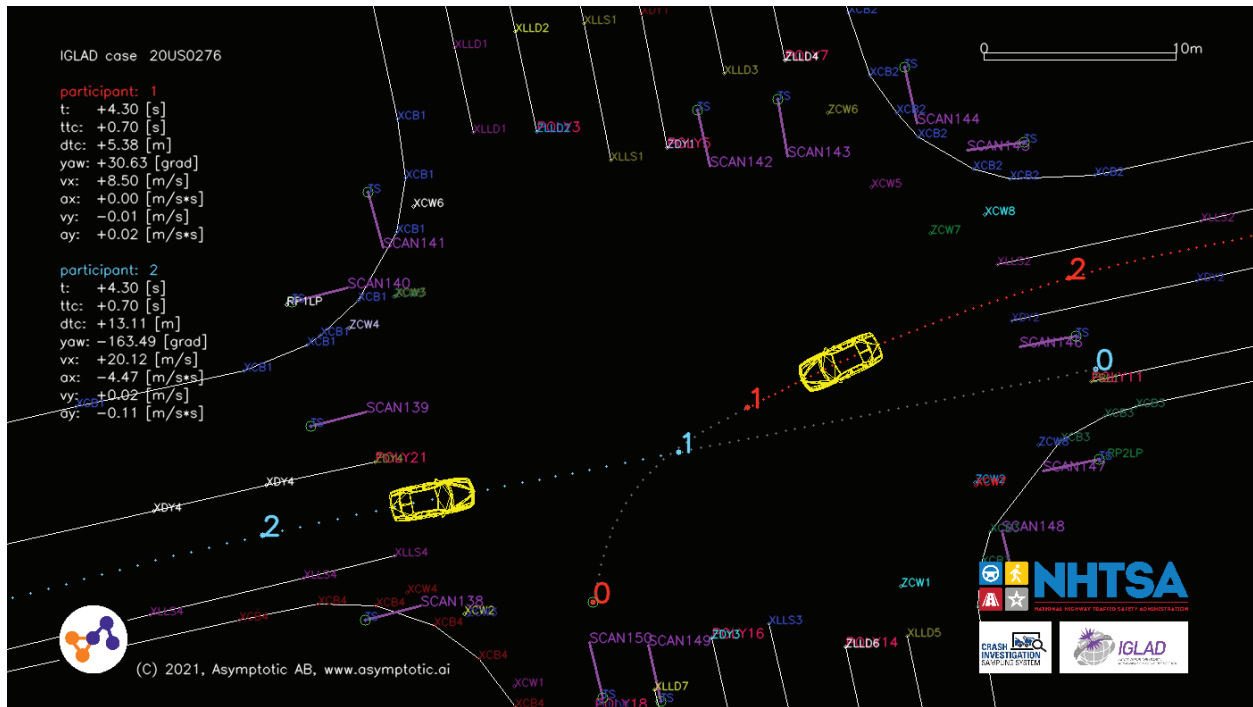
Figure 11. **US IGLAD-PCM with clothoid-spline interpolation of vehicle trajectory and intended course.**

Stage 4. Additionally, to the trajectory points all road-, lane-markings and object positions like signs and obstacles are extracted from the sketches and then grouped, rotated if necessary, and mapped to the coding conventions of the PCM tables "road_marks", "standard_road_marks", "standard_objects", and "standard_traffic_signs".

Stage 5. The PCM provides the "participant_shape" table with a geometric outline of each participant. The CISS sketches already include an accurate CAD mesh for the exact model of each participant. However, the PCM requires a different geometric representation which is created by extruding the 2D shape of the model's mesh. This is accomplished by calculating the convex hull of the projection of the vehicle model to the ground surface and extruding the resulting shape to the height of the vehicle in vertical direction. An example of the shape extrusion is shown in Figure 12.
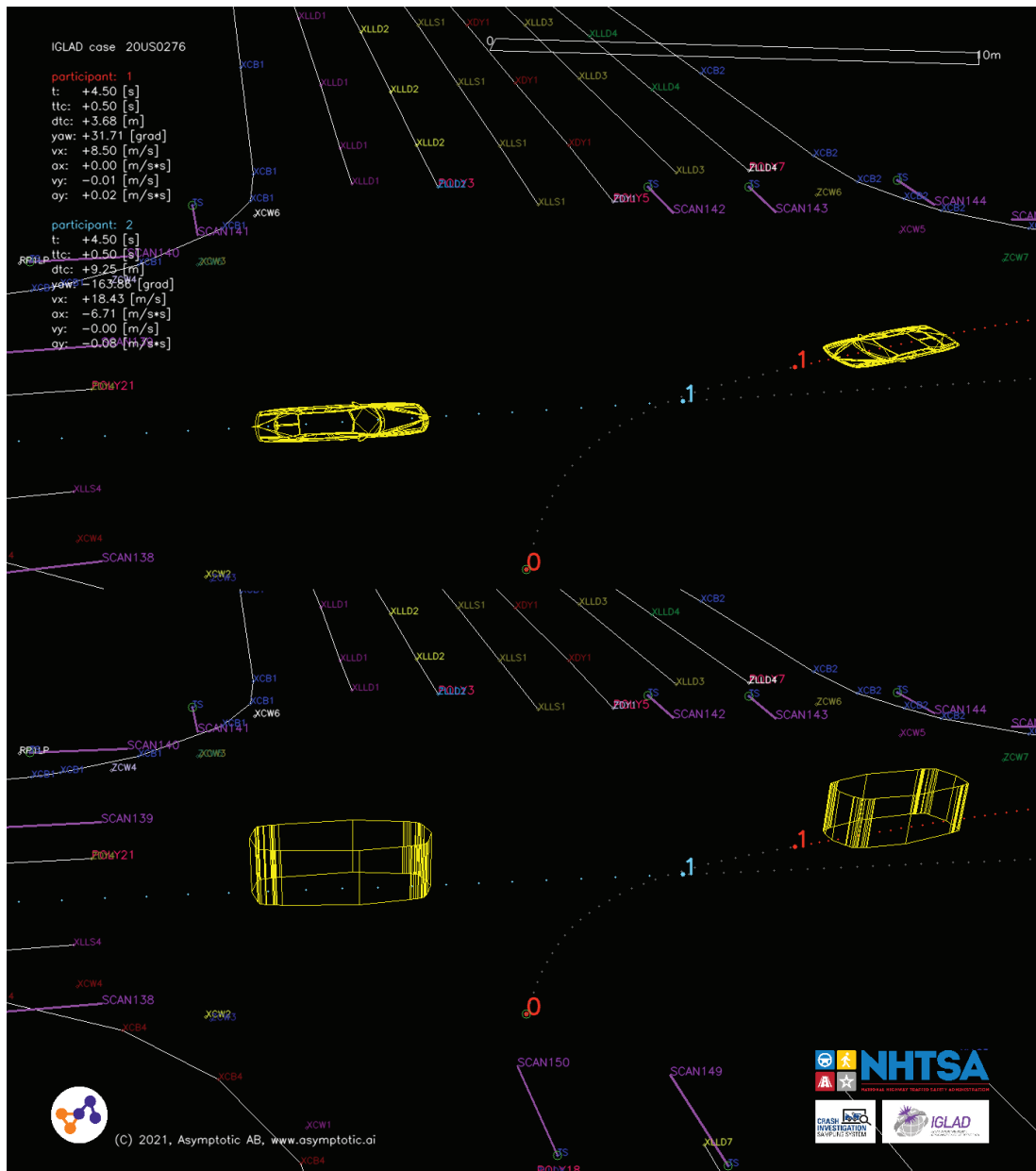
Figure 12. **PCM vehicle shape extruded (right) from the convex hull of the CISS CAD mesh (left).**

The resulting PCM generated from the US CISS data offers a complete data set with a high-quality standard which conforms to the latest PCM specifications. One central piece of the PCM data is the "dynamics" table where the US IGLAD-PCM can excel by providing data which is based on real sensor measurements supplied by the EDR units in the participating vehicles. Opposed to reconstruction based PCMs there are less assumptions involved in the underlying data. Differences to reconstruction based PCMs are for example pre-crash maneuvers that are visible in the EDR measurements but would usually not appear in a reconstruction because there is no on-scene evidence present for these. Examples found in the data showing these differences were short braking maneuvers or accelerations of a participant at a crossing that attempts to avoid a collision when recognizing a car approaching from behind or a quick acceleration followed by sharp braking at traffic lights that most likely were switching from green to red.

The upcoming CISS releases are expected to include more detailed data from updated EDR units and also to extend to a greater variety of accident types. This will even further improve quality and richness of the US IGLAD-PCMs.

Quality assurance process
As the vast majority of data providers have never created PCM files before, the aspect of quality is quite important. From VUFO's more than 10 years of experience with PCM creation and format development, it is known that there are many pitfalls and many small details to consider. For this reason, each of the 200 cases was subjected to a quality check by VUFO on a case-by-case basis. The focus was on compliance with the PCM format specification, e.g. use of the correct units and completeness of the tables on the one hand, and on the other hand on the correct transfer of each individual scenario (case-by-case review). The case-by-case review was performed by using the VUFO PCM Viewer. The following items were analyzed within the process:

- Has all relevant information been transferred from the sketch?
- Do the trajectories match the sketch?
- Are there jumps or interruptions in line segments of the sketch?
- Are the objects and markings rotated correctly?
- Are the speeds and ac-/decelerations plausible?

Finally, all Data Providers managed to deliver PCM data in a good quality after few bilateral iterations between VUFO and the Data Providers.

RESULTS

Content of the IGLAD-PCM
The first ever published IGLAD-PCM contains 200 personal injury accidents from seven different countries, provided by eight data providers. They represent a subset of the regular IGLAD datasets, although the very first release did not have too strict requirements for representativeness in case selection. The primary goal was to prove the feasibility and to establish the corresponding process and tool chains.

However, quite promising results could be derived. Figure 13 shows the distribution of accident configurations in all 9,425 IGLAD accidents and the distribution for the IGLAD-PCM cases respectively. Nearly all configurations are covered in both the IGLAD database and the IGLAD-PCM. Generally, accidents involving a car and a second road user are overrepresented. The most frequent accident configuration in the IGLAD-PCM is the group of car-to-car accidents. Single car accidents are underrepresented as they are particularly challenging because they are usually characterized by unstable driving conditions (understeer or oversteer) in the pre-crash phase. An automatic transfer of the dynamic data into the IGLAD PCM is more difficult than accidents without unstable driving conditions.

Accidents involving two VRU are not included at all so far. The same applies for single bicycle accidents. However, they are usually not of big interest for the current members and stakeholders.
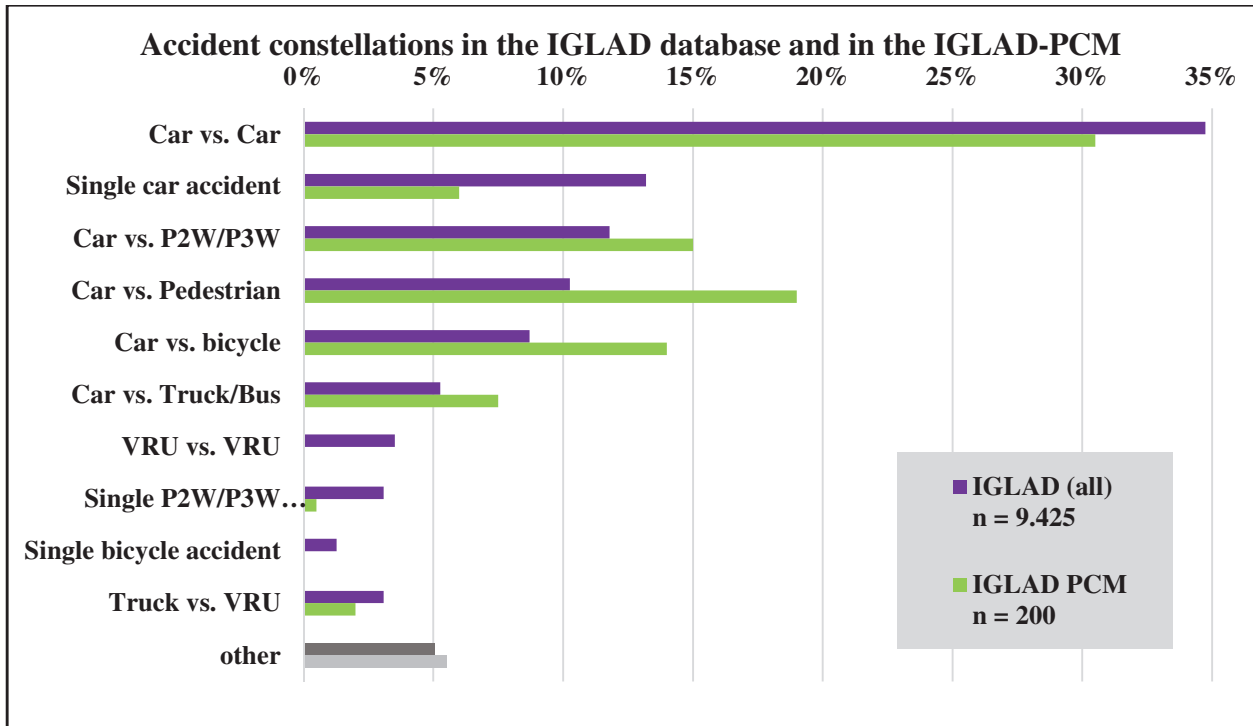
Figure 13. Accident constellations in the IGLAD database and in the IGLAD-PCM

Figure 14 shows the accident severity distribution of the 200 PCM cases. The distributions for most countries is similar to the one in Figure 1. For the Austrian, Chinese as well as the Italian data the accidents in the IGLAD PCM is even more representative for the related country's national statistics. This is due to the fact that the vast majority of PCM cases were selected from the latest IGLAD release (Phase IV / 2021; containing accidents of the years 2019 and 2020). Representativeness aspects are becoming more and more important within IGLAD since years and thus, most countries provide IGLAD data with a good level of representativeness.
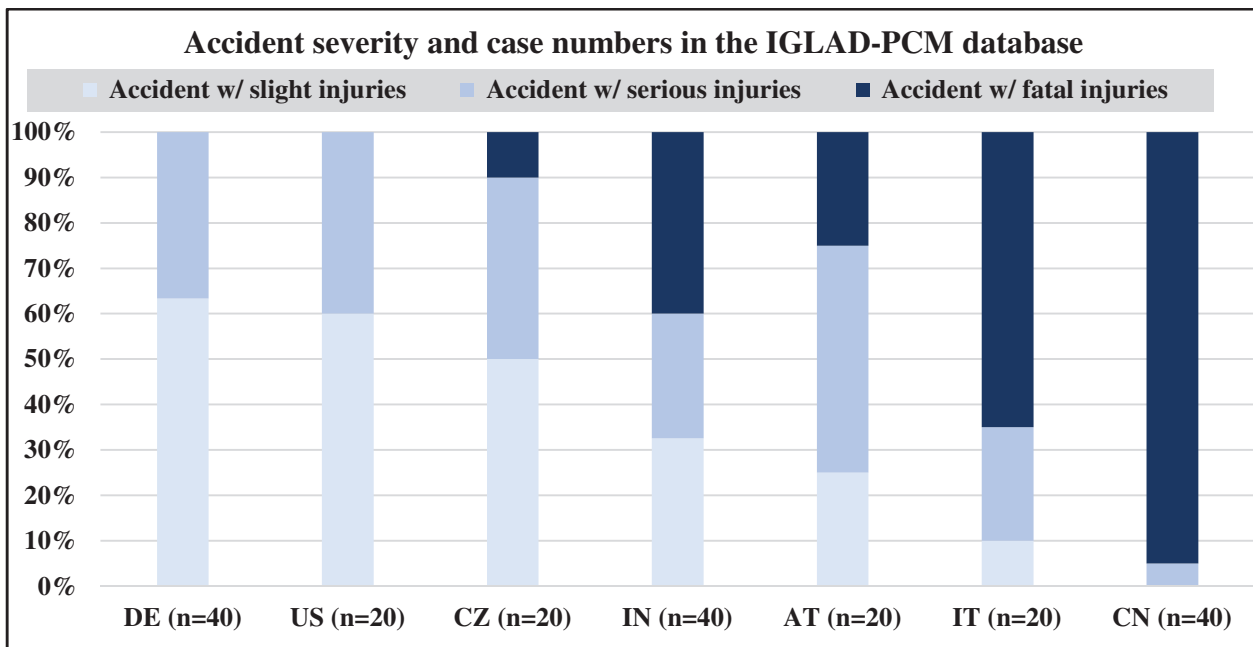
Figure 14. Accident severity and case numbers in the IGLAD-PCM database

Applications of the PCM format

Accident and/or traffic scenarios which are stored in the PCM format can be used in several ways. Most of them base on retrospective analysis to support the development of future vehicle safety systems. Figure 15 shows some examples, which are briefly explained below.
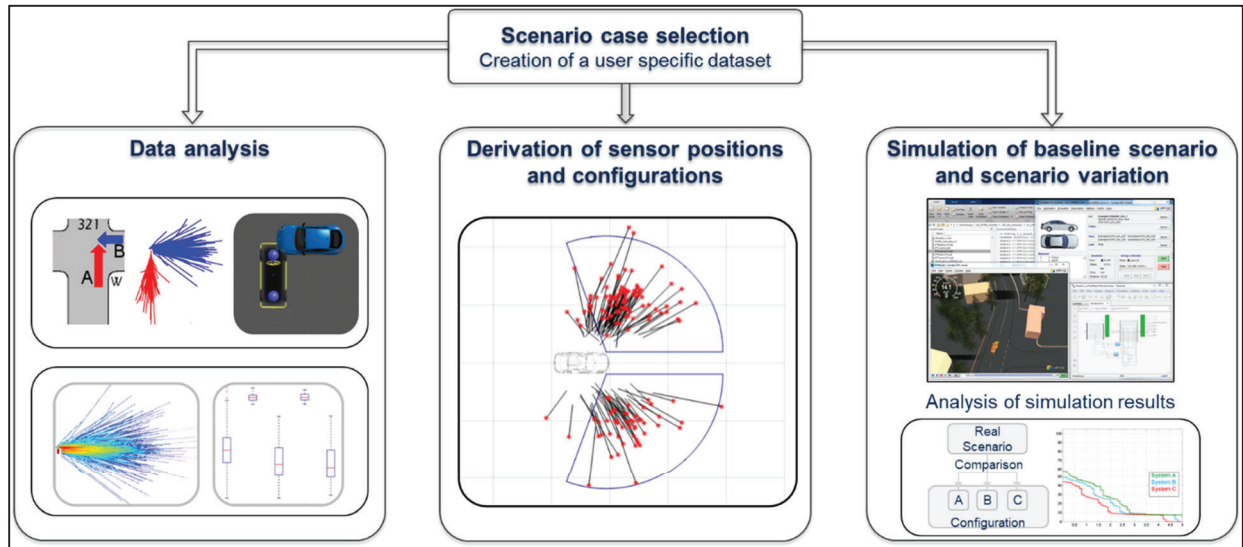
Figure 15. Selected application possibilities of PCM data

Within the field of (retrospective) data analysis, sub-samples from the overall database are examined by means of descriptive analyses. These are, for example, individual or grouped accident types. From these, scenario groups can be formed and analyzed. For example, the left part of the figure above shows the center of gravity trajectories of the accident participants of accident type 321 in the upper section. This allows the approach direction of the accident participants to be analyzed. In addition, the corresponding speeds and accelerations of the participants can also be analyzed, as in the boxplot in the lower section. This means that the following questions can be answered: Which road user is where at which point of time and which maneuver is he carrying out?

Another possibility is the derivation of sensor positions and specifications. This means that an ego vehicle is defined and the position of several participants from different scenarios is examined. Thus, for example, the position or also the specification (opening angle, range, etc.) of a sensor can be examined at a defined time or in a time range. Especially in connection with criticality measures like TTC (Time to Collision) this can be an important tool. Important research and development questions can be answered, as for example: Where should a sensor be positioned on the ego vehicle and which specification should it have in order to provide a high benefit?

In addition, it is possible to transfer scenarios into vehicle dynamics solvers. This offers the possibility to implement a virtual system in the ego vehicle and then to analyze the influenced scenario in relation to the baseline scenario in order to evaluate the effectiveness of the system. This can be used to answer the question if a system has an impact on the accident scenario, and if so, what type and magnitude of impact?

Field-of-View and Speed Analysis

PCM pre-crash data can be used in a variety of ways in the context of automotive engineering. One possible way is the application for deriving system requirements for ADAS. The data provides key performance indicators for sensors, algorithms, and actuation controls. The goal is to make system requirements correct, complete and relevant, and thus support the development of safe and robust products.

Since the PCM only provides a description of the pre-crash trajectories but does not contain metadata on the traffic accidents, the PCM needs to be considered as an add-on to the IGLAD accident data. A two-step approach to analyzing IGLAD accident data and PCM pre-crash data is proposed as shown in Figure 16.

1. Deriving of relevant accident scenarios in IGLAD, such as car-vs-car or car-vs-VRU. Each accident is considered from the viewpoints of the participants in the conflict situation, to generate a set of accident scenarios. For the corresponding method and the used scenario catalog, refer to (20). The car-vs-car accidents can be targeted from the causer or from the non-causer perspectives, therefore the number of accident scenarios that are addressed by ADAS is twice the number of accidents. Car-vs-VRU accidents are only analyzed from the car perspective, as cars are considered responsible for VRU protection. The resulting complete set of IGLAD accident scenarios is the basis for a car safety system development.

2. Analysis of pre-crash characteristics, such as object positions, orientations, and speeds. Subsequently the pre-crash scenarios are retrieved from the PCM and analyzed from the perspective of the ego car. Therefore, the positions, orientation and speeds are transformed into the ego space. This allows for an analysis of sensor fields-of-view in different accident scenarios such as run-up, crossing or turning. The speed information is used for designing real-world test cases. Thus, the validation of safety systems can be supported by virtual simulation of PCM test data.

The current PCM data set, in data year 2021, contains 84 car-vs-car pre-crash scenarios. Furthermore, there are 11 car-vs-motorcycle, 14 car-vs-bicycle, and 21 car-vs-pedestrian pre-crash scenarios.
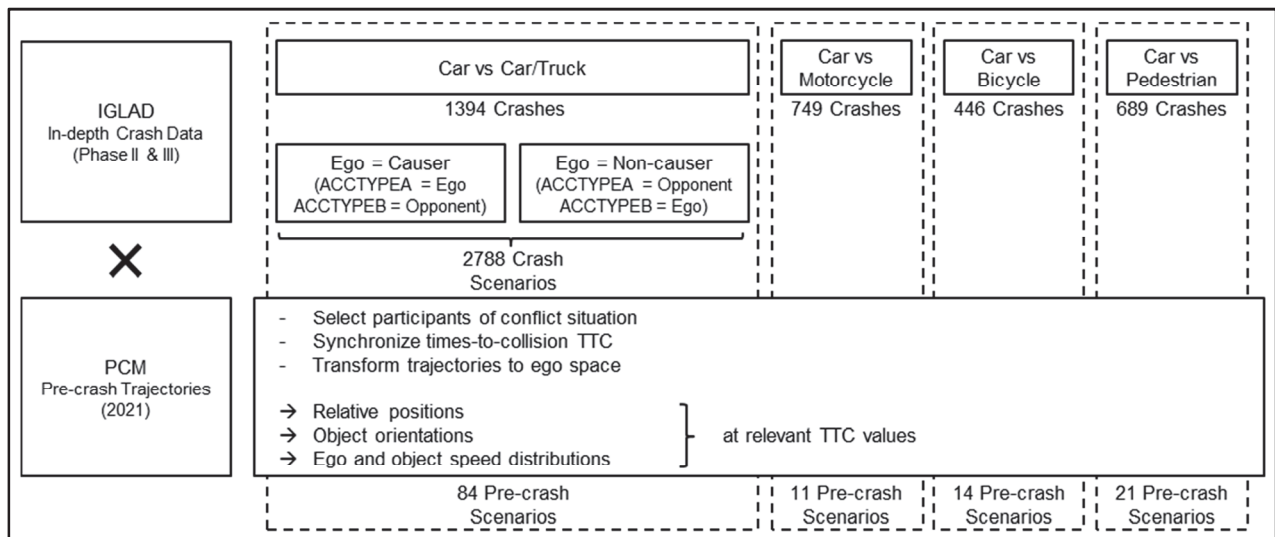
Figure 16. **Method for deriving pre-crash scenarios from IGLAD and PCM.**

PCM data analysis results of car-vs-car accidents are shown in Figure 17. The left-hand side picture depicts the relative positions and orientations of other cars at time-to-collision TTC = 2s. To put the object positions into perspective, generic fields-of-views for typical sensors are drawn: LRR (long range radar), CAM (camera), SRR (short range radar). The count for each scenario type and for each country is given. The most frequent scenarios are "run-up" L1 (13 cases), "rear-end" L4 (13 cases), "crossing from right" C1 (13 cases), and "oncoming same lane" On1 (12 cases). The right-hand side picture shows the speed histograms of ego and object car. Ideally, once the IGLAD-PCM data sample grows, the field-of-view visualization and speed analysis should be performed on a scenario-basis, to get requirements for the different safety functions.
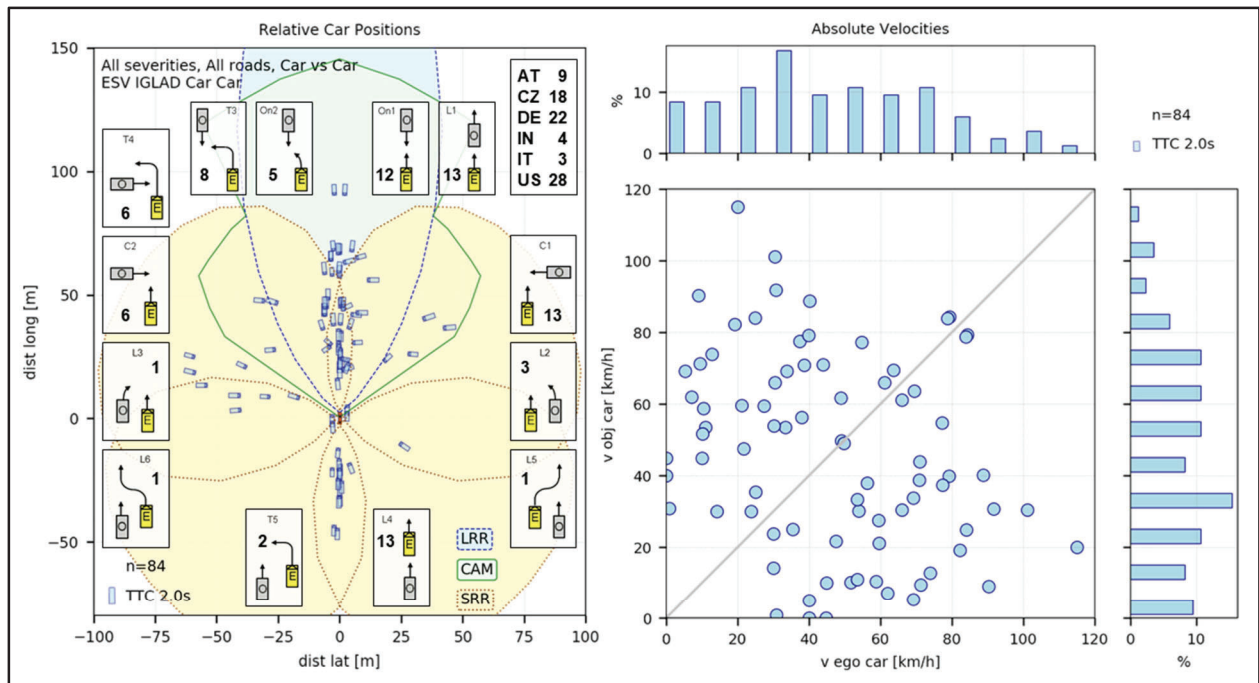
Figure 17. **Field-of-view and speed analysis of car-vs-car pre-crash scenarios**

The car-vs-VRU accidents are also analyzed and visualized in Figure 18 (car-vs-motorcycle), Figure 19 (car-vs-bicycle), and Figure 20 (car-vs-pedestrian). Again, each figure shows the field-of-view and speed analysis. Also, the counts per scenario type and country within the IGLAD-PCM data sample are given.
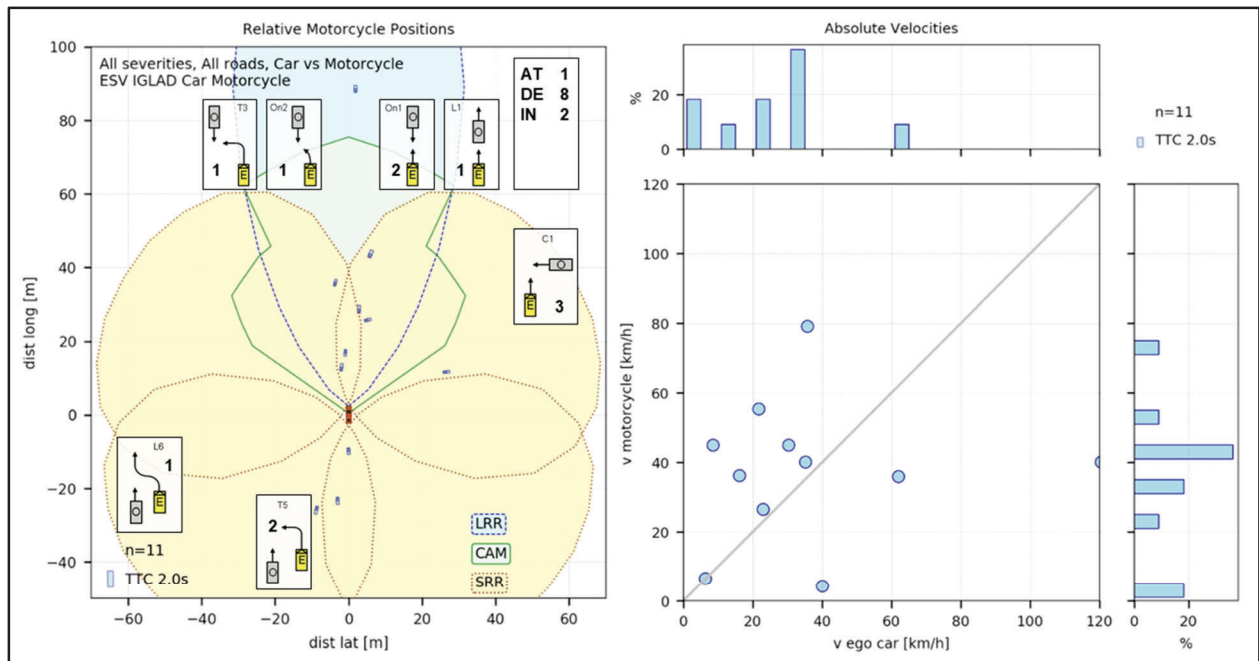

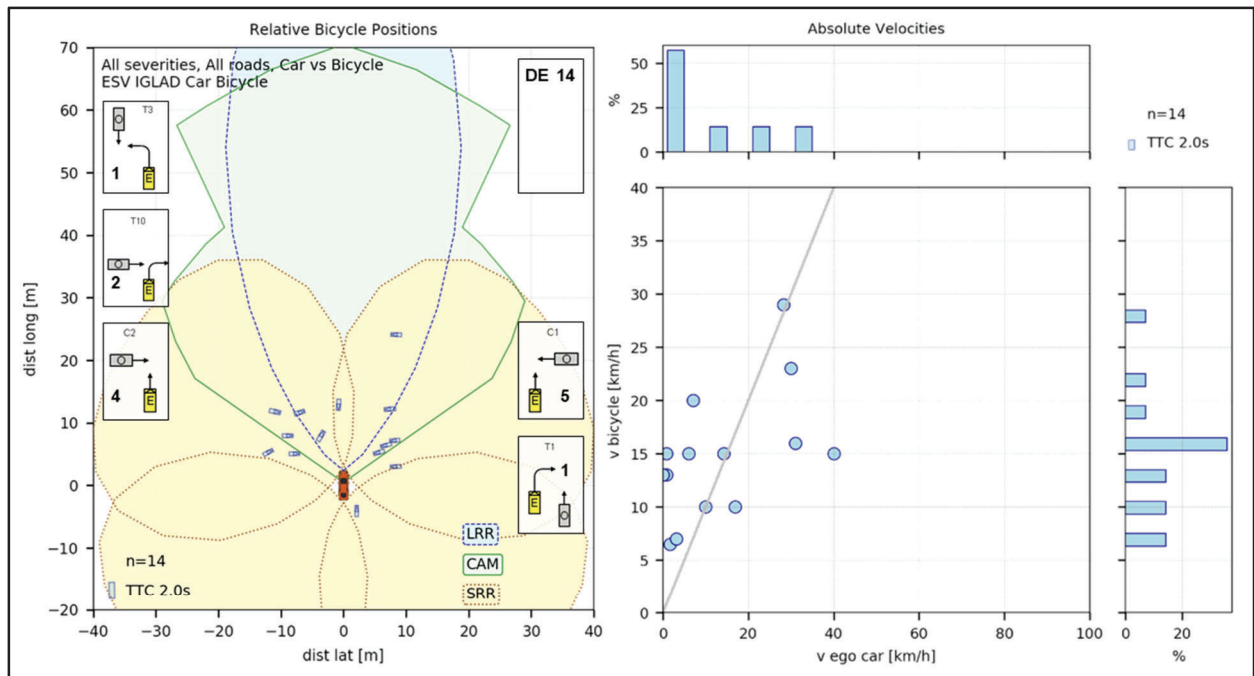***Figure 18.*** **Field-of-view and speed analysis of car-vs-motorcycle pre-crash scenarios**

Figure 19. **Field-of-view and speed analysis of car-vs-bicycle pre-crash scenarios**
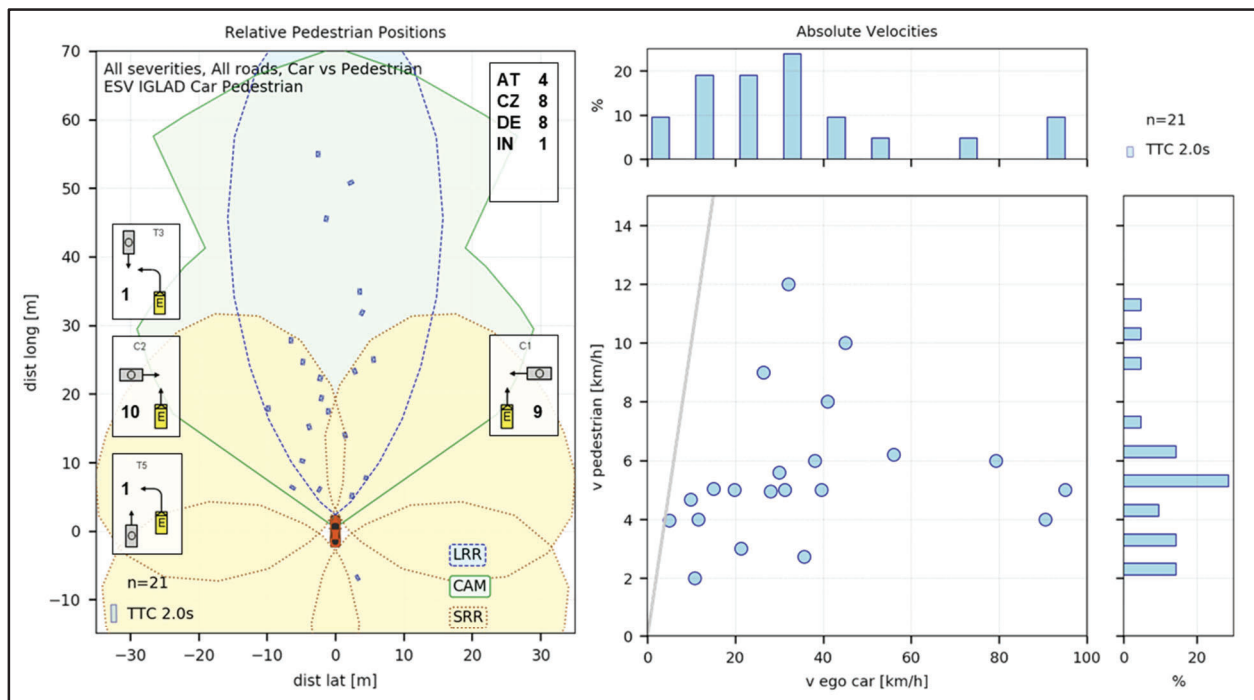
Figure 20. **Field-of-view and speed analysis of car-vs-pedestrian pre-crash scenarios**

DISCUSSION AND LIMITATION

The challenging task of storing data from reconstructed accident scenarios from different data providers in a uniform simulation database was successfully completed. Within one year, eight data providers from seven countries on three continents have transferred a partial data set of their IGLAD accidents into the PCM format V5.

The main challenges were, among others, the transfer of the dynamics data (trajectories, velocities, accelerations), the correct transfer of sketch objects and the first-time application of the PCM format specifications. Nevertheless, it was possible to generate consistent PCM files from the various basic data.

The establishment of an additional quality assurance process proved to be useful, in which the data provider together with VUFO was able to improve the quality of the delivered PCM data in an iterative way. Thus, it can be ensured that the existing 200 PCM cases are consistent, and the contents meet a certain quality standard.

Another benefit of the PCM creation is the fact that the original data and accident sketches are re-examined during the creation and quality check process, which may reveal further errors. However, as the quality checks are done after the PCM has been completely created by the data providers, the effort for correcting errors is rather high (especially for sketches) and could be mitigated with a continuous quality control during the generation of the data. An appropriate visualization tool or quality control of the processed data immediately at the end of the data collection is highly recommended to evaluate the plausibility and quality of the own data.

A limitation, besides the small number of cases so far, is the lack of representativeness of the IGLAD-PCM. As shown in Figure 13, so far mainly accidents involving passenger cars have been transferred to the PCM. These are clearly overrepresented, while accidents between VRUs or truck and bus accidents are underrepresented.

In addition, there are still some challenges. One is the automatic transfer of driving accidents. This main accident type is also underrepresented in the PCM. Another challenge results from the heterogeneous types of road markings and traffic signs around the world. Here, the IGLAD community is working together to create a common catalog of standard objects, at least for the most important and frequently used road markings and traffic signs.

CONCLUSION AND OUTLOOK

We have shown that the PCM specification makes it possible to harmonize pre-crash data from different countries and still take regional specifics into account. Since the PCM specification is an open data format, different scenario descriptions can be easily created and existing development tool chains can be supported. The initial release of the database includes only 200 accidents, but through annual updates the number of scenarios will constantly increase. The example has shown which applications of the IGLAD-PCM are possible.

This first release of the IGLAD-PCM was an important step forward for the IGLAD project. Thanks to the internal start-up funding from the IGLAD consortium, six new data providers have been enabled to convert their reconstructed accident data to PCM format, in addition to VUFO, which has already been delivering PCM data (within the GIDAS project) since 2011.

We have shown how the PCM data can be used to support data-driven system engineering of ADAS and AD systems. Pre-crash data are relevant for deriving key-performance indicators for sensors, controls, and actuation to develop safe and robust systems. Additionally, test scenarios are key for real-world validation by virtual simulation and to show how systems tackle critical crash cases.

The valuable experiences from this project encouraged us to follow-up with additional activities. There are several actions planned or have been already started, e.g.

- the creation of a catalogue of standard objects (mainly road markings) from different countries
- creating appropriate tools for data providers for the efficient and correct creation of PCM files
- enabling more/new data providers to create IGLAD-PCM
- transfer of PCM files into OpenDRIVE and OpenSCENARIO

In addition to the integration of further data sources or data providers, the last point mentioned is particularly important. In the future, the OpenX formats will be used as standard formats for the development, testing, validation, and Periodical Technical Inspection (PTI) of vehicles and functions. Corresponding real-world scenarios should therefore also be made available in these formats in the near future. For this purpose, VUFO already has approaches for conversion, and several hundred (GIDAS, not IGLAD) cases have already been successfully converted into the OpenX formats.

REFERENCES

Literaturverzeichnis

1. **Bakker, J., Jeppson, H., Hannawald, L., Spitzhüttl, F. et al.** *IGLAD - International Harmonized In-Depth Accident Data.* in: NHTSA (ed.), The 25th ESV Conference Proceedings, ESV Conference Proceedings, International Technical Conference on the Enhanced Safety of Vehicles, Michigan, USA, 5.-8.6.2017, NHTSA, 2017.

2. **Bakker, J., Ockel, D. und Schöneburg, R.** *Multinational in-depth accident data: From concept to reality.* In: ESAR (Hg.): 6th International Conference on ESAR "Expert Symposium on Accident Research", June 20-21, Hannover, 2014.

3. **Ockel, D., Bakker, J. und Schöneburg, R.** *Internationale Harmonisierung von Unfalldaten.* Fortschrittsbericht des FIA / ACEA Projekts iGLAD (Initiative for the Global Harmonization of Accident Data). In: VDI-Berichte 2144: VDI Verlag (VDI-Berichte), S. 301–309., 2011.

4. **Ockel, D., Bakker, J., and Schöneburg, R.** *An initiative towards a simplified international in-depth accident database.* in: ESAR (ed.), 5th International Conference on ESAR "Expert Symposium on Accident Research", Hannover, 2012.

5. **Heinig, I., Bakker, J.** IGLAD Homepage. [Online] [Zitat vom: 08. December 2022.] http://www.iglad.net.

6. **Chalmers, SAFER Vehicle and Traffic Safety Center at.** https://www.saferresearch.com/. [Online] [Zitat vom: 24. 11 2022.]

7. **WHO.** *Global status report on road safety 2018.* World Health Organization, Geneva, Switzerland, ISBN 978-92-4-156568-4, 2018.

8. **European Commission.** *Annual statistical report on road safety in the EU, 2021.* 2022.

9. **OECD.** IRTAD road safety database. [Online] [Zitat vom: 20. November 2022.] https://www.itf-oecd.org/irtad-road-safety-database.

10. **Schubert, A., Liers, H., Petzold, M.** *The GIDAS Pre-Crash-Matrix 2016 - Innovations for standardized pre-crash-scenarios on the basis of the VUFO simulation model VAST.* 7th International Conference on ESAR "Expert Symposium on Accident Research", Hannover, June 09/10, 2016.

11. **Verkehrsunfallforschung an der TU Dresden GmbH.** https://www.vufo.de/pcm/. *PCM Specifications.* [Online] [Zitat vom: 18. 11 2022.]

12. **Petzold, M., Schubert, A., et. al.** *Pre-Crash-Matrix (PCM) Format Specification v5.0.* [PDF] VUFO GmbH, 2021.

13. **Tomasch, E., Steffan, H., and Darok, M.** *Retrospective accident investigation using information from court.* in: TRA (ed.), Transport Research Arena Europe 2008 (TRA), Ljubljana, Slovenia, April 21-24, ISBN 978-92-79-10039-0, 2008.

14. **Gruber, M., Kolk, H., Klug, C., Tomasch, E. et al.** *The effect of P-AEB system parameters on the effective-ness for real world pedestrian accidents.* NHTSA (ed.), The 26th ESV Conference Proceedings, International Technical Conference on the Enhanced Safety of Vehicles, Eindhoven, Netherlands, 10-13 June, NHTSA, 2019.

15. **Kolk, H., Tomasch, E., Haberl, M., Fellendorf, M. et al.** *Active safety effectiveness assessment by combination of traffic flow simulation and crash-simulation.* ESAR (ed.), 8th International Conference on ESAR "Expert Symposium on Accident Research", Hannover, 19.-20.04, 2018.

16. **Kolk, H., Sinz, W., Tomasch, E., Bakker, J. et al.** *Evaluation of a momentum based impact model and application in an effectivity study considering junction accidents.* ESAR (ed.), 7th International Conference on ESAR "Expert Symposium on Accident Research", 7th International Conference ESAR, Hannover, 09.-10.06.2016, 2016.

17. **Wimmer, P., Düring, M., Chajmowicz, H., Granum, F. et al.** *Toward harmonizing prospective effectiveness assessment for road safety: Comparing tools in standard test case simulations.* Traffic Injury Prevention 20 (sup1):S139-S145, 2019, doi:10.1080/15389588.2019.1616086.

18. **NHTSA.** https://www.nhtsa.gov/crash-data-systems/crash-investigation-sampling-system. [Online] [Zitat vom: 25. 11 2022.]

19. **Spitzbart, A.** *A Generalization of Hermite's Interpolation Formula.* American Mathematical Monthly, 67 (1): 42–46, doi:10.2307/2308924, JSTOR 2308924.

20. **Feifel, H., Wagner, M.** *Harmonized Scenarios for the Evaluation of Active Safety Systems based on In-Depth-Accident Data.* 8th International Expert Symposium on Accident Research (ESAR), Hanover. 2018.

FRAMEWORK FOR A CONFLICT TYPOLOGY INCLUDING CONTRIBUTING FACTORS FOR USE IN ADS SAFETY EVALUATION

Kristofer D. Kusano
John M. Scanlon
Mattias Brännström
Johan Engström
Trent Victor
Waymo, LLC
United States

ABSTRACT

The aim of a successful conflict typology (also sometimes called crash or maneuver typology) is to group conflicts, some of which may result in a collision, into groups that have common characteristics influencing avoidability and potential severity. A conflict typology can be used in safety impact methodologies that analyze and predict the potential performance of a safety countermeasure or system within a set of defined crash modes. More generally, conflict typologies are used across many traffic safety analyses, including those related to evaluating the safety of an Automated Driving System (ADS). The objective of this paper was to describe a conflict typology including contributing factors that can be used in both Automated Driving System (ADS) and human driven vehicle safety evaluations. The proposed typology is comprised of 5 layers: (1) conflict partners - the types of the actors or objects involved in a conflict, (2) conflict group - the high-level description of a conflict, (3) conflict perspective - assigned to each actor based on their relative maneuvering, (4) the actor role - either the initiator of some surprising action that leads to a conflict or the responder, and (5) contributing factors - factors that in combination contributed to the conflict initiating or non-nominal response that caused the conflict. The main contribution of the proposed conflict typology and contributing factors are applicable conflicts from both retrospective crash data and near-crashes from a naturalistic driving study (NDS), and in the future ADS conflicts. The results also highlight potential difficulties reconciling differences in contributing factors observed in high-severity crash data having limited contributing factor information and those contributing factors observed in lower severity NDS data.

Keywords: Conflict Typology, Contributing Factors, Automated Driving Systems

INTRODUCTION

Conflict typologies, which have also been called crash groups or scenario typology [1], are an essential tool used by traffic safety practitioners to analyze collision data and study the potential effectiveness of proposed countermeasures and systems, such as Advanced Driver Assistance Systems, or other safety systems like Automated Driving Systems (ADS). Traditionally, this has been accomplished by describing the collision geometry, pre-collision maneuvers, and collision actors. Once these crash types are established, different characteristics of the collisions can be compared, such as environmental factors or driver characteristics [2].
Analyzing crash data by first grouping by collision type is necessary, as different collision types often have heterogeneity in their causes, referred to as horizontal heterogeneity (as opposed to vertical heterogeneity in different severity of collisions) [3]. By identifying the characteristics and causes of collisions, traffic safety professionals can investigate countermeasures (directly linked to the causation of the event) that strive to reduce and mitigate collisions. One example of this type of study in vehicle technology is the prospective safety assessment, where the potential benefit of a proposed vehicle safety system, like automated emergency braking, is projected into

the future [4 - 14]. Historical crash databases, such as NHTSA's CRSS, FARS, and CISS databases, have relied on a more general description of the collision geometry and involved partners to describe various conflict types. Relying on these general categorical elements is convenient and practical, as they do provide meaningful context about the nature of the collision event and the information can be generally identifiable using retrospective crash investigation (such as through analyzing on-scene evidence and taking witness statements). However, within each one of these permutations, there is considerable uncertainty as to the nature of the event that affects avoidability and potential severity. For example, in straight crossing path vehicle-to-vehicle collisions, the opportunity for avoidance and injury potential is much different at four-way stop controlled intersections (generally lower travel speeds) when compared to cases involving a red light runner [15].

As different types of naturalistic driving data become more prevalent, from the usage of instrumented vehicles recording driving data for extended periods of time, the typology approach has been extended to use in near-crash, or conflict, events where there is no contact between actors [16]. In this paper and framework, we adopt the definition of a conflict from ISO/TR 21974-1 [17]:

> *Conflict*
> "Situation where the trajectory(ies) of one or more road users or objects (conflict partners) led to one of three results: 1) a crash or road departure, 2) a situation where an evasive maneuver(s) was required to avoid a crash or road departure, or 3) an unsafe proximity between the conflict partners" (ISO/TR 21974-1, [17]).
>
> NOTE 1: Three general classes of traffic conflict are of interest in naturalistic driving analyses: trajectory conflict, single-vehicle conflict, and proximity conflict.

Using the same conflict typology definition between conflicts and collisions allows for studies that attempt to correlate near-crashes to crashes, as crashes are rarely observed in naturalistic driving studies due to their smaller amount of driving compared to police accident report databases [18 - 19]. Additionally, these instrumented vehicles provide meaningful, objective information about the causation of the conflicts/collisions that are often impossible to discern from retrospective crash investigations. Because of this desire to use a common definition between collision and non-collision events, we refer to conflict typologies instead of collision typologies.

As noted above, one of the key areas that conflict typologies are used for is to attempt to understand the causes of collisions so that those causes can be prevented, thus improving traffic safety. Causal relationships between factors in a scenario and the adverse outcomes are becoming ever important in the understanding of how to perform safety assurance for automated vehicles [20]. To avoid confusion with other, more philosophical, definitions of causality, for the rest of this paper we will refer to contributing factors as the factors that in combination contributed to the conflict initiating or non-nominal response that caused the conflict. These contributing factors are a desired property of a conflict typology, but can be difficult to obtain. In retrospective collision databases, some causes are straightforward to extract from the data. For example, if one is studying intersection collisions, a collision database can be queried to determine when drivers perform a traffic control violation that leads to a collision. Due to the retrospective nature of most crash data sources, however, this type of information is considered incomplete and difficult to obtain. For example, distraction or inattention is theorized to be underreported in police accident report data [21]. The possibilities to directly observe driver behavior increase when using naturalistic driving data that often has video recordings of the interior of a vehicle. For example, using the observations of a driver on video, information on the driver's activity (e.g., gaze direction) can be used to infer contributing factors [21].

Selecting the correct level of aggregation or a conflict typology including contributing factors can be challenging as it requires consideration of what is actionable, what can be readily reduced from available data sources, and what will lead to meaningful conclusions in safety impact analysis. In historical, human-driven crash and conflict

analysis, naturalistic data enables more detailed inference on driver state and is useful in determining plausible causes for adverse events. The data sources that allow for this level of detail by having video, however, often have far fewer serious collisions in comparison to near-crash events. Representative crash databases selectively target rare, high severity collisions, but lack the level of detail available from naturalistic driving data sources as the information is often collected retrospectively without video data. The introduction of ADS will add to this difficulty in grouping by contributing factors. These ADS are expected to be exposed to other road users exhibiting many of the same failure modes as human road users expose each other to. The ADS could possibly have many of the same failure modes as humans, but the causes for these failures may be vastly different. For example, an ADS may fail to recognize an object, that causes a late response, and a collision or near collision. This late reaction may be similar in nature to a distracted human driver, but an ADS would not react late for using a smartphone or driving under the influence.

The objective of this paper was to describe a conflict typology including contributing factors that can be used in both Automated Driving System (ADS) and human driven vehicle safety evaluation. Because ADS are augmenting or replacing human drivers, the methodology must also be able to equally describe human conflicts recorded in crash databases and naturalistic driving studies. This paper presents the underlying conflict typology structure and motivation, but is not intended to be a full recitation of the entire typology, which is quite extensive and naturally evolves as novel scenarios are encountered. To demonstrate the typology, the typology methodology is also applied to both a national crash database and a limited naturalistic driving study dataset.

METHODOLOGY

Conflict Typology Layers
The conflict typology uses a layered, hierarchical structure to capture unique sets of scenarios from which safety impact evaluation can be performed. The success of the conflict typology as a tool in safety impact evaluation hinges on its ability to adequately cover at least the reasonably foreseeable conflict and collision space. To accomplish this, our approach was to leverage causation, avoidability, and severity potential as foundational principles in designing our bucketing scheme.

Figure 1 shows an illustrative example of the 5 layers of the proposed conflict typology for an example pedestrian straight crossing path conflict. The layers are: (1) conflict partners - the types of actors involved in a conflict, (2) conflict group - the high-level description of a conflict, (3) conflict perspective - assigned to each actor based on their relative maneuvering, (4) the actor role - either the initiator of some surprising action that leads to a conflict or the responder that is exposed to the surprising event, and (5) contributing factors - factors that in combination directly contributed to the event outcome. Each of the first 4 layers will be discussed in detail in this section. The 5th layer, the contributing factors, will be discussed in the following section.
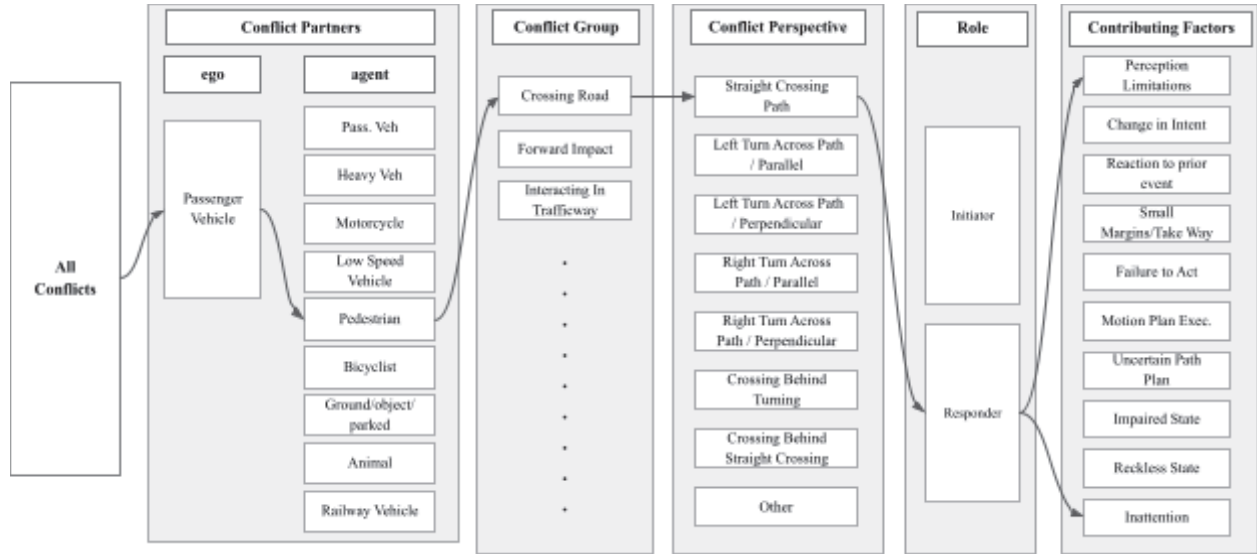
Figure 1. Illustrative example of 5 layers of the conflict typology for a pedestrian straight crossing path conflict.

One important characteristic of the current conflict typology is that a single conflict always involves two partners. One of those partners may be a non-vehicle, such as fixed objects, a road edge or the ground, resulting in what many other typologies refer to as a "single vehicle" conflict type. We find it useful and necessary, however, to retain that all conflicts have exactly two participants (i.e., conflict partners), even if one of those partners is not a road user. A chain of conflicts (each with their own unique conflict type) can occur in succession that can involve more than two parties. This partitioning by conflicts between pairs of actors fits well into the organization of most crash databases, which present collisions as a sequence of events.

Conflict Partners. The collision partners define the type of road users that enter into a conflict. Table 1 describes the collision partners in the conflict typology. The approach for grouping conflict partners was to aggregate road users that have similar maneuver capability and perception qualities. For example, traditional motorcycles and all terrain vehicles often have capabilities to travel at much higher speeds and generally have more maneuverability compared to low speed vehicles such as low powered golf carts. Ambulatory humans, those using wheelchairs, or those using personal means of conveyance have similar perception qualities as pedestrians, although those on personal means of conveyance, such as skateboards, may be able to travel at much higher speeds than ambulatory pedestrians. As this example shows, there can be some variability within conflict partner groups. The analyst may choose to further separate these conflict groups if a particular analysis warrants.

Table 1.
Conflict partners and brief description.

Conflict Partner	Definition
Light vehicle	Sedans, coupes, and station wagons intended to carry passengers and those vehicles pulling light trailers. Additionally includes two-axle, four-tire vehicles, such as pickups and vans.
Heavy vehicle	Buses and other two-plus axle, one-plus unit trucks
Motorcycle	Motorcycles, mopeds, three-wheel motorcycles, all-terrain vehicles, and other recreational vehicles not classified as a low speed vehicle.
Low Speed Vehicle	Powered three-plus wheeled vehicles capable of a maximum speed of less than or equal to 25 mph.
Pedestrian	All non-cyclist human actors, including: ambulatory, wheelchair using (powered and non-powered), and non-ambulatory (e.g., skateboarders)
Bicyclist	Bicyclists, motorized/electric bikes, motorized scooters, and other non-pedestrians on people moving devices that navigate within the flow of all other road user traffic.
Ground/Objects/Parked Vehicle	Contact with the road surface, stationary or moving inanimate objects or structures present, or parked vehicles on or off the trafficway.
Animal	Any living non-human animal variation that may potentially enter a trafficway and poses property damage and/or injury risk.
Railway vehicle	A vehicle that travels on rails.

Conflict Group. The conflict group provides a high-level description of the conflict configuration based on similar geometrical, environmental, and severity related considerations. It describes what the conflict partners were doing just prior to entering the conflict. To adequately describe conflict groups, we will introduce some additional definitions:

Trafficway
"Any right-of-way designated for moving persons or property from one place to another, including the surface on which vehicles normally travel, plus the shoulders, painted medians, and painted gore areas at grade with the roadway".

NOTE 1: The trafficway also includes parking lanes and parking areas (e.g., parking lots, driveways).

NOTE 2: The trafficway is bound by the outer edges of the shoulder or by raised roadside barriers (e.g., curb, guardrail, pylon) and thus does not include raised medians, grassy medians, sidewalks, etc." (ISO/TR 21974-1, [17])

Roadway
"The portion of a trafficway that is designed and ordinarily used for vehicular travel, including all designated or implied travel lanes (through lanes, turn lanes, acceleration and deceleration lanes), but not

shoulders, painted (whether usable or not), medians of any type, roadsides, gore areas, etc., that are of a similar road surface to the parking lanes, parking areas, or driveways" (ISO/TR 21974-1, [17]).

NOTE 1: Some lanes of travel can be partially or fully blocked by parallel parked vehicles during certain times of day. These lanes are part of the roadway when there are no parked vehicles (i.e., traffic is using the lanes) and not part of the roadway when being used as a parallel parking area.
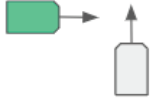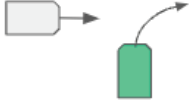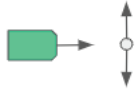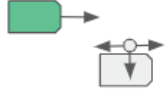
Roadway Actors
A roadway actor is any non-parked stationary or mobile actor that actively navigates along roadways within the flow of vehicle road users. Roadway actors include passenger vehicles, heavy vehicles, motorcycles, low speed vehicles, and cyclists, as defined in the previous section.

An important distinction for the conflict groups is between roadway actors and non-roadway actors. As defined above, roadway actors are using the space dedicated for vehicle traffic. Non-roadway users are traveling in space not dedicated for vehicle traffic, such as sidewalks or unpaved areas adjacent to the road. Conflicts between non-roadway actors with roadway actors can occur when the latter enters the roadway. Pedestrians are most often non-roadway actors, but many actor types can be either roadway actors or non-roadway actors. For example, cyclists, motorcyclists, low speed vehicles, and even motor vehicles can be driving off the roadway (e.g., on a sidewalk) and enter the roadway to be involved in a conflict. For example, a light vehicle driving on a sidewalk into a crosswalk can have many of the same contributing factors as a pedestrian crossing from a sidewalk, and thus it is appropriate to aggregate these types of conflicts together. We use roadway actor to make this distinction to avoid confusion with the term roadway user, which in many other contexts includes all individuals that use the road system, including pedestrians entering the roadway.

Table 2.
Conflict Groups and Short Descriptions. A 🚐 symbol means the conflict group is relevant for conflicts between roadway actors. A 🚶 symbol means the conflict group is relevant for conflicts between a roadway actor and a non-roadway actor.

Conflict Group	Picture	Description
Single Vehicle (SV) 🚐🚶		Includes all actions (or lack thereof) where the ego vehicle is traveling in a trafficway but then experiences an in-trafficway interaction without a conflict partner (e.g., a rollover event) or an off-trafficway interaction (e.g., a road departure).
Front-to-Rear (F2R) 🚐		Involves one road user interacting with another road user in the same direction and same travel lane.
Same-Direction Lateral Incursion (SDLI) 🚐		Occurs when two roadway actors are traveling in the same trafficway but in initially different travel lanes at the time of the initial interaction due to lateral incursion by some actor.
Same-Direction Prior Circumstances (SDPC) 🚐		Involves two roadway actors operating on the same trafficway in the same direction when one road user performs a lateral evasive action, experiences loss of control, or is involved in a prior collision that results in an interaction with the other road user.

Conflict Group	Picture	Description
Opposite Direction Lateral Incursion (ODLI) 🚙		Occurs when a non-turning actor operating in the trafficway's intended travel direction interacts with another actor that is operating opposite of the travel direction in the same trafficway.
Opposite Direction Prior Circumstances (ODPC) 🚙		Involves two roadway actors traveling in opposite direction trafficways in their respective trafficway's direction of travel when one road user performs a lateral evasive action, experiences loss of control, or is involved in a prior collision that results in an interaction with the other road user.
Turn into Path Opposite Direction (TIPOD) 🚙		Occurs as a result of one actor changing vehicle-operated trafficways via a turning maneuver and interacting with another actor, where one of these actors is operating in the opposite direction of the trafficway's direction of travel.
Intersection Cross Traffic (ICT) 🚙		Involves interactions that occur as a result of both actors changing or crossing over trafficways, and where the two actors cross paths with one another.
Intersection Turn Into Path (ITIP) 🚙		Involves interactions that occur as a result of one of the actors moving on to a trafficway via a turning maneuver into the path of another actor that is operating in the trafficway being turned on to.
Perpendicular Direction Prior Circumstances (PDPC) 🚙		Involves two roadway actors operating on crossing roadways that interact with one another following some lateral evasive action, prior loss of control, or prior collision.
Crossing Road 🚶		Involves interactions between an actor moving along a trafficway and another actor crossing that trafficway (while not traveling along or onto another trafficway).
Forward 🚶		Involves vehicle actors moving in the forward direction and interacting with a non-road user conflict partner in the trafficway that is not attempting to cross the road.
Interacting in Trafficway 🚶		Occurs when a forward moving ego is on a trafficway and interacts with an agent that is in the trafficway and moving around, entering, exiting, or interacting with an immediately adjacent vehicle or object.
Backing 🚙 🚶		Includes all interactions where at least one road user is moving in reverse.
Miscellaneous Circumstances		Events that do not fit into the aforementioned conflict groups, and are intended to cover all abnormal circumstance interactions that pose some collision risk.
Other/Unknown		All remaining events that do not fit into a conflict group, but that may need future considerations and those cases that have insufficient information to adequately determine the conflict group.

Conflict Perspectives. The conflict perspectives are subcategories that belong to the conflict groups described in the previous section. Unlike the conflict group that describes an interaction between one or two actors, conflict perspectives apply to one of the actors in a conflict, and describe the specifics of the maneuvers more granularly. For example, an Intersection Cross Traffic conflict perspective is left turn across path, opposite direction, where one agent is the straight traveling vehicle and the other agent is the left turning vehicle. This current paper will not cover a full suite of conflict perspectives as they are too numerous and evolve as new data is compiled and new analysis is performed.

Conflict Role. A conflict, as defined in this framework, involves either one or two actors. In conflicts between two actors, there is an initiator and a responder role, which are defined in more detail below.

> *Initiator*
> The road user in a potential conflict that first initiates a surprising behavior [23] that another road user (the responder) would need to act upon to avoid entering into a conflict. Here we are using surprise to mean a violation of an initial expectation of how a road user should behave given the circumstances.
>
> NOTE 1: The surprising behavior of the initiator may involve both actions (e.g., a lead vehicle braking suddenly) and non-actions (e.g., continuing straight in a turn lane)
>
> NOTE 2: The initiation of a conflict is orthogonal to legal considerations of fault (e.g., in a front-to-rear collision where a lead vehicle brakes suddenly for a child entering the street and is being hit by a tailgating following vehicle, the lead vehicle is the initiator while the legal fault would typically be entirely assigned to the follower).
>
> NOTE 3: Surprise is defined from a third-party perspective, relative to prior expectations produced by a generative model that accurately represents the statistical properties of the traffic environment where the conflict occurs. Thus, surprising behaviors are those that violate the expectations generated by the generative model, irrespective of the surprise actually experienced by the responder or the initiator.
>
> NOTE 4: A road user can play the role of both initiator and responder in a chain of conflicts. For example, consider a scenario where a vehicle A enters the road at an intersection causing a vehicle B to brake which, in turn, causes a vehicle C, which follows B, to brake. Following ISO TR 21974-1 [17], this situation can be divided into two separate conflicts, Conflict 1 (the intersection conflict) and Conflict 2 (the front-to-rear conflict). In Conflict 1, A is the initiator and B the responder. In Conflict 2, B is the initiator and C is the responder. One can also imagine a different scenario where both B and C have to respond to the surprising behavior of A to avoid the conflict. In this case, A is the initiator in both conflicts, B the responder in Conflict 1 and C the responder in Conflict 2.
>
> *Responder*
> The road user in a potential conflict that would be required to act upon a surprising behavior initiated by another road user (the initiator) in order to avoid entering into a conflict.
>
> NOTE: The responder does not necessarily have to exhibit a response for the definition to apply. It suffices that the surprising action of the initiator puts the responder in a situation where they need to respond to avoid entering into a conflict (assuming that the initiator does not take any further evasive action).

Contributing Factors Model of Conflicts

Based on the conflict model presented in the previous section, we aim to develop contributing factors for traffic conflicts based on previous work, in particular Piccinini et al. [22] (but see [24 - 26] for related work). The basic conflict model is presented in Figure 2. In this model, a conflict is the result of a conflict initiating behavior from the initiator, a non-nominal response from the responder, or a combination of both. Examples of conflict initiating behaviors include a vehicle running a red light at an intersection or a pedestrian jaywalking. Examples of non-nominal response behaviors include delayed responses (relative to a reference human reaction model; e.g., [27]) or a complete lack of response.

The goal of the conflict causation analysis is then to identify factors *contributing* to the conflict initiating behavior and/or the non-nominal response. Contributing factors are defined in terms of insufficient and necessary conditions for the observed conflict initiating behavior or non-nominal response to occur. That is, the factor may not by itself have been sufficient to cause the conflict but the conflict would not have occurred if the factor was not present. Factors contributing to conflict initiating behaviors may include surprising or unexpected behaviors from other road users, occlusions or reduced visibility conditions. Non-nominal response is the behavior of the responder that contributes to the responder entering a conflict state, such as a delayed response to initiate avoidance maneuvers or an inappropriate avoidance maneuver. Examples of factors contributing to non-nominal responses include inattention, drowsiness or reduced visibility.
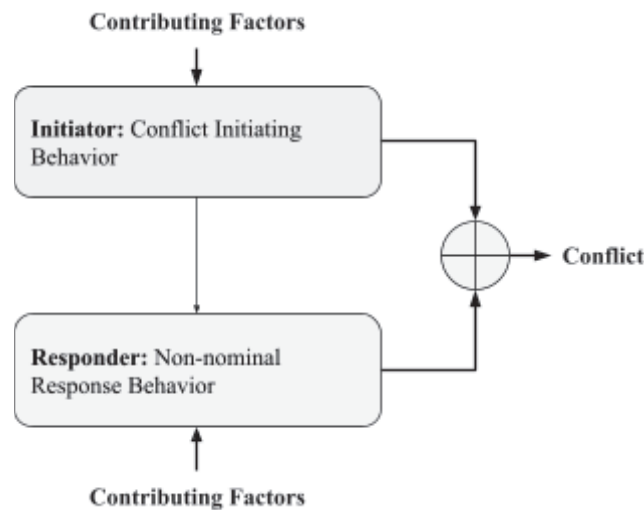
Figure 2. Conflict Model for Contributing Factors.

Assigning contributing factors in crashes is challenging as the number of factors that could be assigned as contributing to an event is potentially infinite. Thus, the assignment of contributing factors always depends on the purpose of the analysis. One could theoretically consider every minutiae of an event, such as prior experiences by actors, demographics-related features, or familiarity with an area. However, such seemingly minor features would end up generating an infinite array of clusters that say little individually about the performance of an ADS. Another difficulty is determining the presence of "internal" cognitive contributing factors. In most crashes, there is no possibility to interview or observe participants to try to determine their thinking or focus prior to a crash. Often, video and recorded vehicle data are the only data sources available. Therefore, to practically assign contributing factors, guidelines must be developed. Two criteria are proposed for identifying case-specific contributing factors to help limit the granularity of the noted factors.

The first criteria is to restrict the contributing factors to physically and easily observable behaviors and environmental features at the time of the event from either ego or agent perspective. This criteria helps classify the

events by features that can be readily detected and objectively measured from existing non-ADS data (e.g., conflict and collision data sets) and ADS data.

The second criteria is to only select factors deemed to meet the INUS conditions proposed in the philosophy literature by authors such as J. L. Mackie [28]. INUS stands for conditions that are "**i**nsufficient but **n**on-redundant parts of a condition which is itself **u**nnecessary but **s**ufficient for the occurrence of the effect". An example of applying the INUS conditions would be to consider the causes for a house burning to the ground. INUS conditions for this outcome could be a short circuit in wiring in the house, the proximity to flammable materials, and a lack of available firefighters. Many other causes could result in the same outcome (e.g., a meteorite falling on the house), but the lack of any of the aforementioned factors could prevent the outcome from occurring. In the traffic conflict application we are considering here, the contributing factors are things that are necessary to produce an observed conflict-initiating action or response failure that also can meet the first laid out criteria of being externally observable.

Like the conflict groups that can be further decomposed into conflict perspectives, we believe it is useful to have a hierarchical structure for contributing factors. Unlike the conflict groups and perspectives which are mutually exclusive for a given conflict, there can be multiple contributing factors that are present for both the initiator's conflicting initiating behavior and the responder's non-nominal response. One of the difficulties with generalizing previous causal models to use in many conflict types is that they develop sophisticated dependencies between different contributing factors. In this study, we strive to introduce a level of aggregation for contributing factors that can be applied across data sources with different types of data available (e.g., retrospective crash databases and naturalistic driving data with video) and meet the overall goal of the conflict typology of grouping conflicts that have common characteristics in studying safety impact.

To accomplish this high-level grouping of contributing factors, the conflict model, principles of observability and INUS introduced previously were applied to contributing factors that are commonly available in crash databases and observable from video and/or sensor data from NDSs. A key distinction from previous studies, such as the many factors reported in crash studies like the the National Motor Vehicle Crash Causation Survey, NMVCCS [29], was that the contributing factors should be directly observable from the conflict initiating behavior of the initiator or non-nominal response of the responder. Factors such as hours of rest or medications taken are not observable directly, but could indirectly be observed as an impaired state by swerving of the vehicle or eye closure captured on video. Clearly, some contributing factors are difficult to reliably determine from retrospective crash data without video recordings (e.g., inattention, occlusions). Even if underreported, most collision databases do include fields for noted inattention (either through violations of state cell phone laws or otherwise). Many of the contributing factor groups at least can be partially inferred from descriptions of scenarios in crash data. For example, some crash scenarios will mention occlusions (e.g., "dashed out"). Grouping into high level contributing factors groups has a benefit of facilitating comparison between crash data with low precision/availability of contributing factors and NDS with higher (but not always complete) availability of contributing factors .

Table 3 lists high-level contributing factor groups with descriptions and example observable indicators. Like the conflict groups and perspectives, these causal factor groups could be further decomposed for specific analyses purposes. The results presented later in this paper, however, demonstrate the utility of grouping contributing factors into the proposed groups. It should be noted that the conflict model and contributing factor group definitions do not require the initiator and responder to have a single or mutually exclusive contributing factors. In practice, there are often multiple contributing factors that in combination contribute to the occurrence of a conflict. For example, inattention and/or an impaired state may contribute to a failure to react. The presence of these different contributing factors, however, may dictate different analyses. For example, when determining the prevalence of a certain type of collision to use for a benchmark to define reasonable human performance, one may want to exclude events that involve impaired state and reckless state.

Table 3.
Description of Contributing Factor Groups.

Contributing Factor Groups	Contributing Factors Description	Example Observable Indicators
Limited Visibility	Limited visibility between conflict partners caused by occlusions and/or environmental factors	Observable regions based on lines of sight. Environmental conditions such as weather, darkness.
Change in Intent	Surprising action, intentional / unintentional change of mind, or unpredictable / non-legible behavior.	Actors that act in ways that violate the predictions of generative models of nominal driving behavior.
Reaction to Prior Event	Reactions to prior conflicts & surprising events	Actors from previous conflicts that create surprising conflicts or events that then cause the initiator to respond, creating a new conflict.
Small Margins	Adopting too small safety margins (following too closely), taking way or allowing for small margins that force others to make space, or unintentionally misjudging gap sizes	Road users are forcing their way to make space, or operate with small margins (either intentionally or unintentionally)
Failure to Act	Failure to act on changes in motion of other road users or change in traffic signals	Road users not responding to the change in motion by others / traffic signals
Motion Plan Failure	Failure in execution of motion / plan (fall, slip, loss of control)	Road users executing plans that might result in loss of control (slippery, difficult to control). Traveling too fast for conditions that results in loss of control or unintended path.
Uncertain Path Plan	Uncertain or unpredictable path planning due to external factors (unstructured environments / difficult to make the right decision)	Uncertainties in the road scene, leading to uncertain path planning for all (e.g., construction, emergency response scene)
Impaired State	Impaired state (DUI/drowsy/repeated inattention/overly cautious behavior)	Road users that are unable to keep a steady course, speed profile, walk straight
Reckless State	Reckless driving state	Road users that are speeding, driving on the shoulder of a road, far from nominal behavior. Includes emergency vehicles operating in emergency situations.
Inattention	Failure in attention to the appropriate area	Not looking in the direction of the conflict (based on head pose, head or eye direction)

RESULTS

To demonstrate the utility of applying the conflict typology proposed in this paper to multiple types of safety data, this results section presents an example analysis of retrospective crash data and human naturalistic crash and near-crashes. First, all layers of the conflict typology are applied to retrospective, police-reported crash databases. The first 3 layers of the conflict typology (actor types, conflict groups, conflict perspectives) are most similar to past conflict typologies that have been primarily used for analyzing retrospective crash databases. These results examine whether, like past typologies, the conflict typology provides insights into the characteristics of crashes in subsets of the crash populations (e.g., in a dense urban ride-hailing environment). Second, we apply the conflict role and causal factors layers to the retrospective crash data. Traditionally, this has been difficult due to the limited information available from retrospective crash data. We then examine whether analyses of the conflict role and causal factors can be done. Finally, we analyze the video data from an NDS dataset to assign conflict role and contributing factors, to enable a comparison of the NDS and retrospective crash data.

Conflict Partners, Collision Groups, and Collision Perspectives

This study analyzed two nationally representative crash databases maintained by the National Highway Traffic Safety Administration: the Crash Report Sampling System (CRSS) and the Fatality Analysis Reporting System (FARS). The CRSS crashes are a nationally representative sample of police-reported collisions that occurred on public roadways in the U.S. Weights are applied to the sampled collisions so that the summed counts correspond to the number of collisions annually in the U.S. FARS is a census of fatal collisions that occur on public roadways. This study examined CRSS and FARS years 2016 to 2020. The 2016 case year was the first year of enhanced pedestrian and bike data reporting and the 2020 case year is the latest year where data was available at the time of writing.

To examine the police-reported crashes in this type of operating environment, we selected collisions from FARS and CRSS with the following properties:

- Involving at least one passenger vehicle (i.e., car, light truck, or van).
- Those that did not have inclement weather or surface conditions (e.g. snow, ice, blowing sand, heavy fog). Rain and wet surface condition was included because the amount of rain is not known.
- Those crashes where at least one vehicle was driving on a road with a speed limit up to 45 mph. Collisions between vehicles traveling on a road with speed limit greater than 45 mph were included if another vehicle was traveling on a road with speed limit 45 mph and below. Speed limits are often missing from these crash databases. If the speed limit was missing, the road type (undivided vs divided) and number of lanes was used to infer which road types would likely be included in the ride-hailing ODD.
- The case was classified as occurring in an urban location (RUR_URB = 2 in FARS and URBANICITY = 1 in CRSS)

To demonstrate the potential effects of collision severity on crash trends, the CRSS data was split into two groups based on the reported KABCO (that is, police reported) collision severity score. "CRSS - A+K" severity were those collisions with either a maximum reported severity of "killed" (K) or "incapacitating" (A). "CRSS - Minor" were those collisions where the maximum reported severity was between "minor" (B), "possible" (C), or "no apparent" (O) injury.

Table 4 summarizes the total number of collisions extracted from CRSS and FARS that met the urban ride-hailing environment conditions. This ride-hailing environment accounted for 41% of minor severity collisions (CRSS - Minor), but fewer severe (32% of CRSS - A+K) and fatal (22% of FARS) collisions.

Table 4.
Considered Cases from CRSS and FARS 2016 - 2020 for a Urban Ride-hailing Environment (passenger vehicle, non-inclement weather, up to 45 mph speed limit)

	Total			Urban Ride-hailing Environment		
Count Description	**CRSS - Minor**	**CRSS - A+K**	**FARS**	**CRSS - Minor**	**CRSS - A+K**	**FARS**
Number of Cases	221,325	31,891	171,972	91,570 (41%)	11,215 (35%)	38,435 (22%)
Weighted Cases	30,044,252	885,436	171,972	12,369,395 (41%)	282,247 (32%)	38,435 (22%)
Average Annualized Weighted Cases	6,008,850	177,087	34,394	2,473,879 (41%)	56,449 (32%)	7,687 (22%)

To demonstrate how the *conflict partner* layer is used, Figure 3 shows the proportion of each conflict partner group in urban ride-hailing environment collisions. In minor collisions, vehicle-to-vehicle partners make up almost three quarters (74%), whereas in serious collisions vehicle collisions with pedestrians, fixed objects, and motorcyclists are more common (between 50% and 65%). This results shows that differences in crash severity can be observed by grouping by actor types. Vulnerable road users (especially pedestrians and motorcyclists) are overrepresented in serious and fatal collisions compared to minor collisions.
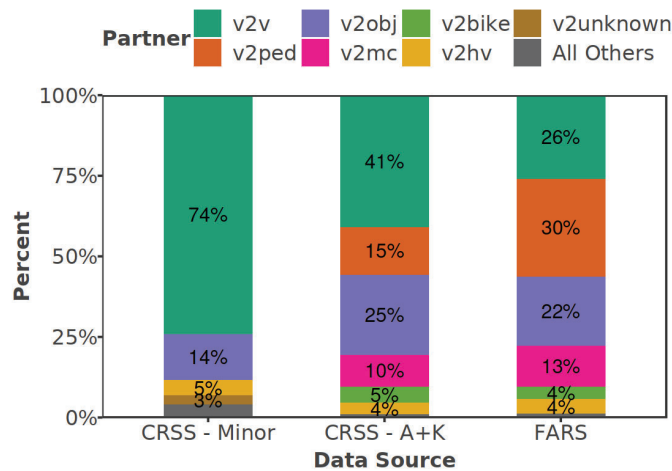

Figure 3. Conflict Partners for Urban Ride-hailing Environment Collisions from CRSS and FARS 2016 - 2020.

To demonstrate the use of the *conflict groups* layer, Figure 4 shows the distribution of conflict groups by data source for an urban ride-hailing environment. Minor collisions have much higher occurrence of front-to-rear (F2R) collisions compared to serious collisions. Serious and fatal collisions have a higher occurrence of single vehicle (SV) and crossing road (CR) collisions compared to minor collisions. This result shows that grouping by collision groups can also provide useful insights into traffic safety trends.
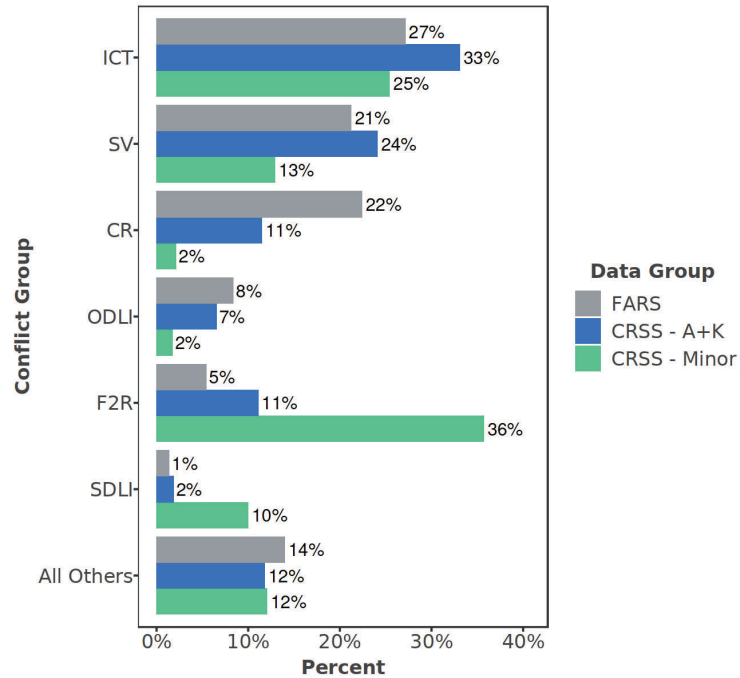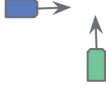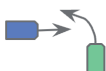
Figure 4. Distribution of Conflict Groups by Data Source in an Urban Ride-Hailing Environment from CRSS and FARS 2016 - 2020.

To demonstrate the use of the *conflict perspectives* layers, Table 5 shows the most frequent conflict perspectives in multi-agent (i.e., excluding the vehicle-to-object collision partner group) from fatal collisions in FARS for the urban ride-hailing environment. The percentages in the table are the proportion of each conflict perspective within the collision partner group (i.e., columns sum to 100%). For the conflict perspectives, the passenger vehicle involved in the collision is presented as the ego role. For example, in vehicle-to-motorcycle collision partners, 42% of collisions were with a motorcyclist going straight and the passenger vehicle turning left across path.

Table 5.
Primary Collision Perspectives in Multi-agent Fatal Collisions from FARS 2016 - 2020 in the Urban Ride-hailing Environment.

Conflict Mode	Picture	Perspective	Vehicle-to-X Conflict Partner				
			Ped.	Veh.	MC	HV	Bike
ICT: Straight Crossing Path (for all but ped.) or CR: Straight Crossing Path (for ped)		SCP from Right (blue)	68%	12%	7%	9%	40%
		SCP from Left (green)		12%	6%	14%	
ICT: Left Turn Across Path, Lateral Direction (for all by ped.) or CR: Left Turn Across Path, Perpendicular Direction (for ped.)		ALTAP/LD (blue)	0%	5%	0%	0%	0%
		ELTAP/LD (green)	0%	5%	13%	11%	0%
ICT: Left Turn Across Path, Opposite Direction (for all but ped.) or CR: Left Turn Across Path, Parallel Direction (for Ped.)		ALTAP/OD (blue)	0%	9%	2%	4%	1%
		ELTAP/OD (green)	4%	9%	42%	7%	3%
ODLI: Lateral Incursion (for all but ped.) or FWD: Opposite Direction (for ped.)		ALO (blue)	0%	10%	3%	2%	0%
		ELO (green)	1%	10%	2%	19%	0%
F2R: Lead Going Straight (for all but ped.) or FWD: Same Direction (for ped.)		ALGS (blue)	5%	4%	4%	11%	24%
		ELGS (green)	0%	4%	5%	4%	0%
All Others			22%	20%	16%	19%	32%
Total			100%	100%	100%	100%	100%

The results in this subsection demonstrate that the first 3 layers of the conflict typology (actor types, conflict groups, conflict perspectives) can provide insights into the characteristics of crashes in subsets of the crash populations. As an example, serious injury and fatal collisions involve a different proportion of actor types (more vulnerable road users) compared to minor collisions in a typical urban ride-hailing environment. We also show that for for fatal collisions in urban ride-hailing environment, 5 collision perspectives account for a majority of collisions (between 68% and 84%).

Conflict Role and Contributing Factors

As shown in Table 5, vehicle-to-pedestrian crossing road collisions where the vehicle is going straight account for a large proportion of serious injury and fatal collisions in the urban ride-hailing environment. As mentioned in the Methodology section, it can be difficult to determine some contributing factors from retrospective collision databases due to a lack of video or other sensor data that can be used to determine the behavior of actors. These crash databases, however, are important data sources to consider, as most NDS data sources lack a large number of collisions, and have few or no serious injury or fatality collisions. How to reconcile these high-severity, yet low fidelity, data with the higher fidelity, yet low severity, data from NDS is an unanswered research question. To demonstrate this difficulty, we first applied the conflict role and contributing factor groups proposed in this paper to pedestrian crossing road conflicts from CRSS and FARS and then compared these results to contributing factors observed in an NDS.

The PEDCTYPE variable is a new addition to CRSS and FARS since case year 2016. The categories of PEDCTYPE are a combination of conflict perspectives and contributing factor groups that attempt to describe which actor (the pedestrian or vehicle) initiated the conflict and the maneuvers taken by both actors. The PEDCTYPE values that are applicable to the pedestrian crossing road, straight crossing path conflict perspective are: "Motorist Failed to Yield", "Pedestrian Failed to Yield", "Dash Out", "Dart Out", "Multiple Threat", "Trapped" and "Crossing Expressway". Table A1 in the appendix lists the full PEDCTYPE variable descriptions for categories used in Table 6 taken from the FARS and CRSS coding manual [30]. All of the PEDCTYPE groups except "Motorist Failed to Yield" were assigned the vehicle as the responder role. Contributing factors were assigned using the primary contributing factors that are associated with the behavior described in the PEDCTYPE variable. For example, the Dart Out scenario is when the pedestrian enters the travel lane of a vehicle from behind some occlusion, which is directly related to the change in intent (surprising) and limited visibility (occlusion) contributing factor groups. The potential contributing factor groups listed are those that are most likely and/or prominent to be present based on the physical scenario described in the PEDCTYPE variable. Other contributing factors can also be present independent of the scenario, such as impaired state.

To show the application of the *conflict role* and *contributing factors* to retrospective crash data, Table 6 shows the proportion of pedestrian crash types (variable PEDCTYPE) in vehicle-to-pedestrian crossing road collisions from CRSS and FARS where the vehicle was in the responder role. Of all pedestrian crossing road collisions, 26% of CRSS - Minor, 14% of CRSS - A+K, and 10% of FARS collisions had the "Motorist Failed to Yield" PEDCTYPE, and thus the vehicle assigned the initiator role. The most common pedestrian crash type in all data groups was pedestrian failed to yield, followed by motorist failed to yield. The CRSS groups, both minor and A+K, had a higher proportion of dash out and dart out crash types compared with the FARS data. Finally, the multiple threat and trapped crash types were the least frequent.

Table 6.

Pedestrian Crash Type Variable from CRSS and FARS 2015 - 2022 for Pedestrian Crossing Road Collisions with the Vehicle in the Responder Role.

Pedestrian Crash Type (PEDCTYPE)	Vehicle Role	Primary Contributing Factor Group	CRSS - Minor	CRSS - A+K	FARS
Pedestrian Failed to Yield	Responder	Change in Intent	56%	66%	82%
Dash Out	Responder	Change in Intent	30%	25%	14%
Dart Out	Responder	Limited Visibility, Change in Intent	12%	7%	3%
Multiple Threat	Responder	Limited Visibility, Change in Intent	1%	1%	1%
Trapped	Responder	Change in Intent	< 1%	1%	< 1%
Crossing Expressway	Responder	Change in Intent	< 1%	1%	1%
Total			100%	100%	100%

As noted above, naturalistic driving data provides a unique opportunity to record video of potential conflicts, which makes determining contributing factors easier compared to retrospective crash databases such as CRSS and FARS. This study examined near-crash events from the Strategic Highway Safety Research 2 (SHRP-2) Naturalistic Driving Study (NDS) [16]. The SHRP-2 NDS included over 3,000 personally owned vehicles that drove over a 3-year period in 6 study locations in the U.S. that resulted in a dataset with almost 50 million miles of data collected. A set of 57 near-crash events from the SHPR-2 NDS were examined. These events were all near-crash events that featured a pedestrian in the crossing road conflict group where the pedestrian was in the initiator role. The video from all pedestrian near-crash events from SHPR-2 were reviewed to determine the pedestrian's role. The contributing factors related to the pedestrian's initiating behavior were also determined by video review. The contributing factors related to the non-nominal response behavior of the responder (vehicle driver) could have also been determined as the SHRP-2 study had in-vehicle video recording. This was not done for this study, however, due to the additional burden necessary to view the potentially identifying information.

To show the application of the *contributing factors* groups to NDS data, Figure 4 shows the contributing factor groups present in pedestrian initiated crossing road conflicts from the SHRP-2 NDS. The figure is an "upset" plot, which shows a histogram (top) for each combination of contributing factors (bottom center). Multiple contributing factors can be present in any given conflict. The histogram at the bottom left shows the frequency of each individual contributing factor in all events. The most frequent contributing factor was perception limitations, which was present in 72% of conflicts and as the sole contributing factor in 33% of conflicts.
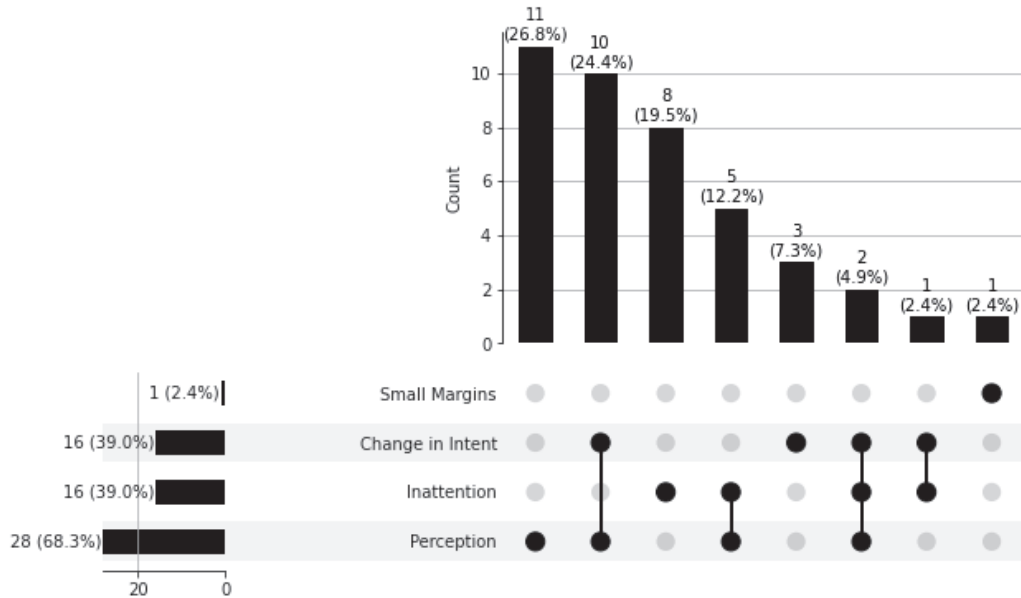
Figure 4. Combinations of Contributing Factor Groups Present for the Pedestrian in the Initiator Role in Crossing Road Near-crashes from the SHRP-2 Naturalistic Driving Study.

Table 7 breaks down the SHRP-2 near-crash events by contributing factor groups into subgroups and attempts to relate the contributing factor to the pedestrian crash type variable from CRSS and FARS presented in Table 6. In general, the contributing factors in the NDS near-crashes match the crash data. Pedestrian failed to yield (due to limited visibility or inattention) made up 37% of NDS cases compared to between 56% and 82% of the crash data. The next most frequent contributing factors in the NDS data were suddenly entering traffic (dart-out and dash-out, 22%) compared to between 17% and 42% of the crash data. One difference, however, was that the NDS data had a large number of events that were related to the multiple threat scenario, where yielding behavior of one vehicle prompts the pedestrian to cross creating a conflict with a vehicle traveling in the same direction (24% of NDS events). This multiple threat scenario made up only 1% of the crash data, across all severities.

Table 7.
Contributing Factor Groups and Subgroups and their Relationship to the CRSS/FARS Pedestrian Crash Type.

Contributing Factor Groups	Subgroup	Approximate Pedestrian Crash Type	Description	N (%)
Limited Visibility	Environmental Visibility	Pedestrian Failed to Yield	The pedestrian enters a multi-lane road when the conflict partner is far away and traveling at a high speed. The pedestrian continues to cross even as the ego vehicle continues to travel. Other environmental factors such as darkness or rain may be present.	7 (17%)
	Occlusions (static and dynamic)	Dart-out	An in-transport vehicle (dynamic occlusion) or static objects (e.g., not in-transport vehicles, bushes/trees, structures) make an occlusion between the pedestrian and conflict partner.	4 (10%)

Limited Visibility & Change in Intent	Occlusions (dynamic and static), Other Agent Prompts Crossing	Multiple threat	A pedestrian signals their intent to cross, and some approaching actor in the scene slows to yield to the pedestrian or in a way that mimics yielding (e.g., making a right turn). This slowing behavior prompts the pedestrian to start to cross. The yielding vehicle causes a dynamic occlusion between the pedestrian and conflict partner vehicle traveling in the same direction as the yielding vehicle.	10 (24%)
Inattention	Looking at Other Actors	Pedestrian Failed to Yield	The pedestrian is focusing on other actors in the scene (vehicles, other pedestrians) or at another location (e.g., their destination), causing the pedestrian to not look in the direction of the conflict partner.	4 (10%)
	Looking at object on their person		The pedestrian is interacting with an object (e.g., looking at a cell phone in hand, reaching for objects inside of a bag), causing the pedestrian to not look in the direction of the conflict partner.	2 (5%)
	Not looking, other		The pedestrian does not check for traffic in the direction of the conflict partner.	2 (5%)
Limited Visibility & Inattention	Occlusion (static and dynamic) & Looking elsewhere	Dart-out	Static objects (e.g., not in-transport vehicles, bushes/trees, structures) create an occlusion between the pedestrian and conflict partner. Further, the pedestrian is looking at a pedestrian on the other side of the street, making them unaware of the potential conflict with a conflict partner.	5 (12%)
Change in Intent	Sudden change in velocity	Dash-out	A pedestrian enters the path of a conflict partner, then suddenly changes their velocity (slow down, speed up, change direction) violating the expectation of the conflict partner and entering into a conflict.	3 (7%)

The results of this subsection demonstrated how the conflict role and contributing factors can be applied to both crash data and NDS data. There are challenges with determining conflict role and contributing factors from retrospective crash data because some information is either missing or may suffer from underreporting. These results demonstrated, however, that in certain collision modes and data sources, at least a partial assignment of conflict role and contributing factors can be done for retrospective collision databases. The conflict role and contributing factors can also be applied to NDS data, where the conflict role and contributing factor information can be observed from the video recordings of conflicts. This ability to apply the conflict role and contributing factors to both data sources allows for comparison between data sources of different quality, like retrospective crash and NDS data.

DISCUSSION

This paper presented a novel conflict typology that describes the conflict partners, groups, perspectives, role, and contributing factors. The paper describes the definitions and framework used to derive these layers of the conflict typology. The conflict perspectives, which are the further decomposition of the conflict groups into more specific

maneuver types, were not presented in great detail in this paper. As they currently stand, there are over 100 conflict perspectives. Although all of the current perspectives could have been listed with short narrative descriptions, this provides limited use to researchers. A full publication and/or application of the conflict perspectives is the topic for future work.

Although the results presented in this paper were exclusively human crash and near-crash data, the conflict typology has been developed to also be applicable to describe ADS conflicts, even if there is no human driver in the ADS vehicle. The study of human conflict types and contributing factors is useful for ADS safety evaluations because ADS will continue to operate in environments with human participants, who will likely continue to initiate conflicts with ADS in similar ways that the humans initiate conflicts with each other today. There are also likely conflict types and/or contributing factor groups that will become more frequent for ADS when compared to human drivers. Many of the conflict actors, groups, perspectives, and roles apply, however, equally to human driven vehicles and ADS operated vehicles. Although many of the contributing factor groups are applicable to both human and ADS operated vehicles (e.g., perception limitations, change in intent), some contributing factor groups may manifest themselves in different ways or be entirely not applicable to ADS equipped vehicles. Most notably, whereas humans must choose where to apply their attention, ADS can monitor their surroundings in multiple directions simultaneously. For example, the contributing factor of inattention may not be applicable to an ADS. Because the contributing factors focus on describing the observable behaviors of actors and not internal reasoning or states of actors, we demonstrated in this study that the contributing factors can be successfully applied to conflicts involving an ADS operated vehicle.

Notably, the results of this study showed that there were different contributing factors in pedestrian crossing road collisions from CRSS and FARS than observed in the SHRP-2 near-crash events. Specifically, the multiple threat scenario made up under 1% of the CRSS - A+K and FARS data and 24% of the SHRP-2 events. Further research is needed to determine if this difference is in fact a difference between conflicts (near-crashes) and serious outcome collisions, or if there is underreporting of this type of scenario in the crash report data. Regardless of the potential differences in observed proportions of contributing factors in these data sets, the results of this study showed that the entire conflict typology, including conflict role and contributing factors, can be applied to both retrospective crash and NDS data. This enables comparisons between different data sources. The PEDCTYPE variable in CRSS and FARS compactly provide pertinent information regarding the conflict role and contributing factors. In other conflict types, like those between vehicles, other types of variables like traffic control presence and moving violations may need to be used to determine role and contributing factors.

Ideally, there would be a data source that had both a representative sample of high severity collisions from crash databases and the video and sensor data that exist in NDS data. Most public NDS datasets require retrofitting equipment onto vehicles that results in recorded mileage on the order of millions of miles. With the advent of cloud connected cell-phone- and consumer electronics-based dash cameras, there is an opportunity to extract collision events from billions of driven miles, increasing the likelihood that some of the collisions will have a serious outcome.

As discussed in the introduction, conflict typologies have been a tool used by traffic safety researchers, especially in the areas of crash data analysis, naturalistic driving, and prospective safety benefits research. Scenario description languages, which describe the trajectories of actors and how the actors interact with the environment often in machine readable format (e.g., [31]), are a related but separate topic. These scenario description languages are useful for defining abstract, logical, and concrete scenarios, especially for scenario-based testing. They focus on describing scenarios in a way that can be translated into simulations or evaluations of an ADS. The conflict typology could be used in conjunction with a set of scenarios to organize them by actor types, groups, perspectives, and contributing factors. For example, this conflict typology is the basis for the aggregation used in the Collision Avoidance Testing

scenario-based testing program at Waymo, where collision avoidance competency is evaluated relative to a reference behavior model in conflicts where the ADS is the responder role vehicle [32 - 33].

The appropriate level of aggregation in the conflict typology is one that allows for a safety impact assessment of a potential system, in our application an ADS. As larger-scale naturalistic driving data becomes available (e.g., from commercial dash cam companies) and as ADS are more widely deployed, it is possible that relevant distinctions between conflict perspectives are not fully captured by the conflict typology presented here. The way the conflict typology presented in this study has been constructed is a layered approach, which can easily accommodate additions of newly discovered actor types and conflicts.

CONCLUSION

This paper introduced a conflict typology for traffic conflicts that includes a definition of conflict partners, groups, perspectives, role, and contributing factors. The results showed that these layers of the conflict typology are useful for organizing conflicts into groups of similar causes, which can aid in retrospective or prospective analysis of traffic safety. To demonstrate the utility of this conflict typology, we presented results of an analysis of nationally representative crash data from the US (CRSS and FARS) and naturalistic driving data (SHRP-2). The main contribution of the proposed conflict typology and contributing factors are applicable to a wide range of conflicts (i.e., collisions from retrospective crash data and near-crashes from an NDS). The results also highlight potential difficulties reconciling differences in contributing factors observed in high-severity crash data having limited contributing factor information and those contributing factors observed in lower severity NDS data.

REFERENCES

[1] Najm, W. G., Smith, J. D., & Yanagisawa, M. (2007). *Pre-crash scenario typology for crash avoidance research* (No. DOT-VNTSC-NHTSA-06-02). United States. National Highway Traffic Safety Administration.

[2] Najm, W. G., Koopmann, J., Smith, J. D., & Brewer, J. (2010). *Frequency of target crashes for intellidrive safety systems* (No. DOT HS 811 381). United States. National Highway Traffic Safety Administration.

[3] Knipling, R. R. (2017). Crash heterogeneity: Implications for naturalistic driving studies and for understanding crash risks. *Transportation research record*, *2663*(1), 117-125.

[4] Kusano, K. D., & Gabler, H. C. (2012). Safety benefits of forward collision warning, brake assist, and autonomous braking systems in rear-end collisions. *IEEE Transactions on Intelligent Transportation Systems*, *13*(4), 1546-1555.

[5] Haus, S. H., Sherony, R., & Gabler, H. C. (2019). Estimated benefit of automated emergency braking systems for vehicle–pedestrian crashes in the United States. *Traffic injury prevention*, *20*(sup1), S171-S176.

[6] Riexinger, L., Sherony, R., & Gabler, H. (2019). *Has electronic stability control reduced rollover crashes?* (No. 2019-01-1022). SAE Technical Paper.

[7] Dean, M. E., & Riexinger, L. E. (2022). *Estimating the Real-World Benefits of Lane Departure Warning and Lane Keeping Assist* (No. 2022-01-0816). SAE Technical Paper.

[8] Bareiss, M., Scanlon, J., Sherony, R., & Gabler, H. C. (2019). Crash and injury prevention estimates for intersection driver assistance systems in left turn across path/opposite direction crashes in the United States. *Traffic injury prevention*, *20*(sup1), S133-S138.

[9] Cicchino, J. B. (2017). Effectiveness of forward collision warning and autonomous emergency braking systems in reducing front-to-rear crash rates. *Accident Analysis & Prevention*, *99*, 142-152.

[10] Cicchino, J. B. (2018). Effects of lane departure warning on police-reported crash rates. *Journal of safety research*, *66*, 61-70.

[11] Cicchino, J. B. (2022). Effects of automatic emergency braking systems on pedestrian crash risk. *Accident Analysis & Prevention*, *172*, 106686.

[12] Spicer, R., Vahabaghaie, A., Murakhovsky, D., Lawrence, S. S., Drayer, B., & Bahouth, G. (2021). Do driver characteristics and crash conditions modify the effectiveness of automatic emergency braking?. *SAE International Journal of Advances and Current Practices in Mobility*, *3*(2021-01-0874), 1436-1440.

[13] Spicer, R., Vahabaghaie, A., Murakhovsky, D., Bahouth, G., Drayer, B., & Lawrence, S. S. (2021). Effectiveness of advanced driver assistance systems in preventing system-relevant crashes. *SAE International Journal of Advances and Current Practices in Mobility*, *3*(2021-01-0869), 1697-1701.

[14] Sander, U. (2017). Opportunities and limitations for intersection collision intervention—A study of real world 'left turn across path'accidents. *Accident Analysis & Prevention*, *99*, 342-355.

[15] Scanlon, J. M., Sherony, R., & Gabler, H. C. (2017). Injury mitigation estimates for an intersection driver assistance system in straight crossing path crashes in the United States. *Traffic injury prevention*, *18*(sup1), S9-S17.

[16] Antin, J. F. (2011). *Design of the in-vehicle driving behavior and crash risk study: in support of the SHRP 2 naturalistic driving study*. Transportation Research Board. DOI: https://doi.org/10.17226/14494.

[17] International Organization for Standardization. (2018). *Naturalistic driving studies — Vocabulary — Part 1: Safety critical events* (ISO Standard No. ISO/TR 21974-1:2018). https://www.iso.org/standard/75786.html

[18] Guo, F., Klauer, S. G., McGill, M. T., & Dingus, T. A. (2010). Evaluating the relationship between near-crashes and crashes: Can near-crashes serve as a surrogate safety metric for crashes?.

[19] Guo, F., Klauer, S. G., Hankey, J. M., & Dingus, T. A. (2010). Near crashes as crash surrogate for naturalistic driving studies. *Transportation Research Record*, *2147*(1), 66-74.

[20] Neurohr, C., Westhofen, L., Butz, M., Bollmann, M. H., Eberle, U., & Galbas, R. (2021). Criticality analysis for the verification and validation of automated vehicles. *IEEE Access*, *9*, 18016-18041.

[21] Stutts, J. C., Reinfurt, D. W., Staplin, L., & Rodgman, E. (2001). The role of driver distraction in traffic crashes.

[22] Piccinini, G. B., Engström, J., Bärgman, J., & Wang, X. (2017). Factors contributing to commercial vehicle rear-end conflicts in China: A study using on-board event data recorders. *Journal of safety research*, *62*, 143-153.

[23] Dinparstdjadid, A., Supeene, I. and Engström, J. (2023). Measuring Surprising Behavior in Traffic. In Press.

[24] Ljung Aust, M., Habibovic, A., Tivesten, E., Sander, U., Bärgman, J., & Engström, J. (2012). *Manual for DREAM version 3.2*. Retrieved from http://publications.lib.chalmers.se/records/fulltext/204828/204828.pdf

[25] Habibovic, A., Tivesten, E., Uchida, N., Bärgman, J., & Aust, M. L. (2013). Driver behavior in car-to-pedestrian incidents: An application of the Driving Reliability and Error Analysis Method (DREAM). *Accident Analysis & Prevention*, 50, 554–565.

[26] Engström, J., Werneke, J., Bärgman, J., Nguyen, N., & Cook, B. (2013). Analysis of the role of inattention in road crashes based on naturalistic on-board safety monitoring data. *Proceedings of the 3rd International Conference on Driver Distraction and Inattention*, Gothenburg, Sweden (September 4–6, 2013).

[27] Engström, J., Liu, S. Y., Dinparastdjadid, A., & Simoiu, C. (2022). Modeling road user response timing in naturalistic settings: a surprise-based framework. *arXiv preprint arXiv:2208.08651*.

[28] Mackie, J. L. (1980). *The cement of the universe: A study of causation*. Clarendon Press.

[29] Singh, S. (2015). *Critical reasons for crashes investigated in the national motor vehicle crash causation survey* (No. DOT HS 812 115).

[30] National Highway Traffic Safety Administration (2019). *2019 FARS/CRSS Pedestrian Bicyclist Crash Typing Manual: A Guide for Coders Using the FARS/CRSS Ped/Bike Typing Tool; Revision Date: August 26, 2020*. National Highway Traffic Safety Administration, Washington, D.C. Report Number DOT HS 813 025.

[31] Association for Standardization of Automation and Measuring Systems (2022). ASAM OpenSCENARIO®. Accessed on December 5, 2022 from https://www.asam.net/standards/detail/openscenario/

[32] Webb, N., Smith, D., Ludwick, C., Victor, T., Hommes, Q., Favaro, F., ... & Daniel, T. (2020). Waymo's safety methodologies and safety readiness determinations. *arXiv preprint arXiv:2011.00054*.

[33] Kusano, K., Beatty, K., Schnelle, S., Favarò, F., Crary, C., Victor, T. (2022). Collision Avoidance Testing of the Waymo Automated Driving System. *arXiv preprint arXiv:2212.08148*.

APPENDIX

Table A1.
PEDCTYPE Variable Descriptions (Quoted from FARS/CRSS Pedestrian/Cyclist Coding Manual [30]).

PEDCTYPE Category	Description
Pedestrian Failed to Yield	'**760 (Pedestrian Failed to Yield)** is used when the pedestrian was involved in a collision with a vehicle while crossing the roadway (not an expressway). The involved motorist had the right-ofway and was traveling or intending to travel straight through. This code should not be used if any of the following apply: 710 (Multiple Threat), 730 (Trapped), 741 (Dash), and 742 (DartOut). If it is NOT apparent that either party had the right-of-way, select "Other/Unknown."'
Motorist Failed to Yield	'**770 (Motorist Failed to Yield)** is used when the pedestrian had the right-of-way and was involved in a collision with a vehicle while crossing the roadway (not an expressway) by a vehicle that was traveling or intending to travel straight through. This code should not be used if any of Crash Type - Pedestrian PB30 2019 FARS/CRSS Pedestrian/Bicyclist Manual 15 the following apply: 710 (Multiple Threat), 730 (Trapped), 741 (Dash), and 742 (Dart-Out). If it is NOT apparent that either party had the right-of-way, select "Other/Unknown."'
Dash Out	'**741 (Dash)** is used when the pedestrian ran into the roadway and was involved in a collision with a vehicle and there is no mention in the case materials that the driver's view of the pedestrian was obstructed. The case materials should state that the pedestrian ran.'
Dart Out	'**742 (Dart-Out)** is used when the pedestrian walked or ran into the roadway and was involved in a collision with a vehicle where the driver's view of the pedestrian was blocked until an instant before impact. A dart-out can only occur if there is some documented visual obstruction (e.g., parked vehicle, building or vegetation).'
Multiple Threat	'**710 (Multiple Threat)** is used when the pedestrian entered the traffic lane in front of stopped or slowing traffic and was involved in a collision with a vehicle traveling in the same direction as the stopped or slowing traffic. If there is a traffic signal present and the light changes while the person is crossing, see 730 (Trapped).'
Trapped	'**730 (Trapped)** is used when the pedestrian was involved in a collision with a vehicle while crossing at a signalized intersection or signalized midblock crossing when the light changed, and traffic started moving.'
Crossing Expressway	'**910 (Crossing Expressway)** is used when the pedestrian was attempting to cross an expressway or expressway ramp when involved with collision with a motor vehicle. An expressway is a major thoroughfare without intersecting cross streets, having specific entrance and exit ramps. It includes superhighways, interstates, freeways, turnpikes, and parkways. Entrance and exit ramps are considered part of an expressway. The pedestrian does not have to be in a travel lane of the expressway or expressway ramp. The case materials need to indicate that the pedestrian was attempting to cross not just walking along or in the expressway.'